HAL
open science

Caractérisation des modifications post-transcriptionnelles des ARN non codants chez Staphylococcus aureus en réponse à divers stress environnementaux : analyse dynamique et fonctionnelle

Laura Antoine

To cite this version:

Laura Antoine. Caractérisation des modifications post-transcriptionnelles des ARN non codants chez Staphylococcus aureus en réponse à divers stress environnementaux : analyse dynamique et fonctionnelle. Médecine humaine et pathologie. Université de Strasbourg, 2021. Français. NNT : 2021STRAJ086 . tel-03701854

HAL Id: tel-03701854

https://theses.hal.science/tel-03701854v1

Submitted on 22 Jun 2022

HAL is a multi-disciplinary open access archive for the deposit and dissemination of scientific research documents, whether they are published or not. The documents may come from teaching and research institutions in France or abroad, or from public or private research centers.

L'archive ouverte pluridisciplinaire **HAL**, est destinée au dépôt et à la diffusion de documents scientifiques de niveau recherche, publiés ou non, émanant des établissements d'enseignement et de recherche français ou étrangers, des laboratoires publics ou privés.

UNIVERSITÉ DE STRASBOURG

ÉCOLE DOCTORALE 414 : Sciences de la vie et de la santé

Architecture et Réactivité de l'ARN – IBMC Strasbourg

THÈSE présentée par :

Laura ANTOINE

Soutenue le : 21 juillet 2021

Pour obtenir le grade de : **Docteur de l'université de Strasbourg**

Discipline/ Spécialité : Aspects Moléculaires et Cellulaires de la Biologie

Caractérisation des modifications post-transcriptionnelles des ARN non codants chez *Staphylococcus aureus* en réponse à divers stress environnementaux : analyse dynamique et fonctionnelle

THÈSE dirigée par :

M. MARZI Stefano	CR1, CNRS, Université de Strasbourg

RAPPORTEURS :

Mme TISNÉ Carine	DR1, CNRS, Université de Paris
M HELM Mark	Associate Professor (W2), Johannes Gutenberg University (JGU), Mainz

EXAMINATEUR INTERNE:

Mme FRUGIER Magali	DR2, CNRS, Université de Strasbourg

A la mémoire de Clément,

Remerciements

Je tiens tout d'abord à remercier les membres du jury d'avoir accepté d'évaluer mon travail ; Carine Tisné, Mark Helm et surtout Magali Frugier, qui suit l'évolution de ma thèse depuis le début. Merci à toi et à Philippe Giegé pour votre disponibilité et vos conseils.

Pascale, merci pour ta patience et ta gentillesse. Merci à toi ainsi qu'à Eric Westhof de m'avoir laissé ma chance et accueillie au sein de l'unité, pour votre soutien et les nombreuses discussions, toujours passionnantes et instructives.

Merci à Stefano de m'avoir encadrée, encouragée et pour les conversations toujours enrichissantes. Merci d'avoir eu la patience de m'expliquer un nombre incalculable de trucs, d'avoir écouté mes suggestions et surtout, merci pour ta bienveillance à toute épreuve, même quand je rate l'avion pour Krakow.

Les membres du labo 436, merci pour les conversations pendant les tea-time et tous les bons moments passés au labo avec vous.
Merci beaucoup à Isa et Papy pour les conseils de microbiologistes, votre disponibilité et votre écoute. Merci Papy Chulo pour la miniature du clip !
Merci beaucoup à Emma d'avoir été là, de m'avoir soutenue et conseillée depuis le tout début du master. Et surtout merci de m'avoir rappelé à chaque fois qu'il y avait des inscriptions à faire ou des papiers à rendre ça m'a sauvé plus d'une fois
Noémie, merci pour les pauses clopes à m'écouter me plaindre et parler de mes animaux et de mes plantes. Et merci aussi d'avoir gardé mon chat quand je n'étais pas là le weekend.
Lucas, merci d'être l'homme de la situation, l'homme du ribosome profiling, qui a retiré les tubes bloqués dans le rotor ! Quel homme ce Lucas ! Merci de m'avoir aidé !
Laura B, merci d'avoir tué la plante que je t'ai offert à noël. Tu n'es plus Laura 2 maintenant, profites bien de ton nouveau statut d'unique Laura du labo ;).
Hiroki and Roberto, it was a pleasure to work with you, I hope I helped with your tRNA and ribosome purifications. Thank you Hiroki for the conversations about french pastries. Thank you Roberto for the conversations during evenings in the lab.

Je remercie également Philippe Wolff de m'avoir mis le pied à l'étrier et formée à la spectrométrie de masse des ARN. Merci de m'avoir supportée et conseillée dès de début de mon stage de master. Merci également à tous les membres de la plateforme protéomique pour leur soutien et leur aide pour les analyses de protéines

Merci aussi à tous les phD de l'unité pour les phD seminars et les phDrink. Merci surtout à José et Luc pour leur amitié et leur soutien. Merci aussi pour les soirées et les débats devant des russes blancs

Je remercie aussi les personnes de la promo du master chimie-bio de Strasbourg pour leur accueil incroyable et leur soutien. Merci à Najet, Mike, Juline pour les soirées. Merci à Marine et Camille pour les brunchs du dimanche au restaurant végétarien et merci à Jérémy pour les poissons et les soirées tartes flambées au gîte. Merci à Stéphane pour les randos ensemble et les soirées à l'o'brien.

Merci à Myriam Seemann et Philippe Chaignon pour m'avoir pris pour mon premier stage, m'avoir appris les enzymes à cluster et m'avoir encouragée comme vous l'avez fait.

Un grand merci à OC, Mika et surtout Nanoo, merci pour tout, merci d'avoir été là, même de loin, depuis plus de 20ans !

Merci à la famille, les cousins et cousines, les oncles et tantes pour leur soutien infaillible et les moments inoubliables au cabaret vert et bon courage Solweig pour ta thèse, que du bonheur, tu verras !
Merci également à Jérémy et aux parents, spécialement à maman, merci pour tout Maman. Je t'aime.

Enfin merci à Nemo d'être à mes côtés depuis 15 ans maintenant, de m'avoir soutenue et supportée depuis toutes ces années et surtout d'avoir été si gentil et si patient avec moi ces derniers mois (ou ces dernières années ?). Je t'aime.

Résumé de la thèse

Caractérisation des modifications post-transcriptionnelles des ARN non codants chez *Staphylococcus aureus* en réponse à divers stress environnementaux : analyse dynamique et fonctionnelle

Introduction :

Les ARN non codants jouent un rôle essentiel pour la cellule, notamment lors de la traduction. En effet, les ribosomes sont constitués essentiellement d'ARN ribosomiques (ARNr) et les ARN de transfert (ARNt) assurent le décodage des ARN messagers (ARNm). Le processus de traduction des ARNm en protéines peut être régulé par d'autres ARN non codants appelés petits ARN régulateurs (sARN).

Les modifications post-transcriptionnelles influencent la structure de l'ARN et les propriétés chimiques des nucléosides. Les ARNt et les ARNr présentent le plus grand nombre de modifications, qui par conséquent jouent un rôle prépondérant pour leurs fonctions, pour l'efficacité et pour la vitesse de la traduction. Par exemple, la modification en position 34 (la base « wobble ») des ARNt est indispensable tant pour le décodage de différents codons correspondant à un même acide aminé que pour la discrimination de codons proches[1]. Pour les bactéries pathogènes, ces modifications post-transcriptionnelles sont impliquées dans l'adaptation à l'environnement, dans l'expression de gènes de virulence[2] et dans les interactions avec l'hôte lors d'infections. La présence de modification en position 34 des ARNt est liée à la virulence chez *Streptococcus pyogenes*[3]. Par ailleurs, la présence ou l'absence d'une modification sur les ARNr peut conférer une résistance aux antibiotiques ciblant le ribosome[4].

Dans ce contexte, cette étude a porté sur *Staphylococcus aureus*, une bactérie commensale de l'Homme présente chez 1 individu sur 3 et aussi un pathogène opportuniste responsable d'infections nosocomiales et communautaires [5]. L'émergence de souches multi-résistantes aux antibiotiques est un véritable problème de santé publique, notamment dans le milieu hospitalier. En tant qu'opportuniste, *S. aureus* possède une grande capacité d'adaptation en réponse aux changements environnementaux. Cette capacité lui permet, via la régulation très fine de l'expression des facteurs de virulence, d'être à l'origine de nombreuses infections pouvant être très graves. A ce jour, le rôle des modifications post-transcriptionnelles dans les processus adaptatifs et l'infection par *S. aureus* reste encore inconnu.

A l'aide d'analyses de spectrométrie de masse associées à différentes méthodes de séquençage à haut débit des ARN (RNA-Seq), cette étude consiste à établir une cartographie des modifications post-transcriptionnelles des ARN non codant chez *S. aureus*. Elle vise ensuite à déterminer leurs potentielles variations en fonction de conditions de stress mimant l'environnement durant une infection afin de mieux comprendre leur impact sur la croissance bactérienne, les réponses aux stress et dans la virulence.

Résultats :

Afin de caractériser les modifications post-transcriptionnelles des ARNt de *S. aureus*, j'ai mis en place, en collaboration avec Philippe Wolff (UPR 9002, responsable de l'analyse de spectrométrie de masse appliquée aux ARN), une méthode de purification et d'identification par chromatographie liquide couplée à la spectrométrie de masse UPLC-MS/MS (Ultra Performance Liquid Chromatography Tandem Mass Spectrometry)[6,7]. La cartographie réalisée par spectrométrie de masse dans les ARNt de *S. aureus* étant partielle, elle a été complétée et confirmée par différentes méthodes de RNA-Seq telles que le Psi-Seq, le RiboMethSeq et l'Alkaniline-Seq[8], en collaboration avec le Pr Yuri Motorin et la Dr Virginie Marchand de la plateforme Epitranscriptomique et Séquençage (EpiRNA-Seq) de Nancy. Les données RNA-Seq ont également permis d'obtenir des informations sur les modifications présentes sur les ARNr (**Figure 1**). Celles détectées dans les ARNt de *S. aureus* sont très proches de celles caractérisées chez d'autres bactéries à Gram positif tel que *Lactococcus lactis*[9]. De façon inattendue, mon étude a également révélé des éléments uniques aux ARNt de *S. aureus*. Précisément, les ARNt de la glycine qui en plus d'être impliqués dans la traduction des protéines, participent également à la formation du pont pentaglycine présent dans la paroi cellulaire des Staphylocoques. Les ARNt responsables du transport de la glycine vers la paroi ont été analysés et ne possèdent pas les modifications spécifiques des ARNt impliqués dans l'incorporation des glycines dans les protéines, specifiquement au niveau de leurs anticodons. De plus, la présence d'une modification dont la masse ne correspond à aucune modification connue à ce jour a pu être détectée en position 37 de l'ARNt de la lysine. Ces résultats ont conduit à un nouveau projet d'étude dans le laboratoire pris en charge par un chercheur post-doctorant afin de déterminer le rôle des modifications (ou leur absence) dans la discrimination des $ARNt_{Gly}$.

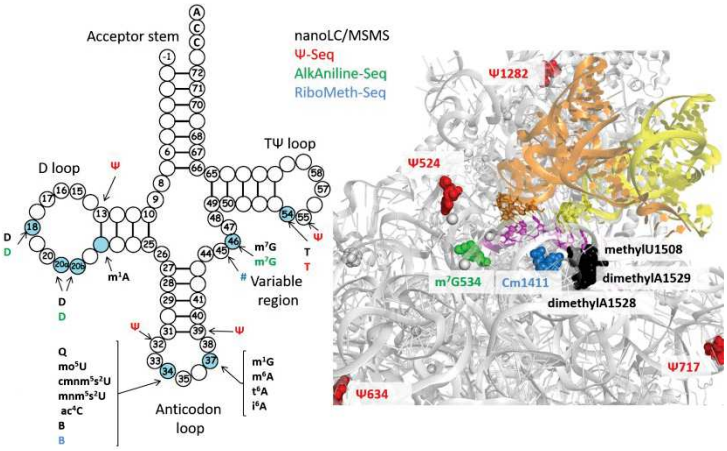

Figure 1. Modifications cartographiées par différentes méthodes dans les ARNt à gauche et l'ARNr 16S de *S. aureus* à droite

Une fois la cartographie établie en condition normale de croissance en laboratoire, différentes conditions de stress mimant ceux rencontrés lors de l'infection et les interactions avec l'hôte (augmentation de la température, privation de nutriments, hypoxie, stress oxydant ou nitrique et présence d'antibiotiques) ont été réalisés. Plusieurs de ces conditions, montrent des variations flagrantes dans le profil de migration des ARNt sur gel de polyacrylamide qui peut résulter de changements dans les modifications (**Figure 2A**). Dans certaines conditions, tel que le stress induit par l'oxyde nitrique (NO), une analyse complète de spectrométrie de masse ainsi que de RNA-Seq de chaque ARNt sera nécessaire pour déterminer si un changement a lieu. Cependant, une condition spécifique qui a montré clairement une variation de migration d'ARNt est le stress oxydant induit par l'addition de méthylviologen entrainant la formation d'espèces réactives de l'oxygène (ROS). La production de ROS est une des défenses principales du système immunitaire contre les infections. Les macrophages produisent des anions superoxydes, du peroxyde d'hydrogène ainsi que des oxydes nitriques en réponse à la phagocytose de bactéries. De plus, ces espèces réactives de l'oxygène et de

l'azote sont impliquées dans l'inflammation et les lésions tissulaires qui sont également hypoxiques[10]. Dans ce contexte, j'ai donc décidé d'étudier l'impact du stress oxydant induit par le méthylviologen sur les modifications des ARNt ainsi que les conséquences qu'une modification différentielle peut avoir sur le processus de traduction.

L'analyse des modifications des ARNt par UPLC-MS/MS montre un clivage par la RNase T1 de l'ARNt$_{TyrGUA}$ en 3' de la queuosine en position 34 qui n'a pas lieu en absence de l'agent oxydant (**Figure 2A**). Cet effet suggère que la queuosine, modification complexe et importante impliquée dans le décodage de l'ARNm lors de la traduction, est absente en condition de stress oxydant. L'absence de queuosine dans les bactéries cultivées en en condition de stress oxydant a été confirmée dans les quatre ARNt (ARNt Tyr, His, Asp et Asn) contenant cette modification par électrophorèse d'affinité au boronate et par analyse UPLC-MS/MS des ARNt purifiés. Pour l'électrophorèse d'affinité, des ARN totaux provenant d'une souche de *S. aureus* n'exprimant pas l'enzyme Tgt, responsable du transfert de l'intermédiaire preQ1 sur l'ARNt ont été également utilisés (**Figure 2B**). Grâce à cette méthode, j'ai également montré qu'il était possible de restaurer la présence de queuosine par l'ajout du preQ1 dans le milieu de culture des bactéries soumises au stress oxydant (**Figure 2B**) indiquant une possible inactivation d'une des enzymes impliquées dans la voie de biosynthèse du preQ1 lors du stress.

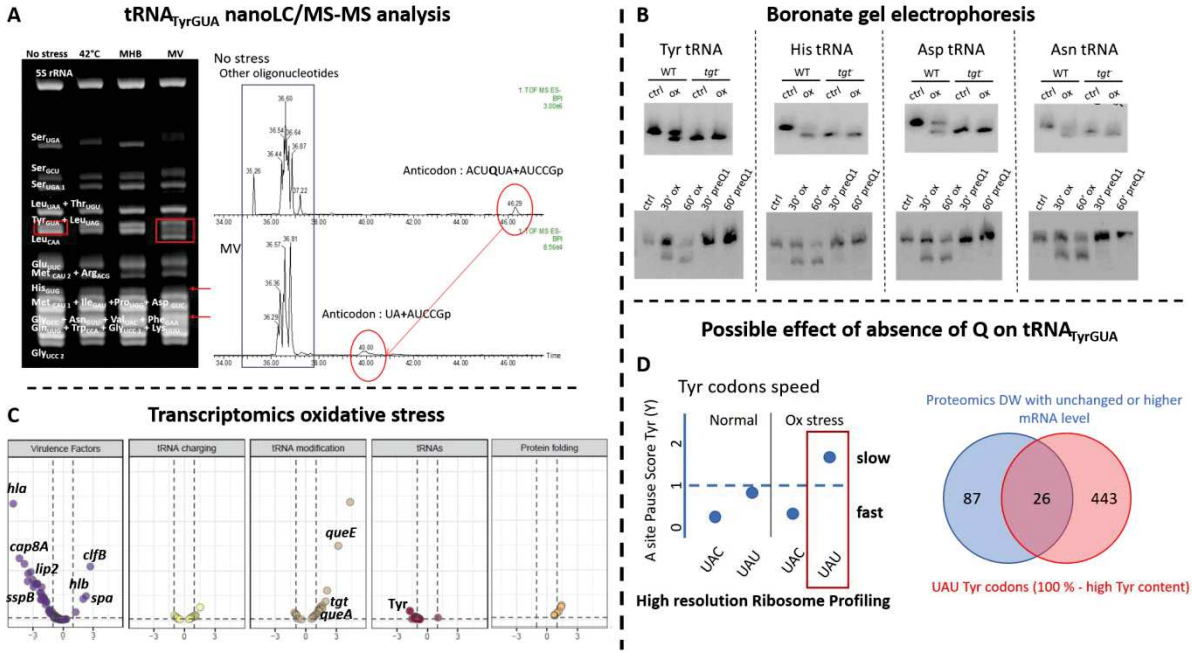

Figure 2. A. Analyse des ARNt dans différentes conditions de stress environnementaux, à gauche : gel de polyacrylamide (12,5%, 8 M urée) des ARNt de *S. aureus* cultivés en conditions normales (no stress), à 42°C (augmentation de la température), en milieu MHB (Mueller-Hinton Broth : privation de nutriments) ou stress oxydant (MV : méthylviologen). Les ARN présents dans chaque bande ont été identifiés par UPLC-MS/MS. A droite : chromatogrammes obtenus à partir des bandes encadrées en rouge contenant l'ARNt$^{Tyr}_{GUA}$, encerclés en rouge les pics correspondants aux anticodons, non clivé par la RNase T1 pour l'ARNt issu de la culture non stressée, clivé pour celui issu de la culture soumise au stress oxydant. Q: queuosine; +: N6-isopentyl Adénosine. **B. Electrophorèse d'affinité au boronate,** ligne du haut : profil de migration des 4 ARNt contenant la queuosine de la souche WT en condition normale et en condition de stress oxydant et de ces ARNt sans queuosine provenant de la souche n'exprimant pas le gène *tgt*. Ligne du bas : profil de migrations des ARNt en conditions de stress oxydant et après addition de l'intermédiaire de la queuosine preQ1. **C. Volcano plot représentant la transcription différentielle de plusieurs types de gènes** tels que les facteurs de virulence, ceux impliqués dans le repliement des protéines et dans les fonctions des ARNt en conditions de stress oxydant. **D. Impact de l'absence de queuosine de l'ARNt^{Tyr} sur la traduction.** A gauche : taux de pause des deux codons UAC et UAU de la tyrosine montrant un décodage plus lent du codon UAU en condition de stress oxydant. A droite : diagramme de Venn indiquant les gènes sous exprimés en protéomique pour lesquels le niveau de transcription ne change pas, voire augmente et dont les ARNm sont riches en codons UAU.

Une altération de la queuosine en position 34 implique d'inévitables conséquences au niveau de l'efficacité de la traduction. L'absence de cette modification peut impacter la vitesse et la finesse de la reconnaissance des codons par l'ARNt, ainsi que la fidélité d'incorporation des acides aminés, entrainant la production de protéines anormales. Afin d'étudier les possibles causes et conséquences de l'anomalie de queuosine en position 34, des analyses protéomiques et transcriptomiques ont été réalisées montrant d'importantes variations dans l'expression des gènes marqueurs du stress oxydant mais également de nombreux facteurs de virulence impliqués dans la dissémination et la protection contre le système immunitaire (**Figure 2C**). Ces résultats sont à corréler avec une analyse de « high resolution ribosome profiling » (hRibo-seq) pour étudier la vitesse de traduction codon par codon. Les résultats préliminaires obtenus, montrent que durant le stress oxydant, les codons UAU nécessitent la présence de la queuosine en 34 de l'ARNt^{Tyr} pour être décodés efficacement. En effet, ils présentent une diminution importante de leur vitesse de décodage, tandis que celle des codons UAC ne semble pas être impactée par l'absence de queuosine (**Figure 2D**). De manière remarquable, l'analyse protéomique en condition de stress oxydant révèle une dérégulation de la traduction pour de nombreux gènes alors que les niveaux d'ARNm demeurent inchangés, voire augmentent. Certains de ces ARNm présentent une composition particulièrement riche en codon UAU. L'analyse de hRibo-seq a été répétée en condition de stress oxydant mais aussi en présence de preQ1 pour discriminer plus clairement les effets exclusivement dus à l'absence de queuosine sur les 4 ARNt concernés. Cette étude est actuellement en cours.

Conclusions et perspectives :

La mise en place de L'UPLC-MS/MS en association avec les méthodes de RNA-Seq a permis d'établir les cartographies partielles des modifications présentes dans les ARN non codants de *S. aureus* afin d'étudier leurs variations, en particulier dans les ARNt lors de stress environnementaux mimant les conditions rencontrées lors de l'infection. J'ai ainsi mis en évidence, d'une part une altération de la queuosine des 4 ARNt possédant cette modification en position wobble de l'anticodon et d'autre part étudié l'impact sur la traduction de l'absence de cette modification. L'expérience de hRibo-Seq complète est en cours afin d'élucider la fonction de la queuosine sur le décodage de l'ensemble des codons nécessitant cette modification. Cette étude est réalisée en parallèle avec une analyse de la composition en nucléosides modifiés des ARNt afin de déterminer l'impact du stress oxydant sur les autres modifications post-transcriptionnelles présentes sur les ARNt totaux. Les données d'analyses de RNA-Seq de ribosomes provenant de bactéries soumises au stress oxydant induit par le méthylviologen sont en cours d'analyse. L'étude structurale de l'impact des variations de modifications des ARNt et ARNr sur l'ensemble de la machinerie traductionnelle se déroule en collaboration avec Roberto Bahena, qui est actuellement en première année de thèse.
Pour compléter l'étude de l'épitranscriptome de *S. aureus*, 4 sARN régulateurs (RsaA, C, G et I) ont également été analysés par RNA-Seq. Cependant, les résultats n'ont pas montré la présence de modifications post-transcriptionnelles. Des analyses UPLC-MS/MS seront nécessaires afin de confirmer l'absence de modifications dans ces sARN.
Cette approche que j'ai mise en place pour l'étude des variations des modifications des ARN en réponse au stress oxydant et de leur impact traductionnel, pourra être appliquée à l'adaptation de la bactérie à d'autres conditions environnementales rencontrées lors de l'infection pour lesquelles des profils différents de migration des ARNt ont été observés.
Bibliographie :

1. Rozov A, Demeshkina N, Khusainov I, Westhof E, Yusupov M, Yusupova G. Novel base-pairing interactions at the tRNA wobble position crucial for accurate reading of the genetic code. Nat Commun. 2016;7:10457. doi:10.1038/ncomms10457

2. Koh CS, Sarin LP. Transfer RNA modification and infection – Implications for pathogenicity and host responses. Biochim Biophys Acta BBA - Gene Regul Mech. 2018;1861(4):419-432. doi:10.1016/j.bbagrm.2018.01.015

3. Cho KH, Caparon MG. tRNA Modification by GidA/MnmE Is Necessary for Streptococcus pyogenes Virulence: a New Strategy To Make Live Attenuated Strains. Infect Immun. 2008;76(7):3176-3186. doi:10.1128/IAI.01721-07

4. Stojković V, Noda-Garcia L, Tawfik DS, Fujimori DG. Antibiotic resistance evolved via inactivation of a ribosomal RNA methylating enzyme. Nucleic Acids Res. 2016;44(18):8897-8907. doi:10.1093/nar/gkw699

5. Lowy FD. Staphylococcus aureus Infections. N Engl J Med. 1998;339(8):520-532. doi:10.1056/NEJM199808203390806

6. Antoine L, Wolff P. Mapping of Posttranscriptional tRNA Modifications by Two-Dimensional Gel Electrophoresis Mass Spectrometry. Methods Mol Biol Clifton NJ. 2020;2113:101-110. doi:10.1007/978-1-0716-0278-2_8

7. Antoine L, Wolff P, Westhof E, Romby P, Marzi S. Mapping post-transcriptional modifications in Staphylococcus aureus tRNAs by nanoLC/MSMS. Biochimie. 2019;164:60-69. doi:10.1016/j.biochi.2019.07.003

8. Motorin Y, Helm M. Methods for RNA Modification Mapping Using Deep Sequencing: Established and New Emerging Technologies. Genes. 2019;10(1):35. doi:10.3390/genes10010035

9. Puri P, Wetzel C, Saffert P, et al. Systematic identification of tRNAome and its dynamics in Lactococcus lactis. Mol Microbiol. 2014;93(5):944-956. doi:10.1111/mmi.12710

10. Eltzschig HK, Carmeliet P. Hypoxia and inflammation. N Engl J Med. 2011;364(7):656-665. doi:10.1056/NEJMra0910283

Liste des Abbreviations

Acides nucléiques :

ADN : acide désoxyribonucléique

ARN : acide ribonucléique

ARNm : ARN messager

ARNr : ARN ribosomique

ARNt : ARN de transfert

Composés chimiques et milieux de cultures

NO : oxyde nitrique

ROS : espèces réactives de l'oxygène

APB : Acide phénylboronique

BHI : Brain heart infusion : infusion cœur cerveau

MV : Méthylviologen

TEA-Cl : chlorure de tetraéthyl ammonium.

Bactéries

S. aureus : Staphylococcus aureus

B. subtilis : Bacillus subtilis

L. lactis : Lactococcus lactis

E. coli : Escherichia coli

MRSA : Methicillin Resistant *S. aureus* (résistante à la méthicilline)

Protéines et facteurs de virulence :

Ahp : Alkyl hydroperoxyde réductase

Clf: Clumping factor (facteur d'agglutinement)

Efb : Extracellular fibrinogen binding protéine (protéine de liaison au fibrinogène extracellulaire)

Fnbp : Fibronectin binding protein (Protéine de liaison à la fibronectine)

Isd : Iron-Regulated Surface Determinant

MSCRAMM : microbial surface components recognizing adhesive matrix molecules (composants de la surface microbienne reconnaissant les molécules adhésives de la matrice)

PSM : Phenol Soluble Modulins

Sod : Superoxyde dismutase

SpA : Staphylococcal protein A (protéine staphylococcique A)

TSST : Toxic shock syndrome toxin (toxine du syndrome de choc toxique)

Techniques

LC : chromatographie liquide

MS : Spectrométrie de masse

Table des Matières

Remerciements 1

Résumé de la thèse 5

Liste des Abbreviations 11

Table des Matières 12

I. Introduction 15

1. Rôle des modifications post-transcriptionnelles chez bactéries pathogènes 15

2. *Staphylococcus aureus* 40

3. L'oxydation comme défense contre les pathogènes 43

4. *S. aureus* et son adaptation au stress oxydant 44

5. Objectifs de la thèse 46

II. Résultats : 47

1. Mise en place de la méthode d'analyse des ARN par gel en 2 dimensions et NanoLC-MS/MS 47

2. Cartographie des modifications post-transcriptionnelles des ARNt de *S.aureus* 58

3. Analyse de RNA-Seq des ARN non codants de *S.aureus* 70

4. Réponse au stress oxydant : 71

i. Analyse transcriptomique et protéomique 72

ii. Dynamique des modifications des ARNt en réponse au stress oxydant 74

iii. Analyse des ARNt contenant la Q34 issus de cultures stressées 75

iv. Le précurseur preQ1 restaure la queuosine dans les 4 ARNt contenant la Q34 76

III. Discussion 77

1. Mise en place de la méthode et cartographie des modifications 77

i. Limites et méthodes complémentaires : le pouvoir de la coopération 77

ii. Cartographie des modifications des ARN non codants de *S. aureus* 78

2. Réponse globale de *S. aureus* au stress oxydant 81

i. Système SOS de réparation de l'ADN et gènes phagiques 81

ii. Détoxification des espèces réactives de l'oxygène 82

iii. Métabolisme des acides aminés 83

iv. Homéostasie du fer 83

v. La voie de respiration en anaérobie 83

vi. L'implication des ARNt et des enzymes de modifications 84

vii. La persistance de la bactérie privilégiée au détriment de la dissémination et de l'infection aiguë 85

3. Modifications des ARNt et stress oxydant 85

i. Dynamique des modifications des ARNt durant le stress 85

ii. Causes de l'absence de queuosine 86

iii. Conséquences traductionnelles de l'absence de Q34 89

IV. Conclusions 91

V. Matériels et méthodes 93

1. Produits et sondes utilisés 93

2. Souches bactériennes et conditions de culture 93

i. Souches 93

ii. Conditions de culture 94

3. Analyse par NanoLC-MS/MS de l'ARNr 16S 95

4. Analyse transcriptomique 96

5. Analyse protéomique 96

6. Gel d'acide phénylboronique et Northern blot 97

7. Purification des ARNt 97

8. Digestion à la RNAse U2 des ARNt purifiés. 98

9. Modèlisation des structures de QueE et QueF de *S. aureus* 98

10. Ribosome profiling à haute résolution 98

Références bibliographiques 100

Annexes 111

Annexe 1 : Tableau de la transcription différentielle durant le stress oxydant 111

Annexe 2 : Tableau de l'expression différentielle des protéines durant le stress oxydant : 125

Annexe 3 : Tableau de l'expression différentielle selon les voies métaboliques impliquées. 134

I. Introduction

1. Rôle des modifications post-transcriptionnelles chez bactéries pathogènes

Les modifications post-transcriptionnelles des ARN sont impliquées dans de nombreux processus biologiques et sont présentes dans toutes les classes d'ARN. Ces modifications sont constitutives ou modulées en réponse à des processus adaptatifs. Elles remplissent de nombreuses fonctions puisqu'elles peuvent impacter l'appariement des bases, la reconnaissance par les protéines, le décodage ainsi que la structure et la stabilité des ARN. Cependant, leurs rôles dans les adaptations aux stress environnementaux ainsi que durant les infections causées par des bactéries pathogènes commencent juste à être appréciées. Avec le développement de technologies modernes de spectrométrie de masse et de séquençage, des exemples récents de modifications régulant les interactions hôte-pathogène ont été étudiés. Ils révèlent comment les modifications des ARN peuvent réguler la réponse immunitaire, la résistance aux antibiotiques, l'expression des gènes de virulence et la persistance bactérienne. Dans la revue suivante, écrite avec l'aide de Roberto Bahena, Stefano Marzi, Pascale Romby, ainsi que 3 étudiants de master, nous illustrons quelques-unes de ces découvertes et soulignons les stratégies utilisées pour caractériser les modifications des ARN et leur potentiel pour de nouvelles applications thérapeutiques. La revue sera soumise à Genes pour le numéro spécial "Functions and Dynamics of RNA Modifications".

Review

RNA modifications in pathogenic bacteria: Impact on host adaptation and virulence

Laura Antoine [1], Roberto Bahena-Ceron [1], Heemee Devi Bunwaree[1], Martin Gobry[1], Victor Loegler [1], Pascale Romby [1] and Stefano Marzi [1,*]

[1] Université de Strasbourg, CNRS, Architecture et Réactivité de l'ARN, UPR 9002, F-67000 Strasbourg, France.
* Correspondence: s.marzi@ibmc-cnrs.unistra.fr

Received: date; Accepted: date; Published: date

Abstract (200 words max: 138 words):

RNA modifications are involved in numerous biological processes and are present in all classes of RNA. These modifications are constitutive or modulated in response to adaptive processes. RNA modifications play multiple functions since they can impact RNA basepairings, recognition by proteins, decoding, as well as RNA structure and stability. However, their roles in stress, environmental adaptation and during infections caused by pathogenic bacteria have just started to be appreciated. With the development of modern technologies in mass spectrometry and deep sequencing, recent examples of modifications regulating host-pathogen interactions have been demonstrated. They show how RNA modifications can regulate immune responses, antibiotic resistance, expression of virulence genes, and bacterial persistence. Here, we illustrate some of these findings, and highlight the strategies used to characterize RNA modifications, and their potential for new therapeutic applications.

Keywords: RNA modifications 1; pathogenic bacteria 2; host-adaptation 3; stress adaptation 4; ribosomal RNA 5; tRNA 6; small non coding RNA 7; mRNA 8;

1. Introduction

Bacteria are remarkably versatile organisms, which can survive and grow in numerous environmental niches on the planet. They modulate the expression of their genes to respond and adapt their growth to environmental stress such as temperature and pH shifts, nutrient availability, antimicrobials or dangerous chemical reactive species. This is particularly the case for pathogenic bacteria, which must adapt their metabolism to the host environment and ensure their survival facing the human/animal immune systems and antibiotic therapies. Bacteria can sense the environment directly via the effect that physical and chemical stresses might have on different macromolecules, or via signaling systems, very often two-component systems (TCS), transducing the stress signal from a specific sensor histidine kinase to a corresponding response regulator [1]. The responses are aimed at eliminating the stressor or its effects, at repairing damages or at inducing the escape from the stress, but sometime the external stimuli are signals for switching to programmed life-style changes. They produce profound changes in cell physiology and behaviors, and affect gene expression at transcriptional, post-transcriptional, translational, and post-translational levels. In these processes, an interplay between various TCS, transcriptional protein regulators, and regulatory RNAs orchestrates complex regulatory networks in order to link metabolism adaptation and virulence [2]. Because RNAs, occupy a central position in translation (tRNAs, rRNAs, mRNAs), they actively contribute to these regulatory networks.

In bacteria, the rate of translation is modulated by multiple signals present in mRNAs affecting translation initiation, elongation, termination, and ribosome recycling [3-6]. The mRNA translation initiation signals can be masked or liberated by the binding of proteins or small regulatory RNAs (sRNAs), or by structural rearrangements occurring in response to metabolite binding or to physical cues changes, which also directly affect transcription and RNA folding [7-12]. Besides, codon usage specific for each gene (codon bias) is used in relation to variation of the tRNA pool to fine tune gene expression [13]. Moreover, many studies have emphasized the physiological importance of ribosome heterogeneity to rapid modulation of selective gene expression in response to environmental conditions [14, 15]. These mechanisms are influenced by base or ribose modifications present in RNAs [16] adding another sophisticated layer of regulation. In fact, stresses can alter RNA modification states of various RNA species (i.e., rRNA, tRNA, sRNA and mRNA) with effect on translation rates, on RNA regulatory properties, or on codon recoding.

The number of newly detected modifications enhances at a constant pace [17]. They can be very simple like methylation or deamination, or be more complicated. Some of them require the consecutive action of several modification enzymes and cofactors [18]. These modifications modulate

the chemical and physical properties of the nucleotides and in turn the RNA functions (for a review see [19]). They might change any of the nucleotide interacting edges, which can potentially affect Watson-Crick base-pairing and non-canonical interactions [20]. For example, the A-form RNA helix, favored by C3′-*endo* sugar pucker, is stabilized by 2′-OH methylation of ribose [21, 22] while dihydrouridine (D) significantly destabilizes the C3′-*endo* sugar conformation, providing structure flexibility [23]. Interestingly, D is predominantly found in psychrophile bacteria and archaea [23]. Methylation on the bases can influence hydrogen-bonding and stacking interactions [24]. Pseudouridine (Ψ) can shift between *syn*/*anti* conformations with relatively greater ease [25]. The dynamic nature and the regulatory functions of some of these RNA modifications [26] have generated a new field referred to 'epitranscriptomics' [27]. The detection of the bacterial epitranscriptome relies on cutting edge methodologies involving combination of mass spectroscopy (LC/MSMS) and RNA-seq based methodologies. Nevertheless, identification of the epitranscriptome of pathogenic bacteria and its modulation upon stress and during the infection process is only in its infancy.

In this review, we illustrate several examples of the involvement of RNA modifications on the expression of virulence genes and in stress responses of different pathogenic bacteria. Even though these studies provide mechanistic explanations for only few cases, they already reveal a multitude of strategies developed by pathogenic bacteria to survive, persist, and fight against host immune defenses based upon the modulation of RNA modifications.

2. Technological advances: Detecting RNA modifications

A prerequisite to analyze the functions of RNA modifications is obviously to be able to detect the modified nucleosides, to quantify them, to map their localization within specific RNA. A detailed description of the available methods is outside the scope of the review. We will give here a summary of the most employed approaches with their limits and advantages (**Table 1**), and details will be found in more specific articles.

Mapping of post-transcriptional RNA modifications using mass spectrometry (MS) existed for over 30 years [28]. The precise measurement of molecular masses (less than 1 Da) provided the possibility to characterize known modified residues in tRNAs using liquid chromatography coupled to mass spectrometry (LC/MSMS). Two complementary MS approaches are routinely used to get a complete repertoire of modified nucleosides obtained either from tRNA extracts in a single experiment [29-31], or from tRNA fragments produced from specific endoribonuclease digestion to determine both the nature of modifications and their location in the tRNA sequence [32, 33]. The analysis of a pure RNA or a class of RNAs hydrolyzed into nucleosides allows precise characterization and quantification of modifications, while oligonucleotide analysis allows precise localization of

modified sites on sequence, but no quantification can be achieved. Moreover, the method does not allow complete sequence coverage and the use of RNases with different sequence specificity can increase it. Capillary electrophoresis coupled to MS (CE/MSMS) allows precise analysis of a wide range of molecules (reviewed in [34]), and can also be used for the characterization of tRNA modifications with the two approaches. Because capillary electrophoresis allows analysis of small oligonucleotide fragments, the combination of LC/MSMS and CE/MSMS leads to a better sequence coverage on pure tRNAs [35]. Nevertheless, one of the major limitations of these MS methods is the detection of Ψ, which is an isomer of uridine and for this reason is a mass-silent modification. The MS analysis of Ψ can be done because they can be selectively modified by 1-cyclohexyl-(2-morpholinoethyl)carbodiimide metho-p-toluene sulfonate (CMCT) [36]. The carbodiimide (CMC) moiety of CMCT modifies the N1 of guanosine, the N3 of uridine, and the N1 and N3 of Ψ, but alkaline treatment at pH 10.3 easily removes it from them, with the exception of the N3 of Ψ, therefore producing a detectable mass increment of 252 Da [37]. More recently, pseudouridines have been also detected directly in RNA fragments by pseudo-MS^3 (MS/MS/MS) analysis [38] thanks to the specific signature ion at *m*/*z* 207.041 for double dehydrated Ψ [39].

Various high throughput sequencing methods are often used to characterize specific modifications by Reverse Transcriptase (RT) signatures after chemical treatment. These methods do not need to purify the RNA prior to the analysis but they need bioinformatics data treatment and statistical evaluation of errors. NGS-based methods are often not quantitative, have high false-positive rates [40] and require multiple ligation steps and extensive polymerase chain reaction amplification during the library preparation, introducing undesired biases in the sequencing data [41]. Currently, customized protocols must be optimized for each RNA modification type, leading to experimental designs in which the RNA modification type to be studied is chosen beforehand, limiting the ability to characterize the plasticity of the epitranscriptome in a systematic and unbiased manner. A recent review described in details the RNAseq based approaches [42]. We will just mention here the very recent development of single molecule direct RNA sequencing methods developed by Oxford Nanopore Technologies (ONT), which are promising for the analysis of modification landscape on a specific RNA sequence [43-46].

Combination of these highly complementary methods allows a precise localization and characterization of post-transcriptional modifications and their dynamics, a prerequisite to a better understanding of the roles of RNA modification in bacterial adaptation.

Methods			Modifications detected	Quantification	Genome wide	Positional information	Remarks (Pros/Cons)
Structure determination	X-ray Cristallography		All modifications	✗/✓	✗	✓	Difficult to obtain crystals
	Cryo Electron Microscopy						Heterogeneous resolution
	Nuclear Magnetic Resonance						Size limit
LC/MSMS	Nucleoside analysis	DMRM [28]	Known modifications	✓	✓	✗	Fragmentation pattern and retention time of modifications must be known
		NLS [28]	Various modifications	✓	✓	✗	NLS is less suitable for quantification than DMRM
	Fragment analysis	With a reference (SILNAS/CARD/SILCARD) [47, 48]	Known modifications	✓	✗	✓	Relative quantification can be assessed with reference *in vitro* RNA
		Without reference (RNase digests) [33]	Known modifications	✗	✗	✓	Determination of base composition and localization by comparing mass-spectrometry results with expected RNase fragments
NGS-based methods	RNA deep-sequencing direct method		A-to-I [49]	✓	✓	✓	To be accompanied by DNA sequencing to distinguish editing events from SNPs
			Methylations [50]	✗	✗		Based on RT stops or missincorporations
	Nanopore RNA sequencing [51, 52]		m^6A, m^5C, A-to-I, Ψ and others	✓	✓		Based on the use of systematic base-calling 'errors' caused by the presence of RNA modifications. Software is still in development
	Indirect methods: chemical treatments	ICE-Seq [53, 54]	A-to-I	✓	✓		No need of DNA seq
		Bisulfite-Seq [55]	m^5C				
		Riboxi-Seq [56]	Nm				
		RiboMethSeq[57, 58]					
		Pseudo-Seq[59]	Ψ				
		Ψ-Seq					
		PSI-Seq[60]					
		HydraPsi-Seq [61]					
		SLAM-Seq[62]	s^4U				
		ARM-Seq[63]	m^1A, m^3C, m^1G				
		TRAC-Seq[64]	m^7G				
		AlkAniline-Seq[65]	m^7G, m^3C, D				
	Indirect methods: IP	miCLIP[66]	Methylation	✓	✓		
		m^6A-Seq[67]	m^6A				
		meRIP-Seq[68]					
		m^6A-LAIC-Seq[69]					
		Nm-Seq / 2OMe-Seq[70]	Nm				
		acRIP-Seq[71]	ac^4C				
		NAD capture-Seq[72]	5'-NAD cap				
Affinity gel electrophoresis	Mercury-sulfur affinity[73]		s^2U, s^4U	✗?	✗	✗	APM treatment (Acrylo-aminophenylmercuric chloride)
	Boronate affinity[74]		NAD- or FAD-modified RNAs	✓	✓	✗	APB treatment (Acryloylaminophenyl boronic acid); fast screening (easy and quick); quantification possible as per intensity of bands

Table 1. Summary of main techniques for the detection of RNA modifications.

3. Impact of RNA Modifications on Pathogenic Bacteria Stress Responses and Host Adaptation

3.1. rRNA Modifications

The ribosome is a powerful molecular machine and a huge ribonucleoprotein complex (2.3 MDa in bacteria), which performs the crucial task of translating the genetic information into proteins. The ribosome is also a ribozyme with its catalytic centers made by RNAs [75]. To carry out translation, the ribosome needs to balance between speed and accuracy and rRNA base modifications participate to fine tune ribosome structure and function. Indeed, *in vitro* reconstituted *E. coli* ribosomes lacking rRNA modifications were severely defective in catalytic activity [76] and the ribosome assembly was also altered (Ofengand's lab). Numerous studies showed that the loss of rRNA modifications perturbs the active site structures [77, 78], and causes altered rates and accuracy of translation [79]. In bacterial ribosomes, there are three major types of rRNA modifications: Ψ, methylation of the 2'-hydroxyl group of riboses (Nm), and methylation of base (mN) [80]. Even if specific role for several of these modifications was not yet attributed, they confer specific properties to the nucleotides. For instance, they can induce enhanced (Ψ) or decreased (D) base stacking, structure rigidity (Ψ and Nm) or flexibility (mN) to both single- and double-stranded regions with possible altered hydrogen-bonding [25, 81]. These modifications are clustered in highly conserved areas devoted to decoding, peptidyl transfer, binding sites of A- and P- tRNAs, the peptide exit tunnel, and inter-subunit bridges [82, 83](**Fig. 1A and 1B**).

Bacterial rRNA modifications have been investigated by Mass Spectrometry (MS), Reverse Transcriptase extension (RT), RNAseq, and structure analysis. Several high-resolution structures of 70S ribosomes have been achieved both by cryo-EM and X-ray studies. However, cryo-EM structures can be non-uniform in local resolution and confident assignment of modifications is often possible on their most structurally stable core. Assignment of 35 modifications on bacterial rRNAs was first obtained on the cryo-EM structure of *E. coli* 70S-EF-Tu-tRNA complex solved at 2.65-2.9 Å resolution [84]. This study provides clues on their roles in fine-tuning ribosome structure and function and in modulating the action of antibiotics. In this structure, the methyl group of nucleosides could be clearly visualized as extra densities, as well as the non-planar dihydrouridine at position 2449 of 23S rRNA, while Ψs were identified indirectly by polar residues within hydrogen-bonding distance of the N1 position. Besides, the rRNA modifications were unambiguously identified in the *T. thermophilus* and *E. coli* crystal structures at 2.3-2.5-Å resolution, respectively [85, 86]. More recently, sub-stoichiometric modified nucleotides, like m^7G527 and m^6A1519 of the 16S rRNA, could be assigned on the structure of *E. coli* 70S solved at 2 Å resolution, and some antibiotic resistance mechanisms could be proposed [82] (**Fig. 1A**). In the past three years, cryo-EM analyses of 70S [83] and 50S [87] from *S. aureus* allowed the placing of 10 rRNA modifications (**Fig. 1B**).

Because the literature about the functions of rRNA modifications is very rich, we have chosen specific examples in different bacteria, which illustrate the variety of their functional impact. For clarity, we refer to the *E. coli* numbering of the 16S and 23S rRNA sequences. In the decoding region of the small 30S subunit, several modified nucleotides contact tRNA or mRNA, or are close to positions known to be important for translation, contributing to the building of the decoding site. For example, the *E. coli* m^2G966 contacts the P-site tRNA through stacking with nucleotide at position 34 of the tRNA [88]. Particularly, they stabilize the binding of initiator fMet-$tRNA^{fMet}$ to the 30S pre-initiation complex prior to start codon recognition [89]. The correct folding of the 16S rRNA around the initiator tRNA helps to discriminate the initiator tRNA against other tRNAs. In this context, m^2G966, $m^{6}{}_{2}A1518$ and $m^{6}{}_{2}A1519$ monitor the characteristic presence of the three consecutive GC pairs of the anticodon stem of the initiator tRNA [90]. In addition, $m^4Cm1402$ and m^3U1498 contact the P-site mRNA codon and play a role in fine-tuning the shape and function of the P-site [82] to increase initiation decoding fidelity [91]. In *S. aureus*, the $m^4Cm1402$ modifications are important for infection since *rsmI* and *rsmH* genes encoding the two methylases of C1402 protect *S. aureus* from oxidative stress and restore translational fidelity [92].

On the large ribosomal subunit, *E. coli* Gm2251 and Um2552 are located in the P- and A-loops, respectively, to establish interactions with the CCA end of tRNAs in P- and A- sites. Gm2251 is conserved in all three kingdoms of life [93], whereas Um2552 is present in many bacteria except that in some Bacillus species, like *B. subtilis* and *B. stearothermophilus,* methylation at the neighboring G2553 was observed [94]. Absence of Um2552 modification (*rlmE*-deficient mutant) increases the flexibility of the nucleotides next to it, and induces 50S maturation delay, slower subunit association, and slower translocation rate [95]. Surprisingly, translation with unmethylated U2552 appears to be more accurate suggesting that a certain degree of recoding provided by methylation of this residue is important for cell physiology [96].

The ribosome and more generally the translation apparatus are main targets of antibacterial therapies [97-100]. However, bacteria are continuously evolving resistance mechanisms for antibiotics. Acquisition of additional rRNA modifications is one of the most direct marks of antibiotic resistance. For example, aminoglycosides target the 30S subunit to prevent translocation and A-site tRNA binding, and promotes miscoding (**Fig. 1C**), while macrolides bind to the nascent peptide exit tunnel on the 50S subunit to prevent peptide bond formation and translocation [101, 102] (**Fig. 1D**). Methylation of their rRNA target sites inhibits antibiotics binding [103]. Interestingly, the modification enzymes responsible for the resistance are often inducible and only synthetized when necessary for survival. For example, in *S. aureus* sub-inhibitory concentrations of the macrolide erythromycin (**Fig. 1D**) stall ribosomes on the leader peptide for the methylase (*ermC*) responsible for the dimethylation

of A2058 at the ribosomal peptide exit tunnel of the 50S subunit [104] (**Fig. 1D**). This pausing induces the transcript to form a structure in which the Shine and Dalgarno sequence for *ermC* is exposed, allowing translation of *ermC* [104]. ErmC induced-dimethylation of A2058 prevents erythromycin binding (**Fig. 1D**), but also results in inefficient translation of selected polypeptides [104]. It is interesting to note that, *S.* aureus strains bearing $m^{6}{}_{2}A2058$ are not only erythromycin-resistant, but can also better escape host immune system, avoiding recognition by specific Toll-like receptors [105]. Other mechanisms of modifications inducing resistance but compromising bacterial fitness involve methylations of G1405 and A1408 in 16S rRNA, which are required for aminoglycoside resistance in Gram-negative bacteria (**Fig. 1C**). In fact, these additional modifications interfere with the natural methylation at the neighboring C1407 residue ($m^{5}C1407$) and decrease translation accuracy [106]. Conversely, antibiotic resistance could also arise from the lack of modifications at naturally occurring sites. Indeed, mutation of the *ksgA* gene encoding methyltransferase, causes a defect of modifications at A1518 and A1519 in the 16S rRNA, and induces kasugamycin resistance [107] accompanied by assembly defects and a cold sensitive phenotype [108]. Similarly, loss of methylation at $m^{7}G527$, which is located near the mRNA decoding site has been shown to confer low-level streptomycin and neomycin resistance [109, 110].

Finally, induction of rRNA modifications has been reported to be a key step in the ribosome reactivation during resuscitation of persistence state [111]. Indeed, antibiotic stresses together with a myriad of other stresses, are sometimes inducing the differentiation of a subpopulation of cells, which become dormant and multi-stress tolerant (persisters) [112]. This transient phenotype, which does not involve genetic changes, can be reverted via different mechanisms to re-activate ribosomes [113-115]. For instance, it has been recently shown by single-cell studies, that in *E. coli* cells resuscitate and ribosome activity is resumed by the action of the RluD enzyme, which is responsible of 23S rRNA pseudouridine (5-ribosyl-uracil) modification at positions 1911, 1915, and 1917 [111].

3.1. tRNA Modifications

tRNAs are key molecules in translational process, their main purpose is to participate to protein synthesis by decoding the mRNA codons into the corresponding amino acids. They contain the largest number of modifications and the widest chemical diversity. Their modifications are known to improve tRNA decoding capacity, to decrease codon sensitivity, and to dictate codon choice and the maintenance of reading frame. Their localization concentrates in two hotspots - the anticodon loop and the tRNA core region, where the D- and TΨ -loops interact with each other (**Fig. 2**) (reviewed in [116, 117]).

Modifications in the tRNA core are important for the stability of tRNA structure and can contribute to temperature adaptation in thermophilic as well as in psychrophilic organisms [118]. Because they are involved in the tertiary interactions maintaining the L-shape, they are also expected to influence the binding of several proteins to the tRNA (i.e. EF-Tu, aminoacyl-tRNA synthetases, and anticodon modification enzymes) [119-121]. Different mutagenesis studies have demonstrated the role of these modifications in tRNA structure stabilization and their consequences on bacterial physiology during stress adaptation and on pathophysiology. The 2′-O methylation of Gm18, present on several tRNAs and common to all Gram-negative bacteria, is lacking in most Gram-positive species despite the presence of putative *trmH*-like genes. Methylation of the ribose stabilizes G18 in its C3′-endo form increasing its rigidity [122, 123] and promotes Gm18-Ψ55 base pairing (**Fig. 2**). The 5-methylation of U54 and the isomerization of U55 into Ψ55 enhance base stacking and stabilize the tRNA [124-126]. In the mesophilic *E. coli*, lack of the modification enzymes coded by the genes *trmH* (Gm18), *trmA* (m^5U54) and *truB* (Ψ55), reduces growth rate particularly at high temperature [127]. In the thermophilic *T. thermophilus*, adaptation to low temperature requires maintaining a sufficient flexibility of tRNAs. In this condition, methylation of the ribose of G18 is prevented but only if Ψ55 is present [128]. Moreover, the lack of some of these modifications induces changes in decoding and modulates frameshifting. In the pathogenic bacteria *Shigella flexneri*, Ψ55 is linked to the expression of several virulence factors, which are responsible of shigellosis, an intestinal infection causing diarrhea. Deletions of *trmH, trmA,* and *truB* genes in *S. flexneri* are associated with a reduction of the hemolytic activity and a decrease of the secretion system expression [127]. Furthermore, Gm18 is known to be responsible for TLR-7 dependent suppression of the immune response of dendritic cells, allowing a better tolerance of several enterobacteria by the host immune system [129-131].

The anticodon loop (ASL) is the other hotspot for modifications, which affect the geometry and physicochemical determinants governing the decoding process [132, 133]. The anticodon regions of all tRNAs bind to their cognate mRNA codons on the ribosome with similar affinities, despite diverse codon–anticodon pairings that should exhibit differences in basepairing strengths [134]. The modifications in the tRNA anticodon loop compensate for potential binding differences and ensures uniform affinities of all tRNAs to their cognate codons [135]. Perturbations of these modifications selectively alter the spectrum of proteins during adaptation via rare codon usage and translational frameshifting [136]. Specifically, modifications of nucleotide at position 37 and at the position 34 (wobble) have a strong impact on maintaining the reading frame [136, 137]. Modifications at positions 32 and 38, the first and last nucleotides of the loop, have also important consequences in modulating the affinity for specific codons, by inducing 32-38 basepairing and reducing the size of the loop [138]. This interaction is coordinated with the identity of codons. Strong GC-rich codon–anticodon

interactions are always balanced by a weaker 32–38 pairing and conversely, a weak AU-rich codon–anticodon interaction is coupled with a stronger 32–38 pairing [138]. Several studies have analyzed the link between modifications of anticodon loop residues and gene expression regulation. For example, the introduction of queuosine (Q) in the $tRNA^{Tyr}_{GUA}$, $tRNA^{Asn}_{GUU}$, $tRNA^{Asp}_{GUC}$ and $tRNA^{His}_{GUG}$ at the wobble position (G34) in Eukaryotes and Bacteria, permits efficient recognition of both NAC and NAU codons. This Q modification allows fine-tuning of translation and has been correlated with low-level translation of *Shigella* virulence factors, including the main transcriptional regulator VirF [139]. Its efficient translation depends on the presence of Q34 and 2-methylthio-N6-isopentenyladenosine (ms^2i^6A37) tRNA modifications. Deletion of either *tgt* (tRNA-guanine transglycosylase, for Q) or *miaA* (tRNA dimethylallyltransferase, for ms^2i^6A) genes leads to a less efficient synthesis of VirF in *S. flexneri* and reduces its pathogenicity [139]. In *E. coli*, it has been shown that ms^2i^6A is important for translation of RpoS, the general stress response alternative sigma factor, which is particularly rich in UUX-Leu codons over CUX-Leu codons [140]. Similarly, *S. flexneri virF* contains a high proportion of UUX-Leu codons [141]. Although the mechanism by which Q induces *virF* translation is not known, it is noticeable that putrescine or a combination of methionine and arginine metabolically related to putrescine, restore VirF expression of *S. flexneri tgt* mutant [142]. Since polyamine like putrescine can modulate translational fidelity and maintenance of reading frame [143, 144], it is possible that translation misreading of *virF* could occur in absence of Q.

Studies on U34 hypermodifications reveal the central role of wobble U modifications and associated enzymes in bacterial adaptation to environmental conditions and virulence in pathogens. Even if the precise mechanism remains unclear, in the absence of modifications, frameshift occurs resulting in the expression of alternate proteins [136, 145]. Deletion of *gidA* and *mnmE*, encoding two enzymes of the 5-methylaminomethyl-2-thiouridine (mnm^5s^2U34) modification pathway, was shown to significantly reduce the colonization of *Salmonella Typhimurium* in liver and spleen, accompanied by decreased invasion of epithelial cells and compromised ability to survive and replicate inside macrophages [146]. This effect can be explained in part by the fact that several colonization genes important for host cell invasion, including the T3SS genes *invAEG*, *spaPQ*, and *prgHJ* were downregulated in the attenuated mutants [147]. In addition, in this strains it has been also observed the repression of several other proteins as the oxidoreductase Ygh, and the thiol peroxidase Tpx, which promote the survival of *S. Typhimurium* under the stressful conditions experienced within host macrophages [148]. The modified nucleotide mnm^5s^2U34 is also important for virulence in other bacteria. In *Streptococcus* species, Gram-positive bacteria responsible for a wide range of infections from skin infection to sepsis, GidA/MnmE modification enzymes are essential for acid stress and high temperature adaptation [149], for pathogenicity [150], reduced ability of adhesion and invasion in

epithelial cells, and increased sensitivity to phagocytosis [151]. Transposon mutagenesis in GidA gene is leading to sensitivity to acidic conditions also in *Cronobacter sakazakii*, an opportunist pathogen causing neonatal meningitis, enterocolitis, septicemia, bloody diarrhea and brain abscesses, decreasing its ability to growth in host digestive system [152]. One of the best-characterized example of host adaptation via the induction of specific tRNA modification at U34 to selectively translate codon-biased mRNAs for persistence genes, has been described for *Mycobacterium bovis* [153]. When mycobacteria species infect host lungs, they are phagocytized by alveolar macrophages, which are unable to kill and digest them. Consequently, the bacteria multiply and promote the formation of granulomas, which are symptomatic of chronic infections. Human granulomas lacking endothelial and blood vessel are highly hypoxic [154], and mycobacteria enter a quiescent state in which cell replication is halted or slowed [155]. In this condition, DosR, the master regulator of hypoxic bacteriostasis, mediates the expression of approximately 50 genes necessary for dormancy survival [156]. Translation activation of DosR requires shifting from mo^5U, presents at U34 in $tRNA^{Thr}_{UGU}$ in aerobic conditions, to cmo^5U and $mcmo^5U$. This change of modification type, facilitates decoding of ACG codons, particularly abundant in *dosR* transcript [153]. The rationale for this decoding has been described by structural analysis [157]. The presence of cmo^5U34 induces a classical Watson-Crick base-pairing geometry involving the wobble position, which allows better stacking between U34 and purine 35, and as a consequence increases the stability of the codon-anticodon interaction.

In addition to wobble position, 2′-O-methylations of A, C, and U at position 32 by methyltransferases of the Trm family, have been shown to confer resistance to oxidative stress in *P. aeruginosa*, allowing its survival during infection [158]. Hypomethylation of the 2′-O-ribose moiety at position 32, linked to reduced catalase activity, perturbs codon-anticodon interaction and results in translation insufficiency and transcript misreading [159, 160]. Thiolation of cytidine at position 32 catalyzed by TtcA, a [Fe-S] cluster enzyme, has been shown to play a role in the response to oxidative stress during infections caused by *P aeruginosa* [161].

Finally, modifications of nucleotides in the variable loop have been shown to contribute to host adaptation. For example, m^7G46 catalyzed by tRNA guanine-N7-methyltransferase (*trmB*) is important for decoding efficiency of $tRNA^{AspGUC}$ and $tRNA^{Phe}_{GAA}$. In *P. aeruginosa*, loss of *trmB* has a strong negative effect on the translation of Phe- and Asp-enriched mRNAs, including those coding for the major peroxide detoxifying enzymes, the catalases KatA and KatB, resulting in oxidative stress-sensitive phenotype [162]. Using tRNA-seq and mass spectrometry performed on *Vibrio cholera* revealed specific modifications in various tRNAs that were not described in *E. coli* tRNAs [163]. These modifications include an acetylated acpU at either position 20 in the D-loop and at positions 46 or 47 in the variable loop. More interestingly, an editing process C-to- Ψ was for the first time identified at

position 32 of the anticodon loop of $tRNA^{Tyr}$. Although the physiological consequences of these specific features have to be defined, it is tempting to propose that RNA modifications contribute to the speciation of the bacteria and to the adaption of the organism to its specific niches.

3.1. sRNA Modifications

Small trans-acting regulatory RNAs (sRNAs) belong to a very heterogeneous class of RNAs regulating several processes including virulence gene expression, stress adaptation, and quorum sensing [164]. They exert their functions through specific interactions with diverse targets such as mRNAs, sRNAs, tRNA precursors, proteins or even with the ribosome [165]. The sRNAs are very different in length, sequence, structure and regulate gene expression using various mechanisms. So far only few examples of RNA modifications have been reported in bacterial sRNAs [166].

The best examples of regulatory RNAs, where modifications have been identified, are tmRNA and Y RNA, both mimicking the tRNA structure (**Fig. 3**). The tmRNA together with the small protein B (SmpB) is involved in trans-translation, the major and ubiquitous ribosome rescue system in bacteria [4]. This mechanism is taking place when ribosomes and tRNAs are stalled on problematic and often truncated mRNAs, which can lead to reduced translation [167]. Ribosome halting resulted from i) chemical mRNA damages produced by environmental stresses, ii) rare codons or problematic polypeptide stretches, iii) drugs inducing translational misreading, non-programmed frameshifting, or stop codons readthrough, and from iv) spurious RNase activity or cleavage of the mRNA in the A-site by RelE in response to starvation stress [168-172]. In these situations, trans-translation operates to liberate the ribosome, and simultaneously to degrade the nascent truncated peptide [4]. A vacant ribosomal A-site is the signal recognized by tmRNA/SmpB complex, which is delivered to the ribosome by the translation elongation factor EF-Tu. The tmRNA is characterized by two functional domains embedded into a conserved and complex structure, which are a tRNA-like domain (TLD) specifically aminoacylated with alanine and a mRNA-like domain (MLD) encoding a peptide tag targeting proteolysis [173, 174]. TLD presents a typical tRNA TΨ-loop with two Ψs and one m^5U [175]. These modifications most probably enhance tRNA structural mimicry and its use in translation as a canonical tRNA (**Fig. 3**). Most probably that m^5U54 in tmRNA is introduced by the SAM-dependent methyltransferase TrmA as it is for the tRNAs [176]. Although tmRNA has been shown to be essential for the expression of virulence factors during *S. Typhimurium* infection [177], to our knowledge no studies have been conducted to establish the role of its modifications in bacterial adaptation or infection.

The non-coding Y RNAs are present in both eukaryotes and in several bacteria including some pathogens [178]. Bacterial Y RNA, known as YrlA (Y RNA-like A) RNA, is a modular RNA of variable

length (between 90 and 150 nucleotides) characterized by a large stem involving pairings between nucleotides at the 5′ and 3′ ends (**Fig. 3**) and a tRNA-like domain [179]. This domain shows high similarities to the D, TΨ and acceptor arms of tRNA (**Fig. 3**). Due to this structure similarity, YrlA is a substrate for two tRNA modification enzymes DusA and TruB, which introduce a dihydrouridine and a Ψ in the D and TΨ loops, respectively [180]. The basal stem of YrlA tethers the monomeric ring Rsr protein similar to eukaryotic Ro60 protein, while the effector tRNA-like domain binds the ring-shaped 3′ to 5′ exoribonuclease polynucleotide phosphorylase (PNPase), forming a double-ringed RNA degradation machine called RYPER [179]. Although the functions and mechanism of RYPER are still under investigation, Rsr and YrlA have been shown to alter PNPase substrate specificity to preferentially direct the degradation of structured RNAs (including rRNAs) [179, 181]. By altering the levels of specific RNA populations, RYPER has been proposed to be involved in stress responses, such as UV irradiation or prolonged stationary phase [182, 183]. In *Salmonella enterica*, expression of YrlA appears to be confined to certain infection stages [184]. Surprisingly, it was reported that lupus autoimmunity might be triggered and sustained by commensal bacteria expressing Rsr RNPs [185]. Noteworthy, in some bacteria including *S. Typhimurium*, *rsr* and Y RNA genes are located within an "RNA repair" operon together with the *rtcA* encoding RNA cyclase and *rtcB* encoding RNA ligase [179], which transcription is activated by tRNA fragments resulting from the SOS response to DNA damage [186]. tRNA fragments also accumulate when tRNAs are hypomodified, such as in *ΔtruA* strain where Ψ at positions 38, 39, and 40 in the anticodon arm of some tRNAs cannot be introduced anymore [187]. Since tRNA fragments are both natural substrates of PNPase and of RtcB religation, it is possible that assembly of RYPER protects them from degradation and that the expression of RtcB could restore tRNAs from halves and translation [186]. Interestingly, in *E. coli* RtcB re-ligates a 16S rRNA 3′ fragment containing the anti-Shine-Dalgarno sequence cleaved by the MazF toxin [188]. This indicates a tight link between RNA modification levels, translation regulation, and RNA metabolism in response to stress.

Another example of sRNA modification in pathogenic bacteria derives from a transcriptome-wide profiling of m^6A distribution in *Pseudomonas aeruginosa*. Methylation sites were found present in two major sRNAs, RsmY and RsmZ [189], which sequester the regulatory protein RsmA to control its activity which is associated with acute and chronic virulence phenotypes [12, 190]. The involvement of these modifications in the regulatory mechanisms of RsmY/Z has not been studied yet.

Recently, one of the best characterized sRNA in *S. aureus*, an opportunistic pathogen causing a large variety of infections, has been shown to contain at its 5′end a peculiar modification which is co-transcriptionally introduced [191]. The expression of RNAIII is under the control of a two-component system, which senses bacterial cell density, to orchestrate the regulation of virulence gene expression

[192, 193]. This dual RNA codes for the cytotoxic δ-hemolysin peptide, while its 5′ and 3′ UTRs act as antisense RNA to regulate at the post-transcriptional level the expression of virulence genes associated with infectious diseases [193]. Hence, through basepairing interactions with its target mRNAs, it represses several cell wall associated proteins involved in adhesion and tissue colonization, and the transcriptional repressor of toxins Rot while it activates directly or indirectly the synthesis of many secreted proteins and toxins required for infection dissemination. A new RNAseq based approach has been developed to detect the incorporation of NAD, the nicotinamide-adenine dinucleotide, at the 5 ends of RNA transcripts [194]. This study found only few *S. aureus* transcripts containing this 5′ cap, including RNAIII. In Gram-negative bacteria, NAD has been reported to have a stabilization effect protecting the RNA from the 5′ processing enzyme RppH, which produces monophosphate at the end of RNAs that are substrates of RNase E [194]. In *Bacillus subtilis*, NAD protects RNAs from the exonucleolytic activity of RNase J1/J2 [195]. In *S. aureus*, the presence of NAD in RNAIII does not induce its stabilization nor affects its structure, but it has important consequences on pathophysiology. By a yet unknown mechanism, the NAD modified RNAIII leads to a decreased expression of δ-hemolysin and reduced cytotoxicity [191].

3.1. mRNA Modifications

Besides the classical 5′-cap m^7G modification of eukaryotic mRNAs, other modifications have been described, including the 6-methyladenosine (m^6A), the 5-methylcytosine (m^5C), inosine (I) derived from adenine deamination and pseudouridine (Ψ). These modifications, which are present within 5′- and 3′-untranslated regions (UTRs) and the coding sequences of mRNAs, contribute to fine tune gene regulation [196-202]. In bacteria, the presence and the roles of mRNA modifications is relatively unexploited in pathogenic bacteria. In bacterial mRNAs, the presence of non-canonical 5′ ends has recently been reported for a subset of mRNAs. As described above, co-transcriptionally introduced 5′ NAD cap has also been detected in some *E. coli* mRNAs and is thought to modulate mRNA stability and translation efficiency [194, 203]. Recently, NAD cap has been found in mRNAs expressed in *B. subtilis* spores, a dormant state developed in response to different stresses [204]. Its role in these mRNAs remains to be analyzed. Other studies have shown additional types of 5′ capping directly incorporated into mRNAs during transcription initiation, which might increase mRNA stability. For example, dinucleoside tetraphosphates, very often Np4A, have been reported in *E. coli* [205]. Interestingly, the incorporation of such dinucleosides depends on their cellular concentration, which increases in some stress conditions such as heat shock [206] and oxidative stress [207].

Bacterial mRNAs can also contain post-transcriptional modifications. In *E.* coli, Ψs have been detected in some mRNAs. They can be located at specific codons and as a consequence they alter

translation speed or mRNA decoding [208], and at stop codons to induce nonsense suppression [209, 210]. Ψs have been proposed to influence the kinetics of RNase E-directed degradation in Gram-negative bacteria [211]. Another abundant mRNA modification is m^6A, which has been detected in genes involved in energy metabolism in Gram-negative bacteria, including pathogenic *P. aeruginosa* [189]. Very recently, it has been shown that m^6A reduces both sense and stop codon reading accuracy [212, 213]. The molecular explanation for this decoding perturbation could be due to the formation of less stable codon-anticodon interactions with cognate tRNAs [212]. Indeed, when compared with unmodified A, m^6A forms less stable basepairing with uridine (U) and destabilizes local RNA structures and short duplexes [214, 215]. It remains to be studied whether these modifications in mRNAs vary significantly in response to metabolic changes or stress.

Adenosine deamination is most probably the major modification in mRNAs, which can directly influence the activity of the synthesized protein. Adenosine-to-inosine (A-to-I) mRNA editing is catalyzed by the tRNA adenosine deaminase enzyme TadA, which recognizes stem-loop structures resembling the anticodon arm of $tRNA^{Arg}$ [216]. Because inosine (I) is recognized as guanosine (G) by the translational machinery, A-to-I editing expands the decoding rules resulting in protein diversification. In *E. coli* and in the two pathogenic bacteria *Klebsiella pneumonia* and *Yersinia enterocolitica*, recoding tyrosine (UAC) to cysteine (UGC) has been reported in mRNAs encoding self-killing toxins like HokB, increasing its toxicity [216]. HokB induces cellular growth arrest in response to starvation as a function of cellular density, via membrane depolarization. By doing so, it was found to mediate antibiotic tolerance leading to persistence [217]. Since bacteria persistence is characterized by the existence of sub-populations of bacteria that are tolerant to an antibiotic treatment with a fitness cost [218], the heterogeneous RNA editing levels of *hokB* mRNA could promote non-genetic cell heterogeneity [219].

3.2. Figures and Table

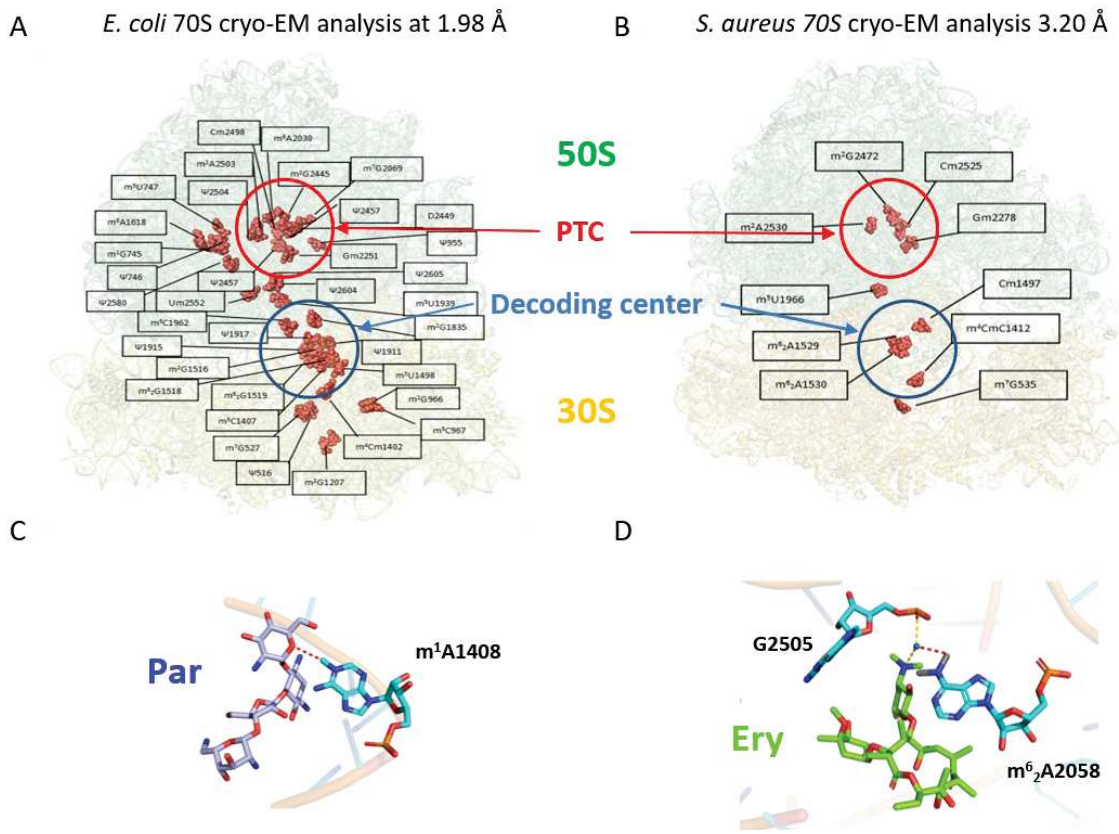

Figure 1. Natural ribosomal RNA modifications and additionally modification implicated in antibiotic resistance mechanisms as indicated by structural analyses. (**A**) Cryo-EM structure at 1.98 Å of *E. coli* 70S ribosome (pdb file 7K00). 11 and 24 RNA modifications (red spheres) could be visualized in the 30S (16S rRNA) and 50S (23S rRNA) subunits, respectively [82]. (**B**) Cryo-EM structure at 3.20 Å of *S. aureus* 70S ribosome (pdb file 6YEF). The limited resolution allowed the visualization of 4 RNA modifications in the 16S rRNA and 6 in 23S rRNA [83]. PTC, Peptidyl Transferase Center on the large 50S subunit. (**C**) Mechanism of aminoglycoside (Par, paromomycin) resistance induced by methylation of A1408 (pdb file 5ZEJ [220]). The presence of the methyl group directly perturbs antibiotic interaction. (**D**) Mechanism of macrolide (Ery, erythromycin) resistance induced by dimethylation of A2058 (pdb file 6XHV [221]). The two methyl groups on A2058 prevent the coordination of a water molecule with G2505, which stabilizes erythromycin binding.

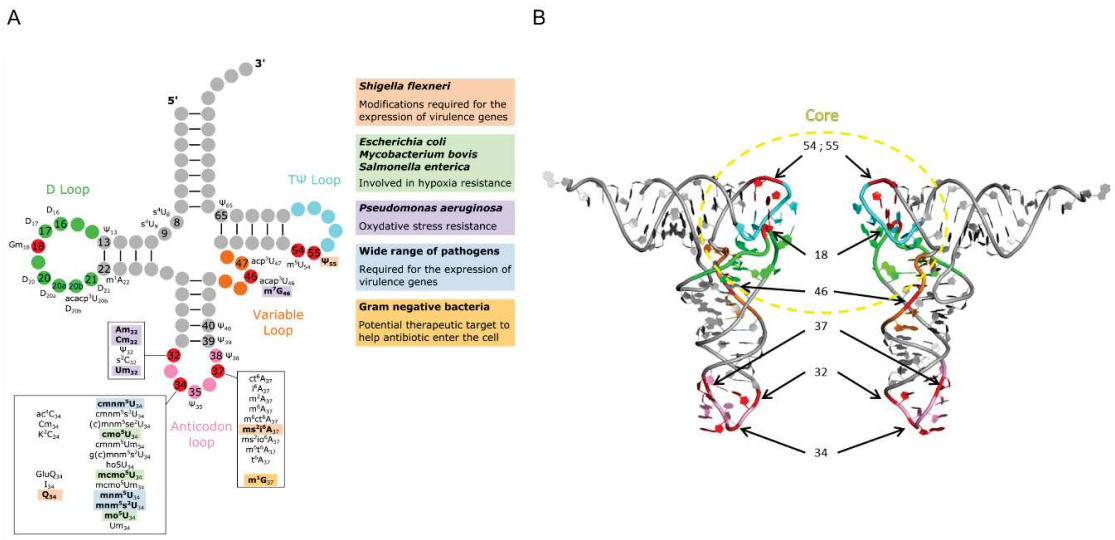

Figure 2. Pathogenic bacteria tRNA modifications involved in virulence and stress adaptation. (**A**) Secondary structure of tRNA. The nucleotides in the loops, where the majority of modifications accumulate, are colored as follow: D loop in green, anticodon loop in pink, variable loop in orange, and TΨ loop in light blue. The nucleotides for which the modifications are associated with a specific phenotype specified in the figure are in red. (**B**) Tertiary L-shape structure of tRNA. The 3D model corresponded to the crystal structure of *Saccharomyces cerevisiae* $tRNA^{Phe}{}_{GAA}$ (pdb file 1EHZ [222]). The same color code is used for the secondary (A) and tertiary (B) tRNA structures. The core domain of the tRNA comprises the D-, TΨ- and variable loops.

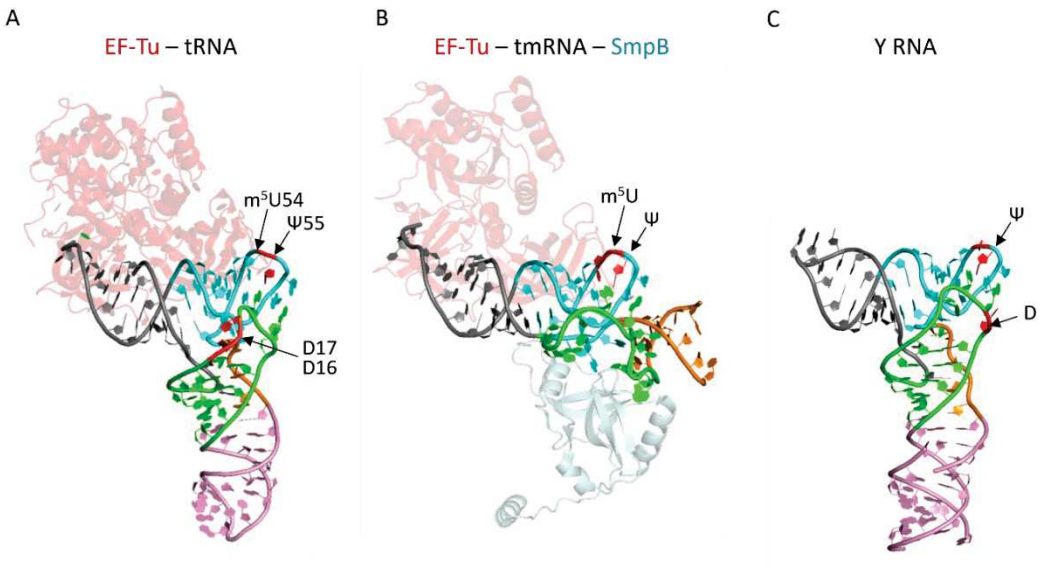

Figure 3. The structures of tmRNA and Y RNA mimic part of the tRNA structure. (**A**) The structure of EF-Tu-tRNA^{Phe} complex (with GDPNP, GTP analog) from *Thermus aquaticus* (pdb file 1TTT [223]). Each domain of the tRNA is colored: acceptor am in grey, TY-arm in light blue, the variable region in orange, the D-arm in green, and the anticodon-arm in pink. EF-Tu structure is represented in light pink. (**B**) The structure of the tmRNA fragment in complex with EF-Tu (with GDP and kirromycin antibiotic, in light pink) and SmpB (in light grey) from *Thermus thermophilus* (pdb file 4V8Q [224]). The regions of tmRNA mimicking tRNA are shown with the same color code as for the tRNA. (**C**) *Salmonella Typhimurium* Y RNA (YrlA, pdb file 6CU1 [225]). The regions of YrlA mimicking tRNA are shown with the same color code as for the tRNA.

4. Conclusion and perspectives

The review presented several examples, which unveiled the diversity of functions of RNA modifications in translation and RNA degradation in bacterial pathogens. Because technologies are constantly improving, it is expected that the whole set of modifications will be mapped in RNA molecules as well as their quantifications. This will be the prerequisite to better study their dynamics upon stress or during bacterial infection. Further works correlating the modifications with the characterization of their protein co-factors (referred as writers, readers, and erasers) will be another step necessary to get an in-depth overview of their functions and the physiological consequences on bacterial pathogens. Many questions still remain to be addressed: what is the extent of chemical modifications diversity and complexity among evolutionary distant bacteria? Are there specific classes of bacterial sRNAs and mRNAs that could be modified extensively as it is for tRNAs and rRNAs? What are the consequences of RNA modification defects on bacterial physiology and pathogenesis? Some of the data suggested that some tRNA modifications are species-specific. Hence, it is expected that modifications might contain some metabolites issued from specific metabolic pathways resulting from the bacterial adaption to its ecological niches. Meanwhile during the infection process, the pathogens have to face metabolic burden and should counteract the host defenses mechanisms. It would not be so surprising that some of the modifications might be acquired or disrupted during the infection process with consequences on the bacterial proteome. The functional studies of the modification enzymes might also led to biotechnological applications, to design gene reprogramming or new tools for RNA studies, or to select novel anti-microbial strategies. Many of these studies will require the development of more simple technologies, such as the direct RNA sequencing methodologies, to facilitate the mapping and the discovery of RNA modifications among bacterial species. Although many studies have been done on tRNA and rRNA modifications, we are still far to fully appreciate the impact of modifications on RNA functions. We are only at the beginning of the tip of the iceberg.

Author Contributions: All authors have contributed to the review, searching the literature, writing the text and preparing the figures. All authors have read and agreed to the published version of the manuscript.

Funding: This work was supported by the Centre National de la Recherche Scientifique (CNRS). This work of the Interdisciplinary Thematic Institute IMCBio, as part of the ITI 2021-2028 program of the University of Strasbourg, CNRS and Inserm, was supported by IdEx Unistra (ANR-10-IDEX-0002) and by SFRI-STRAT'US project, and

EUR IMCBio (IMCBio ANR-17-EURE-0023) under the framework of the French Investments for the Future Program.

Acknowledgments:

Conflicts of Interest: The authors declare no conflict of interest.

References

1.Papon, N. and A.M. Stock, Curr Biol, 2019. 29(15): p. R724-R725.
2.Beier, D. and R. Gross, Curr Opin Microbiol, 2006. 9(2): p. 143-52.
3.Samatova, E., et al., Front Microbiol, 2020. 11: p. 619430.
4.Müller, C., C. Crowe-McAuliffe, and D.N. Wilson, Front Microbiol, 2021. 12: p. 652980.
5.Duval, M., et al., Biochimie, 2015. 114: p. 18-29.
6.Tollerson, R., 2nd and M. Ibba, J Biol Chem, 2020. 295(30): p. 10434-10445.
7.Loh, E., et al., Microbiol Spectr, 2018. 6(2).
8.Ignatova, Z. and F. Narberhaus, Curr Opin Microbiol, 2017. 36: p. 14-19.
9.Giuliodori, A.M., et al., Mol Cell, 2010. 37(1): p. 21-33.
10.Geissmann, T., S. Marzi, and P. Romby, RNA Biol, 2009. 6(2): p. 153-60.
11.Marzi, S., et al., Biol Chem, 2008. 389(5): p. 585-98.
12.Pourciau, C., et al., Front Microbiol, 2020. 11: p. 601352.
13.Quax, T.E., et al., Mol Cell, 2015. 59(2): p. 149-61.
14.Sauert, M., H. Temmel, and I. Moll, Biochimie, 2015. 114: p. 39-47.
15.Kurylo, C.M., et al., Cell Rep, 2018. 25(1): p. 236-248 e6.
16.Grosjean, H., Nucleic Acids Are Not Boring Long Polymers of Only Four Types of Nucleotides: A Guided Tour, in DNA and RNA Modification Enzymes: Structure, Mechanism, Function and Evolution, H. Grosjean, Editor. 2009, Landes Bioscience: Austin. p. 1-18.
17.Boccaletto, P., et al., Nucleic Acids Research, 2017. 46(D1): p. D303-D307.
18.Shetty, S. and U. Varshney, J Biol Chem, 2020. 296.
19.Frye, M., et al., Nat Rev Genet, 2016. 17(6): p. 365-72.
20.Motorin, Y. and M. Helm, Biochemistry, 2010. 49(24): p. 4934-44.
21.Davis, D.R., Biophysical and Conformational Properties of Modified Nucleosides in RNA (Nuclear Magnetic Resonance Studies), in Modification and Editing of RNA. 1998. p. 85-102.
22.Yokoyama, S., K. Watanabe, and T. Miyazawa, Adv Biophys, 1987. 23: p. 115-47.
23.Dalluge, J.J., et al., Nucleic Acids Res, 1996. 24(6): p. 1073-9.
24.Song, Q., et al., Structural Chemistry, 2013. 24(1): p. 55-65.
25.Charette, M. and M.W. Gray, IUBMB Life, 2000. 49(5): p. 341-51.
26.Yue, Y., J. Liu, and C. He, Genes Dev, 2015. 29(13): p. 1343-55.
27.Meyer, K.D. and S.R. Jaffrey, Nat Rev Mol Cell Biol, 2014. 15(5): p. 313-26.
28.Thuring, K., et al., Methods, 2016. 107: p. 48-56.
29.Edmonds, C.G., et al., J Bacteriol, 1991. 173(10): p. 3138-48.
30.Pomerantz, S.C. and J.A. McCloskey, Methods Enzymol, 1990. 193: p. 796-824.
31.Russell, S.P. and P.A. Limbach, J Chromatogr B Analyt Technol Biomed Life Sci, 2013. 923-924: p. 74-82.
32.Pomerantz, S.C., J.A. Kowalak, and J.A. McCloskey, J Am Soc Mass Spectrom, 1993. 4(3): p. 204-9.
33.Kowalak, J.A., et al., Nucleic Acids Res, 1993. 21(19): p. 4577-85.

34.Stolz, A., et al., ELECTROPHORESIS, 2019. 40(1): p. 79-112.
35.Lechner, A., et al., Anal Chem, 2020. 92(10): p. 7363-7370.
36.Addepalli, B. and P.A. Limbach, J Am Soc Mass Spectrom, 2011. 22(8): p. 1363-72.
37.Ho, N.W. and P.T. Gilham, Biochemistry, 1971. 10(20): p. 3651-7.
38.Raska, C.S., et al., J Am Soc Mass Spectrom, 2002. 13(9): p. 1034-41.
39.Yamauchi, Y., et al., Nucleic Acids Res, 2016. 44(6): p. e59.
40.Anreiter, I., et al., Trends Biotechnol, 2021. 39(1): p. 72-89.
41.Lahens, N.F., et al., Genome Biol, 2014. 15(6): p. R86.
42.Motorin, Y. and V. Marchand, Genes (Basel), 2021. 12(2).
43.Begik, O., et al., Nat Biotechnol, 2021.
44.Gao, Y., et al., Genome Biol, 2021. 22(1): p. 22.
45.Ramasamy, S., et al., bioRxiv, 2021: p. 2020.05.19.105338.
46.Begik, O., et al., bioRxiv, 2021: p. 2020.07.06.189969.
47.Paulines, M.J. and P.A. Limbach, Methods Mol Biol, 2017. 1562: p. 19-32.
48.Taoka, M., et al., Nucleic Acids Res, 2015. 43(18): p. e115.
49.Bahn, J.H., et al., Genome Res, 2012. 22(1): p. 142-50.
50.Vandivier, L.E., Z.D. Anderson, and B.D. Gregory, Methods Mol Biol, 2019. 1870: p. 51-67.
51.Garalde, D.R., et al., Nat Methods, 2018. 15(3): p. 201-206.
52.Workman, R.E., et al., Nat Methods, 2019. 16(12): p. 1297-1305.
53.Sakurai, M., et al., Genome Res, 2014. 24(3): p. 522-34.
54.Suzuki, T., et al., Nat Protoc, 2015. 10(5): p. 715-32.
55.Schaefer, M., et al., Nucleic Acids Res, 2009. 37(2): p. e12.
56.Zhu, Y., S.P. Pirnie, and G.G. Carmichael, RNA, 2017. 23(8): p. 1303-1314.
57.Marchand, V., et al., Nucleic Acids Res, 2016. 44(16): p. e135.
58.Ayadi, L., Y. Motorin, and V. Marchand, Methods Mol Biol, 2018. 1649: p. 29-48.
59.Carlile, T.M., et al., Nature, 2014. 515(7525): p. 143-6.
60.Schwartz, S., et al., Cell, 2014. 159(1): p. 148-162.
61.Marchand, V., et al., Nucleic Acids Res, 2020. 48(19): p. e110.
62.Herzog, V.A., et al., Nat Methods, 2017. 14(12): p. 1198-1204.
63.Cozen, A.E., et al., Nat Methods, 2015. 12(9): p. 879-84.
64.Lin, S., et al., Nat Protoc, 2019. 14(11): p. 3220-3242.
65.Marchand, V., et al., Angew Chem Int Ed Engl, 2018. 57(51): p. 16785-16790.
66.Hussain, S., et al., Cell Rep, 2013. 4(2): p. 255-61.
67.Dominissini, D., et al., Nature, 2012. 485(7397): p. 201-6.
68.Meyer, K.D., et al., Cell, 2012. 149(7): p. 1635-46.
69.Molinie, B., et al., Nat Methods, 2016. 13(8): p. 692-8.
70.Dai, Q., et al., Nat Methods, 2017. 14(7): p. 695-698.
71.Arango, D., et al., Cell, 2018. 175(7): p. 1872-1886 e24.
72.Winz, M.L., et al., Nat Protoc, 2017. 12(1): p. 122-149.
73.Igloi, G.L., Biochemistry, 1988. 27(10): p. 3842-9.
74.Nübel, G., F.A. Sorgenfrei, and A. Jäschke, Methods, 2017. 117: p. 14-20.
75.Cech, T.R., Science, 2000. 289(5481): p. 878-9.
76.Baxter-Roshek, J.L., A.N. Petrov, and J.D. Dinman, PLoS One, 2007. 2(1): p. e174.
77.Demirci, H., et al., RNA, 2010. 16(12): p. 2319-24.
78.Desaulniers, J.P., et al., Org Biomol Chem, 2008. 6(21): p. 3892-5.
79.Liang, X.H., Q. Liu, and M.J. Fournier, Mol Cell, 2007. 28(6): p. 965-77.
80.Decatur, W.A. and M.J. Fournier, Trends Biochem Sci, 2002. 27(7): p. 344-51.
81.Arnez, J.G. and T.A. Steitz, Biochemistry, 1994. 33(24): p. 7560-7.
82.Watson, Z.L., et al., Elife, 2020. 9.
83.Golubev, A., et al., FEBS Lett, 2020. 594(21): p. 3551-3567.

84.Fischer, N., et al., Nature, 2015. 520(7548): p. 567-70.
85.Polikanov, Y.S., et al., Nat Struct Mol Biol, 2015. 22(4): p. 342-344.
86.Noeske, J., et al., Nat Struct Mol Biol, 2015. 22(4): p. 336-41.
87.Halfon, Y., et al., Sci Rep, 2019. 9(1): p. 11460.
88.Jenner, L.B., et al., Nat Struct Mol Biol, 2010. 17(5): p. 555-60.
89.Burakovsky, D.E., et al., Nucleic Acids Res, 2012. 40(16): p. 7885-95.
90.Das, G., et al., EMBO J, 2008. 27(6): p. 840-51.
91.Kimura, S. and T. Suzuki, Nucleic Acids Res, 2010. 38(4): p. 1341-52.
92.Kyuma, T., et al., FEBS J, 2015. 282(13): p. 2570-84.
93.Sergeeva, O.V., A.A. Bogdanov, and P.V. Sergiev, Biochimie, 2015. 117: p. 110-8.
94.Hansen, M.A., et al., RNA, 2002. 8(2): p. 202-13.
95.Wang, W., et al., Proc Natl Acad Sci U S A, 2020. 117(27): p. 15609-15619.
96.Widerak, M., et al., Gene, 2005. 347(1): p. 109-14.
97.Francklyn, C.S. and P. Mullen, J Biol Chem, 2019. 294(14): p. 5365-5385.
98.Ho, J.M., et al., RNA Biol, 2018. 15(4-5): p. 667-677.
99.Lin, J., et al., Annu Rev Biochem, 2018. 87: p. 451-478.
100.Wilson, D.N., Nat Rev Microbiol, 2014. 12(1): p. 35-48.
101.Doi, Y., J.I. Wachino, and Y. Arakawa, Infect Dis Clin North Am, 2016. 30(2): p. 523-537.
102.Vázquez-Laslop, N. and A.S. Mankin, Trends Biochem Sci, 2018. 43(9): p. 668-684.
103.Gupta, P., et al., Nat Commun, 2013. 4: p. 1984.
104.Arenz, S., et al., Mol Cell, 2014. 56(3): p. 446-52.
105.Oldenburg, M., et al., Science, 2012. 337(6098): p. 1111-5.
106.Lioy, V.S., et al., RNA, 2014. 20(3): p. 382-91.
107.Helser, T.L., J.E. Davies, and J.E. Dahlberg, Nat New Biol, 1972. 235(53): p. 6-9.
108.Sharma, H. and B. Anand, Nucleic Acids Res, 2019. 47(21): p. 11368-11386.
109.Okamoto, S., et al., Mol Microbiol, 2007. 63(4): p. 1096-106.
110.Mikheil, D.M., et al., J Antibiot (Tokyo), 2012. 65(4): p. 185-92.
111.Gutgsell, N.S., M.P. Deutscher, and J. Ofengand, RNA, 2005. 11(7): p. 1141-52.
112.Van den Bergh, B., M. Fauvart, and J. Michiels, FEMS Microbiol Rev, 2017. 41(3): p. 219-251.
113.Kim, J.S., et al., Environ Microbiol, 2018. 20(6): p. 2085-2098.
114.Yamasaki, R., et al., iScience, 2020. 23(1): p. 100792.
115.Wood, T.K., S. Song, and R. Yamasaki, J Microbiol, 2019. 57(3): p. 213-219.
116.Helm, M. and J.D. Alfonzo, Chem Biol, 2014. 21(2): p. 174-85.
117.Jackman, J.E. and J.D. Alfonzo, Wiley Interdiscip Rev RNA, 2013. 4(1): p. 35-48.
118.Lorenz, C., C.E. Lunse, and M. Morl, Biomolecules, 2017. 7(2).
119.Eargle, J., et al., J Mol Biol, 2008. 377(5): p. 1382-405.
120.Zhang, J. and A.R. Ferre-D'Amare, Life (Basel), 2016. 6(1).
121.Giege, R. and M. Springer, EcoSal Plus, 2016. 7(1).
122.Kawai, G., et al., Nucleic Acids Symp Ser, 1991(25): p. 49-50.
123.Kawai, G., et al., Biochemistry, 1992. 31(4): p. 1040-6.
124.Davanloo, P., et al., Nucleic Acids Res, 1979. 6(4): p. 1571-81.
125.Davis, D.R., Nucleic Acids Res, 1995. 23(24): p. 5020-6.
126.Wang, S. and E.T. Kool, Biochemistry, 1995. 34(12): p. 4125-32.
127.Urbonavicius, J., J.M. Durand, and G.R. Björk, J Bacteriol, 2002. 184(19): p. 5348-57.
128.Ishida, K., et al., Nucleic Acids Res, 2011. 39(6): p. 2304-18.
129.Gehrig, S., et al., J Exp Med, 2012. 209(2): p. 225-33.
130.Jockel, S., et al., J Exp Med, 2012. 209(2): p. 235-41.
131.Rimbach, K., et al., J Innate Immun, 2015. 7(5): p. 482-93.
132.Grosjean, H. and E. Westhof, Nucleic Acids Res, 2016. 44(17): p. 8020-40.
133.Rozov, A., et al., Trends Biochem Sci, 2016. 41(9): p. 798-814.

134.Fahlman, R.P., T. Dale, and O.C. Uhlenbeck, Mol Cell, 2004. 16(5): p. 799-805.
135.Gromadski, K.B., T. Daviter, and M.V. Rodnina, Mol Cell, 2006. 21(3): p. 369-77.
136.Gustilo, E.M., F.A. Vendeix, and P.F. Agris, Curr Opin Microbiol, 2008. 11(2): p. 134-40.
137.Agris, P.F., F.A. Vendeix, and W.D. Graham, J Mol Biol, 2007. 366(1): p. 1-13.
138.Olejniczak, M. and O.C. Uhlenbeck, Biochimie, 2006. 88(8): p. 943-50.
139.Durand, J.M., et al., Mol Microbiol, 2000. 35(4): p. 924-35.
140.Aubee, J.I., M. Olu, and K.M. Thompson, RNA, 2016. 22(5): p. 729-42.
141.Thompson, K.M. and S. Gottesman, J Bacteriol, 2014. 196(4): p. 754-61.
142.Durand, J.M. and G.R. Björk, Mol Microbiol, 2003. 47(2): p. 519-27.
143.Jelenc, P.C. and C.G. Kurland, Proc Natl Acad Sci U S A, 1979. 76(7): p. 3174-8.
144.Matsufuji, S., et al., Cell, 1995. 80(1): p. 51-60.
145.Bregeon, D., et al., Genes Dev, 2001. 15(17): p. 2295-306.
146.Shippy, D.C., et al., Microb Pathog, 2013. 57: p. 1-9.
147.Shippy, D.C. and A.A. Fadl, Int J Mol Sci, 2014. 15(10): p. 18267-80.
148.Shippy, D.C., et al., Microb Pathog, 2011. 50(6): p. 303-13.
149.Li, D., et al., Appl Environ Microbiol, 2014. 80(1): p. 97-103.
150.Gao, T., et al., Front Cell Infect Microbiol, 2019. 9: p. 173.
151.Gao, T., et al., Front Cell Infect Microbiol, 2016. 6: p. 44.
152.Alvarez-Ordóñez, A., et al., Int J Food Microbiol, 2014. 178: p. 21-8.
153.Chionh, Y.H., et al., Nat Commun, 2016. 7: p. 13302.
154.Tsai, M.C., et al., Cell Microbiol, 2006. 8(2): p. 218-32.
155.Chao, M.C. and E.J. Rubin, Annu Rev Microbiol, 2010. 64: p. 293-311.
156.Voskuil, M.I., K.C. Visconti, and G.K. Schoolnik, Tuberculosis (Edinb), 2004. 84(3-4): p. 218-27.
157.Weixlbaumer, A., et al., Nat Struct Mol Biol, 2007. 14(6): p. 498-502.
158.Jaroensuk, J., et al., Nucleic Acids Res, 2016. 44(22): p. 10834-10848.
159.Pintard, L., et al., EMBO J, 2002. 21(7): p. 1811-20.
160.Guy, M.P., et al., RNA, 2012. 18(10): p. 1921-33.
161.Romsang, A., et al., Sci Rep, 2018. 8(1): p. 11882.
162.Thongdee, N., et al., Nucleic Acids Res, 2019. 47(17): p. 9271-9281.
163.Kimura, S., P.C. Dedon, and M.K. Waldor, Nat Chem Biol, 2020. 16(9): p. 964-972.
164.Desgranges, E., et al., Microbiol Spectr, 2019. 7(2).
165.Dutta, T. and S. Srivastava, Gene, 2018. 656: p. 60-72.
166.Felden, B. and D. Gilot, Genes (Basel), 2018. 10(1).
167.Moore, S.D. and R.T. Sauer, Mol Microbiol, 2005. 58(2): p. 456-66.
168.Abo, T., et al., Genes Cells, 2002. 7(7): p. 629-38.
169.Ueda, K., et al., Genes Cells, 2002. 7(5): p. 509-19.
170.Bandyra, K.J. and B.F. Luisi, RNA Biol, 2013. 10(4): p. 627-35.
171.Thomas, E.N., et al., Elife, 2020. 9.
172.Christensen, S.K., et al., Proc Natl Acad Sci U S A, 2001. 98(25): p. 14328-33.
173.Rae, C.D., Y. Gordiyenko, and V. Ramakrishnan, Science, 2019. 363(6428): p. 740-744.
174.Karzai, A.W., E.D. Roche, and R.T. Sauer, Nat Struct Biol, 2000. 7(6): p. 449-55.
175.Felden, B., et al., EMBO J, 1998. 17(11): p. 3188-96.
176.Ranaei-Siadat, E., et al., RNA Biol, 2013. 10(4): p. 572-8.
177.Julio, S.M., D.M. Heithoff, and M.J. Mahan, J Bacteriol, 2000. 182(6): p. 1558-63.
178.Sim, S. and S.L. Wolin, Microbiol Spectr, 2018. 6(4).
179.Chen, X., et al., Cell, 2013. 153(1): p. 166-77.
180.Chen, X., et al., RNA, 2014. 20(11): p. 1715-24.
181.Chen, X., et al., Genes Dev, 2007. 21(11): p. 1328-39.
182.Chen, X., A.M. Quinn, and S.L. Wolin, Genes Dev, 2000. 14(7): p. 777-82.
183.Wurtmann, E.J. and S.L. Wolin, Proc Natl Acad Sci U S A, 2010. 107(9): p. 4022-7.

184.Westermann, A.J., et al., Nature, 2016. 529(7587): p. 496-501.
185.Greiling, T.M., et al., Sci Transl Med, 2018. 10(434).
186.Hughes, K.J., et al., Cell Rep, 2020. 33(12): p. 108527.
187.Cortese, R., et al., J Biol Chem, 1974. 249(4): p. 1103-8.
188.Temmel, H., et al., Nucleic Acids Res, 2017. 45(8): p. 4708-4721.
189.Deng, X., et al., Nucleic Acids Res, 2015. 43(13): p. 6557-67.
190.Marzi, S. and P. Romby, Mol Microbiol, 2012. 83(1): p. 1-6.
191.Morales-Filloy, H.G., et al., J Bacteriol, 2020. 202(6).
192.Novick, R.P., Mol Microbiol, 2003. 48(6): p. 1429-49.
193.Bronesky, D., et al., Annu Rev Microbiol, 2016. 70: p. 299-316.
194.Cahová, H., et al., Nature, 2015. 519(7543): p. 374-7.
195.Frindert, J., et al., Cell Rep, 2018. 24(7): p. 1890-1901 e8.
196.Pan, T., Trends Biochem Sci, 2013. 38(4): p. 204-9.
197.Anders, M., et al., Life Sci Alliance, 2018. 1(4): p. e201800113.
198.Squires, J.E., et al., Nucleic Acids Res, 2012. 40(11): p. 5023-33.
199.Nombela, P., B. Miguel-López, and S. Blanco, Mol Cancer, 2021. 20(1): p. 18.
200.Kumar, S. and T. Mohapatra, Front Cell Dev Biol, 2021. 9: p. 628415.
201.Bazak, L., et al., Genome Res, 2014. 24(3): p. 365-76.
202.Palladino, M.J., et al., Cell, 2000. 102(4): p. 437-49.
203.Vvedenskaya, I.O., et al., Mol Cell, 2018. 70(3): p. 553-564 e9.
204.Craft, D.L., et al., FEMS Microbiol Lett, 2020. 367(17).
205.Luciano, D.J. and J.G. Belasco, Proc Natl Acad Sci U S A, 2020. 117(7): p. 3560-3567.
206.Lee, P.C., B.R. Bochner, and B.N. Ames, Proc Natl Acad Sci U S A, 1983. 80(24): p. 7496-500.
207.Bochner, B.R., et al., Cell, 1984. 37(1): p. 225-32.
208.Eyler, D.E., et al., Proc Natl Acad Sci U S A, 2019. 116(46): p. 23068-23074.
209.Fernández, I.S., et al., Nature, 2013. 500(7460): p. 107-10.
210.Karijolich, J. and Y.T. Yu, Nature, 2011. 474(7351): p. 395-8.
211.Islam, M.S., et al., bioRxiv, 2021: p. 2021.05.23.445298.
212.Ieong, K.W., et al., Nucleic Acids Res, 2021. 49(5): p. 2684-2699.
213.Choi, J., et al., Nat Struct Mol Biol, 2016. 23(2): p. 110-5.
214.Roost, C., et al., J Am Chem Soc, 2015. 137(5): p. 2107-15.
215.Micura, R., et al., Nucleic Acids Res, 2001. 29(19): p. 3997-4005.
216.Bar-Yaacov, D., et al., Genome Res, 2017. 27(10): p. 1696-1703.
217.Verstraeten, N., et al., Mol Cell, 2015. 59(1): p. 9-21.
218.Harms, A., E. Maisonneuve, and K. Gerdes, Science, 2016. 354(6318).
219.Bar-Yaacov, D., Y. Pilpel, and O. Dahan, RNA Biol, 2018. 15(7): p. 863-867.
220.Kanazawa, H., et al., Nucleic Acids Res, 2017. 45(21): p. 12529-12535.
221.Svetlov, M.S., et al., Nat Chem Biol, 2021. 17(4): p. 412-420.
222.Shi, H. and P.B. Moore, RNA, 2000. 6(8): p. 1091-105.
223.Nissen, P., et al., Science, 1995. 270(5241): p. 1464-72.
224.Neubauer, C., et al., Science, 2012. 335(6074): p. 1366-9.
225.Wang, W., et al., Structure, 2018. 26(12): p. 1635-1644 e3.

2. *Staphylococcus aureus*

Les Staphylocoques sont des coques à Gram positif commensales de l'Homme, dont plusieurs espèces sont des pathogènes opportunistes. Parmi elles, *Staphylococcus aureus* représente l'espèce la plus virulente, responsable d'un grand nombre d'infections de gravité variable et touchant un large éventail de tissus, allant des infections cutanées bénignes à la pneumonie, l'endocardite, voire la septicémie. *S. aureus* est aussi capable de s'adapter pour persister à la surface et à l'intérieur de tissus humains. Elle est présente sur la peau et dans le nez chez environ 30% de la population (Wertheim *et al.*, 2005). La colonisation de la peau inclus l'implantation de la bactérie à sa surface en tant que constituant du microbiome (Oh *et al.*, 2016). Mais également l'insertion entre les couches de l'épiderme (Nakatsuji *et al.*, 2013), la modulation de la réponse immunitaire et la persistance dans les cellules immunitaires, endothéliales et épithéliales (Soong et al., 2015). Cette internalisation lui permet d'échapper complètement aux défenses immunitaires de celui-ci.

L'émergence de souches multi résistantes aux antibiotiques est une préoccupation majeure de santé publique, particulièrement en milieu hospitalier, les souches MRSA (*S. aureus* résistante à la méthicilline) provoquant des infections nosocomiales graves et difficiles à traiter. La diversité des symptômes cliniques provoqués et les mécanismes de résistance aux traitements dépendent de l'expression de nombreux facteurs de virulence et des voies de réponse au stress.

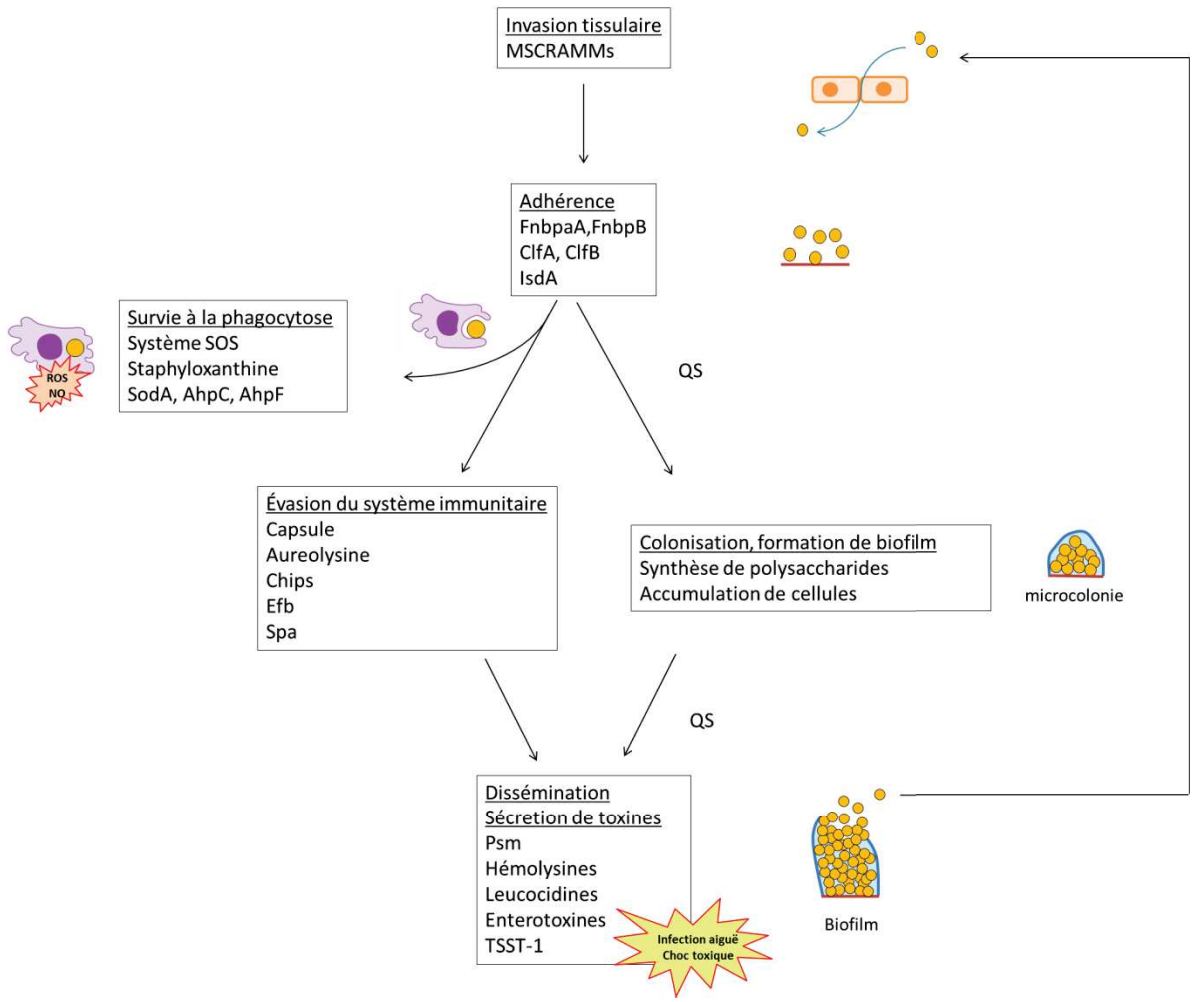

Figure 1 : Schéma représentant les étapes de l'infection de *S. aureus*. La colonisation des tissus amorce l'infection grâce aux adhésines permettant aux bactéries de se fixer sur différents types cellulaires. Au sein des tissus, les bactéries sont confrontées aux défenses immunitaires de l'hôte. Elles doivent donc échapper aux cellules immunitaires, former des colonies et entrer dans une phase de croissance grâce à la formation du biofilm les protégeant des stress environnementaux. Lorsque les colonies sont assez grandes, la phase de dissémination est déclenchée par la production de toxines et exoprotéines (nucléases et protéases) entrainant la rupture du biofilm et conduisant à une infection aiguë ou un choc toxique. En cas de phagocytose, la bactérie est capable de résister au stress généré dans les phagosomes grâce aux systèmes de détoxification et de réparation, elle va ainsi survivre sous forme quiescente. Les flèches annotées « QS » présentent des transitions entre les étapes du cycle d'infection qui sont réalisées sous le contrôle du Quorum Sensing, système à deux composants permettant à la bactérie de détecter la densité cellulaire et moduler l'expression de nombreux facteurs de virulences grâce à l'ARNIII. Cet ARN régulateur permettant simultanément de réprimer les facteurs impliqués dans l'adhérence et la colonisation et activer l'expression des toxines et exoprotéines

Le cycle de l'infection par *S. aureus* est assez précisément établi. A chaque étape du cycle, la bactérie va s'adapter grâce à la production d'un arsenal de facteurs de virulence dont l'expression est coordonnée en fonction de son environnement (**Fig. 1**).

Lors de l'adhérence et l'invasion tissulaire, l'étape initiatrice fondamentale à l'infection, des protéines de la famille des MSCRAMM (microbial surface components recognizing adhesive

matrix molecules) sont produites. Parmi elles, les protéines de liaison à la fibronectine (FnbpA et FnbpB) ou les facteurs de liaisons au fibrinogène, les Clumping factor A et B (ClfA et ClfB) permettent à la bactérie de se fixer sur différents types cellulaires de l'hôte (Eidhin *et al.*, 1998; Heilmann *et al.*, 2004). De plus, la protéine SpA (Staphylococcal protein A) lui permet non seulement de se lier aux immunoglobulines mais également d'échapper aux défenses immunitaires de l'hôte (Falugi *et al.*, 2013).

Afin de se protéger de la phagocytose, *S. aureus* est capable de produire une capsule de polysaccharides (Luong and Lee, 2002). La production de protéases telles que la Staphopain B et l'Aureolysine lui permet de dégrader l'élastine de l'hôte et entrainer la mort des monocytes (Shaw *et al.*, 2004; Smagur *et al.*, 2009; Elmwall *et al.*, 2017). Les CHIPS (chemotaxis inhibitory proteins of *S.aureus*) et Efb (extracellular fibrinogen binding protein) sont également sécrétées afin d'empêcher le recrutement de neutrophiles et l'activation du système du complément (Postma *et al.*, 2004; Rooijakkers *et al.*, 2006).

Pour assurer la prolifération de la bactérie dans les tissus, une structure de protection est produite sous forme de biofilm. Cette structure permet aux cellules de résister aux antibiotiques, d'échapper aux défenses immunitaires de l'hôte et ainsi devenir persistantes en diminuant leur métabolisme. (Arciola *et al.*, 2015; Otto, 2018)

La dissémination de la bactérie est facilitée par la production de toxines et d'exoprotéines (nucléases, lipases et protéases) entrainant la dispersion du biofilm. Ces toxines induisant la lyse des cellules ciblées, telles que les hémolysines (Jarry *et al.*, 2008; Berube and Wardenburg, 2013), les leucocidines (Spaan *et al.*, 2017) et les PSM (phenol soluble modulins) permettent également la propagation de l'infection à d'autres tissus (Periasamy *et al.*, 2012). Elles stimulent la libération de cytokines pro-inflammatoires (IL-18) des kératinocytes et sont indispensables à l'induction de l'inflammation de la peau (Syed *et al.*, 2015). Les cytokines pro-inflammatoires sont importantes pour maintenir les macrophages dans leur rôle de nettoyage des pathogènes avec une production d'oxyde nitrique et d'espèces réactives de l'oxygène importante (Pidwill *et al.*, 2021). Ces toxines sont responsables d'infections aiguës, les entérotoxines par exemple causent des intoxications alimentaires et les TSST-1 (Toxic shock syndrome toxin-1) causent les chocs toxiques Staphylococciques. Il existe une dualité claire entre la production de toxines (infection aiguë)

et la tolérance de l'hôte (infection chronique) durant laquelle *S. aureus* évite de stimuler les processus inflammatoires.

L'expression de l'ensemble de ces facteurs de virulence est orchestrée en réponse à de nombreux signaux environnementaux tels que la densité cellulaire, la disponibilité des nutriments ainsi que les stress imposées par les mécanismes de défense de l'hôte. Des systèmes de quorum sensing, codés notamment par le gène *agr* (accessory gene regulator) chez *S. aureus* permettent cette régulation fine de la virulence de la bactérie (Wang and Muir, 2016).

3. L'oxydation comme défense contre les pathogènes

La production d'espèces réactives de l'oxygène (ROS) tel que les superoxydes (O_2^-) et les peroxydes (H_2O_2) fait partie de la première ligne de défense mise en place par l'hôte pour lutter contre les bactéries pathogènes. Les ROS sont produits au sein des neutrophiles et des macrophages grâce au complexe de la phagocyte NADPH oxidase (Fang, 2004). Les superoxydes et les peroxydes entrainent la libération d'un atome de fer des metalloenzymes contenant un cluster [4Fe-4S] catalytique, entrainant la destruction du cluster et l'inactivation de l'enzyme (Imlay, 2006). Ces enzymes à cluster [4Fe-4S] sont impliquées dans un grand nombre de mécanismes indispensables pour tous les organismes, notamment les modifications post-transcriptionnelles.

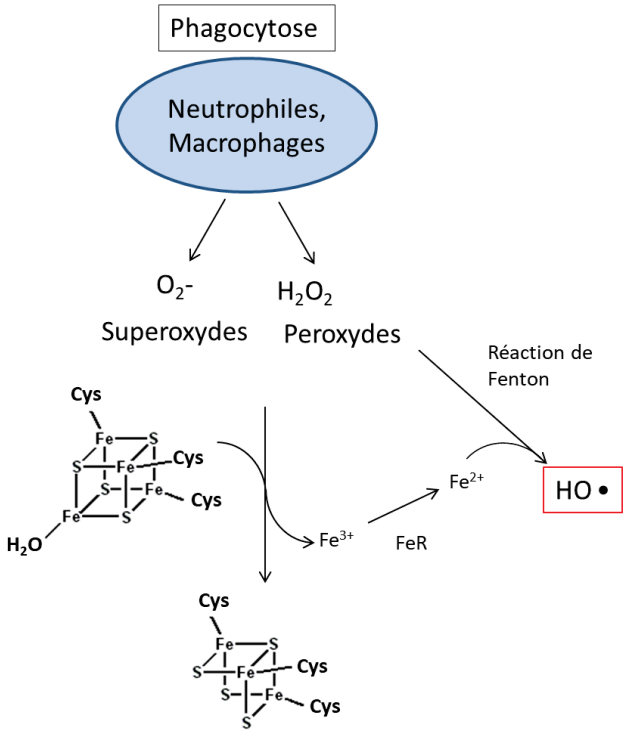

Figure 2 : Schéma de la formation des radicaux hydroxyles induite par la destruction de centres [4Fe-4S] en présence de peroxyde. L'ion ferreux libéré va réagir avec le peroxyde produit par les neutrophiles et macrophages entrainant la formation du HO•, encadré en rouge, par une réaction de Fenton.

Les radicaux hydroxyles (HO•) créés par des réactions de Fenton, sont fortement réactifs et interagissent avec toutes les molécules biologiques à proximité en causant des dommages parfois irréversibles. Les molécules les plus spécifiquement touchées sont les acides nucléiques, entrainant des mutations sur l'ADN (Keyer and Imlay, 1996). Les protéines sont également des cibles majeures des ROS, qui peuvent subir des modifications entrainant la formation d'agrégats (Davies, 2005, 2016). Les acides aminés contenant un groupement thiol (méthionine et cystéine) sont particulièrement sensibles à l'oxydation pouvant entrainer l'inactivation des protéines les contenant (Dean *et al.*, 1997; Grimaud *et al.*, 2001).

4. *S. aureus* et son adaptation au stress oxydant

S. aureus possède de nombreuses défenses pour s'adapter aux ROS, parmi lesquelles le pigment staphyloxanthine, responsable de sa couleur dorée caractéristique. Présents chez une grande partie des souches de *S. aureus* provenant d'infections humaines, ces pigments caroténoïdes sont connus pour désactiver les singulets d'oxygène. De par leur nombreuses

double-liaisons conjuguées, les caroténoïdes sont des molécules importantes pour la détoxification des ROS. La présence de staphyloxanthine confère ainsi une résistance aux ROS et améliore la survie de la bactérie lors d'infections (Liu *et al.*, 2005).

D'autres systèmes sont également connus pour réduire la concentration de ROS. Les superoxyde dismutases (SOD) sont des metalloenzymes de détoxification des ROS qui catalysent la dismutation du $O2^-$ en oxygène et H_2O_2, qui sera ensuite réduit en H_2O par des catalases ou l'alkyl hydroperoxyde reductase (Clements *et al.*, 1999; Cosgrove *et al.*, 2007). *S. aureus* possède deux gènes codant pour des SOD, *sodA* et *sodM*. L'enzyme SOD majeure SodA dépend strictement du manganèse Mn^{2+}, tandis que l'enzyme alternative SodM est active lorsqu'elle est chargée en Mn^{2+} ou en Fe^{2+} (Treffon *et al.*, 2020).

L'homéostasie des ions métalliques, plus spécifiquement celle du fer, occupe donc une place importante dans la réponse des bactéries aux conditions oxydantes. De nombreux facteurs liés à l'apport du fer indispensable pour la survie de la cellule, sont mobilisés durant l'infection. Chez l'hôte, les ions Fe^{2+} sont séquestrés au sein de complexes moléculaires les rendant très peu disponibles pour les pathogènes qui doivent mettre en place des stratégies afin de pouvoir acquérir le fer nécessaire à leur survie.

Chez *S. aureus*, les protéines du système Isd (Iron-Regulated Surface Determinant) sont des protéines exprimées lors d'un déficit de fer, ces protéines permettent l'utilisation du fer provenant de l'hème de l'hôte. (Clarke *et al.*, 2004; Muryoi *et al.*, 2008). Le système Isd est constitué de 10 protéines, permettant de capter l'hémoglobine et l'haptoglobine avec les recepteurs IsdB et IsdH (Dryla *et al.*, 2003; Torres *et al.*, 2006). L'hème est ensuite transféré à travers la paroi cellulaire via IspA et IspC (Liu *et al.*, 2008; Zhu *et al.*, 2008) vers le transporteur IsdDEF permettant son internalisation dans le cytoplasme. IsdDEF est un abc transporteur dans lequel IsdE est une lipoprotéine se liant à l'hème, IsdD est une ATPase et IsdF est une perméase. Enfin, la porphyrine est dégradée par IsdG ou IsdI qui sont des oxygènases produisant la staphylobiline (Skaar et al., 2004; Reniere et al., 2010). En plus de ce système Isd, la bactérie produit des staphyloferrines qui sont des sidérophores capables d'extraire le fer de la ferritine, les staphyloferrines A sont codés par les opérons *sfaABCD* (Beasley et al., 2009) et les staphyloferrines B par *sbnABCDEFGHI* (Park et al., 2005; Cheung et al., 2009)

Les systèmes de réparation de l'ADN tels que le système SOS est activé par la protéine RecA, impliquée dans la reconnaissance et la recombinaison de l'ADN simple brin qui est elle-même réprimée par la fixation de la protéine LexA. Lors de dommage sur l'ADN, LexA va être clivé, et permettre l'activation du système SOS (Cirz *et al.*, 2007; Butala *et al.*, 2009). L'opéron *rexBA* fait également partie de la réponse SOS également mis en place par la bactérie afin de survivre aux attaques des ROS produits par les défenses de l'hôte. Les protéines RexAB font partie de la famille des protéines AddAB hélicases-nucléases et sont indispensables pour la survie de la bactérie lors de l'infection. Elles sont impliquées dans la réparation des cassures du double brin (Chang *et al.*, 2006; Ha *et al.*, 2020b).

5. Objectifs de la thèse

La cartographie des modifications post-transcriptionnelles dans les ARN non codants de *S. aureus* reste encore peu connue ainsi que leurs implications dans l'adaptation de la bactérie à son environnement, notamment lors de l'infection.

Cette étude a pour but principal dans un premier temps d'établir une cartographie des modifications présentes dans les ARN non codants, plus spécifiquement dans les ARNt de *S. aureus*. Pour cela, une méthode d'analyse permettant de les isoler un à un et de caractériser les modifications présentes doit être mise en place et adaptée aux moyens matériels disponibles ainsi qu'à l'organisme étudié.

Dans un second temps, la cartographie établie pourra permettre une étude dynamique des modifications en adaptation à différentes conditions environnementales rencontrées par la bactérie durant les interactions avec l'hôte, plus spécifiquement les stress rencontrés durant l'infection.

Enfin, l'étude des causes et des conséquences traductionnelles des changements observés pourra être réalisée afin de déterminer le potentiel rôle des modifications post-transcriptionnelles dans l'adaptation aux stress

II. Résultats :

1. Mise en place de la méthode d'analyse des ARN par gel en 2 dimensions et NanoLC-MS/MS

Le chapitre de Methods in molecular biology présente un protocole détaillé pour isoler les ARNt bactériens un a un par gel de polyacrylamide en 2 dimensions ainsi que l'identification des ARNt et la caractérisation des modifications post-trancriptionelles par l'analyse LC-MS/MS. Ce protocole mis en place au sein de l'unité pour l'analyse des ARNt de *E. coli* sera également appliqué sans modifications majeures à cette étude sur les ARNt de *S.aureus*.

Chapter 8

Mapping of Posttranscriptional tRNA Modifications by Two-Dimensional Gel Electrophoresis Mass Spectrometry

Laura Antoine and Philippe Wolff

Abstract

RNA modification mapping by mass spectrometry (MS) is based on the use of specific ribonucleases (RNases) that generate short oligonucleotide digestion products which are further separated by nano-liquid chromatography and analyzed by MS and MS/MS. Recent developments in MS instrumentation allow the possibility to deeply explore posttranscriptional modifications. Notably, development of nano-liquid chromatography and nano-electrospray drastically increases the detection sensitivity and allows the identification and sequencing of RNA digested fragments separated and extracted from two-dimensional polyacrylamide gels, as long as the mapping and characterization of ribonucleotide modifications.

Key words 2D Gel isolation, Posttranscriptional tRNA modifications, Nano-LC-MS/MS

1 Introduction

RNA modification mapping recently experienced a renewed interest because of the development of new sensitive detection technologies and implication of RNA modifications in the deciphering of gene expression regulation or antibiotic resistance [1, 2]. In this chapter, we provide a detailed protocol for *E. coli* tRNA modification mapping. We present the sequencing by mass spectrometry of two tRNAs, tRNA Ser GCU and tRNA Leu CAG. To obtain the largest sequence coverage, three different nucleotide-specific RNases are used: RNase T1 (cleaves at 3′ end of G), RNase A (cleaves at 3′ end of U and C), and RNase U2 (cleaves at 3′ end of purine but preferably at 3′ end of A). The RNA modification mapping and data analysis workflow are shown in Fig. 1. This protocol had been applied successfully to different organisms such as bacteria, archaea, and eukaryotes.

The MS analysis procedure presents several caveats. First, as different tRNAs share similar sequences, it may be difficult to

Véronique Arluison and Frank Wien (eds.), *RNA Spectroscopy: Methods and Protocols*, Methods in Molecular Biology, vol. 2113, https://doi.org/10.1007/978-1-0716-0278-2_8, © Springer Science+Business Media, LLC, part of Springer Nature 2020

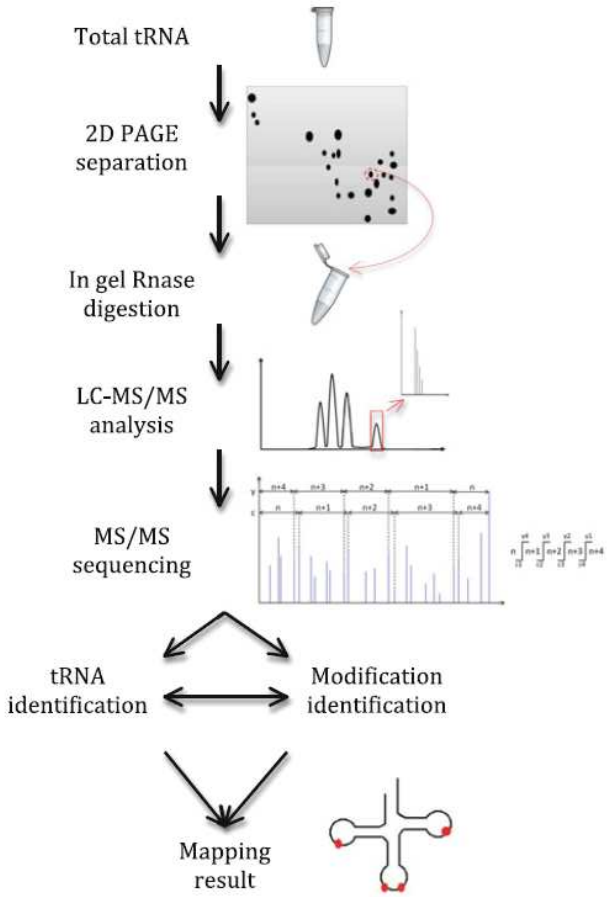

Fig. 1 Workflow for posttranscriptional tRNA modifications mapping by two-dimensional gel electrophoresis followed by mass spectrometry analysis. tRNA is separated by 2D gel electrophoresis. Individual tRNA spots are sliced out and in-gel digested by nucleoside-specific RNases. RNase digests are sequenced by LC-MS/MS in order to identify tRNA and to localize modifications

unambiguously attribute such sequences to a single tRNA. Additionally, different sequences can have the same mass (same nucleotide composition) or similar mass (there is a difference of only 1 Da between cytosine and uridine). In those cases, there is often an isotopic pattern overlay, and it can be very difficult to sequence correctly MS/MS spectra. In order to simplify MS/MS analysis and tRNA identification, two-dimensional polyacrylamide gels (2D gels) were used to separate tRNAs (Fig. 2) [3, 4].

After "in-gel RNase digestion," oligonucleotide products (passively eluted from the gel) are separated by nano-ion-pair reversed-phase high-performance liquid chromatography (nano-IP-RP-HPLC) [5]. Eluted digests are directly injected in the spectrometer

spot	tRNA
S02	Ser GCU
S03	Leu CAG
S05	Leu CAA
S08	Ile GAU
S08	Asp GUC
S09	Asn GUU
S11	Glu UUC
S10	Gln UUG
S10	Gln CUG
S09	Pro CGG
S09	Ala UGC
S07	Val UAC
S07	Gly GCC
S06	His GUG
S06	Arg ACG
S06	ProUGG
S13	Leu UAG
S03	Ser GGA
S14	Tyr GUA

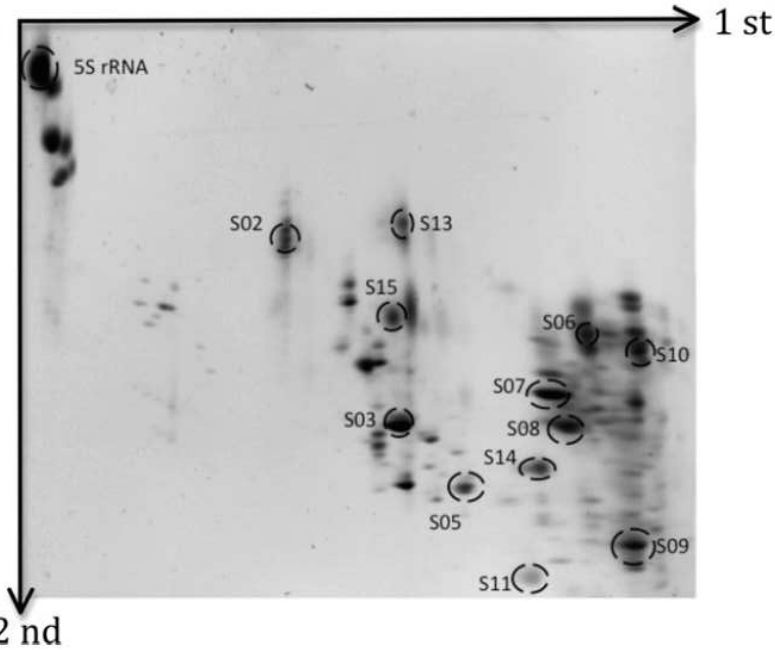

Fig. 2 2D polyacrylamide gel (20%) of *E. coli* total tRNA. 10 μg of total tRNA from *E. coli* were loaded; tRNA spots are revealed by ethidium bromide staining. The spots containing tRNA identified by MS/MS sequencing are indicated (black circles) and annotated in the table on the left

via a commercial NanoLockSpray ionization source to provide exact mass measurement. All oligonucleotides are fragmented by collision-induced dissociation (CID) and produce preferential fragments from y and c series for RNA sequencing [6]. Sequencing results are compared to genomic sequence in order to identify tRNA and to map RNA modifications in the sequence.

2 Materials

2.1 Instruments and Equipment

1. Polyacrylamide gel electrophoresis (PAGE) apparatus for 50 cm glass plates, 1 mm spacers (first dimension).
2. Polyacrylamide gel electrophoresis (PAGE) apparatus for 30 cm glass plates, 1 mm spacers (second dimension).
3. Electrophoresis power supply.
4. UV transilluminator and UV safety glasses.
5. Sterile surgical blades.
6. SpeedVac vacuum concentrator.
7. NanoAcquity UPLC system (Waters, Manchester, UK).

8. Synapt G2-S mass spectrometer equipped with NanoLock-Spray ionization source (Waters, Manchester, UK).
9. MassLynx mass spectrometry software with MaxEnt3 module (Waters, Manchester, UK).
10. Acquity UPLC peptide BEH C18 column (130 Å, 1.7 μm, 75 μm × 200 mm) (Waters, Manchester, UK).
11. Basic laboratory materials (vortex, thermoblock, etc.)

2.2 Two-Dimensional Gel Electrophoresis

1. Total tRNA from *E. coli* used in this study was prepared by Gérard Keith (personal gift), but it is also commercially available.
2. 12.5% Acrylamide/bis-acrylamide (19:1), 8 M urea, 1× Tris-Borat-EDTA (TBE) (first dimension).
3. 20% Acrylamide/bis-acrylamide (19:1), 4 M urea, 1× TBE (second dimension).
4. Ethidium bromide (EtBr).

2.3 In-Gel Digestion of Separated tRNA

1. RNase T1 and A (Thermo Fischer Scientific).
2. RNase U2 was homemade prepared as described [7].
3. Ammonium acetate 100 mM.
4. ZIP Tip C18 (Millipore).

2.4 Nano-liquid Chromatography

1. Mobile phase A.
   - 200 mM Hexafluoropropanol (HFIP).
   - 7 mM Triethylamine (TEA).
   - 7.5 mM Triethylamine acetate (TEAA) pH 7.5.
2. Mobile phase B.
   - 100% Methanol LC-MS grade.

3 Methods

3.1 Two-Dimensional Gel Electrophoresis (See Note 1)

3.1.1 First Dimension (Denaturing Conditions)

1. Cast the first-dimensional, 12.5% acrylamide/bis-acrylamide, 8 M urea.
2. Pre-run the gel in 1× TBE buffer for 30 min at 30 W (constant power).
3. Load 10 μg per well of *E. coli* total tRNA in a minimum volume (less than 10 μL).
4. Run the gel for 7 h at 30 W (constant power).
5. Stain the gel with an EtBr solution (10 μg/L) for 10 min.

6. Visualize the bands containing tRNAs under UV light (302 nm). Beware of wearing appropriate protections for handling gel containing EtBr and manipulation under UV light.
7. Excise the gel fragments containing tRNAs with a clean razor blade.

3.1.2 Second Dimension (Semi-denaturing Condition)

1. Put the excised gel lanes on the top of the second polyacrylamide gel, and cast the second-dimensional gel 20% acrylamide/bis-acrylamide, 4 M urea. The excised gel fragment from the first electrophoresis should be embedded in the gel.
2. Run the gel for 24 h at 6 W (constant power).
3. Stain the gel with an EtBr solution (10 μg/L) for 10 min.
4. Using UV transilluminator, excise the spots containing tRNAs (Fig. 2). Beware of wearing appropriate protections for handling gel containing EtBr and manipulation under UV light.
5. Dry gel spots in Eppendorf tubes under vacuum for 10 min without heating.

3.2 In-Gel RNase Digestion

Rehydrate excised gel fragments with 20 μL of RNase T1 (1 U/μL) solution or 20 μL of RNase A (0.01 U/μL) solution in 100 mM ammonium acetate (pH is not adjusted), and incubate at 50 °C for 3 h, followed by 12 h at 37 °C.

For RNase U2 digestion, rehydrate gel fragments with 50 μL of RNase U2 at 0.3 ng μL^{-1} in 100 mM ammonium acetate (pH is adjusted to 5.3), and incubate at 37 °C for 1 h.

3.3 RNA Digest Product Desalting

1. Prepare ZipTip C18 with 50% acetonitrile in water (3 × 10 μL).
2. Equilibrate the ZipTip for sample binding with 200 mM ammonium acetate (1 × 10 μL).
3. Bind the digested sample, and wash oligonucleotides with 200 mM ammonium acetate (5 × 10 μL).
4. Elute oligonucleotides with 10 μL of 50% acetonitrile in water.
5. Dry under vacuum for 20 min without heating.

3.4 LC-MS/MS

3.4.1 Nano-liquid Chromatography

Nano-LC is performed at a 0.3 μL/min flow rate for 1 h. RNase digestion products are eluted using a gradient from 15% to 35% B in 2 min followed by an increase of B to 50% in 20 min and then returning to 15% B in 25 min.

Table 1
List of natural and modified nucleotides identified in this study

Name	Short name	Symbol	Nucleotide mass (Da)	$[M-H]^-$ Np (Da)	$[M-H]^-$ N > p (Da)	Neutral loss (Da)
Guanosine	G	G	345	362	344	
Cytidine	C	C	305	322	304	
Uridine	U	U	306	323	305	
Adenosine	A	A	329	346	328	
2′-*O*-Methylguanosine	Gm	#	359	376	358	
1-Methylguanosine	m1G	K	359	376	359	
2′-*O*-Methylcytidine	Cm	B	319	336	318	
5-Methyluridine	m5U	T	320	337	319	
Dihydrouridine	D	D	308	325	307	
N6-Threonylcarbamoyladenosine[a]	t6A	6	329	346	328	145

A full list of modified nucleosides is available in the Modomics database (http://modomics.genesilico.pl/modifications/)
[a]Due to the neutral loss of threonylcarbamoyl, nucleotide mass fragmentation of t6A corresponds to the mass without modification. This modification occurs exclusively at position 37 in the anticodon loop

3.4.2 Mass Spectrometry Analysis

All experiments are performed in negative mode. The eluted RNase digests are injected on line into the mass spectrometer via Nano-LockSpray. Capillary voltage is set to 2.6 kV and sample cone to 30 V. Source is heated to 130 °C. For MS, a mass range from 500 to 1500 (m/z) is used, followed by collision-induced dissociation (CID) fragmentation of most intense signals using fast data directed acquisition (FastDDA) mode with a m/z detection range of fragments from 50 to 2000. A collision energy ramp (18–28 V at m/z 500 and 28–38 V at m/z 1500) is applied in the trap collision cell to provide the maximum fragment ions.

3.5 Data Analysis

All the fragment spectra are manually sequenced (*see* **Note 2**).

1. Deconvolute CID spectra by using MaxEnt3 software (*see* **Note 3**).
2. Using Table 1, listing the masses of the most common natural and modified nucleotides, reconstruct the sequence by following the y and/or c series (*see* **Note 4**). Three sequencing examples are shown in Fig. 3. Additionally, Fig. 4 gives a list of all the different masses obtained by nano-LC-MS/MS and the corresponding sequences.
3. Note that pseudouridine, an isomer of uridine, is a silent mass and cannot be detected by this method (*see* **Note 5**).

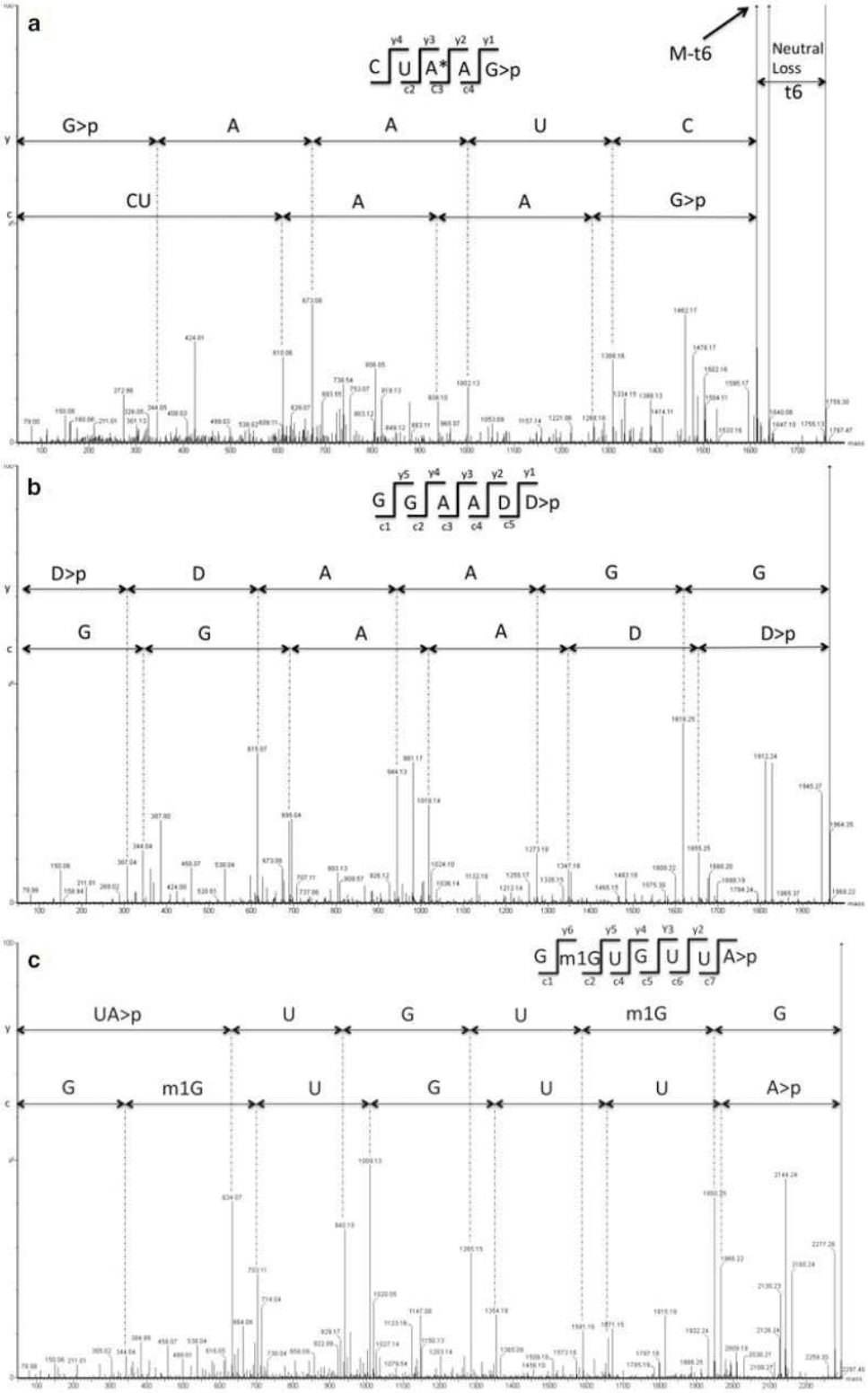

Fig. 3 Typical MS/MS spectra of RNase digested tRNA fragments. Only series y and c have been sequenced. (**a**) MS/MS sequencing spectrum of CU**t6A**AG>p after RNase T1 digestion. In the case of t6A modification,

theoretical m/z	observed m/z	z	molecular mass (Da)	sequence	tRNA	theoretical m/z	observed m/z	z	molecular mass (Da)	sequence	tRNA
RNase T1											
878,62	878,63	-2	1758,3	CU6AG>p	Ser GCU	947,11	947,10	-2	1895,2	CUUCAG>p	Leu CAG
946,62	946,62	-2	1894,2	CAUCCG>p	Ser GCU	956,11	956,10	-2	1913,2	CUUCAGp	Leu CAG
955,62	955,62	-2	1912,2	CAUCCGp	Ser GCU	966,12	966,09	-2	1933,2	TUCAAG>p	Leu CAG
1135,15	1135,13	-2	2271,3	UCAAAAG>p	Ser GCU	975,13	975,10	-2	1951,2	TUCAAGp	Leu CAG
1144,16	1144,13	-2	2289,3	UCAAAAGp	Ser GCU	988,14	988,13	-2	1977,3	AADD#G>p	Leu CAG
1240,14	1240,1	-2	2481,2	CUCCCCUG>p	Ser GCU	997,15	997,13	-2	1995,3	AADD#Gp	Leu CAG
1249,15	1249,12	-2	2499,2	CUCCCCUGp	Ser GCU	1252,64	1252,60	-2	2506,2	UCCUUACG>p	Leu CAG
1251,66	1251,63	-2	2504,3	CCUCACCG>p	Ser GCU	1261,65	1261,62	-2	2524,2	UCCUUACGp	Leu CAG
1263,66	1263,64	-2	2528,3	AAUCCCCG>p	Ser GCU	1233,15	1233,11	-3	3701,3	UCCCCCCCCUCG>p	Leu CAG
1272,67	1272,63	-2	2546,3	AAUCCCCGp	Ser GCU	1239,15	1239,10	-3	3719,3	UCCCCCCCCUCGp	Leu CAG
RNase A											
858,11	858,11	-2	1717,2	GGGGTp	Ser GCU	662,09	662,09	-2	1325,2	AGACp	Leu CAG
991,15	991,16	-2	1983,3	AAAAGCp	Ser GCU	1326,18	1326,17	-1	1326,2	AAGUp	Leu CAG
1007,14	1007,15	-2	2015,3	GAAGGCp	Ser GCU	836,12	836,12	-2	1673,2	GGAADp	Leu CAG
1179,66	1179,69	-2	2360,3	GAGAGGCp	Ser GCU	981,13	981,14	-2	1963,3	GGAADD>p	Leu CAG
1417,20	1417,18	-2	2835,4	6AGGGAGUp	Ser GCU	1007,63	1007,64	-2	2016,3	GAAGGUp	Leu CAG
1046,47	1046,49	-3	3141,5	U6AGGGAGUp	Ser GCU	1030,64	1030,64	-2	2062,3	GGGGGTp	Leu CAG
RNase U2											
706,10	706,1	-2	1413,2	CU6A>p	Ser GCU	823,61	823,63	-2	1648,3	ADD#G>p	Leu CAG
807,11	807,11	-2	1615,2	CDGAA>p	Ser GCU	865,60	865,59	-2	1732,2	pGCGAA>p	Leu CAG
915,15	915,15	-2	1831,3	CCGCCA	Ser GCU	927,60	927,60	-2	1856,2	UCCUUA>p	Leu CAG
966,62	966,62	-2	1934,2	GCUGCA>p	Ser GCU	977,63	977,64	-2	1956,3	DD#GDA>p	Leu CAG
1240,14	1240,14	-2	2481,3	CUCCCCUG>p	Ser GCU	1142,16	1142,17	-2	2285,3	ADD#GDA>p	Leu CAG
1388,19	1388,21	-2	2777,4	CU6AGGGA>p	Ser GCU	1147,13	1147,13	-2	2295,3	GKUGUUA>p	Leu CAG
1273,15	1273,16	-3	3821,5	GGCGCUCCCCUG>p	Ser GCU	1425,66	1425,67	-2	2852,3	GUGUCCUUA>p	Leu CAG
						1479,21	1479,20	-2	2959,4	ADD#GDAGA>p	Leu CAG
						1233,15	1233,17	-3	3701,5	UCCCCCCCCUCG>p	Leu CAG

tRNA Ser GCU
pGGUGAGGUGGCCGAGAGGCDGAAGGCGCUCCCCUGCU6AGGGAGUAUGCGGUCAAAAGCUGCAUCCGGGGTUCGAAU CCCCGCCUCACCGCCA
Sequence coverage 77%
tRNA Leu CAG
pGCGAAGGUGGCGGAADD#GDAGACGCGCUAGCUUCAGKUGUUAGUGUCCUUACGGACGUGGGGGTUCAAGUCCCCC CCCUCGCACCA
Sequence coverage 82%

Fig. 4 List of all digested products experimentally observed for tRNA Ser GCU and Leu CAG, after individual digestion with RNases T1, A, and U2. The MS/MS sequenced products are indicated in red in the full tRNA sequences below the table. Although sequence coverage is close to 100%, some parts of the sequences are still missing. Thus, in the case of uncharacterized tRNA, modifications existing in vivo may be missed

4. For methyl groups, it is not possible to localize the group on the base and/or the ribose with this technique (*see* **Note 6**).
5. When a digested tRNA fragment is sequenced, the parent ion and the fragments' masses have to be checked using Mongo Oligo mass calculator (https://mods.rna.albany.edu/masspec/Mongo-Oligo). A maximum tolerance of 0.05 Da between the measured and calculated mass is routinely tolerated.
6. Comparison of the resulting sequences with *E. coli* genomic sequences (http://gtrnadb.ucsc.edu) identifies tRNA (*see* **Note 7**).

Fig. 3 (continued) collision-induced dissociation (CID) fragmentation leads to a neutral loss of 145 Da corresponding to the leaving of the threonylcarbamoyl group. ∗ corresponds to the location of the neutral loss. (**b**) MS/MS sequencing spectra of GGAA**DD**>p after RNase A digestion. (**c**) MS/MS sequencing spectra of G**m1G**UGUUA>p after RNase A digestion

7. Map modifications on the tRNA sequence. Figure 4 shows a list of all digested tRNA fragments sequenced by MS/MS.

4 Notes

1. In the first-dimension electrophoresis, tRNAs are completely heat denatured due to the dual action of gel temperature (70 °C) and urea (8 M) and are separated by their length. In the second dimension, urea concentration was decreased to 4 M, and the gel is run at room temperature. Under these conditions, tRNAs are partially refolded, and the separation is based on the partial secondary conformation.
2. Software have been developed for interpretation and annotation of MS/MS data (Ariadne [8], RoboOligo [9]), but to obtain unambiguous localization of modifications, manual interpretation of MS/MS spectra is still required.
3. Electrospray spectrum produces multiple charged ions. Typically, RNase digest products are two or three times charged. Spectrum deconvolution allows to simplify spectrum reading by transforming multiple charges spectrum (m/z) to mono charge spectrum (mass).
4. Generally, the most intense series are y and c. Mongo Oligo online calculator (https://mods.rna.albany.edu/masspec/Mongo-Oligo) could be helpful to find and/or check ion series.
5. Pseudouridine may be specifically derivatized using *N*-cyclohexyl-*N*′-(2-morpholinoethyl)carbodiimide metho-*p*-toluenesulfonate (CMCT) in order to be detectable [10].
6. LC-MS/MS of digestion products allows the localization of methylation in the correct nucleotide but does not allow the localization on the ribose and/or on the base. Using known tRNA modification sequences, it could be possible to predict the type of methylation. Modomics tRNA database (http://modomics.genesilico.pl/sequences/list/tRNA/) [11] provides a large collection of modified tRNA sequences. Furthermore, based on phylogenetic conservation of modification locations, tRNAmodviz (http://genesilico.pl/trnamodviz/) [12], an online software tool, allows the visualization of modification pattern in tRNAs.
7. As with proteomics strategy, RNase digestion generates a set of oligonucleotides, specific to a unique tRNA. tRNA identification is possible by using a genomic tRNA database.

Acknowledgments

The authors would like to thank Gérard Keith for the total *E. coli* tRNA preparation and Dominique Burnouf for critical reading of the manuscript and useful comments. We are grateful to Pascale Romby and Eric Westhof for their constant support. This work was supported by Labex NetRNA.

References

1. Helm M, Motorin Y (2017) Detecting RNA modifications in the Epitranscriptome: predict and validate. Nat Rev Genet 18:275–291
2. Gaston KW, Limbach PA (2014) The identification and characterization of non-coding and coding RNAs and their modified nucleosides by mass spectrometry. RNA Biol 11:1568–1585
3. Fradin AH, Gruhl H, Feldmann H (1975) Mapping of yeast tRNAs by two-dimensional electrophoresis on polyacrylamide gels. FEBS Lett 50:185–189
4. Dong H, Nilsson L, Kurland GC (1996) Co-variation of tRNA abundance and codon usage in *Escherichia Coli* at different growth rates. J Mol Biol 260:649–663
5. Masato T, Ikumi M, Nakayama H, Masaki S, Matsuda R, Nobe Y, Yamauchi Y, Takeda J, Takahashi N, Toshiaki I (2010) In-gel digestion for mass spectrometric characterization of RNA from fluorescently stained polyacrylamide gels. Anal Chem 82:7795–7803
6. McLuckey SA, Van Berkel GJ, Glish GL (1992) Tandem mass spectrometry of small, multiply charged oligonucleotides. J Am Soc Mass Spectrom 3:60–70
7. Houser WM, Butterer A, Addepalli B, Limbach PA (2015) Combining recombinant Ribonuclease U2 and protein phosphatase for RNA modification mapping by liquid chromatography-mass spectrometry. Anal Biochem 478:52–58
8. Hiroshi N, Akiyama M, Taoka M, Yamauchi Y, Nobe Y, Ishikawa H, Takahashi N, Isobe T (2009) Ariadne: a database search engine for identification and chemical analysis of RNA using tandem mass spectrometry data. Nucleic Acids Res 37:e47
9. Sample PJ, Gaston KW, Alfonzo JD, Limbach PA (2015) RoboOligo: software for mass spectrometry data to support manual and de novo sequencing of post-transcriptionally modified ribonucleic acids. Nucleic Acids Res 43:e64
10. Durairaj A, Limbach PA (2008) Matrix-assisted laser desorption/ionization mass spectrometry screening for Pseudouridine in mixtures of small RNAs by chemical Derivatization, RNase digestion and signature products. Rapid Commun Mass Spectrom 22:3727–3734
11. Boccaletto P, Machnicka MA, Purta E, Piatkowski P, Baginski B, Wirecki TK, de Crécy-Lagard V (2018) MODOMICS: a database of RNA modification pathways. 2017 update. Nucleic Acids Res 46:D303–D307
12. Machnicka MA, Olchowik A, Grosjean H, Bujnicki JM (2014) Distribution and frequencies of post-transcriptional modifications in tRNAs. RNA Biol 11:1619–1629

2. Cartographie des modifications post-transcriptionnelles des ARNt de *S.aureus*

La spectrométrie de masse est un outil puissant pour la caractérisation des modifications post-transcriptionnelles des ARN. La méthode de purification et d'analyse par NanoLC-MS/MS mise en place a ainsi permis d'établir une cartographie partielle des modifications présentes dans 40 ARNt de *S. aureus*. Les modifications spécifiques des bactéries à gram positives telles que le mo^5U présente notamment dans les ARNt de *B. subtilis* a été localisé en position 34 des ARNt de *S. aureus*. La cartographie des ARNt établie permet l'étude dynamique des modifications des ARNt en réponse aux conditions environnementales rencontrées durant l'infection.

Biochimie 164 (2019) 60–69

Contents lists available at ScienceDirect

Biochimie

journal homepage: www.elsevier.com/locate/biochi

Research paper

Mapping post-transcriptional modifications in *Staphylococcus aureus* tRNAs by nanoLC/MSMS

Laura Antoine [a, 1], Philippe Wolff [a, b, 1], Eric Westhof [a], Pascale Romby [a, **], Stefano Marzi [a, *]

[a] Université de Strasbourg, CNRS, Architecture et Réactivité de L'ARN, UPR 9002, F-67000, Strasbourg, France
[b] Plateforme Protéomique Strasbourg Esplanade, CNRS, FR1589, F-67000, Strasbourg, France

ARTICLE INFO

Article history:
Received 15 March 2019
Accepted 3 July 2019
Available online 8 July 2019

Keywords:
Post-transcriptional tRNA modifications
nanoLC/MSMS
Staphylococcus aureus
2D gel isolation

ABSTRACT

RNA modifications are involved in numerous biological processes. These modifications are constitutive or modulated in response to adaptive processes and can impact RNA base-pairing formation, protein recognition, RNA structure and stability. tRNAs are the most abundantly modified RNA molecules. Analysis of the roles of their modifications in response to stress, environmental changes, and infections caused by pathogens, has fueled new research areas. Nevertheless, the detection of modified nucleotides in RNAs is still a challenging task. We present here a reliable method to identify and localize tRNA modifications, which was applied to the human pathogenic bacteria, *Staphyloccocus aureus*. The method is based on a separation of tRNA species on a two-dimensional polyacrylamide gel electrophoresis followed by nano liquid chromatography-mass spectrometry. We provided a list of modifications mapped on 25 out of the 40 tRNA species (one isoacceptor for each amino acid). This method can be easily used to monitor the dynamics of tRNA modifications in *S. aureus* in response to stress adaptation and during infection of the host, a relatively unexplored field.

© 2019 Elsevier B.V. and Société Française de Biochimie et Biologie Moléculaire (SFBBM). All rights reserved.

1. Introduction

1.1. A brief tour on the roles of tRNA modifications in bacteria

RNA modifications alter the chemical and physical properties of nucleotides and the biological functions of RNA. They are involved in numerous biological processes because they can impact RNA base-pairing formation, the structure of specific RNA motifs, protein recognition, translation and decoding properties, and RNA stability (for a review see Ref. [1]). RNA modifications can be present in many RNA species, but abundant noncoding RNAs such as tRNAs, rRNAs, and spliceosomal RNAs are the most heavily modified ones and depend on the modifications for their biogenesis and function. Today more than 170 modifications have been identified, primarily in tRNAs and rRNAs (http://modomics.genesilico.pl/modifications/) [2], and numerous RNA-modifying enzymes have been characterized [3–8]. The expression and activity of these enzymes can be modulated in response to environmental stresses, adding another layer of complexity in gene regulation. For example, in bacteria, deregulations of modifications in ribosomal RNAs (rRNA) can promote antibiotic resistance [9–11]. In tRNAs, modifications are central for folding, quality control, and efficient and accurate decoding. Also, they control gene expression during stress adaptation [12] and modulate interaction with human host [13].

tRNAs contain the largest number of modifications and the widest chemical diversity [2]. The complexity of tRNA modifications ranges from simple methylations on the base or the ribose to rather complex and large base hypermodifications, the synthesis of which generally depend on a cascade of enzymatic reactions [14]. Modifications have been shown to contribute to the highly conserved L-shaped structure, which is crucial for the interaction with a variety of proteins, the ribosome, and mRNAs. Interestingly, the distribution of the modified nucleotides along the tRNA molecule is conserved across evolution and reflects their two major functions in maintaining the tRNA structure and, ultimately, in decoding. Modified nucleotides concentrate in two hotspots - the anticodon loop and the tRNA core region, where the D- and

* Corresponding author.
** Corresponding author.
E-mail address: s.marzi@ibmc-cnrs.unistra.fr (S. Marzi).
[1] These authors contributed equally to this work.

https://doi.org/10.1016/j.biochi.2019.07.003
0300-9084/© 2019 Elsevier B.V. and Société Française de Biochimie et Biologie Moléculaire (SFBBM). All rights reserved.

Abbreviations

LC	Liquid Chromatography
MS	Mass Spectrometry
BHI	Brain Heart Infusion
EtBr	Ethidium Bromide
TBE	Tris Borate EDTA
HFIP	Hexafluoro Isopropanol
TEA	Triethylamine
TEAA	Triethylamine Acetate

TΨ-loops interact with each other (reviewed in Refs. [15,16]). tRNA modifications of the core are important for the stability of the tRNA structure. In this context, it was shown that they affect temperature adaptation in thermophilic as well as in psychrophilic organisms [17]. The modifications of the core region are also thought to be important for EF-Tu binding (U to T change at position 54 in the TΨ loop) [18] and since they are involved in the tertiary interactions maintaining the L-shape, they are expected to influence the binding of several proteins to the tRNA (i.e. aminoacyl tRNA synthetases and anticodon modification enzymes) [19,20]. tRNA modifications also facilitate tRNA-mediated transcriptional control through T-box riboswitches to sense intracellular availability of amino acids [21] and participate in quality control of tRNA integrity [22,23]. More recently, it was demonstrated that hypomodification of tRNAs in *Vibrio cholerae* induces their rapid decay mediated by the degradosome, demonstrating a new quality control mechanism [24].

Their major role in translation is due to their direct or indirect influence on the decoding process and fidelity of translation (i.e., [25]). Because the genetic code is degenerated, the 20 natural amino acids are encoded by 61 triplets that are recognized by 22–46 distinct tRNAs depending on the organism. Therefore, several tRNAs recognize more than one synonymous codon (i.e., the tRNA isoacceptors carry the same amino acid). The first nucleotide at position 34 of the anticodon (wobble base) can potentially form pairs non-complementary in the Watson-Crick sense (for a review see Refs. [26,27]). Detailed structural, physicochemical and kinetic studies of bacterial ribosomes associated with mRNA and aminoacyl-tRNAs have shown that the decoding center of the ribosome imposes specific constraints for the selection of a given codon by its cognate aminoacyl-tRNA by strongly favoring Watson-Crick pairs [25,28–34]. In miscoding induced by GU pairs, these pairs are in a Watson–Crick-like state promoted by tautomerization [27–29]. Interestingly, post-transcriptional modifications of nucleotide 34 can change the physicochemical behavior of the base (frequency of tautomerism), the spatial preference of the nucleotide (*syn/anti*, puckering of the ribose), the stability of codon-anticodon base-pairing and the structure of the anticodon loop itself, all contributing to the fidelity of the decoding process [25,35–40]. A typical example is given by $tRNATyr_{GUA}$, $tRNAAsn_{GUU}$, $tRNAAsp_{GUC}$ and $tRNAHis_{GUG}$, which can recognize both NAU and NAC codons, allowing G-C Watson-Crick base-pair with NAC codons and wobble G·U pair with NAU codons. These tRNAs (collectively harboring GUN anticodons), in eukaryotes and bacteria, present the Queuosine (Q) hypermodification on G34 [41]. Recently, Tuorto and colleagues [42] have demonstrated that, in mammals, the presence of Q affected translation speed. In the absence of Q modification, ribosomes pause on NAU codons, while NAC codons are much less affected [42]. Protein aggregation was observed for those genes enriched in NAU codons. This phenomenon seems to be species-specific since Q-modification in tRNAs in *S. pombe* has been shown to improve translation increasing the decoding speed of C-ending codons relative to U-ending codons [43]. Although not yet investigated, such deregulation based on mRNA codon content in response to the tRNA anticodon modification states, might take place in bacteria which display distinct codon usage bias (GtRNAdb [44]). Because tRNA modifications including the anticodon loop modifications can be modulated by various environmental changes, the proteome is expected to vary during adaptation [12]. To date, perturbations of tRNA modifications following physiological stress such as oxidation, temperature, pH, salinity, and nutrient starvation are well established in eukaryotes, but less well studied in bacteria [45,46].

1.2. Roles of tRNA modifications in pathogenic bacteria

During infection, pathogenic bacteria must adapt to the host environment, which is often scarce in nutrients and oxygen, and fastened with toxic metabolites and enzymes. They express virulence genes to interact with host tissues, to compete with the commensal flora, to avoid detection of the bacteria by the host immune system or to fight against it. Thus, pathogenic bacteria rapidly adapt to continuously changing environmental conditions and often regulate virulence gene expression at both the transcriptional and post-transcriptional levels. The analysis of the impact of RNA modifications in pathogenic bacteria during growth adaptation and infection has just started to be appreciated [47]. Recent studies in Gram-negative bacteria, have demonstrated that deletion of genes encoding RNA modification enzymes leaded to infection attenuation in mice, reduced colonization, decreased levels of the pro-inflammatory cytokines, reduced bacterial motility, replication in macrophages, and invasion of epithelial cells ([48] and references therein). For example, the deletion of the tRNA guanine transglycosylase gene (*tgt*) responsible for Q modifications reduces the translation of VirF, the transcription factor orchestrating *Shigella flexneri* virulence [49]. Moreover, tRNA modifications in pathogenic bacteria have been shown to modulate interaction with human host [13], or to regulate the expression of genes involved in the protection from oxidative stress, one of the main challenges that pathogenic bacteria must cope with during infection [50]. In mycobacteria, hypoxia modulates tRNA modification state to selectively translate codon-biased mRNAs for persistence genes [51]. In numerous Gram-negative (*Escherichia coli*, *Salmonella enterica*, *Aeromonas hydrophila*, *Pseudomonas fluorescens*, *P. aeruginosa* and *P. syringae*) and some Gram-positive pathogens (*Streptococcus pyogenes* and *S. suis*), the GidA/MnmE tRNA modification pathway, which leads to methylation of U34 in different tRNAs, has been implicated in the regulation of bacterial virulence [52]. Even if the precise mechanism remains unclear, an increased frequency of two-base frameshift has been reported [53]. Although these examples illustrate how the dynamic nature of tRNA modifications regulates virulence in various pathogenic bacteria, the roles of RNA modifications in *Staphylococcus aureus* have not been yet studied.

S. aureus is a Gram-positive opportunistic pathogen that is present in a third of the population on skin and in nostrils [54] as commensal bacteria, but is also responsible for a wide range of infections from minor skin abscesses to life-threatening diseases such as septicemia or toxic shock syndrome [55]. *S. aureus* represents a major health problem due to the insurgence of antibiotic multi-resistant strains in the hospital and community settings. Given the importance of tRNA modifications in several aspects of bacterial life, we decided to implement a rapid and easy method for their detection in *S. aureus* tRNAs for which little knowledge existed.

1.3. Analysis of tRNA modifications by mass spectrometry approaches

Mapping of post-transcriptional RNA modifications using mass spectrometry (MS) has existed for over 30 years [56]. The ability to get precise measure of molecular masses (less than 1 Da) provided the possibility to characterize modified residues in tRNAs using liquid chromatography coupled to mass spectrometry (LC/MSMS). Two complementary MS approaches have been developed. The first one implies total digest of tRNAs into nucleosides in order to identify the whole repertoire of modified nucleosides in one experiment [57]. The resulting nucleosides are thereby separated by reversed-phase high-performance liquid chromatography (HPLC) [58] and modifications detected using spectroscopy (e.g., UV) or by mass spectrometry [59]. The comparison of the HPLC chromatogram with known standard profiles and the characteristic measured mass-to-charge ratio (m/z) of the ionized nucleosides are contributing to the precise nucleoside identification. Atomic composition is finally obtained *via* collision induced dissociation (CID) tandem mass spectrometry (MSMS), providing a sensitive method for obtaining a survey of modified nucleosides in the tRNA sample. The second method is based on the generation of tRNA fragments produced from specific endoribonuclease digestion (e.g., RNase T1 cleaves every guanosine at their 3' side). The generated oligonucleotides with known 5′ and 3′-nucleotide identity [60] are then separated by HPLC and detected by MS. Fragments along the phosphodiester backbone by CID MSMS can be manually interpreted to localize the modification to a specific nucleotide. Thus, the mass and the sequence of each oligonucleotide is precisely identified by LC/MSMS allowing determination of the nature of each modification and their location in the tRNA sequence [61].

These two complementary methods have provided the first insights into tRNA modification dynamics following various stresses [56,62,63]. For nucleoside analysis, an ensemble of tRNAs can be studied to follow easily the changes of their modification patterns upon growth conditions while the LC/MSMS analysis of oligonucleotides requires purification of specific tRNA prior to digestion. This is usually done by affinity chromatography with a complementary DNA oligonucleotide linked to a solid resin or bead [63]. The recent development of Ultra-Performance LC (nanoLC) permits the careful separation of RNA fragments prior to the mass spectrometry analysis at very slow flow rates (hundreds of nL/min) in a column with a reduced resin diameter (<2 μm). This method requires smaller sample amounts, generates less chromatographic dilution and higher sensitivity. Because it is possible to detect very small amounts of tRNA-derived oligonucleotides, a two-dimensional gel electrophoresis (2D-PAGE) can be used to fractionate each tRNA species from bulk RNA extracts.

Here, we describe the use of this method and its application to the analysis of post-transcriptional modifications in *S. aureus* tRNAs. We also provide here for the first time a map of *S. aureus* tRNA modifications present in 26 out of the 40 tRNAs with different sequences, including at least one isoacceptor tRNA for each amino acid. We will also discuss applications to better address the roles of tRNA modifications in the physiopathology of *S. aureus*.

2. Material and methods

2.1. Bacterial growth

S. aureus HG001 strain, a derivative of RN1 (NCT8325) strain with restored *rbsU* (a positive activator of SigB), was used for tRNA isolation. The strain still contains a mutation at *tcaR*, a transcriptional regulator involved in teicoplanin susceptibility and biofilm [64]. *S. aureus* strain was manipulated under a specific hood in a dedicated room for manipulating class II pathogens. Stock culture in glycerol 25%, conserved at −80 °C were plated on a blood-agar Petri dish and grown at 37 °C overnight in Memmert model 100 incubator. One single clone was picked and grown in 2 mL Brain Heart Infusion (BHI from Sigma-Aldrich), incubated at 37 °C with a 180 rpm agitation overnight in a Stuart® orbital incubator S1600C. A preculture (100 μL) was added in 10 mL BHI medium ($OD_{600nm} = 0.05$), the bacterial growth was regularly checked until it reached an $OD_{600nm} = 3$ with a Thermospectronic Genesys 20 spectrophotometer (~4 h of culture at 37 °C stirring at 180 rpm).

2.2. Cell lysis and total RNA extraction

Cells were pelleted by centrifugation at 3750 rpm (3000 g) for 15 min at 4 °C in a Beckman Coulter Allegra X12-R centrifuge with a SX4750A rotor. Supernatant was carefully removed and the pellet (200 mg) was resuspended in 1 mL of RNAPro® Solution (MP Biomedicals, CA). Cells lysis was performed using a FastPrep®-24 with the 24 × 2 mL holder at 6 m/s speed in 2 mL FastPrep® tubes containing 0.1 mm zirconium silicate beads from FastRNA® pro blue kit (MP biomedicals, CA).

Total RNA purification followed the procedure described for the FastRNA Pro Blue Kit (MP Biomedicals, CA). RNA was further purified by adding 1/2 volume of chloroform:isoamyl alcohol (19:1), vortexed 10 s before precipitation of the RNA in the aqueous phase obtained by adding 3 vol of cold absolute ethanol (1.2 mL) in 2 mL Eppendorf tubes at −20 °C overnight. RNA was precipitated by centrifugation at 13000 rpm (18000 g) for 15 min at 4 °C using an Eppendorf 5417R centrifuge with a F45-30-11 rotor. The RNA pellet was washed with 500 μL of 80% cold ethanol and dried 20 min under vacuum in a Speed Vac® from Savant, before being resuspended in 200 μL of milliQ water. RNA concentration was determined by measuring absorbance at 260 nm with a Nanodrop ND-1000 spectrophotometer. Total RNA concentration was adjusted to 2 μg/μL. For phenol or chloroform extraction, work has to be done under a fume hood. Eppendorf tubes, tips, and buffers were RNase-free.

2.3. tRNA purification, 1st dimension PAGE

The first dimension gel electrophoresis was performed under denaturing conditions using 15% polyacrylamide gel (15% acrylamide:bisacrylamide 19:1 solution from Roth, 8 M urea, 1 × TBE buffer from Euromedex®) (Fig. 1A). Before loading the RNA sample, the gel was pre-run at 900 V for 20 min. One volume of urea-blue solution (urea 8 M, bromophenol blue and xylen cyanol 0.025%) was added to 5 μL containing 10 μg of total RNA. The sample was heated at 90 °C during 2 min before loading on the gel. After 15 h migration at 500 V at 20 °C, the gel was stained with 0.5 μg/mL EtBr solution (from Sigma-Aldrich) by soaking the gel during 5 min, then washed with milliQ water and visualized on a High performance 2UV™ transilluminator from UVP. The gel slice containing 5S rRNA and tRNAs was cut to perform the second dimension gel.

2.4. Individual tRNA purification, 2nd dimension PAGE

The second dimension was performed under semi-denaturing conditions. The first dimensional gel slice (see § 2.3) was first placed horizontally at the top and between two glass plates (20 × 20 cm). Then a solution containing 20% polyacrylamide (polyacrylamide-bisacrylamide 19:1), 4 M urea, 1X TBE and 0.06% of ammonium persulfate and TEMED was poured between the plates. Once polymerized, the gel was run at 6 W (200 V) for 24 h at 20 °C using BioRad Protean II xi Cell. The gel was stained with EtBr as described in paragraph § 2.3 before UV visualization (Fig. 1B). Gel

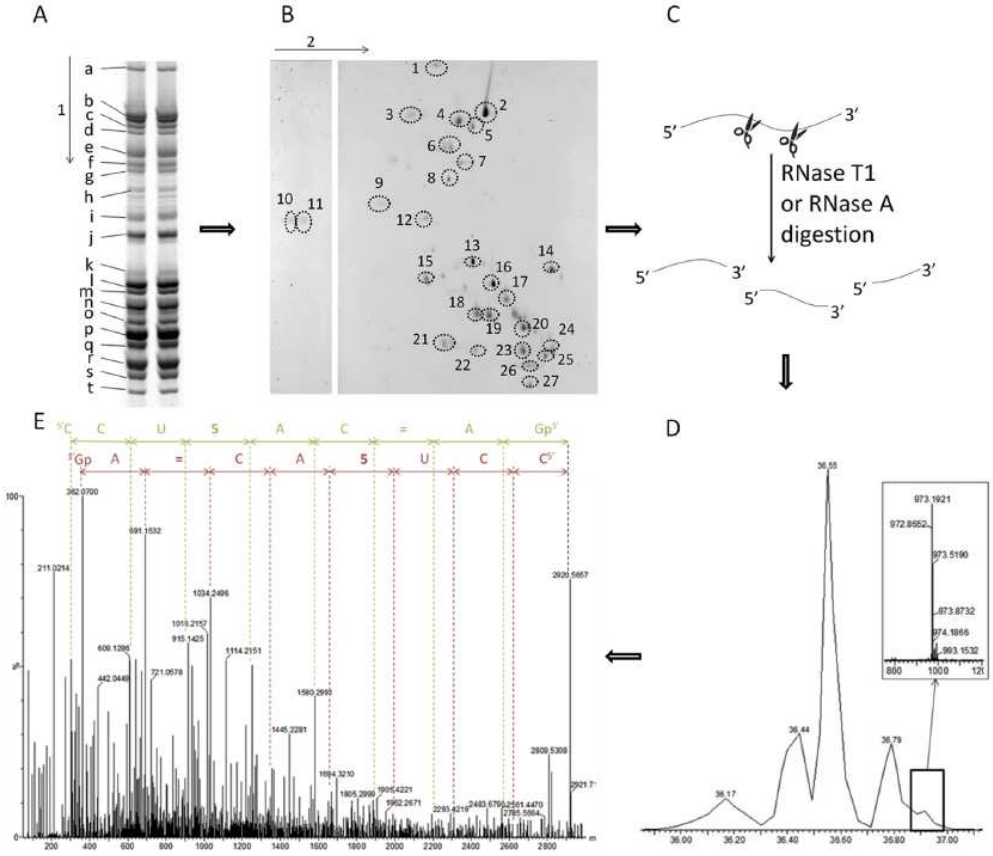

Fig. 1. Complete protocol for nanoLC/MSMS analysis of *S. aureus* tRNAs from isolation to modification mapping. The five main steps of the protocol are as follow. *A. First-dimension PAGE.* Total RNA was migrated on the first-dimension gel electrophoresis (denaturing 15% PAGE with 8 M Urea). The gel slice containing "tRNA-size" (25000–150000 Da) RNA species migrating close to 5S rRNA, was cut. Arrow 1 indicates the direction of gel migration. The gel slice containing the tRNAs is deposited on the top of the second-dimension gel. In parallel, the 21 visible bands (colored by Ethidium Bromide and named from *a* to *t*) were cut individually, digested with RNase T1 and analyzed by nanoLC/MSMS to determine which tRNAs are present in each band (see at the end of the legend). *B. Second-dimension PAGE.* Separation of the tRNAs from the first-dimension gel slice in the second-dimension gel electrophoresis (semi-denaturing 20% PAGE with 4 M Urea). Arrow 2 indicates the direction of migration. After staining, the gel was divided into three large areas to be analyzed by the Gel Doc™ EZ imager. Here only the middle (left) and bottom (right) parts are reported but the two pieces are coming from the same experiment. No spots were visible on the upper part of the gel (not shown). Each of the 23 spots (numbered from 1 to 23) was cut and used for the following steps. The identity of these spots, as obtained from the complete analysis is given at the end of the legend. *C. RNases in gel digestion.* The spots were subjected to RNase T1 or RNase A digestion, desalted, and used for the liquid chromatography separation of the fragments. *D. nanoLC (Ultra-Performant Liquid Chromatography) and MS analysis.* The RNase derived fragments from each 2D spot are separated on the BEH C18 column with a 300 nL/min flow rate. An example from spot 17 (tRNAVal$_{UAC1-2-3}$) digested with RNase T1 is given. Each peak is subjected to MS (insert) and MSMS (E) to determine its sequence and the presence of modifications. *E. MSMS analysis.* Electrospray-Ionization Collision-Induced Dissociation (ESI CID) spectrum obtained for the $^{5'}$CCUSUAC = AGp$^{3'}$ oligonucleotide (m/z = 972.87, triple charged (-3H$^+$)) from the *S. aureus* tRNAVal$_{UAC1-2-3}$. The profile obtained from the MSMS (fragmentation) analysis is shown with its sequence given from its 5′ nucleotide (sequence in green, c ion series) or from its phosphorylated 3′ nucleotide (sequence in red, y ions series). The localization of a N6-methyladenosine (m^{6}A) is showed with its symbol " = ". **1D bands**: *a*: tRNASer$_{UGA3}$; *b*: 5S rRNA fragment + tRNASer$_{GCU}$; *c*: 5S rRNA fragment + tRNASer$_{UGA1}$; *d*: tRNATyr$_{GUA2}$; *e*: tRNALeu$_{UAG}$; *f*: tRNALeu$_{UAA1-2}$; *g*: tRNALeu$_{CAA}$; *h*: tRNAHis$_{GUG1-2}$; *i*: tRNAThr$_{UGU1-2-3}$ + tRNAHis$_{GUG1-2}$; *j*: tRNAArg$_{ACG1-2}$ + tRNAMet$_{CAU1}$; *k*: tRNAGly$_{GCC1-2p}$ (proteinogenic); *l*: tRNAAsp$_{GUC1-2-3-4}$ + tRNAIle$_{GAU1-2}$; *m*: tRNAMet$_{CAU1I}$; *n*: tRNAVal$_{UAC1-2-3}$; *o*: tRNAVal$_{UAC1-2-3}$ + tRNAGlu$_{UUC1}$; *p*: tRNAPro$_{UGG1-2}$ + tRNAAla$_{UGC1-2-3}$; *q*: tRNAAla$_{UGC1-2-3}$ + tRNAPhe$_{GAA}$; *r*: tRNAGly$_{UCC1-2p}$ + tRNAAsn$_{GUU1-2-3}$ + tRNALys$_{UUU2-3}$; *s*: tRNAGln$_{UUG1-2}$ + tRNATrp$_{CCA}$; *t*: tRNAGly$_{UCC1-3np}$ (non-proteinogenic). **2D spots**: 1: tRNASer$_{UGA3}$; 2: 5S rRNA fragment; 3: tRNASer$_{GCU}$; 4: tRNASer$_{UGA1}$; 5: tRNATyr$_{GUA2}$; 6: tRNALeu$_{UAG}$; 7: tRNALeu$_{UAA1-2}$; 8: tRNALeu$_{CAA}$; 9: tRNAHis$_{GUG1-2}$; 10: tRNAArg$_{ACG1-2}$; 11: tRNAThr$_{UGU1-2-3}$; 12: tRNAMet$_{CAU1}$; 13: tRNAGly$_{GCC1-2}$; 14: tRNAAsp$_{GUC1-2-3-4}$; 15: tRNAIle$_{GAU1-2}$; 16: tRNAMet$_{CAU1I}$; 17: tRNAVal$_{UAC1-2-3}$; 18: tRNAGlu$_{UUC1}$;: 19: tRNAPro$_{UGG1-2}$; 20: tRNAAla$_{UGC1-2-3}$; 21: tRNAPhe$_{GAA1}$; 22: tRNAGly$_{UCC1-2p}$ (proteinogenic); 23: tRNAAsn$_{GUU1-2-3}$; 24: tRNALys$_{UUU2-3}$; 25: tRNATrp$_{CCA}$; 26: tRNAGln$_{UUG1-2}$; 27: tRNAGly$_{UCC1-3np}$ (non-proteinogenic). 1D bands and 2D spots are also summarized in Table 1.

pictures were taken with a Gel Doc™ EZ imager with its corresponding 16 × 12 cm UV tray.

2.5. In gel RNase digestion

Gel spots containing tRNAs were excised with a blade scalpel and dried under vacuum for 10 min (Speed Vac®). Digestion of the tRNAs with specific RNase was carried out directly on the gel fragments. The gel spots were incubated with 20 μL of 1U/μL of RNase T1 from Thermo Fisher Scientific (cleavage at G residues) in ammonium acetate 100 mM (pH 6.8) and incubated at 50 °C for 3 h followed by a 37 °C overnight incubation under 300 rpm constant

agitation. Alternatively, 20 μL of 0.01 U/μL of RNase A from Thermo Fisher Scientific (cleavages at C and U residues) in ammonium acetate 100 mM were added to the gel spots and the samples were incubated at 60 °C during 3 h, followed by a 37 °C overnight incubation under 300 rpm constant agitation. The samples were stored at −20 °C or immediately desalted, after removal of the gels by centrifugation (10 min, at 18000 g, at 4 °C), using ZipTIP C18 (Millipore) prewet with acetonitrile 50% in milliQ water (3 × 10 μL) and 200 mM ammonium acetate (3 × 10 μL). The supernatant containing the digested tRNA fragments passively eluted from the gel, was loaded on the column, which was then washed with 200 mM ammonium acetate (7 × 10 μL) followed by milliQ water (5 × 10 μL). Finally, the fragments were eluted with 10 μL of 50% acetonitrile in milliQ water and dried for 25 min under vacuum (Speed Vac®) (Fig. 1C).

2.6. nanoLC/MSMS of RNA oligonucleotides

The pellet containing the oligonucleotides is resuspended in 3 μL of milliQ water. The oligonucleotides were then separated on nanoLC Acquity UPLC peptide BEH C18 column (130 Å, 1.7 μm, 75 μm × 200 mm) using a nanoAcquity UPLC system (Waters). The column was pre-equilibrated in Buffer A (200 mM HFIP (Hexafluoroisopropanol), 7 mM TEA (Triethylammonium), 7.5 mM TEAA (Triethylammonium acetate, pH 7.5) at a flow rate of 300 nL/min. After loading on the column, the RNase digestion products were eluted using a step gradient with two segments. The first consists of a gradient 15–35% of solution B (100% methanol (MeOH)) for 2 min, followed by the second step where the solution B reaches 50% (during 20 min at the same flow rate). Finally, the MeOH solution is decreased to 15% during 25 min. The column is then re-equilibrated in Buffer A during 20 min (Fig. 1D).

MS and MSMS analysis were performed using a SYNAPT G2-S HDMS from Waters equipped with a NanoLockSpray-ESI source in negative sensitivity mode with a capillary voltage set to 2.6 kV and sample cone to 30 V. Source was heated to 130 °C. For MS analysis, a mass range from 550 to 1500 (m/z) was used followed by Collision Induced Decay (CID) fragmentation of most intense signals with a m/z detection range of fragments from 50 to 2000 with 1s scans (Fig. 1E).

2.7. Data analysis

Chromatograms and spectra were processed using the Masslynx software from Waters (V4.1). CID fragment spectra were deconvoluted by MaxEnt3 tool to convert the m/z measured from multicharged ions into singly charged ones. Spectra were then manually sequenced using oligonucleotide fragmentation ion nomenclature [65]. Sequences are deduced by calculating mass difference between consecutive fragment ions singly charged. Typically, the most intense ion series (y and c) were used. Correct manual annotation was checked using MongoOligo online calculator (http://mods.rna.albany.edu/masspec/Mongo-Oligo), with a maximum tolerance of 0.05 Da between the calculated mass and the measured mass for parent and fragment ions. The tRNA genomic sequences were obtained from the HG001 genome [66].

3. Results and discussion

3.1. A global view of S. aureus tRNA modifications

The above protocol is fast and easily implementable. Briefly, the pool of tRNAs extracted from *S. aureus* cultures was isolated by collecting RNA species of sizes smaller than the 5S rRNA (118 nucleotides), which are clearly visible on a denaturing (8 M Urea) 1D gel (Fig. 1A). The tRNA samples were loaded on two different lanes on 1D gel. One lane was used for direct nanoLC/MSMS analysis and the other one was deposited on top of semi-denaturing gel for the second-dimension. The bands from the 1D gel were cut and analyzed by nanoLC/MSMS method to assign each tRNA (Fig. 1A). Several bands contained different RNA species (i.e., band *b* contains both a 5S fragment and $tRNASer_{GCU}$; and band *j* contains both $tRNAArg_{ACG1\text{-}2}$ and $tRNAMet_{CAU1}$). To assign unambiguously fragments to the different tRNAs, we then proceeded to a further purification step using the second-dimension gel electrophoresis under semi-denaturing conditions (4 M urea) (Fig. 1B). The 1D bands gave rise to several spots where tRNAs are migrating individually (i.e. band *b* was resolved into spots 2 and 3 containing 5S rRNA and $tRNASer_{GCU}$, respectively; and band *j* was resolved into spots 10 and 12 corresponding to $tRNAArg_{ACG1\text{-}2}$ and $tRNAMet_{CAU1}$, respectively). Each spot was subjected to the in-gel RNase T1 digestion (Fig. 1C) followed by nanoLC/MSMS analysis (Fig. 1D–E), which provided information on the sequences and on the presence of modifications.

Sixty-one tRNA genes are present in *S. aureus* HG001 [63]. They are transcribed from eleven *loci* as single genes ($tRNASer_{UGA1}$, $tRNAArg_{CCG}$, $tRNAArg_{UCU}$ and $tRNAGln_{UUG3}$) or organized into seven operons (I to VII, Fig. 2) sometimes together with rRNAs. The number of isoacceptor tRNAs varies between one (Cys, Trp and elongator tRNAMets) to seven (tRNAGly) (Fig. 2). With the exclusion of the non-proteinogenic tRNAGly and the tRNACys, we could determine fragments belonging to 25 different tRNAs (Table 1) representing 46 tRNA genes, at least one isoacceptor for each tRNA. Some isoacceptors have identical sequences and cannot be distinguished in our analysis (the three $tRNAAla_{UGC}$, the two $tRNAArg_{ACG}$, the three $tRNAAsn_{GUU}$, the four $tRNAAsp_{GUC}$, two of the three $tRNAGln_{UUG}$, the two $tRNAGly_{GCC}$, the two proteinogenic $tRNAGly_{UCC}$, two of the three non-proteinogenic $tRNAGly_{UCC}$, the two $tRNAIle_{GAU}$, the two $tRNALeu_{UAA}$, the two $tRNAPro_{UGG}$, the three $tRNAThr_{UGU}$ and the three $tRNAVal_{UAC}$). For the other tRNAs, we could determine exactly from which gene they were transcribed. Only fourteen tRNAs could not be detected (indicated with blue dots in Fig. 2; $tRNAGlu_{UUC2}$ and $tRNAGlu_{UUC3}$ are identical and therefore counted as single species). Three of them are transcribed from a single gene while the others belong to operons from which other tRNAs were isolated in our analysis. Since the most intense spots on the 2D-gel were all analyzed, it is possible that they are less abundant (less transcribed or more rapidly degraded) and more difficult to be detected. To complete the *S. aureus* tRNA analysis, it would be necessary to purify them individually using biotinylated oligonucleotides, which could specifically fish them from total RNA extracts [63].

Several modifications were detected on the tRNA fragments (Fig. 3) deriving from the core region (D and TΨ stem-loops), the variable region, and the anticodon loop. Modifications at nucleotides in the core region and variable loop include dihydrouridine (D), 1-methyladenosine (m^1A), 7-methylguanosine (m^7G), and thymidine (T). A high diversity of modifications was found in the anticodon loop and ten of them concentrate at positions 34 and 37 (Table 1, Fig. 3). Using the present strategy, pseudouridine (Ψ) cannot be detected since its mass is indistinguishable from that of uridine. In order to trace them, we use *N*-cyclohexyl-N′-β-(4-methylmorpholinium) ethylcarbodiimide *p*-tosylate (CMC) derivatization which modified only Ψ under alkaline conditions (at pH above 10) [67]. Although such modification can be visualized by mass spectrometry [68,69], we unfortunately lost it during the MSMS fragmentation step preventing the detection of any Ψ. This technical issue could be solved by the use of acrylonitrile, which is

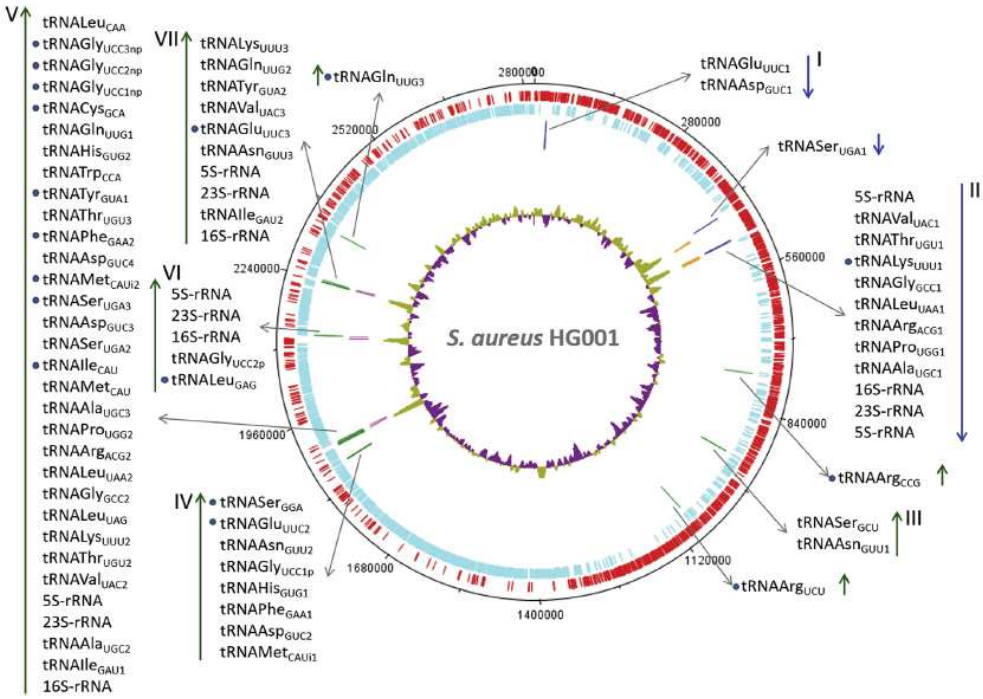

Fig. 2. ***Staphylococcus aureus*** **HG001 tRNA operons organization.** The sixty-one genes present in *S. aureus* HG001 [66] were placed on a circular genome representation using DNAPlotter [96]. The tRNA genes are expressed from eleven loci sometimes as single gene, and more often as operons, which also contain rRNA genes. tRNAs which were not detected in the present study are marked with a blue dot. tRNA genes on the positive and negative strands are represented as long blue and green tracks, respectively. rRNA genes on the positive and negative strands are represented as yellow and pink tracks, respectively. Coding sequences on the positive and negative strands are represented as red and cyan tracks, respectively. Mean centered GC% plot is represented in mustard (above-mean) and violet (below mean).

more resistant to the fragmentation [70].

Table 1 shows the regions that were probed for each analyzed tRNA. Four tRNAs are almost complete (coverage > 70% for the tRNASer$_{UGA3}$, the tRNAPro$_{UGG1-2}$, the tRNALys$_{UUU2-3}$ and the tRNAGlu$_{UUC1}$). On average almost 60% of the tRNA sequences were analyzed and, for most of the tRNAs, the core region and the anticodon loop were covered with the exception of tRNALeu$_{UAA1-2}$ and tRNATrp$_{CCA}$, for which we could not cover any nucleotide of the anticodon loop, and tRNAArg$_{ACG1-2}$ and tRNAGln$_{UUG1-2}$, for which we could not detect fragments including their anticodons (nucleotides 34–36). In this study, we used RNase T1 and RNase A since they are highly active enzymes able to hydrolyze RNA in the gel. RNase T1 cleaves specifically at guanosines while RNase A cleaves at pyrimidine residues. To enhance the coverage, we tested other RNases. We first used RNase MC1, which cleaves at the 5′ of uridine and pseudouridine [71] but no significant gel digestion of the tRNAs could be obtained (data not shown). We finally adapted RNase U2, which cleaves at purines with a slight specificity to adenosine [72], and preliminary data revealed that RNase U2 is able to digest RNAs contained in gel. By using multiple RNases with different base specificity, oligonucleotide fingerprints can be overlapped to provide full sequence coverage and to complete the mapping of tRNA modifications.

Overall, *S. aureus* tRNA modification types and their localization are similarly found in other Gram-positive bacteria such as *Bacillus subtilis* [2] and *Lactococcus lactis* [73] (Fig. S1). *S. aureus* specific features are discussed thereafter.

3.2. Individual tRNA modification maps

All modifications that were detected in the analyzed *S. aureus* tRNAs are detailed in Table 1. As expected, most of them were localized in the core regions and in the anticodon loops. In general, the modifications were also conserved in many other bacteria.

Our work highlights the possible roles of the modifications at position 34 and 37 in tRNA anticodons for fidelity maintenance, codon selection and discrimination in *S. aureus*. For instance, Q at position 34 of tRNATyr$_{GUA}$ was proposed to efficiently discriminate tyrosine codons (UAU and UAC) from stop codon during translation in eukaryotes (review in Ref. [14]) and to increase affinity for UAU codons [42] in bacteria. As expected, we could detect Q34 in tRNATyr$_{GUA2}$, but also in tRNAAsn$_{GUU1-3}$, tRNAAsp$_{GUC1-4}$ and tRNAHis$_{GUG1-2}$.

Modification at U34 is regularly found in tRNAs that read split codon-box families where the synonymous A- and G-ending codons encode a different amino acid than the U- and C-ending codons. We detected three major modifications at U34 (Table 1). The mo^{5}U (5-methoxyuridine (5)) [74] was present in eight *S. aureus* tRNAs. This modification is only found in Gram-positive bacteria and is believed to enhance translational fidelity by the ribosome [27,39,75]. We found cmnm^{5}s^{2}U (5-carboxymethylaminomethyl-2-thiouridine ($)) in the *S. aureus* tRNALys$_{UUU2-3}$. This hypermodification is ubiquitous in all bacteria and is usually detected in several tRNAs (Lys$_{UUU}$, Gln$_{UUG}$, Glu$_{UUC}$, Trp$_{UCA}$ or Leu$_{UAA}$). Finally, mnm^{5}s^{2}U (5-methylaminomethyl-2-thiouridine (S)) was observed

Table 1
Characterization of RNA modifications in 26 *Staphylococcus aureus* tRNAs. Sequences of characterized tRNAs are reported with their respective coverage percentages. In the sequences the color code is as follow: **red** nucleotides indicate oligonucleotides fragments obtained by RNase T1 digestion, **green** nucleotides indicate oligonucleotides fragments obtained by RNase A digestion (overlapping sequences are in red) while **black** nucleotides represent regions that could not be analyzed. The various regions of the tRNAs are visualized by colors according to the tRNA database http://trna.bioinf.uni-leipzig.de/as follow: sequences highlighted in orange are for the two complementary strands of the anticodon arm; sequences highlighted in green are for the two complementary strands of the D-stem; sequences highlighted in blue are for the two complementary strands of the acceptor-stem; sequences highlighted in pink are for the two complementary strands of the T-stem; sequences highlighted in light blue are for the CCA at the 3'. Modifications are indicated with symbols described in Fig. 3B.

1D	2D	A. A.	Antioc.		Acc-stem		D-stem	D-loop	D-stem		Ac-stem	Ac-loop	Ac-stem	V-region	T-stem	T-loop	T-stem	Acc-stem		CCA	Cover. (%)	HG001	Operon
				-1	1	8	10	14	22	26	27	32	39	44	49	53	61	66	73	74			
p/q	20.	Ala	UGC 1-2-3	-	GGGGGCU	UA	GCUC	AGCUGGGA	GAGC	G	CCUGC	UU5GCAC	GCAGG	AGGUC	AGCGG	UUCGAUC	CCGCU	AGUCUCC	A	CCA	38	00443 01812 01823	II V V
j	10.	Arg	ACG 1-2	-	GCGCCCG	UA	GCUC	AAUDGGAUA	GAGC	G	UUUGA	CUACGKA	UCAAG	AG7UU	AUGGG	UUCGACU	CCUAU	CGGGCGC	G	CCA	38	00441 01814	II V
r	23.	Asn	GUU 1-2-3	-	UCCACAG	UA	GCUC	AGUGGUA	GAGC	U	AUCGG	CUQUU6A	CCGAU	CGGUC	GUAGG	UUCGAGU	CCUAC	CUGUGGA	G	CCA	49	00874 01758 02198	III IV VII
l	14.	Asp	GUC 1-2-3-4	-	GGUCUCG	UA	GUGU	AGCGGDDA	ACAC	G	CCUGC	CUQUCAC	GCAGG	AGAUC	GCGGG	TUCGAUU	CCCGU	CGAGACC	G	CCA	63	00021 01762 01805 01808	I IV V V
s	26.	Gln	UUG 1-2	-	UGGGCUA	UA	GCCA	AGCGGUA	AGGC	A	ACGGA	CUUUGAC	UCCGU	CACUC	GUUGG	UUCGAAU	CCAGC	UAGCCCA	G	CCA	27	01799 02194	V VII
o	18.	Glu	UUC 1	-	GGCUCCU	UG	GUCA	AGCGGDDA	"GAC	A	CCGCC	CUSUCAC	GGCGG	UAAC	ACGGG	TUCGAGU	CCCGU	AGGAGUC	A	CCA	85	00020	I
k	13.	Gly	GCC 1-2	-	GCAGAAG	UA	GUUC	AGCGGUA	GAAU	A	CAACC	UUGCCAA	GGUUG	GGGUC	GCGGG	UUCGAAU	CCCGU	CUUCUGC	U	CCA	59	00439 01816	II V
r	22.	Gly	UCC 1-2 p	-	GCGGGUG	UA	GUUU	AAUGGCA	AAAC	C	UCAGC	CUSCCAA	GCUGA	UGUU	GUGGG	UUCGAUU	CCCAU	CACCCGC	U	CCA	61	01759 02088	IV VI
i/h	9.	His	GUG 1-2	G	GCGGUUG	UG	GUGA	AGUGGDDA	"CAC	A	UCGGA	UUQUGK/GU	UCCGA	CAUUC	GAGGG	TUCGAUC	CCCUU	CAGCCGC	C	CCA	68	01760 01800	IV V
l	15.	Ile	GAU 1-2	-	GGGCCUA	UA	GCUC	AGCUGGDDA	GAGC	G	CACGC	CUGAU6A	GCGUG	AGGUC	GGUGG	UUCGAGU	CCACU	UAGGCCC	A	CCA	53	01824 02201	V VII
g	8.	Leu	CAA	-	GCCGGUG	UG	GCGG	AAUDGGCAG	ACGC	G	CGGGA	CUBAA+A	UCCCG	UUCCACUUGUGGAGU	GUCGG	UUCGACC	CCGAC	CACCGGU	A	CCA	52	01794	V
f	7.	Leu	UAA 1-2	-	GCCGGGG	UG	GCGG	AACDGGCAG	ACGC	A	CAGGA	CUUAAAA	UCCUG	CGGUGAGAGAUCACCGU	ACCGG	TUCGAUU	CCGGU	CCUCGGC	A	CCA	57	00440 01815	II V
e	6.	Leu	UAG	-	GCGGGUG	UG	GCGG	AAUDGGCAG	ACGC	A	CUAGA	CUSAGKA	UCUAG	CGCCUUACGGCGU	GGGGG	TUCGACU	CCCUU	CACCCGC	A	CCA	66	01817	V
r	24.	Lys	UUU 2-3	-	GAGCCAU	UA	GCUC	AGUUGGUA	GAGC	A	UCUGA	CUS/SUU6/HA	UCAGA	GGGUC	AGAGG	TUCGAAU	CCUCU	AUGGCUC	A	CCA	74	01818 02193	V VII
m	16.	Met	CAU i1	-	CGCGGGA	UG	GAGC	AGUUCGGUA	GCUC	G	UCGGG	CUCAUAA	CCCGA	AGGUC	GGUGG	TUCAAAU	CCGCC	UCCCGCA	A	CCA	44	01763	IV
j	12.	Met	CAU	-	GGCGGUG	UA	GCUC	AGCUGGCDA	GAGC	G	UACGG	UUMAU=C	CCGUG	AGGUC	GGGGG	TUCGAUC	CCCUC	CACCGCC	A	CCA	65	01811	V
q	21.	Phe	GAA 1	-	GGUUCAG	UA	GCUC	AGUUGGUA	GAGC	A	AUGGA	UUGAAKC	UCCAU	GUGUC	GGCAG	UUCGACU	CUGUC	CUGAACC	A	CCA	45	01761	IV
p	19.	Pro	UGG 1-2	-	CGGGAAG	UA	GCUC	AGCUUGGUA	GAGC	A	CUUGG	UUSGGKA	CCAAG	GGGmUC	GCAGG	TUCGAAU	CCUGU	CUUCCCG	A	CCA	72	00442 01813	II V
b	3.	Ser	GCU	-	GGAAACG	UA	CUCA	AGUUGGCUGA	"GAG	G	GCCC	CUGCU6A	GGGUG	UAGUCGCGAAAGCGGCGC	GAGGG	TUCGAAU	CCCUC	CGUUUCC	G	CCA	66	00873	III
c	4.	Ser	UGA 1	-	GGAGGAA	UA	CCCA	AGUCCGGCUGA	AGGG	A	UCGGU	CUSGA+A	ACCGA	CAGGGGCUUAACGGCUCGC	GGGGG	UUCGAAU	CCCUC	UUCCUCC	G	CCA	31	00383	-
a	1.	Ser	UGA 3	-	GGAGGAA	UA	CCCA	AGUCCGGCUGA	"GGG	A	UCGGU	CUSGA+A	ACCGA	CAGGGCCUUAACGGGCCGC	GGGGG	TUCGAAU	CCCUC	UUCCUCC	G	CCA	70	01807	V
i	11.	Thr	UGU 1-2-3	-	GCCGGCC	UA	GCUC	AAUDGGUA	GAGC	A	ACUGA	CUSGU6A	UCAGU	AGGUU	GGGGG	TUCAAGU	CCUCU	GGCCGGC	A	CCA	34	00437 01803 01819	II V V
s	25.	Trp	CCA	-	AGGGGCA	UA	GUUC	AACGGUA	GAAU	A	GAGGU	CUCCAAA	ACCUU	UGGU	GUGGG	UUCGAUU	CCUAC	UGCCCCU	G	CCA	45	01801	V
d	5.	Tyr	GUA 2	-	GGAGGGG	UA	GCGA	AGUGGCDAA	"CGC	G	GCGGA	CUQUA+A	UCCGC	UCCUUCGGGUUC	GGCAG	UUCGAAU	CUGCC	CCCCUCC	A	CCA	64	02195	VII
n/o	17.	Val	UAC 1-2-3	-	GGAGAAU	UA	GCUC	AGCUGGGA	GAGC	A	UCUGC	CUSAC=A	GCAGA	GGGUC	GGCGG	UUCGAAC	CCGUC	AUUCUCC	A	CCA	54	00436 01820 02196	II V VII

in tRNAGlu$_{UUC}$ and tRNALys$_{UUU}$ as shown in several Gram-negative bacteria like *Escherichia coli*. The hypermodifications (S and $) at U34 are primarily observed on tRNAs carrying U34 and U35 (Table 1). In fact, these two uridines are essential recognition determinants for the enzyme MnmA, which catalyzes the thiolation at position 2 of U34 [76]. Intriguingly, *S. aureus* tRNALys$_{UUU2-3}$ presented both "$" and "S" modifications at U34 (Fig. S2). Such heterogeneity was also observed at position 37 where t^{6}A (N6-threonylcarbamoyladenosine (6)) was present on the same fragment presenting S at U34, while an unknown adenosine hypermodification (for a total mass of 530 Da for the nucleotide) was observed for the fragment containing $34. To estimate the relative abundance of the two different modification patterns of tRNALys$_{UUU2-3}$, the area of the peaks of the two distinct oligonucleotides in the mass chromatogram was determined (Figs. S2E–F). The comparison reveals that the oligonucleotide containing the anticodon with unknown modified adenosine (H) represents 34.6% of the total tRNALys$_{UUU2-3}$. Further analysis will be required to identify this novel modification, to carefully quantify its abundance and to understand the functional consequences of such heterogeneity in tRNALys.

The modification contents were also analyzed on the unique elongator tRNAMet$_{CAU}$ and one initiator tRNAMet$_{iCAU}$ species. The important determinants of the initiator tRNA in all bacteria are the absence of a Watson–Crick base pair between positions 1 and 72 in the acceptor stem and the presence of three conserved consecutive G:C base pairs in the anticodon stem [77]. The peculiarity of the acceptor stem accounts for the high specificity of the methionyl-tRNA^{fMet} transformylase (FMT) for methionylated tRNAs over other aminoacylated species [78,79], while the anticodon stem-loop is important for IF3 discrimination of non-initiator tRNAs in the 30S translation initiation complex [80–83]. In addition, formylation of the methionine prevents misrecognition of the initiator tRNA by EF-Tu [84,85]. No modification could be detected in the anticodon of the initiator tRNAMet (Table 1). A search in the Modomics database (http://modomics.genesilico.pl [2,86]) shows that the absence of modification in the anticodon is a trait common to other bacterial initiator tRNAs (e.g., *Lactococcus lactis* and *Streptomyces griseus*), except that a methylation on the ribose at C32 was observed in *Thermus thermophilus* and in *E. coli*. The absence of modification for the initiator tRNA anticodon could be another peculiarity of the translation initiation complex in which decoding is monitored at level of the 30S subunit bound to the initiation factors IF1, IF2 and IF3 [87].

For the elongator tRNAMet$_{CAU}$, we identified a N4-acetylcytidine (M) at position 34 and a N6-methyladenosine (=) at position 37. Modifications at C34 and A37 are present in most of the bacterial elongator tRNAMet and believed to be important to maintain fidelity. For instance, the M34 modification in *E. coli* elongator tRNAMet was shown to prevent misreading of the AUA isoleucine codon [88]. Indeed, the NAU anticodons are particular because besides the tRNAMet, one tRNAIle isoacceptor also carries the anticodon CAU (Fig. 2). In addition, *S. aureus* encode two other tRNAIle isoacceptors with the GAU anticodons. In various

A

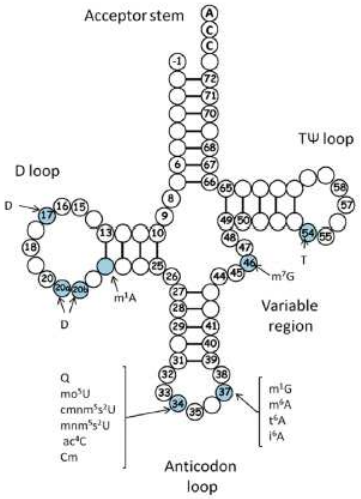

B

Modification	Symbol	tRNA	position
Dihydrouridine	D	Leu UAA, Leu UAG, Leu CAA, Thr UGU, Arg ACG, Asp GUC, His GUG, Met CAU, Tyr GUA, Glu UUC	U 17, U 20a, b
1-methyladenosine	" (m^1A)	His GUG, Tyr GUA, Glu UUC, Ser GCU, Ser UGA	A 22
2'-O-methylcytidine	B (Cm)	Leu CAA	C 34
N4-acetylcytidine	M (ac^4C)	Met CAU	C 34
Queuosine	Q	His GUG, Tyr GUA, Asn GUU, Asp GUC	G 34
5-methoxyuridine	5 (mo^5U)	Gly UCC, Val UAC, Pro UGG, Ala UGC, Leu UAG, Thr UGU, Ser UGA	U 34
5-carboxymethylaminomethyl-2-thiouridine	Ş ($cmnm^5s^2U$)	Lys UUU	U 34
5-methylaminomethyl-2-thiouridine	S (mnm^5s^2U)	Glu UUC, Lys UUU	U 34
1-methylguanosine	K (m^1G)	His GUG, Pro UGG, Arg ACG, Leu UAG	G 37
N6-methyladenosine	= (m^6A)	Met CAU, Val UAC	A 37
N6-threonylcarbamoyladenosine	6 (t^6A)	Ile GAU, Asn GUU, Thr UGU, Ser GCU	A 37
N6-isopentenyladenosine	+ (i^6A)	Tyr GUA, Ser UGA, Leu CAA	A 37
Unknown modified adenosine	H (xA)	Lys UUU	A 37
7-methylguanosine	7 (m^7G)	Arg ACG, Pro UGG	G 46
5-methyluridine	T (m^5U)	Met CAU, Asp GUC, Pro UGG, Leu UAG, Thr UGU, Glu UUC, Leu UAA, Ser GCU, Ser UGA	U 54

Fig. 3. Atlas of modifications characterized on *S. aureus* tRNAs. *A.* The different modifications observed on *S. aureus* tRNAs are reported on the typical cloverleaf two-dimensional structure of a tRNA. The acceptor stem, the variable region, the D, TΨ and anticodon loops are indicated. The nucleotide positions where the modifications were found are highlighted by light blue filled circles. *B.* Table summarizing the modifications with their abbreviations, the tRNAs for which each modification was found and its nucleotide position.

organisms, there are some variations in the tRNAIle content. Indeed, only in some bacteria, some tRNAIle have the UAU anticodons, common also in eukaryotes. Most eukaryotes have two isoacceptor tRNAIle, one with the anticodon IAU (I = inosine), which reads all three isoleucine codons (AUU, AUC and AUA) [89], while the other, with the anticodon ΨAΨ, is thought to read only AUA [90]. In bacteria, $tRNAIle_{GAU}$ reads two of the isoleucine codons (AUU and AUC) and carries a t^6A modification at position 37, as it is also in *S. aureus* (Table 1). The other $tRNAIle_{CAU}$ reads the third isoleucine codon AUA and usually carries a lysidine residue (Lysine modified C at position 34). The enzyme TilS, responsible for this modification, is not only essential for the correct recognition of the AUA codon but also for the amino-acid specificity from methionine to isoleucine [91,92]. This modification enzyme is also present in the *S. aureus* genome suggesting that the lysidine modification is most likely present in $tRNAIle_{CAU}$ to maintain fidelity. Purification of this isoacceptor tRNAIle will be necessary to assert this hypothesis.

3.3. tRNA modification dynamics under different stress conditions

The protocol presented here can be easily applied to analyze specific stress conditions that might alter the modification state or the nature of modifications in tRNAs. The possibility to probe several tRNAs in one single experiment using 2D-gel isolation procedure, without the need of biotinylated probes to capture (single) tRNA, has removed one of the major bottlenecks for the LC/MSMS analyses. The recent advances in mass spectrometry technologies and software [93,94] now enable the routine sequence mapping of modifications from much less material than in the past. Prior to modification mapping on individual tRNAs, a complete nucleoside profile of total tRNAs would be complementary to screen for modification changes taking place under specific conditions. The analysis of the dynamics of tRNA modifications upon stress encountered during infection in *S. aureus* might reveal unexpected strategies developed by the pathogen to survive, persist, and fight against host immune defenses. The increase in the sensitivity of nanoLC/MSMS methodologies and the new development of high throughput RNA sequencing analysis [95] are promising developments amenable to gain a full picture of RNA modifications, opening new areas in the field of RNA regulatory functions in bacteria.

Funding

This work was supported by the Agence Nationale de la Recherche (ANR, grant ANR-16-CE11-0007-01, RIBOSTAPH, to [P.R.] and ANR-15-CE11-0021-01 to [E.W.]), and from "Fonds Régional de Cooperation Pour la Recherche" (Région Grand Est, project EpiRNA). It has also been supported and published under the framework of the LABEX: ANR-10-LABX-0036 NETRNA as part of the investments for the future program and of ANR-17-EURE-0023 to [E.W. and P.R.] from the French National Research Agency. L.A. received the support for the Grand Est region and the labEx NetRNA for her PhD contract.

Author contributions

LA conducted the experiments, analyzed the data and wrote the paper; PW developed the MS analysis approach, conducted the preliminary experiments, analyzed the data and wrote the paper; EW designed the research and wrote the paper; PR and SM designed the research, analyzed the data and wrote the paper; All authors have read and approved the manuscript.

Acknowledgments

The authors thank P. Hammann, L. Kuhn and J. Chicher from the IBMC Proteomic Platform (Strasbourg), and all members of the team for their helpful discussions.

Appendix A. Supplementary data

Supplementary data to this article can be found online at https://doi.org/10.1016/j.biochi.2019.07.003.

References

[1] M. Frye, et al., RNA modifications: what have we learned and where are we headed? Nat. Rev. Genet. 17 (6) (2016) 365–372.
[2] P. Boccaletto, et al., MODOMICS: a database of RNA modification pathways. 2017 update, Nucleic Acids Res. 46 (D1) (2018) D303–D307.
[3] K. Chatterjee, et al., The archaeal COG1901/DUF358 SPOUT-methyltransferase members, together with pseudouridine synthase Pus10, catalyze the formation of 1-methylpseudouridine at position 54 of tRNA, RNA 18 (3) (2012) 421–433.
[4] B. Desmolaize, et al., A single methyltransferase YefA (RlmCD) catalyses both m5U747 and m5U1939 modifications in Bacillus subtilis 23S rRNA, Nucleic Acids Res. 39 (21) (2011) 9368–9375.
[5] M.P. Guy, et al., Yeast Trm7 interacts with distinct proteins for critical modifications of the tRNAPhe anticodon loop, RNA 18 (10) (2012) 1921–1933.
[6] M. Kempenaers, et al., New archaeal methyltransferases forming 1-methyladenosine or 1-methyladenosine and 1-methylguanosine at position 9 of tRNA, Nucleic Acids Res. 38 (19) (2010) 6533–6543.
[7] E. Purta, et al., YgdE is the 2'-O-ribose methyltransferase RlmM specific for nucleotide C2498 in bacterial 23S rRNA, Mol. Microbiol. 72 (5) (2009) 1147–1158.
[8] J.P. Wurm, et al., The ribosome assembly factor Nep1 responsible for Bowen-Conradi syndrome is a pseudouridine-N1-specific methyltransferase, Nucleic Acids Res. 38 (7) (2010) 2387–2398.
[9] S. Douthwaite, D. Fourmy, S. Yoshizawa, Nucleotide methylations in rRNA that confer resistance to ribosome-targeting antibiotics, in: Topics in Current Genetics, Fine-Tuning of RNA Functions by Modification and Editing, Springer-Verlag, Berlin, Heidelberg, 2005, pp. 285–307.
[10] L. Fernandez, R.E. Hancock, Adaptive and mutational resistance: role of porins and efflux pumps in drug resistance, Clin. Microbiol. Rev. 25 (4) (2012) 661–681.
[11] S.M. Toh, A.S. Mankin, An indigenous posttranscriptional modification in the ribosomal peptidyl transferase center confers resistance to an array of protein synthesis inhibitors, J. Mol. Biol. 380 (4) (2008) 593–597.
[12] E.M. Gustilo, F.A. Vendeix, P.F. Agris, tRNA's modifications bring order to gene expression, Curr. Opin. Microbiol. 11 (2) (2008) 134–140.
[13] S. Gehrig, et al., Identification of modifications in microbial, native tRNA that suppress immunostimulatory activity, J. Exp. Med. 209 (2) (2012) 225–233.
[14] B. El Yacoubi, M. Bailly, V. de Crecy-Lagard, Biosynthesis and function of posttranscriptional modifications of transfer RNAs, Annu. Rev. Genet. 46 (2012) 69–95.
[15] M. Helm, J.D. Alfonzo, Posttranscriptional RNA Modifications: playing metabolic games in a cell's chemical Legoland, Chem. Biol. 21 (2) (2014) 174–185.
[16] J.E. Jackman, J.D. Alfonzo, Transfer RNA modifications: nature's combinatorial chemistry playground, Wiley Interdiscip Rev RNA 4 (1) (2013) 35–48.
[17] C. Lorenz, C.E. Lunse, M. Morl, tRNA modifications: impact on structure and thermal adaptation, Biomolecules 7 (2) (2017).
[18] J. Eargle, et al., Dynamics of recognition between tRNA and elongation factor tu, J. Mol. Biol. 377 (5) (2008) 1382–1405.
[19] J. Zhang, A.R. Ferre-D'Amare, The tRNA elbow in structure, recognition and evolution, Life (Basel) 6 (1) (2016).
[20] R. Giege, M. Springer, Aminoacyl-tRNA synthetases in the bacterial world, EcoSal Plus 7 (1) (2016).
[21] J. Zhang, A.R. Ferre-D'Amare, Structure and mechanism of the T-box riboswitches, Wiley Interdiscip Rev RNA 6 (4) (2015) 419–433.
[22] R.K. Gudipati, et al., Extensive degradation of RNA precursors by the exosome in wild-type cells, Mol. Cell 48 (3) (2012) 409–421.
[23] S. Vanacova, et al., A new yeast poly(A) polymerase complex involved in RNA quality control, PLoS Biol. 3 (6) (2005) e189.
[24] S. Kimura, M.K. Waldor, The RNA degradosome promotes tRNA quality control through clearance of hypomodified tRNA, Proc. Natl. Acad. Sci. U. S. A. 116 (4) (2019) 1394–1403.
[25] H. Grosjean, E. Westhof, An integrated, structure- and energy-based view of the genetic code, Nucleic Acids Res. 44 (17) (2016) 8020–8040.
[26] P.F. Agris, F.A. Vendeix, W.D. Graham, tRNA's wobble decoding of the genome: 40 years of modification, J. Mol. Biol. 366 (1) (2007) 1–13.
[27] E. Westhof, M. Yusupov, G. Yusupova, The multiple flavors of GoU pairs in RNA, J. Mol. Recognit. (2019), e2782.
[28] A. Rozov, et al., Tautomeric G*U pairs within the molecular ribosomal grip and fidelity of decoding in bacteria, Nucleic Acids Res. 46 (14) (2018) 7425–7435.
[29] N. Demeshkina, et al., A new understanding of the decoding principle on the ribosome, Nature 484 (7393) (2012) 256–259.
[30] I. Wohlgemuth, et al., Evolutionary optimization of speed and accuracy of decoding on the ribosome, Philos. Trans. R. Soc. Lond. B Biol. Sci. 366 (1580) (2011) 2979–2986.
[31] R.P. Fahlman, T. Dale, O.C. Uhlenbeck, Uniform binding of aminoacylated transfer RNAs to the ribosomal A and P sites, Mol. Cell 16 (5) (2004) 799–805.
[32] J. Zhang, et al., Accuracy of initial codon selection by aminoacyl-tRNAs on the mRNA-programmed bacterial ribosome, Proc. Natl. Acad. Sci. U. S. A. 112 (31) (2015) 9602–9607.
[33] J.M. Ogle, et al., Selection of tRNA by the ribosome requires a transition from an open to a closed form, Cell 111 (5) (2002) 721–732.
[34] J.M. Ogle, V. Ramakrishnan, Structural insights into translational fidelity, Annu Rev Biochem 74 (2005) 129–177.
[35] J.W. Stuart, et al., Functional anticodon architecture of human tRNALys3 includes disruption of intraloop hydrogen bonding by the naturally occurring amino acid modification, t6A, Biochem. 39 (44) (2000) 13396–13404.
[36] V.Y. Vare, et al., Chemical and conformational diversity of modified nucleosides affects tRNA structure and function, Biomolecules 7 (1) (2017).
[37] F.V.t. Murphy, V. Ramakrishnan, Structure of a purine-purine wobble base pair in the decoding center of the ribosome, Nat. Struct. Mol. Biol. 11 (12) (2004) 1251–1252.
[38] F.V.t. Murphy, et al., The role of modifications in codon discrimination by tRNA(Lys)UUU, Nat. Struct. Mol. Biol. 11 (12) (2004) 1186–1191.
[39] A. Weixlbaumer, et al., Mechanism for expanding the decoding capacity of transfer RNAs by modification of uridines, Nat. Struct. Mol. Biol. 14 (6) (2007) 498–502.
[40] S. Kurata, et al., Modified uridines with C5-methylene substituents at the first position of the tRNA anticodon stabilize U.G wobble pairing during decoding, J. Biol. Chem. 283 (27) (2008) 18801–18811.
[41] F. Harada, S. Nishimura, Possible anticodon sequences of tRNA His , tRNA Asm , and tRNA Asp from Escherichia coli B. Universal presence of nucleoside Q in the first postion of the anticondons of these transfer ribonucleic acids, Biochem. 11 (2) (1972) 301–308.
[42] F. Tuorto, et al., Queuosine-modified tRNAs confer nutritional control of protein translation, EMBO J. 37 (18) (2018).
[43] M. Muller, et al., Queuine links translational control in eukaryotes to a micronutrient from bacteria, Nucleic Acids Res 47 (7) (2019) 3711–3727.
[44] P.P. Chan, T.M. Lowe, GtRNAdb 2.0: an expanded database of transfer RNA genes identified in complete and draft genomes, Nucleic Acids Res. 44 (D1) (2016) D184–D189.
[45] M. Vinayak, C. Pathak, Queuosine modification of tRNA: its divergent role in cellular machinery, Biosci. Rep. 30 (2) (2009) 135–148.
[46] T. Pan, Modifications and functional genomics of human transfer RNA, Cell Res. 28 (4) (2018) 395–404.
[47] C.N. Marbaniang, J. Vogel, Emerging roles of RNA modifications in bacteria, Curr. Opin. Microbiol. 30 (2016) 50–57.
[48] T. Kyuma, et al., Ribosomal RNA methyltransferases contribute to Staphylococcus aureus virulence, FEBS J. 282 (13) (2015) 2570–2584.
[49] J.M. Durand, et al., Transfer RNA modification, temperature and DNA superhelicity have a common target in the regulatory network of the virulence of Shigella flexneri: the expression of the virF gene, Mol. Microbiol. 35 (4) (2000) 924–935.
[50] L. Lan, et al., Pseudomonas aeruginosa OspR is an oxidative stress sensing regulator that affects pigment production, antibiotic resistance and dissemination during infection, Mol. Microbiol. 75 (1) (2010) 76–91.
[51] Y.H. Chionh, et al., tRNA-mediated codon-biased translation in mycobacterial hypoxic persistence, Nat. Commun. 7 (2016) 13302.
[52] D.C. Shippy, A.A. Fadl, tRNA modification enzymes GidA and MnmE: potential role in virulence of bacterial pathogens, Int. J. Mol. Sci. 15 (10) (2014) 18267–18280.
[53] D. Bregeon, et al., Translational misreading: a tRNA modification counteracts a +2 ribosomal frameshift, Genes Dev. 15 (17) (2001) 2295–2306.
[54] H. Grundmann, et al., Emergence and resurgence of meticillin-resistant Staphylococcus aureus as a public-health threat, Lancet 368 (9538) (2006) 874–885.
[55] F.D. Lowy, Staphylococcus aureus infections, N. Engl. J. Med. 339 (8) (1998) 520–532.
[56] K. Thuring, et al., Analysis of RNA modifications by liquid chromatography-tandem mass spectrometry, Methods 107 (2016) 48–56.
[57] C.G. Edmonds, et al., Posttranscriptional modification of tRNA in thermophilic archaea (Archaebacteria), J. Bacteriol. 173 (10) (1991) 3138–3148.
[58] S.C. Pomerantz, J.A. McCloskey, Analysis of RNA hydrolyzates by liquid chromatography-mass spectrometry, Methods Enzymol. 193 (1990) 796–824.
[59] S.P. Russell, P.A. Limbach, Evaluating the reproducibility of quantifying modified nucleosides from ribonucleic acids by LC-UV-MS, J Chromatogr B Analyt Technol Biomed Life Sci 923–924 (2013) 74–82.
[60] S.C. Pomerantz, J.A. Kowalak, J.A. McCloskey, Determination of oligonucleotide composition from mass spectrometrically measured molecular weight, J. Am. Soc. Mass Spectrom. 4 (3) (1993) 204–209.
[61] J.A. Kowalak, et al., A novel method for the determination of post-transcriptional modification in RNA by mass spectrometry, Nucleic Acids Res. 21 (19) (1993) 4577–4585.
[62] D. Su, et al., Quantitative analysis of ribonucleoside modifications in tRNA by HPLC-coupled mass spectrometry, Nat. Protoc. 9 (4) (2014) 828–841.
[63] R. Ross, et al., Sequence mapping of transfer RNA chemical modifications by liquid chromatography tandem mass spectrometry, Methods 107 (2016) 73–78.
[64] S. Herbert, et al., Repair of global regulators in Staphylococcus aureus 8325 and comparative analysis with other clinical isolates, Infect. Immun. 78 (6) (2010) 2877–2889.
[65] J. Wu, S.A. McLuckey, Gas-phase fragmentation of oligonucleotide ions, Int. J. Mass Spectrom. 237 (2) (2004) 197–241.

[66] I. Caldelari, et al., Complete genome sequence and annotation of the Staphylococcus aureus strain HG001, Genome Announc. 5 (32) (2017).
[67] N.W. Ho, P.T. Gilham, Reaction of pseudouridine and inosine with N-cyclohexyl-N'-beta-(4-methylmorpholinium)ethylcarbodiimide, Biochem. 10 (20) (1971) 3651–3657.
[68] K.G. Patteson, L.P. Rodicio, P.A. Limbach, Identification of the mass-silent post-transcriptionally modified nucleoside pseudouridine in RNA by matrix-assisted laser desorption/ionization mass spectrometry, Nucleic Acids Res. 29 (10) (2001). E49-9.
[69] A. Durairaj, P.A. Limbach, Matrix-assisted laser desorption/ionization mass spectrometry screening for pseudouridine in mixtures of small RNAs by chemical derivatization, RNase digestion and signature products, Rapid Commun. Mass Spectrom. 22 (23) (2008) 3727–3734.
[70] J. Mengel-Jorgensen, F. Kirpekar, Detection of pseudouridine and other modifications in tRNA by cyanoethylation and MALDI mass spectrometry, Nucleic Acids Res. 30 (23) (2002) e135.
[71] B. Addepalli, N.P. Lesner, P.A. Limbach, Detection of RNA nucleoside modifications with the uridine-specific ribonuclease MC1 from Momordica charantia, RNA 21 (10) (2015) 1746–1756.
[72] W.M. Houser, et al., Combining recombinant ribonuclease U2 and protein phosphatase for RNA modification mapping by liquid chromatography-mass spectrometry, Anal. Biochem. 478 (2015) 52–58.
[73] P. Puri, et al., Systematic identification of tRNAome and its dynamics in Lactococcus lactis, Mol. Microbiol. 93 (5) (2014) 944–956.
[74] K. Murao, T. Hasegawa, H. Ishikura, 5-methoxyuridine: a new minor constituent located in the first position of the anticodon of tRNAAla, tRNAThr, and tRNAVal from Bacillus subtilis, Nucleic Acids Res. 3 (10) (1976) 2851–2860.
[75] S. Okumura, et al., Codon recognition by tRNA molecules with a modified or unmodified uridine at the first position of the anticodon, Nucleic Acids Symp. Ser. (34) (1995) 203–204.
[76] T. Numata, et al., Snapshots of tRNA sulphuration via an adenylated intermediate, Nature 442 (7101) (2006) 419–424.
[77] J. Shepherd, M. Ibba, Bacterial transfer RNAs, FEMS Microbiol. Rev. 39 (3) (2015) 280–300.
[78] C.P. Lee, B.L. Seong, U.L. RajBhandary, Structural and sequence elements important for recognition of Escherichia coli formylmethionine tRNA by methionyl-tRNA transformylase are clustered in the acceptor stem, J. Biol. Chem. 266 (27) (1991) 18012–18017.
[79] J.M. Guillon, et al., Nucleotides of tRNA governing the specificity of Escherichia coli methionyl-tRNA(fMet) formyltransferase, J. Mol. Biol. 224 (2) (1992) 359–367.
[80] D. Hartz, et al., Domains of initiator tRNA and initiation codon crucial for initiator tRNA selection by Escherichia coli IF3, Genes Dev. 4 (10) (1990) 1790–1800.
[81] T. Meinnel, et al., Discrimination by Escherichia coli initiation factor IF3 against initiation on non-canonical codons relies on complementarity rules, J. Mol. Biol. 290 (4) (1999) 825–837.
[82] T. Hussain, et al., Large-scale movements of IF3 and tRNA during bacterial translation initiation, Cell 167 (1) (2016) 133–144 e13.
[83] D. Petrelli, et al., Translation initiation factor IF3: two domains, five functions, one mechanism? EMBO J. 20 (16) (2001) 4560–4569.
[84] J.M. Guillon, et al., Importance of formylability and anticodon stem sequence to give a tRNA(Met) an initiator identity in Escherichia coli, J. Bacteriol. 175 (14) (1993) 4507–4514.
[85] J.M. Guillon, et al., Interplay of methionine tRNAs with translation elongation factor Tu and translation initiation factor 2 in Escherichia coli, J. Biol. Chem. 271 (37) (1996) 22321–22325.
[86] M.A. Machnicka, et al., MODOMICS: a database of RNA modification pathways–2013 update, Nucleic Acids Res. 41 (2013) D262–D267. Database issue.
[87] A. Simonetti, et al., A structural view of translation initiation in bacteria, Cell. Mol. Life Sci. 66 (3) (2009) 423–436.
[88] L. Stern, L.H. Schulman, The role of the minor base N4-acetylcytidine in the function of the Escherichia coli noninitiator methionine transfer RNA, J. Biol. Chem. 253 (17) (1978) 6132–6139.
[89] C. Kohrer, et al., Life without tRNAIle-lysidine synthetase: translation of the isoleucine codon AUA in Bacillus subtilis lacking the canonical tRNA2Ile, Nucleic Acids Res. 42 (3) (2014) 1904–1915.
[90] B. Senger, et al., The modified wobble base inosine in yeast tRNAIle is a positive determinant for aminoacylation by isoleucyl-tRNA synthetase, Biochem. 36 (27) (1997) 8269–8275.
[91] A. Soma, et al., An RNA-modifying enzyme that governs both the codon and amino acid specificities of isoleucine tRNA, Mol. Cell 12 (3) (2003) 689–698.
[92] T. Muramatsu, et al., Codon and amino-acid specificities of a transfer RNA are both converted by a single post-transcriptional modification, Nature 336 (6195) (1988) 179–181.
[93] H. Nakayama, et al., Ariadne: a database search engine for identification and chemical analysis of RNA using tandem mass spectrometry data, Nucleic Acids Res. 37 (6) (2009) e47.
[94] P.J. Sample, et al., RoboOligo: software for mass spectrometry data to support manual and de novo sequencing of post-transcriptionally modified ribonucleic acids, Nucleic Acids Res. 43 (10) (2015) e64.
[95] D.R. Garalde, et al., Highly parallel direct RNA sequencing on an array of nanopores, Nat. Methods 15 (3) (2018) 201–206.
[96] T. Carver, et al., DNAPlotter: circular and linear interactive genome visualization, Bioinformatics 25 (1) (2009) 119–120.

Supplementary file : Figure S1.

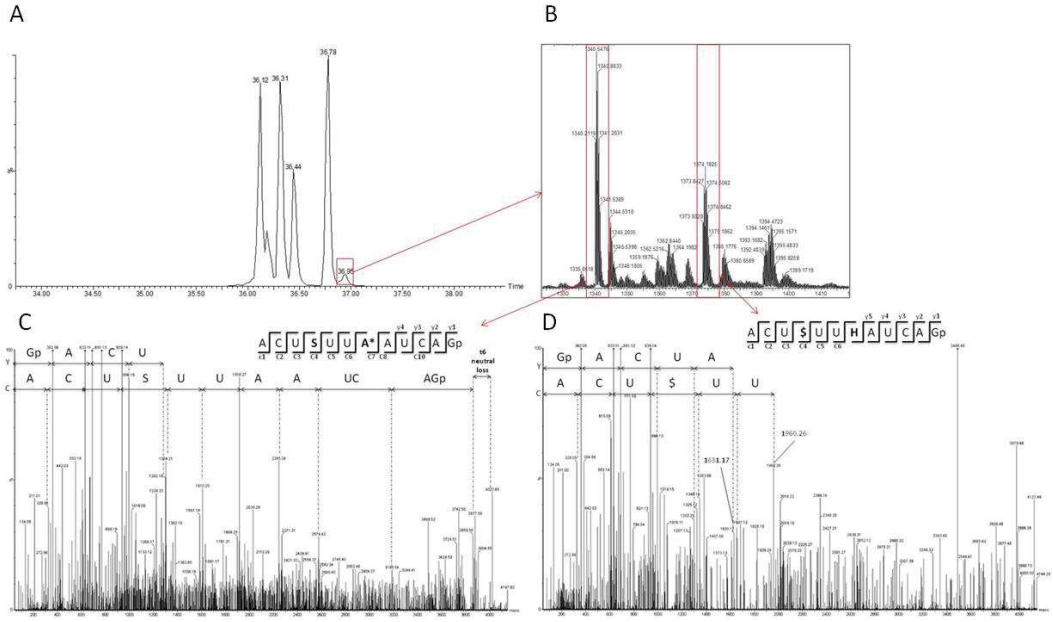

Figure S1. nanoLC/MSMS analysis of spot n°24 containing Lys-tRNA$_{UUU2-3}$ after RNase T1 digestion. *A.* Elution profile of the nanoLC of spot n°24 containing Lys-tRNA$_{UUU2-3}$ after T1 digestion. The different fragments are as follow: *a* acceptor stem (sequence $^{5'}$CUACACCA$^{3'}$ from position 70 to 76); *b* acceptor stem (sequence $^{5'}$CAUCUGp$^{3'}$ from position 25 to 30); *c* acceptor stem (sequence $^{5'}$CCAUUAGp$^{3'}$ from position 4 to 10); *d* TΨ loop and stem (sequence $^{5'}$AAUCCUCUAUGp$^{3'}$ from position 57 to 68); *e* anticodon loop (sequence $^{5'}$ACUUUUAAUCAG$^{3'}$ from position 31 to 42). *B.* MS spectrum of the peak *e* of the nanoLC chromatogram corresponding to the anticodon loop. The two main ions have been selected for further fragmentation. *C.* MSMS spectrum of anticodon loop corresponding to the sequence $^{5'}$ACUSUUA*AUCAGp$^{3'}$ with the 145 Da neutral loos specific of the t6A. A* is present at position 37, carrying the t6A modification. Measured m/z : 1340,19 (-3H^{+}). The specific bonds that fragment most often are the 5′ P-O inter-nucleotide bond. Fragment ions where the charge is retained on the 5′-fragment are denoted as c-type fragment ions, and fragment ions where the charge is retained on the 3′-fragment are denoted as y-type fragment ions {McLuckey, 1992 #79}. *D.* MS/MS spectrum of anticodon loop corresponding to the sequence $^{5'}$ACU$UUHAUCAGp$^{3'}$ without neutral loss. Measured m/z : 1373,50 (-3H^{+}).

3. Analyse de RNA-Seq des ARN non codants de *S.aureus*

Afin de compléter la cartographie des modifications des ARNt (et ARNr), réalisée par NanoLC-MS/MS, des approaches complémentaires basées sur le RNA-Seq ont été combinées (**Fig 3.**). Les trois techniques qui ont été utilisées permettent de détecter les Ψ, m^7G, m^3C, D et 2'-O methylations. Les analyses RNA-Seq telles que l'HydraPsi-Seq (Marchand *et al.*, 2020), l'AlkAniline-Seq (Marchand *et al.*, 2018) et le RiboMeth-Seq (Marchand *et al.*, 2016; Ayadi *et al.*, 2018) ont été réalisées en collaboration avec le Pr. Yuri Motorin et la Dr. Virginie Marchand de la plateforme Epitranscriptomique et Séquençage (EpiRNA-Seq) de Nancy. Ces analyses ont été réalisées sur les ARNt totaux et sur les ARNr. Les résultats d'HydraPsi-Seq révèlent la présence de pseudouridines en position 13, 32 et 55 des ARNt et également en position 524, 634, 717 et 1282 de l'ARNr 16S. L'AlkAniline-Seq spécifique des m^7G, m^3C et D, a confirmé la présence de modifications caractérisées pas NanoLC-MS/MS telles que les dihydrouridines localisées dans la boucle D et le m^7G en position 46 dans la boucle variable de l'$ARNt^{Pro}_{UGG}$. Cette méthode à également permis la caractérisation d'un m^7G en 534 de l'ARNr 16S. Le RiboMeth-Seq a confirmé la présence d'un 2'O-méthyl en position 34 de l'$ARNt^{Leu}_{CAA}$ mais a également révélé la présence d'un Gm en position 45 de l'$ARNt^{Val}_{UAC}$ ainsi que la présence d'un Cm en position 1411 de l'ARNr 16S.

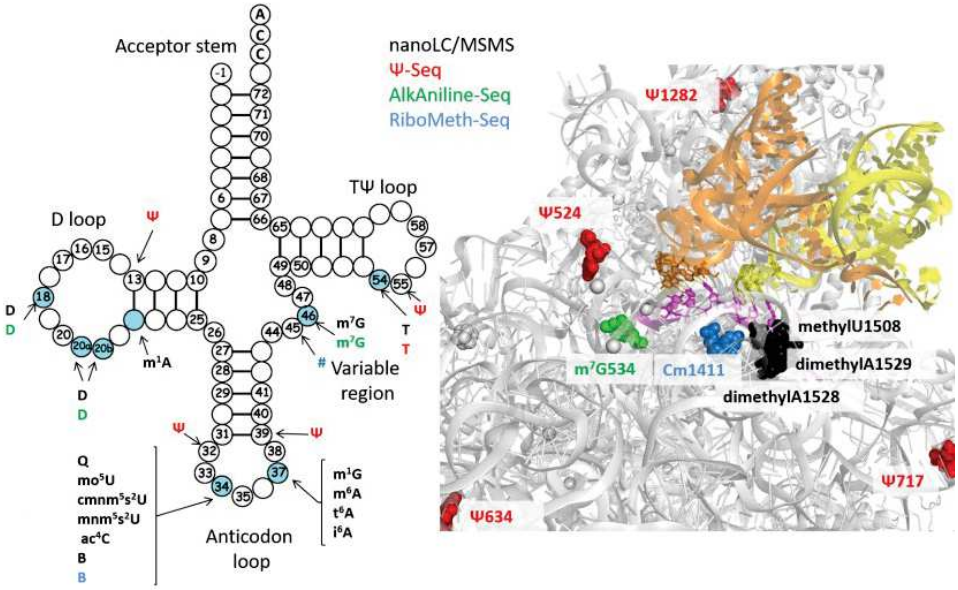

Figure 3 : Modifications cartographiées par différentes méthodes de NanoLC-MS/MS et RNA-Seq dans les ARNt à gauche et l'ARNr 16S de *S. aureus* à droite

4. Réponse au stress oxydant :

Après avoir caractérisé de nombreuses modifications sur des ARNt de *S. aureus*, leur dynamique en réponse à des conditions mimant les stress rencontrés pendant l'infection reste à déterminer. La production par les macrophages et les neutrophiles de ROS générant un stress oxydant est une des lignes de défense du système immunitaire. Tout d'abord, des analyses de transcriptomique différentielle et de protéomique sont réalisées afin de caractériser l'adaptation globale de la bactérie au stress oxydant avant de suivre les changements de modification des ARNt.

L'induction des ROS dans les cultures de S. aureus est réalisée par l'ajout de l'herbicide Méthylviologen (MV ; N,-N'-dimethyl-4,-4'-bipyridinium dichloride ; aussi appelé Paraquat). Le MV est une molécule communément utilisée pour étudier le stress oxydant chez les bactéries et les plantes. La réaction entre le radical du MV et le dioxygène (O_2) génère les espèces toxiques : le radical superoxyde (O_2^-) et le peroxyde d'hydrogène (Hassan, 1984).

i. Analyse transcriptomique et protéomique

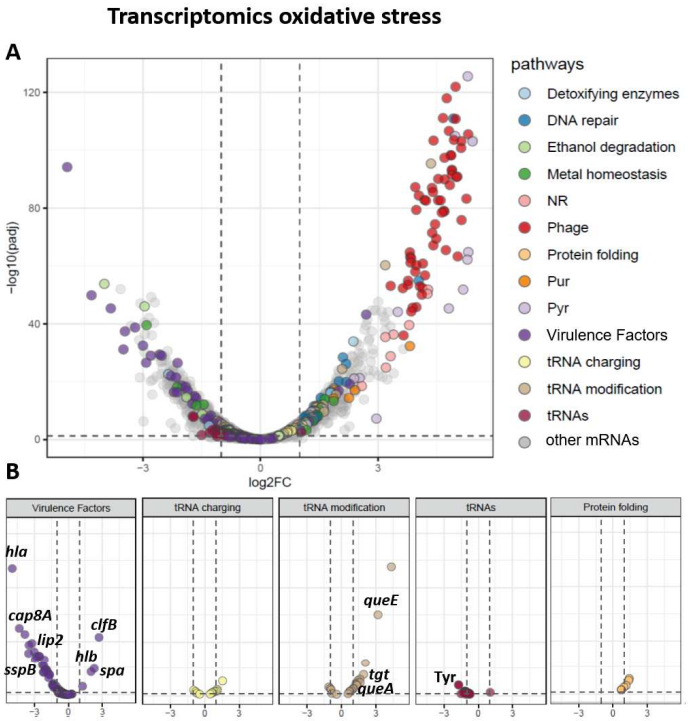

Figure 4 : A) Volcano plot représentant l'analyse transcriptomique différentielle de cultures de *S.aureus* HG001 soumises à un stress oxydant (**Annexe 1**.). Pyr et Pur représentent les voies de biosynthèse des désoxynucléotides et NR représente la voie de réduction des nitrites et des nitrates. **B)** Extraits du volcano plot.

L'analyse transcriptomique différentielle de cultures de *S. aureus* HG001 cultivées en conditions normales ou soumises au stress oxydant généré par le méthylviologen est réalisée en collaboration avec la plateforme EpiRNA-Seq. Ces résultats montrent une surexpression de gènes codants pour des protéines phagiques et des enzymes de détoxification. De même, des protéines impliquées dans les voies de synthèse des acides nucléiques (purines et surtout pyrimidines), de la réparation de l'ADN ainsi que de la réduction des nitrites et des nitrates sont plus exprimées chez les bactéries stressées (**Fig. 4A.**) La plupart des facteurs de virulence sont sous exprimés, notament *cap8A* impliqués dans la synthèse de la capsule, la staphopain, la triacylglycerol lipase (*lip2*) et les toxines (l'alpha-hemolysin *hly*, la delta-hemolysin *hld* présente dans l'ARNII, les gamma-hemolysins *hlgABC* et les peptides PSM). Tandis que l'hémolysine B, le clumping factor B, la protéine A sont surexprimés en condition oxydante. Le niveau de tRNA semble également légèrement plus faible chez les bactéries

stressées, spécifiquement l'ARNt^{Tyr}. Les protéines chaperonnes semblent à l'inverse légèrement plus exprimées durant le stress (**Fig. 4B.**).

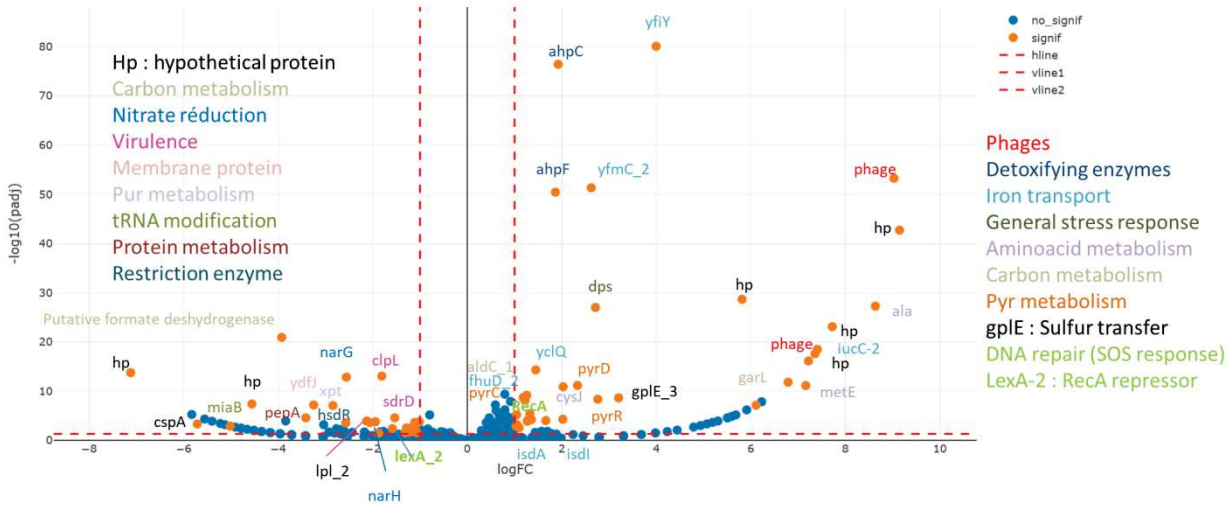

Figure 5 : Volcano plot représentant l'expression différentielle des protéines de cultures de *S.aureus* HG001 soumises à un stress oxydant (**Annexe 2.**).

Les données de protéomique ont été obtenues par analyse LC-MS/MS d'extraits de protéines totales issues de bactéries HG001 cultivées ou non en présence de MV, cette analyse est réalisée en collaboration avec la plateforme protéomique de l'Esplanade de Strasbourg. Cette analyse montre une activation de l'expression des gènes phagiques ainsi qu'une forte augmentation de l'expression de gènes codant pour des protéines de réponse générale au stress (Dps) ainsi que des sous unités C et F de l'alkyl hydroperoxide reductase (AhpC et AhpF). Plusieurs protéines impliquées dans l'import de fer provenant du milieu (YfiY, YfmC_2) ou de l'hôte (IsdI) sont également surexprimées lors du stress oxydant. De même, une protéine dont l'expression est influencée par la disponibilité du fer (IsdA) semble légèrement plus présente dans les bactéries stressées. La protéine de réparation de l'ADN RecA ainsi que des protéines impliquées dans le métabolisme des acides nucléiques, plus spécifiquement des pyrimidines sont surexprimées lors du stress oxydant alors que l'expression de la Xanthine phosphoribosyltransferase codée par le gène *xpt* est inhibée (**Fig. 5**.).

ii. Dynamique des modifications des ARNt en réponse au stress oxydant

L'effet du stress oxydant sur les ARNt peut être caractérisé en analysant leur migration sur gel de polyacrylamide puis en analysant les modifications présentes par NanoLC-MS/MS. Différentes souches ont été utilisées, la souche de laboratoire HG001 mais aussi la souche clinique USA300 et une souche avec un gène *tgt* inactivé (Fey *et al.*, 2013) et ne présentant pas la queuosine.

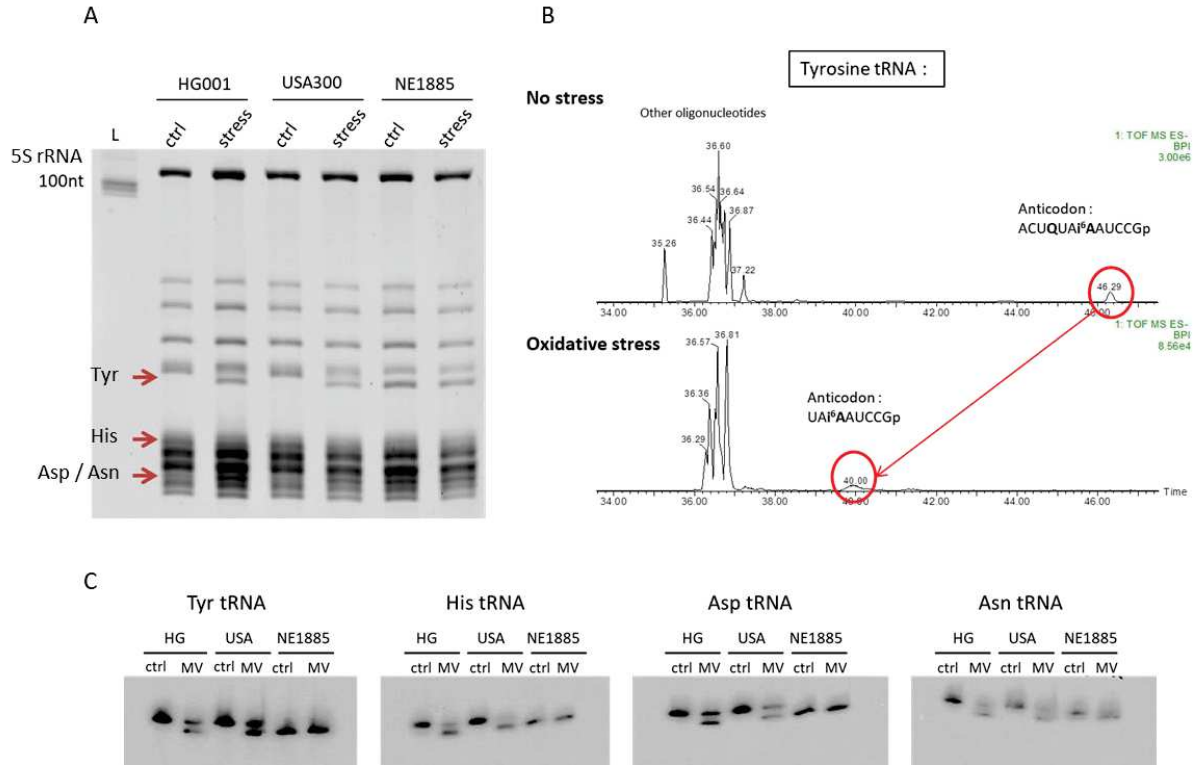

Figure 6 : A) Profil de migration sur gel (polyacrylamide 12%, 8M urée) des ARNt des souches HG001 (souche contrôle), USA300 (souche clinique) et NE1885 (souche possédant le gène *tgt* inactivé) de *S. aureus*. Les flèches rouges indiquent les positions sur le gel des ARNt connus pour posséder une Q en position 34 et correspondant aux bandes présentant un changement de comportement électrophorétique. **B)** Chromatogrammes obtenus à partir des bandes contenant l'ARNt$^{Tyr}_{GUA}$ issus de *S. aureus* HG001. Encerclés en rouge les pics d'élutions correspondants aux anticodons, non clivé par la RNase T1 pour l'ARNt issus de la culture non stressée, clivé pour celui issus de la culture soumise au stress oxydant. **C)** Northern blot sur gel de polyacrylamide et acide phénylboronique des 4 ARNt contenant une Q34 issus de cultures en présence (MV) ou en absence (ctrl) de stress oxydant.

Les profils électrophorétiques des ARNt issus de la souche de laboratoire HG001 sont similaires à ceux des ARNt de la souche clinique USA300. Les ARNt provenant de cellules soumises à un stress oxydant présentent 3 bandes shiftées correspondantes aux profils de

migration de l'ARNt de la Tyrosine, de l'Histidine ainsi que les ARNt de l'Aspartate et l'Asparagine (Antoine *et al.*, 2019). La souche NE1885 provenant de la Nebraska collection est dérivée de la souche USA300 avec le gène *tgt* impliqué dans la voie de biosynthèse de la Q inactivé (Fey *et al.*, 2013). Les ARNt extraits de cette souche montrent un profil de migration similaire à ceux issus des souches HG001 et USA300 soumises au stress oxydant (**Fig. 6A**). L'analyse LC-MS/MS de la bande présentant un changement de migration flagrant provenant de la culture de *S. aureus*, contenant l'ARNt^{Tyr} révèle le clivage de l'anticodon par la RNase T1 en 3' de la Q34 de cet ARNt issus de la culture stressée. Ce clivage n'a pas lieu dans l'ARNt^{Tyr} issus de la culture non stressée, dû à la présence de la modification, empêchant sa reconnaissance par la RNAse T1 (**Fig. 6B**). Les gels d'affinité contenant de l'acide phénylboronique (APB) qui interagit spécifiquement avec la queuosine, ralentissent la migration des ARNt modifiés (Igloi and Kössel, 1985). Le Northern blot des gels avec APB montre que les ARNt ne possédant pas de Q34 (NE1885) ont migré plus rapidement que les ARNt issus de cultures non stressées qui contiennent une Q34. La migration des ARNt issus des cultures stressées semble plus rapide, comparable à la migration des ARNt ne contenant pas de Q34 (**Fig. 6C**).

iii. Analyse des ARNt contenant la Q34 issus de cultures stressées

Chacun des ARNt contenant une Q34 a été purifié par hybridation avec une sonde d'ADN biotinylée spécifique. L'analyse par LC-MS/MS après digestion avec la RNase U2 révèle la présence d'un G non modifié en position 34 pour 3 des 4 ARNt concernés. Les autres modifications telles que les dihydrouridines dans la boucle D, le m7G dans la boucle variable, la thymidine dans la boucle TΨ ainsi que les modifications en position 37 de l'anticodon (t^6A, m^1G et i^6A) ne semblent pas impactées par le stress oxydant.

Amino Acid	Anticodon		Acc-stem		D-stem	D-loop	D-stem		Ac-stem	Ac-loop	Ac-stem	V-region	T-stem	T-loop	T-stem	Acc-stem		CCA
Asp	GUC	-	GGUCUCG	UA	GUGU	AGCGGDDA	ACAC	G	CCUGC	CUGUCAC	GCAGG	AGAUC	GCGGG	TUCGGUU	CCCGU	CGAGACC	G	CCA
Asn	GUU	-	UCCACAG	UA	GCUC	AGUGGDA	GAGC	U	AUCGG	CUGUU6A	CCGAU	CG7UC	GUAGG	TUCGAGU	CCUAC	CUGUGGA	G	CCA
His	GUG	G	GCGGCUG	UG	GUGA	AGUGGDDA	AmCAC	A	UCGGA	UUGUGKU	UCCGA	CAUUC	GAGGG	UUCGAUC	CCCUU	CAGCCGC	C	CCA
Tyr	GUA	-	GGAGGGG	UA	GCGA	AGUGGCUAA	ACGC	G	GCGGA	CUGUA+A	UCCGC	UCCUUCGGGUUC	GGCAG	TUCGAAU	CUGCC	CCCCUCC	A	CCA

Tableau 1 : Séquences des ARNt contenants une Q34 issus d'une culture de *S. aureus* HG001 soumise au stress oxydant. En bleu sont présentés les fragments séquencés par MS/MS après digestion avec la RNase U2.

iv. Le précurseur preQ1 restaure la queuosine dans les 4 ARNt contenant la Q34

A partir des données d'analyses de protéomique et de transcriptomique, aucune des 8 enzymes (**Fig. 7A**) de la voie de synthèse de la queuosine ne présente de changement dans son expression. Cependant, le stress oxydant peut affecter directement l'activité des protéines. Afin de comprendre quelles enzymes sont susceptibles d'être inactivées, les cultures soumises au stress oxydant ont été supplémentées avec le précurseur de la queuosine preQ1. La cinétique d'incorporation de la queuosine a ensuite été vérifiée par électrophorèse d'affinité à l'APB. (**Fig. 7B**).

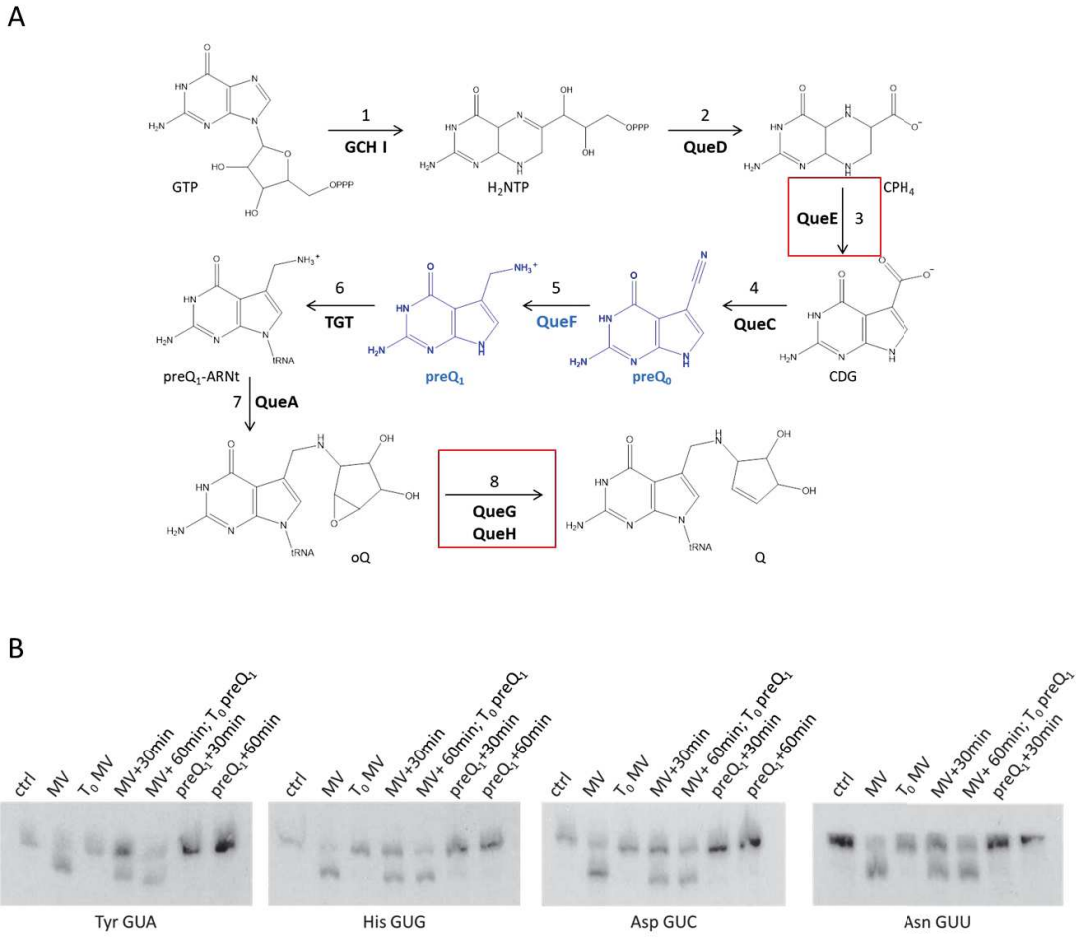

Figure 7 : A) Voie de biosynthèse de la queuosine (adapté de (Dowling *et al.*, 2016). En rouge sont encadrées les étapes catalysées par des enzymes à cluster [4Fe-4S], en bleu l'étape catalysée par la QueF convertissant le$preQ_0$ en $preQ_1$**. B)** Northern blot de gels APB des ARNt contenant une Q34 issus de *S.aureus* HG001 cultivées en condition oxydante. A T_0MV, le stress oxydant est appliqué à la culture et à $T_0$$preQ_1$, 60min après l'ajout de MV, l'intermédiaire $preQ_1$ est ajouté au milieu. La culture ctrl est la culture non stressée, sans ajout de $preQ_1$, la culture MV est la culture stressée sans ajout de $preQ_1$.

Les ARNt issus de cultures stressées présentent des profils de migration semblant indiquer une proportion plus importante d'ARNt ne possédant plus de Q34 au court du stress oxydant. 30 min après l'ajout du précurseur de la queuosine $preQ_1$, les ARNt présentent de nouveau un profil électrophorétique similaire à ceux provenant de cellules cultivées en conditions normales. Ce profil se maintient à $TpreQ_1$+60 min et suggère une restauration de la voie de biosynthèse de la queuosine.

III. Discussion

1. Mise en place de la méthode et cartographie des modifications

i. Limites et méthodes complémentaires : le pouvoir de la coopération

La méthode de NanoLC-MS/MS choisie pour cette étude bénéficie d'une grande sensibilité et précision de mesure, permettant de détecter et localiser sur la séquence tous types de modifications connues. Cependant, elle présente plusieurs limites, principalement les informations fragmentaires obtenues ne permettant pas d'établir une cartographie complète des modifications présentes sur l'ensemble des ARNt.

L'utilisation de plusieurs RNases spécifiques permet d'améliorer par recoupement le recouvrement de séquence des ARNt. Cependant, seules les RNases T1 et A sont capables de digérer les ARNt directement à l'intérieur du gel de polyacrylamide. L'utilisation des RNases MC1 ou U2 par exemple, nécessite d'adapter la méthode de purification des ARNt. Pour cela, la purification d'un ARNt spécifique par hybridation avec un oligodésoxynucléotide biotinylé, suivie d'une chromatographie d'affinité peut permettre d'isoler un ARN ciblé qui n'a pas été détecté à la révélation du gel de polyacrylamide en 2D (*cf* § II. 4. iii.). La séparation des fragments d'ARNt digérés peut également être optimisée grâce à l'utilisation de l'électrophorèse capillaire afin de pouvoir détecter les fragments plus courts (Lechner *et al.*, 2020).

La pseudouridine est une modification de masse silencieuse et n'est pas détectable directement par cette méthode. Un traitement chimique au CMCT est possible mais lors des

tests réalisés, les pseudouridines n'ont pas pu être localisées sur les séquences suite au décrochage du groupement CMC lors de la fragmentation. Une altérnative possible est d'utiliser l'acrylonitrile qui semble plus stable en MS/MS (Mengel-Jørgensen and Kirpekar, 2002).

L'analyse par spectrométrie de masse des nucléosides issus de la digestion complète des ARNt suivi de la déphosphorylation des nucléotides fournit la composition globale en modifications des ARNt. Cette méthode ne nécessite pas de séparation ou de purification préalable des ARNt mais ne fournit pas d'informations concernant la position ou la séquence et permet la quantification relative entre différentes conditions des modifications présentes (Helm and Motorin, 2017; Galvanin *et al.*, 2020). Il est également possible comme alternative, d'utiliser l'approche de marquage SIL-IS in vivo en cultivant les bactéries avec du 13C-glucose comme source majeure de carbone pour faciliter la comparaison relative des modifications par LC-MS/MS (Kellner, Ochel, *et al.*, 2014). En dehors de la spectrométrie de masse, les différentes méthodes de RNA-Seq permettent de localiser certaines modifications spécifiques en fonction du traitement appliqué lors de la préparation des librairies. Les analyses quantitatives sont également possibles avec cette méthode.

Les analyses par des méthodes complémentaires permettent de compléter la cartographie des modifications établie et confirmer les résultats obtenus. La combinaison de différentes méthodes citées apporte une caractérisation plus robuste des modifications des ARNt et de la dynamique de celles-ci.

ii. Cartographie des modifications des ARN non codants de *S. aureus*

Les données de RNA-Seq (HydraPsi-Seq, AlkAniline-Seq et RiboMethSeq) ont permis de confirmer la présence de modifications sur les ARNt de *S. aureus* et de compléter la carte partielle avec les pseudouridines. Les modifications présentes dans les ARNt de *S. aureus* diffèrent peu des modifications présentes dans d'autres bactéries à gram positif telles que *B. subtilis* ou *L. lactis* pour lesquels des cartographies existent (Vold, 1976; Puri, Wetzel, Saffert, W.Gaston, *et al.*, 2014; de Crécy-Lagard *et al.*, 2020). La cartographie des modifications des

ARNt de *S. aureus* demeure encore partielle. Afin de la compléter, une analyse des nucléosides présents sur les ARNt sera réalisée.

La présence de particularités des ARNt de *S.aureus* a été mise en évidence. Plus précisément, la présence d'ARNt isoaccepteurs de la glycine spécifiques impliqués dans la synthèse de la paroi cellulaire. Ces ARNt interviennent dans la constitution du pont pentapeptide spécifique du peptidoglycane des Staphylocoques via les complexe de proteines FemXAB (facteurs essentiels pour la méthicilline (Giannouli *et al.*, 2009; Rietmeyer *et al.*, 2021) (**Fig. 8A**). Ces $ARNt^{Gly}$, dits non protéinogéniques, présentent une séquence différente des $ARNt^{Gly}$ intervenants dans la traduction (protéinogéniques) et j'ai pu déterminer qu'ils ne possèdent pas la modification 5-méthoxyuridine (mo^5U) en 34 permettant le décodage des ARNm. Ils présentent également une boucle T particulière avec un G en position 55, L'absence de la Ψ55 peu inflencer la présence d'autres modifications, comme c'est le cas notamment dans l'$ARNt^{Phe}$ de *Saccharomyces cerevisiae* (Barraud *et al.*, 2019). Chacun de ces $ARNt^{Gly}$ ont été purifiés et analysé par spectrométrie de masse (**Fig. 8B**), confirmant l'absence de modifications dans les régions analysées. Une investigation complète est en cours à ce jour au laboratoire pour déterminer le rôle des modifications dans la discrimination de la machinerie traductionnelle et la redirection de ces ARNt vers la voie de biosynthèse correspondante.

A

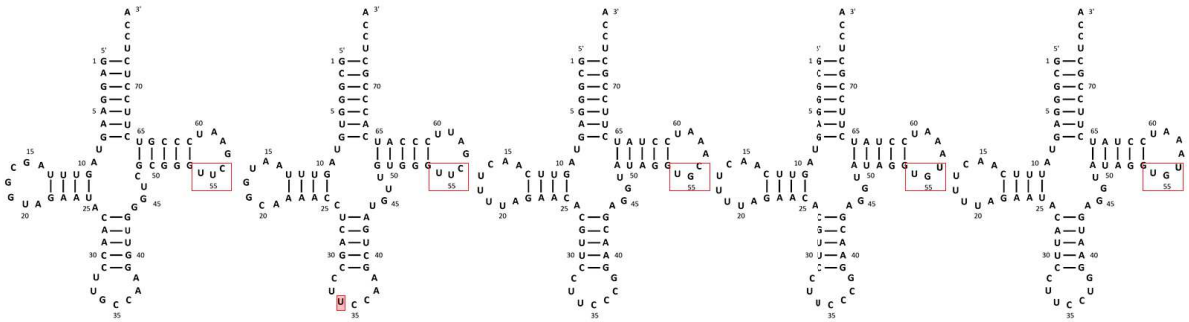

B

Amino Acid	Antiocodon		Acc-stem		D-stem	D-loop	D-stem		Ac-stem	Ac-loop	Ac-stem	V-region	T-stem	T-loop	T-stem	Acc-stem		CCA
		-1	1	8	10	14	22	26	27	32	39	44	49	53	61	66	73	74
Gly P1	GCC	-	GCAGAAG	UA	GUUC	AGCGGUA	GAAU	A	CAACC	UUGCCAA	GGUUG	GGGUC	GCGGG	UUCGAAU	CCCGU	CUUCUGC	U	CCA
Gly P2	UCC	-	GCGGGUG	UA	GUUU	AAUGGCA	AAAC	C	UCAGC	CU5CCAA	GCUGA	UGUU	GUGGG	UUCGAUU	CCCAU	CACCCGC	U	CCA
Gly NP1	UCC	-	GCGGGAG	UA	GUUC	AACUUUUA	GAAC	A	CGUUC	CUUCCCG	GAACG	AGGU	AUAGG	UGCAAAU	CCUAU	CUUCCGC	U	CCA
Gly NP2	UCC	-	GCGGGAG	UA	GUUC	AACUUUUA	GAAC	A	CGUUC	CUUCCCG	GAACG	AGGU	AUAGG	UGUAAAU	CCUAU	CUUCCGC	U	CCA
Gly NP3	UCC	-	GCGGGAG	UA	UUUC	AACUUUUA	GAAU	A	CAUUC	CUUCCUG	GAAUG	AGGU	AUAGG	UGUAAAU	CCUAU	CUUCCGC	U	CCA

Figure 8 : Séquences des ARNt^{Gly} de *S. aureus* adapté de (Giannouli *et al.*, 2009). **A)** P1 et P2 sont les isoaccepteurs protéinogéniques, l'ARNt P2 UCC possède un mo^{5}U en position 34 encadré en rouge. Les ARNt NP123 sont des ARNt non protéinogéniques, encadré en rouge la différence de séquence dans la boucle T. **B)** Dû a leur forte identité de séquence, il est difficile de les identifier spécifiquement un par un. NP1 et NP2 sont alors confondu dans nos analyses. Cependant, aucune modification n'a été détectée dans ces ARNt.

La présence d'une modification de masse inconnue a été établie dans l'ARNt de la Lysine (*cf* § II. 3. **Fig. S1**). Cependant, la caractérisation complète afin d'identifier cette nouvelle modification nécessite de plus amples investigations. Il est en effet possible de cultiver les bactéries en présence d'isotopes afin de déteminer la formule brute de la modification (Kellner, Neumann, *et al.*, 2014).

Il n'existe pas de cartographie globale des modifications présentes sur l'ensemble du ribosome de *S. aureus* à ce jour. Seulement 10 modifications ont pu être assignées pas la structure Cryo-EM du ribosome 70S (Golubev *et al.*, 2020). Les données de RNA-Seq des modifications dans les ARNr sont en cours de traitement par Roberto Bahena qui est doctorant au sein de l'équipe. Les résultats obtenus par cette méthode sur les ARNr sont en cours de confirmation par extension d'amorce (Motorin *et al.*, 2007). Pour caractériser certaines régions spécifiques des ARNr, une adaptation de la NanoLC-MS/MS peut être développée (*cf* § V. 3. **Fig. 13**). L'ARNr 16S a été très partiellement analysé par les différentes techniques mises en place (spectrométrie de masse et RNA-Seq), ce qui a permis de localiser

les modifications situées au niveau du site de décodage impliquant des interactions avec les ARNt et l'ARNm.

2. Réponse globale de *S. aureus* au stress oxydant

La transcriptomique différentielle et les analyses protéomiques ont permis d'établir une représentation globale de l'expression des gènes en condition de stress. Ci-après, Les changements observés seront discutés selon les voies métaboliques impliquées (**Annexe 1**). Il a été mentionné qu'une analyse de transcriptome sur micropuce de la réponse cellulaire de *S. aureus* (NCTC 8325) a déjà été rapportée (Chang *et al.*, 2006). L'étude a été conduite en début de phase exponentielle dans un milieu pauvre, ce qui diffère de notre étude réalisée en milieu riche et plus tard dans la phase de croissance de la bactérie. Cependant, les gènes de la réponse SOS et des mécanismes de réparation de l'ADN ont été retrouvés activés également. D'autres gènes, notamment de nombreux facteurs de virulence pour lesquels nous avons observé des variations significatives, n'ont pas été détectés dans ce rapport.

i. Système SOS de réparation de l'ADN et gènes phagiques

Parmi les ROS, le radical hydroxyle hautement réactif (HO•) réagit avec l'ADN produisant environ 20 produits majeurs d'oxydation des bases ou des sucres de l'ADN, des clivages du brin, et des crosslinks d'ADN et protéines (Cadet and Wagner, 2013). Les dommages sur l'ADN altèrent la réplication et la transcription, causant la mort cellulaire et peut mener à des mutations. Lorsque la DNA polymérase est bloquée sur une lésion, l'hélicase continue de dérouler l'ADN, générant des régions d'ADN simple brin étendues qui vont être ciblées par les protéines du système SOS (Podlesek and Žgur Bertok, 2020). La réponse SOS entraine l'induction de multiples protéines qui renforcent l'intégrité de l'ADN. Cette réponse inclus également des facteurs qui sont des sources d'erreurs, ils vont permettre d'améliorer la survie et la continuité de la réplication en présence de dommages étendus de l'ADN, mais au prix d'une mutagénèse élevée. Dû à son potentiel mutagène, le système de réponse SOS est sujet à une régulation complexe (Maslowska *et al.*, 2019). L'activation du système SOS de

réparation de l'ADN est lié à l'inhibition du répresseur LexA qui va générer l'expression de nombreux gènes, notamment la surexpression de la protéine RecA (Ha *et al.*, 2020b) qui est observé dans nos analyses avec un FoldChange . La protéine RecA est connue pour stimuler l'autoclivage de LexA eu ainsi augmenter l'expression (Bisognano et al., 2004). Nous avons également observé une augmentation de l'expression de *uvrB*, codant pour un facteur requis pendant les étapes précoces de la réparation par excision des nucléotides qui va former un complexe ADN-protéine au niveau du site endommagé permettant l'incision (Gordienko and Rupp, 1997). De plus, de nombreuses protéines impliquées dans la synthèse des purines et des pyrimidines semblent confirmer la mise en place de réparation des acides nucléiques.

L'activation de l'expression de gènes prophagiques suite au stress oxydant était attendue, leur expression étant activée suite au déclenchement du système SOS de réparation de l'ADN (Maiques *et al.*, 2006). Les protéines prophagiques favorisent le transfert horizontal de l'ADN et peuvent entrainer l'acquisition par la bactérie de résistances. Ce transfert génétique entre les bactéries est habituellemnet induit par des stresseurs, comme les antibiotiques (Beaber *et al.*, 2004; Jutkina *et al.*, 2016), les métaux et biocides (Seier-Petersen *et al.*, 2014) et plus généralement par la réponse SOS (Andersson and Hughes, 2014). De plus il a été récemment observé que la diffusion chez *E. coli* de gènes de résistance via la conjugaison et aussi stimulée par le stress oxydant généré par les radiations UV (Chen *et al.*, 2019). Puisque la transduction conditionnée par les bacteriophages est considérée comme un des facteurs principaux des transferts de gènes horizontaux chez les Staphylocoques (Xia and Wolz, 2014; Stanczak-Mrozek *et al.*, 2015), il est possible que chez *S. aureus* le stress oxydant stimule le transfert de gènes via la transduction.

ii. Détoxification des espèces réactives de l'oxygène

Les protéines AhpCF de détoxification des ROS sont très largement surexprimées, cependant, les analyses protéomiques réalisées n'ont pas montré de surexpression détectable des protéines Sod alors que l'analyse transcriptomique indique une surexpression de *sodM* dont l'expression est activée lors d'un manque de manganèse dans le milieu sans lien avec les conditions oxydantes rencontrées (Karavolos et al., 2003; Garcia et al., 2017). La

catalase KatA est légèrement surexprimée au niveau protéique alors que la transcription reste inchangée, suggérant une régulation au niveau traductionnel de son expression. L'expérience de ribosome profiling à haute résolution pourrait nous permettre de mieux comprendre s'il y a une différence d'efficacité de la traduction du gène *katA.*

iii. Métabolisme des acides aminés

L'enzyme MetE impliquée dans la biosynthèse *de novo* de la méthionine à partir d'homocystéine ainsi que la sulfite réductase codée par le gène *cysJ* impliqué dans la biosynthèse de la cystéine sont surexprimées. L'expression de la thioredoxine permettant la réduction des thiols dans le cytoplasme est inchangée alors que la protéine régulatrice Spx, nécessaire à son expression est sous exprimée au niveau protéomique malgré une surexpression en transcriptomique.

iv. Homéostasie du fer

De nombreuses protéines responsables de l'apport du fer sont largement surexprimées, illustrant l'importance vitale de celui-ci pour la survie de la bactérie en conditions oxydantes. Les staphyloferrines et les protéines Isd permettant l'import de celui-ci provenant de son environnement, ou des cellules de l'hôte. Dans un contexte d'infection, la production de ces protéines permettant l'internalisation par la cellule du fer présent dans l'hème ou la transferrine de l'hôte peut permettre à la bactérie de survivre à l'oxydation du Fer induit par les ROS.

v. La voie de respiration en anaérobie

Les protéines impliquées dans la respiration anaérobie codées par les opérons *narGHWX* et *nasDEF* sont surexprimées au niveau transcriptionnel alors qu'elles sont moins exprimées en protéomique durant le stress oxydant. L'inhibition de l'expression de ses protéines peut s'expliquer par une absence de traduction des ARNm transcrits ou une traduction altérée qui

entrainerait la production de protéines instables et ainsi la dégradation de celles-ci. La surexpression de protéines chaperonnes impliquées dans le repliement semble corroborer la deuxième hypothèse. Cependant, La transcription de ces opérons depend de la présence ou non d'oxygène. En effet, la protéine NreB, qui est codé par l'opéron *narGHWX* et fait partie du régulon NreABC, est une kinase à cluster [4Fe-4S] qui va avoir un rôle de capteur de l'oxygène. En absence de O_2, le cluster est intact et l'enzyme est active, elle va s'autophosphoryler et transférer le phospore à NreC qui va pouvoir se lier à l'ADN pour activer l'expression des deux opérons le la voie de réduction du nitrate et du nitrite (Fedtke et al., 2002; Nilkens et al., 2014). En présence d'oxygène, le cluster [4Fe-4S] est dégradé et l'enzyme est inactivée. Dans nos conditions expérimentales de stress oxydant, NreC doit être inactive ce qui suggère que la transcription de l'opéron est activée par un autre facteur qui n'est pas caractérisé et qui n'entraine pas la production de protéines fonctionnelles. Ces résultats indiquent qu'il existe un système de régulation plus complexe de l'expression des opérons de la chaine de respiration anaérobie en lien avec le stress oxydant

vi. L'implication des ARNt et des enzymes de modifications

Les enzymes de modifications des ARNt sont, bien que plus lègérement impactées, également surexprimés en transcriptomique et moins exprimées en protéomique. Les ARNt, plus spécifiquement l'ARNt^{Tyr} sont moins exprimés pendant le stress oxydant. Chez E. coli, le stress induit par le H_2O_2 en milieu minimal entraine une diminution globale de la quantité de ARNt due à leur dégradation et engendrant l'inhibition de l'élongation de la traduction (Zhong et al., 2015). Alors que l'exposition au MV ne touche que l'ARNt^{Gly}, altérant le décodage des codons (Leiva et al., 2020). Chez E. coli, l'expression des ARNt peuvent moduler la réponse au stress oxydant. Il est possible que chez *S. aureus,* même si le niveau global d'ARNt n'est pas fortement impacté, des changements au niveau de leurs modifications puissent participer au contrôle traductionnel et à la réponse au stress oxydant.

vii. La persistance de la bactérie privilégiée au détriment de la dissémination et de l'infection aiguë

Les mécanismes de survie et de réparation des dommages causés par les ROS sont privilégiés durant le stress oxydant au détriment de la production de toxines cytolytiques responsables d'infections aigües telles que les PSM ou les CHIPS. Dans le contexte d'une infection, cela est habituellement observé durant la colonisation des tissus dans lesquels *S. aureus* établit de nouvelles colonies grâce aux adhésines exprimées telles que la protéine SpA et le clumping factor B. D'un autre côté, le stress oxydant est habituellement rencontré lorsque *S. aureus* est internalisé dans les neutrophiles et les macrophages. *S. aureus* a été reconnue comme persistant à l'intérieur des phagocytes ou des cellules endothéliales sur des périodes prolongées (Hamill *et al.*, 1986). Dans ces conditions confinées, le système de quorum sensing Agr devrait normalement augmenter l'expression des toxins et exoprotéines (Carnes *et al.*, 2010). Cependant, chez les bactéries internalisées, il a été démontré que l'inactivation du régulateur Agr empêchant l'expression des facteurs de virulence dépendant du quorum sensing leur permet et persister sous forme de Small Colony Variants (SCV). Ces variants se développent plus lentement mais présentent une plus grande résistance aux antibiotiques, provoquant des infections chroniques (Sendi and Proctor, 2009; Young *et al.*, 2017). Lorsque Les conditions seront plus favorables ou la densité de cellules suffisante, les toxines seront produites afin de disséminer les bactéries et diffuser l'infection (Surewaard *et al.*, 2013; Bojer *et al.*, 2018).

3. Modifications des ARNt et stress oxydant

i. Dynamique des modifications des ARNt durant le stress

En condition de stress oxydant, le profil de migration des ARNt sur gel de polyacrylamide est modifié pour la souche de laboratoire HG001 comme pour la souche clinique de *S.aureus* USA300. La migration des ARNt indique un changement dans l'état de modification de certains ARNt. L'absence de queuosine suggérée par le clivage par la RNAse T1 dans l'ARNt^{Tyr}

est confirmée par les profils de migration sur gel d'APB des 4 ARNt concernés. Les ARNt contenant une Q34 migrent à la même vitesse en condition de stress oxydant que les ARNt provenant d'une souche ne possédant pas de queuosine. Les analyses de 3 des ARNt purifiés par chromatographie d'affinité digérés par la RNase U2 montrent la présence de G34 non modifiés pour ces ARNt provenant de cultures stressées.

L'analyse par RNA-Seq en triplicats d'ARNt totaux issus de cultures stressées ou non est à ce jour en cours afin de déterminer si d'autres modifications sont affectées. Les enzymes de modification des ARN, plus spécifiquement les méthyltransférases, font partie des métalloenzymes à centre [4Fe-4S]. La présence de ROS peut donc entrainer leur inactivation et ainsi une diminution des méthylations des ARNt. Cependant aucun résultat obtenu lors de cette étude ne permet de le démontrer. Les 2'OMe présents en position 32 qui sont impliqués dans la réponse au stress oxydant chez *P. aeruginosa* n'ont pas été détectés par NanoLC-MS/MS chez *S. aureus*. De même, les m^7G en position 46 ont été détectés dans peu d'ARNt, ne permettant pas de réaliser d'analyses sur de potentiels changements lors du stress.

ii. Causes de l'absence de queuosine

L'analyse transcriptomique semble montrer une légère surexpression des enzymes impliquées dans la voie de biosynthèse de la queuosine malgré l'absence de celle-ci dans les ARNt. Ces résultats peuvent indiquer la chute de l'activité enzymatique des protéines produites. Les plus susceptibles d'être inactivées sont les enzymes contenant un cluster [4Fe-4S], il y en a 3 impliquées dans la synthèse de la queuosine : QueE, QueG et QueH. La 7-carboxy-7-deazaguanine synthase (QueE) utilise la SAM et catalyse la synthèse du CDG à partir du CPH_4 (**Fig. 7A**, étape 3) (McCarty *et al.*, 2013). *S. aureus* possède deux époxyqueuosine réductases (**Fig. 7**, étape8), QueG utilisant la cobalamine (Dowling *et al.*, 2016) et QueH qui semble être indépendante de la cobalamine (Zallot *et al.*, 2017).

L'ajout d'un intermédiaire de cette voie, le preQ1 permet de restaurer la présence de la queuosine sur les ARNt indiquant une possible inactivation d'une ou plusieurs enzymes en amont de cet intermédiaire. La réduction de l'époxyqueuosine (oQ) ne semble donc pas être

l'étape impactée par la présence des ROS. Comme deux enzymes sont capables de catalyser cette réaction, deux possibilités se présentent : soit les deux clusters ne sont pas sensibles aux ROS, soit leurs activités peuvent se compenser en cas d'inactivation de l'une des deux enzymes. L'enzyme QueE est potentiellement sensible à l'oxydation par les ROS, le fer apical (non coordiné par une cystéine du motif CXXXCXXC) du cluster peut être protégé de l'oxygène s'il est coordiné par un ligand ou à un autre acide aminé situé à proximité.

Cependant, cela ne semble pas être le cas pour QueE, le fer apical des enzymes à SAM doit être accessible pour permettre la coordination du SAM. Par exemple, l'enzyme QueE de *B. subtilis*, proche de celle de celle de *S.aureus* présente un fer très accessible (**Fig. 9**).

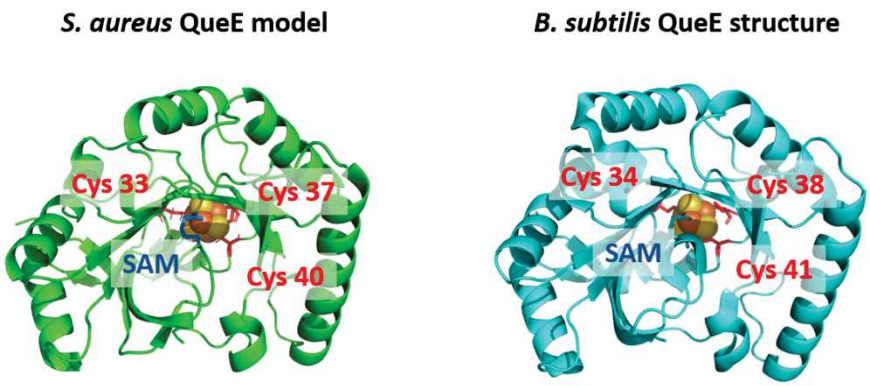

Figure 9. Comparaison structurelle entre la QueE de *S. aureus* modélisée par homologie est la structure obtenue par rayon X de *B. subtilis* (fichier pdb 5TH5; Bruender et al., 2017). Le motif spécifique pour la coordination du cluster [4Fe-4S] (en orange et jaune) est conservé. Il est composé de 3 résidus cystéine. Chez *B. subtilis,* cys 38 et cys 41 (chez *S. aureus,* cys 37 and cys 40 correspondants) sont assez proches our pouvoir former un pont disulfure si ils sont oxydés. Le 4ème fer du cluster interagit avec l'α-amino et l'α- carboxylate du SAM.

L'enzyme catalysant la synthèse du preQ$_1$ à partir du preQ$_0$, QueF (7-cyano-7-déazaguanine réductase NADPH dépendante) (**Fig. 7**, étape 5) possède une cystéine catalytique en position 57 chez *S. aureus* (**Fig. 10**).

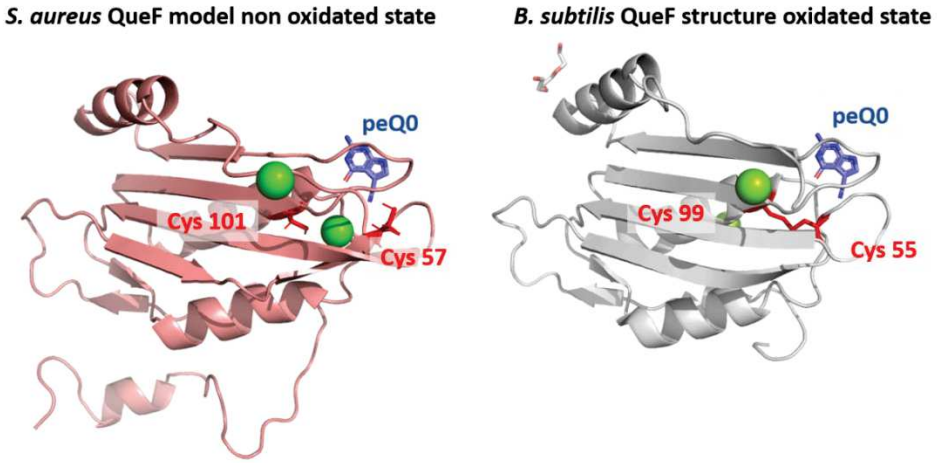

Figure 10 : Comparaison structurale entre le modèle de QueF de *S. aureus* obtenu par homologie avec la structure aux rayons X de QueF de *B.subtilis* en état oxydé (pdb file 5UDG; Mohammad et al., 2017). La Cys 55 de *B. subtilis* (correspondant à la Cys 57 chez *S. aureus*) se lie au substrat preQ$_0$, formant un intermédiaire thiomide. Ce résidu catalytique est sensible à l'oxydation et peut former un pont disulfure avec la Cys 99 (Cys 101 chez *S. aureus*). Le preQ$_0$ ne peut plus se fixer à QueF si la Cys 57 est oxydée, empêchant la formation de la queuosine.

Cette cystéine peut être protégée en conditions oxydantes par la formation d'un pont disulfure avec une deuxième cystéine se situant à proximité (Mohammad et al., 2017). Des analyses de LC-MS/MS ont été réalisées en alkylant les protéines avant la réduction des ponts disulfures mais les cystéines concernées n'ont pas pu être visualisées dû à la trop faible abondance de la protéine d'intérêt. La séparation préalable sur SDS-PAGE n'a pas permis d'éliminer suffisamment les protéines contaminantes. Afin d'enrichir l'échantillon pour l'analyse LC-MS/MS de QueF, il est possible d'exprimer la protéine portant une étiquette (flag-tag) avant purification par chromatographie d'affinité de type co-immunoprécipitation. Après élimination du MV par centrifugation des bactéries, aucune restauration de la queuosine n'a été observée sur gel de polyacrylamide, ce qui semble invalider l'hypothèse de l'inactivation réversible de QueF. De manière identique à preQ$_1$, l'ajout du substrat de QueF, preQ$_0$ au milieu de culture des bactéries cultivées en conditions oxydantes est en cours au laboratoire afin de tenter de restaurer la présence de queuosine.

iii. Conséquences traductionnelles de l'absence de Q34

La queuosine est présente en position 34 des ARNt, la position wobble qui est impliquée dans le décodage des ARNm. L'altération de cette modification peut impacter la vitesse et la précision de la traduction des protéines contenant les 4 acides aminés dont l'incorporation dépend des ARNt qui ont perdu la queuosine.

La légère surexpression observée dans l'analyse transcriptomique des gènes de chaperonnes impliquées dans le repliement des protéines peut indiquer un problème d'agrégation des protéines dû à des variations de vitesse de traduction.

Afin d'étudier la vitesse de décodage des ARNm codon par codon, une expérience de ribosome profiling à haute résolution (hRibo-Seq) permet de révéler les sites de pause du ribosome. Un protocole établi pour *E. coli* (Mohammad *et al.*, 2019) a été adapté à l'étude de *S. aureus* au sein du laboratoire. Cette méthode consiste à immobiliser les ribosomes en cours de traduction grâce à la congélation directe des bactéries dans l'azote liquide en présence d'une concentration élevée de sels de magnésium. Après purification des polysomes, les portions d'ARNm qui ne sont pas protégés par la présence du ribosome sont digérées par une RNase spécifique (MNase) permettant de générer des fragments d'ARNm en cours de décodage. Le séquençage des fragments d'ARNm en cours de traduction permet de déterminer d'une par les gènes traduits spécifiquement durant les conditions données mais également d'obtenir un taux d'occupation des ribosomes le long des ARNm.

L'étape de digestion des ARNm est cruciale pour déterminer précisément les codons particuliers pour lesquels la vitesse de décodage est altérée. En effet, la digestion par la RNAse doit générer des fragments de longueur adaptée, correspondant à la position exacte du ribosome et permettant d'assigner un codon spécifique au site de décodage.

L'étude de l'impact des queuosines sur le décodage des ARNm chez les eucaryotes met en évidence des conséquences différentes de l'absence de queuosine sur la vitesse de décodage des codons contenants un C ou un U en 3' dépendant de l'organisme. La queuosine contribuant ainsi à l'harmonisation de la vitesse de la traduction de manière générale (Tuorto *et al.*, 2018; Müller *et al.*, 2019).

Les données préliminaires obtenues durant les tests réalisés au laboratoire semblent indiquer que chez *S. aureus*, spécialement pour l'ARNt^{Tyr}, l'absence de Q34, entraine une perte de vitesse de décodage des codons UAU durant le stress oxydant alors que la vitesse de décodage des codons UAC n'est pas impactée (**Fig. 11**).

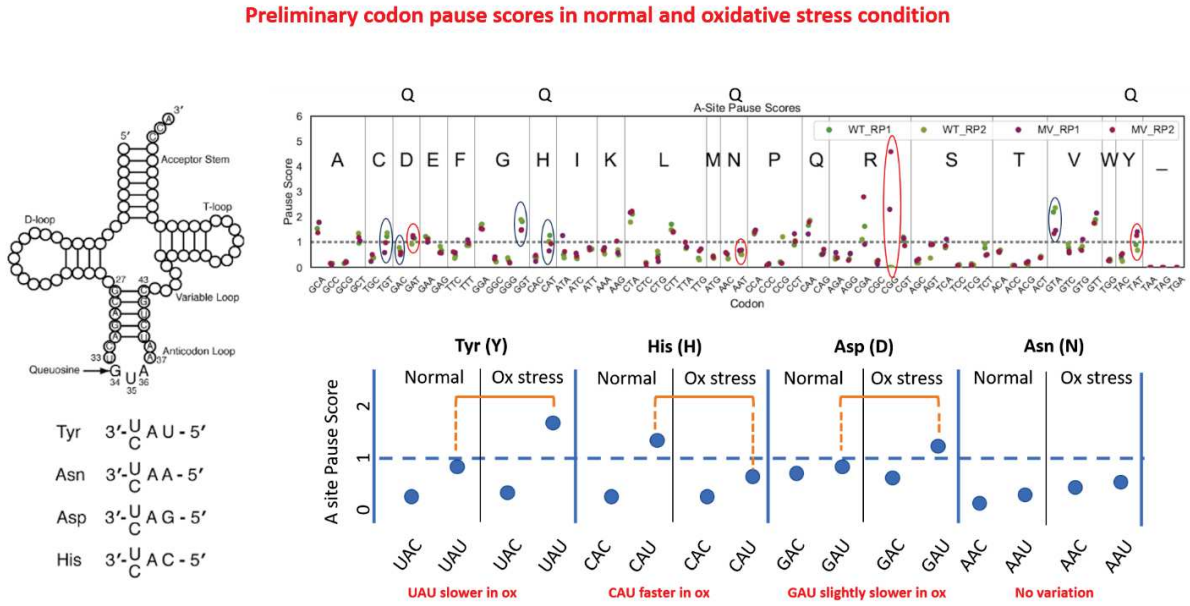

Figure 11. Score de pause des codons dans le site A par analyse préliminaire de hRibo-seq en condition normale (WT, en vert) et stress oxydant (MV, en rouge). Les scores de pauses ont été calculées selon Mohammad *et al.*, 2019. Des variations ont été obsérvées pour les codons synonymes des Cys (C), Asp (D), Gly (G), His (H), Asn (N), Arg (R), Val (V) et Tyr (Y). Les codons Asp (D), Asn (N) et Tyr (Y), et His (H) correspondent aux ARNt contenant une Q34 en condition normale et un G34 en stress oxydant. Parmis eux, les différences les plus importantes sont observées pour l'ARNt^{Tyr} qui montre un décodage plus lent pour le codon UAU durant le stress oxydant.

Le protocole utilisé restreint le volume de culture qui peut être utilisé et dans les conditions de notre analyse, réalisée en fin de phase exponentielle (lorsque la traduction est déjà réduite), nous n'avons pas pu obtenir assez de fragments d'ARNm pour réaliser une analyse correcte et complète. Afin d'obtenir suffisamment d'ARNm en cours de traduction, les cellules doivent être en phase exponentielle et contenir un grand nombre de ribosomes matures et actifs. Cela implique pour nous d'induire le stress plus tôt dans la phase de croissance des bactéries et d'arrêter la culture plus tôt car dans les conditions présentées dans cette étude, de nombreux ribosomes se sont révélés être immatures ou inactifs. Un autre aspect qui peut être amélioré pour obtenir une meilleure résolution pour nos expériences de hRibo-seq est le choix de la RNase utilisée pour produire les fragments

d'ARNm protégés par le ribosome. L'utilisation de la MNase ne semble pas adaptée pour cette étude chez *S. aureus*, car la taille des fragments obtenus indique une dégradation non spécifique des extrémités des ARNm protégés par le ribosome. Cette étape de digestion est réalisée avec la RNase I pour les analyses de ribosome profiling chez les eucaryotes, cette procédure a été testées avec succès et sera donc mise en place au sein du laboratoire

Des perturbations dans la vitesse de traduction des protéines peut impacter le repliement de celles-ci et ainsi leur stabilité. Le décodage de certains ARNm, selon leur composition en codons spécifiques, peut donc participer à la régulation de l'expression de certaines protéines au niveau de la traduction. Cette analyse permettra d'étudier l'impact sur la vitesse de décodage de l'absence de la queuosine sur les 4 ARNt concernés et ainsi d'établir le rôle de cette modification dans l'adaptation de la bactérie au stress oxydant.

IV. Conclusions

J'ai participé à la mise en place de la méthode d'UPLC-MS/MS qui, en association avec les méthodes de RNA-Seq, a permis d'établir les cartographies partielles des modifications présentes dans les ARN non codants de *S. aureus.* L'amélioration de cartographie est en cours avec l'utilisation de méthodes complémentaires permettant de la compléter et d'étendre cette analyse à d'autres ARN tels que les ARN régulateurs pour lesquels aucune modification n'a été caractérisée *chez S. aureus*

Cette cartographie m'a permis d'étudier leurs variations, en particulier dans les ARNt, lors du stress oxydant mimant la production de ROS par les cellules du système immunitaire lors de l'infection. J'ai ainsi pu mettre en évidence une altération de la queuosine des 4 ARNt possédant cette modification en position wobble de l'anticodon. De plus, l'ajout d'un intermédiaire de la voie de biosynthèse restaure la présence de la queuosine, apportant une indication sur la cause possible de l'absence de la modification

Ces résultats ont conduit à la mise en place de la méthode de ribosome profiling à haute résolution et son adaptation pour l'étude de *S.aureus*. Les premières analyses de l'impact sur la traduction de l'absence de cette modification sur les $ARNt^{Tyr}$ ont montré des résultats

encourageants. L'expérience de hRibo-Seq complète peut être réalisée afin d'élucider la fonction de la queuosine sur le décodage de l'ensemble des codons nécessitant cette modification. Les cultures contenant du $preQ_0$ ont été réalisées et peuvent être analysées afin de souligner une potentielle inactivation de l'enzyme QueF lors du stress oxydant.

La cartographie des modifications sur les ARN ribosomiques est en cours de réalisation, les données de RNA-Seq de ribosomes et d'ARNt provenant de bactéries soumises ou non au stress oxydant sont en cours d'analyse. Le projet se poursuit avec l'étude structurale de l'impact des variations des modifications des ARNt et ARNr sur l'ensemble de la machinerie traductionnelle qui est réalisée par Roberto Bahena, qui est actuellement en thèse.

L'analyse des modifications des $ARNt^{Gly}$ non protéinogéniques ne possédant pas de modifications a mené à la création d'un nouveau projet de recherche. L'étude structurale des différents isoaccepteurs de la glycine ainsi que de leurs interactions avec la machinerie traductionnelle (EFTU) ou la machinerie responsable du transfert des ARNt vers la paroi cellulaire telles que les protéines Fem (facteurs essentiels pour la résistance à la méthicilline) est en cours avec Hiroki Kanazawa actuellement en contrat post doctoral.

Cette approche mise en place pour l'étude des variations des modifications des ARN en réponse au stress oxydant et de leur impact traductionnel, pourra être appliquée à d'autres conditions environnementales rencontrées lors de l'infection. La combinaison des informations apportées par l'étude de la réponse du pathogène aux différents stress permettra d'améliorer notre compréhension du rôle des modifications durant l'infection.

V. Matériels et méthodes

1. Produits et sondes utilisés

Les produits chimiques et milieux de culture utilisés proviennent de Sigma-Aldrich. Les enzymes utilisées proviennent de ThermoFischer Scientific.

Sondes utilisées :

	probe for single tRNA purification	probe for Northern blotting
$tRNA^{Asp}_{GUC}$	/5BiosG/GATCTCCTGCGTGACAGGCAGGCGTGTTAACCGCTACAC	GATCTCCTGCGTGACAGGCAGGCGTGTTAACCGCTACAC
$tRNA^{Asn}_{GUU}$	/5BiosG/GACCGATCGGTTAACAGCCGATAGCTCTACCACTGAGC	GACCGATCGGTTAACAGCCGATAGCTCTACCACTGAGC
$tRNA^{His}_{GUG}$	/5BiosG/GAATGTCGGAACCACAATCCGATGTGTTAACCACTTCAC	GAATGTCGGAACCACAATCCGATGTGTTAACCACTTCAC
$tRNA^{Tyr}_{GUA}$	/5BiosG/CGAAGGAGCGGATTTACAGTCCGCCGCGTTTAGCCACTTCGC	CGAAGGAGCGGATTTACAGTCCGCCGCGTTTAGCCACTTCGC
tRNAGly P2	/5Biosg/ATC AGC TTG GAA GGC TGA GGT TTT GCC ATT AAA CTA	/
tRNAGly NP1+NP2	/5Biosg/TCG TTC CGG GAA GGA ACG TGT TCT AAA AGT TGA ACT A	/
tRNAGly NP3	/5Biosg/TCA TTC CAG GAA GGA ATG TAT TCT AAG AGT TGA AAT A	/
rRNA pos	oligonucleotide for rRNA modifications MS analysis	
1202-1241	C GTGTGTAGCCCAAATCATAAGGGGCATGATGATTTGACG	
1395-1440	GGTGTTACAAACTCTCGTGG TGTGACGGGC GGTGTGTACAGACCC	
1497-1542	TCCAGCCGCACCTTCCGATACGGCTACCTTGTTACGACTTCACCCC	

Tableau 2 : Oligonucléotides utilisés pour la purification des ARNt, les Northern blot et l'Analyse par NanoLC-MS/MS des modifications de l'ARNr 16S

2. Souches bactériennes et conditions de culture

i. Souches

La souche principalement utilisée pour cette étude est la souche *S. aureus* HG001 de laboratoire, dérivée de la souche NCTC8325 contenant le gène *rsbU* restauré (Herbert *et al.*, 2010). La souche clinique MRSA (methicillin resistant *S.aureus*) *S. aureus* USA300 (Tenover and Goering, 2009) ainsi que la souche NE1885 provenant de la collection Nebraska qui en est dérivée seront également utilisées. La souche NE1885 possède un transposon contenant plusieurs codons stop en position 9 du gène *tgt* entrainant une absence de queuosine (Bose *et al.*, 2013).

ii. Conditions de culture

Les cultures de bactéries non stressées sont réalisées dans les conditions publiées précédemment (*cf* § II. 2). Brièvement, une préculture sur la nuit est diluée à DO(600nm) = 0,05 dans 20 mL de BHI et est incubée à 37°C sous agitation à 180rpm durant 4h jusqu'à une $DO(600nm)_{finale}$ = 3.

Les cultures soumises au stress oxydant sont cultivées comme les bactéries non stressées pendant 120 min. A t= 120 min, 10mM final de méthylviologen est ajouté à la culture, les bactéries sont ensuite cultivées dans les conditions de température et d'agitation inchangées pendant 120 min jusqu'à atteindre une $DO(600nm)_{finale}$ = 2,5-3.

Pour l'étude de l'effet de l'intermédiaire $preQ_1$, le stress est appliqué par l'ajout de méthylviologen au milieu de culture après 90min d'incubation. Après 1h de croissance en condition de stress oxydant, le $preQ_1$ est ajouté à une concentration finale de 1µM, les cellules sont ensuite incubées dans les mêmes conditions de température et d'agitation.

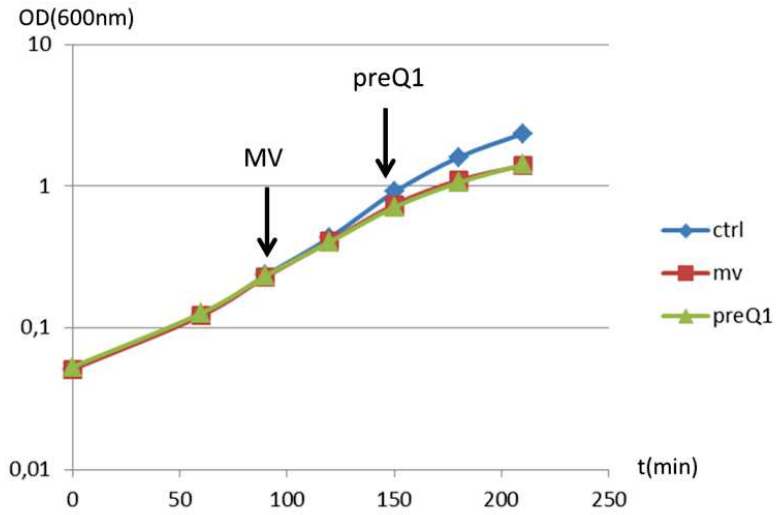

Figure 12 : Courbe de croissance des cultures de *S. aureus* HG001 cultivées en condition oxydante dont la queuosine est réstaurée par l'ajout de $preQ_1$.

3. Analyse par NanoLC-MS/MS de l'ARNr 16S

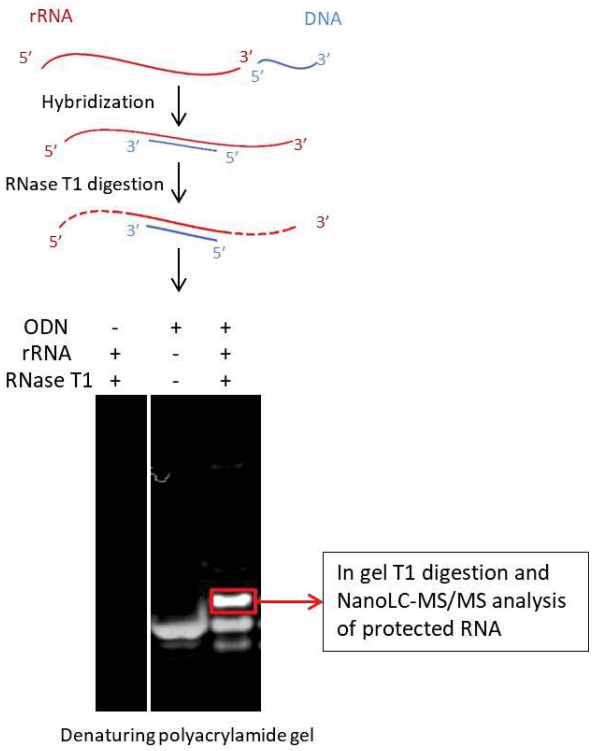

Figure 13 : Adaptation de la méthode NanoLC-MS/MS à l'analyse des ARNr. Brièvement, une partie ciblée de l'ARN est protégée par hybridation d'un oligodésoxynucléotide puis digérée avec la RNAse T1. Le duplexe ARN-ADN est ensuite séparé sur gel de polyacrylamide dénaturant avant une seconde digestion à la RNaseT1 et analyse NanoLC-MS/MS.

L'analyse est réalisée à partir d'ARNt totaux, préparés comme publié précédemment (*cf* § II. 2). 10 µg d'ARN totaux sont dénaturés en présence de l'oligonucléotide (**tableau 2**)dans un tampon cacodylate 10 mM ; 50 mM NaCl ; 25 mM KCl à 90°C pendant 5 min puis renaturés avec l'oligonucléotide d'ADN dans la glace pendant 30 min. L'ARN non protégé est ensuite digéré avec la RNase T1 à 37°C pendant 2h (100 mM Acétate d'ammonium). Les échantillons sont ensuite déposés sur gel de polyacrylamide 10%, 8M urée et migrés dans le TBE pendant 2h à10W constants.

Les ARN sont révélés par bromure d'éthidium, les bandes de gel sont découpées puis les ARN sont digérés en gel et analysés par NanoLC-MS/MS comme publié précédemment ((*cf* § II. 1).

4. Analyse transcriptomique

Les triplicats d'ARN totaux sont extraits suivant les protocoles publiés précédemment (*cf* § II. 2.). Brièvement, les cultures sont centrifugées à 3750 rpm et 4°C pendant 15min puis les cellules sont resuspendues dans 1mL de solution RNA Pro (MP biomedicals) et lysées mécaniquement au fastprep (MP biomedical) 2 fois 40s à vitesse maximale. Les ARN totaux sont extraits au chloroforme, puis précipités à l'éthanol et traités avec 1U de DNase I par µg d'acides nucléiques (estimés par mesure de l'absorbance à 260nm) pendant 45min à 37°C sans agitation. La DNase est éliminée par une nouvelle extraction au phénol/chloroforme/alcool isoamylique et les ARN sont précipités à l'éthanol. La concentration et la pureté des acides nucléiques sont mesurées par nanodrop avant la préparation des librairies et séquençage par la plateforme EpiRNA-Seq de Nancy. Les données sont traitées avec Galaxy comme détaillé dans (Lalaouna *et al.*, 2018) pour l'élimination des séquences des adaptateurs, le seuil de qualité, l'alignement sur le génome et le comptage des reads par feature annotée. Pour l'analyse différentielle, Deseq2 est utilisé.

5. Analyse protéomique

Les triplicats de protéines totales sont extraits de cellules resuspendues dans le tampon 50 mM Tris pH 8, 50 mM NaCl, 1% triton × 100 et lysée 40s au fastprep. Le dosage des protéines est réalisé par Bradford, les protéines (5 µg) sont précipitées au méthanol contenant 0,1 M d'acétate d'ammonium, puis réduites et alkylées (5 mM DTT, 10 mM iodoacetamide). Les protéines sont ensuite digérées à la trypsine puis les peptides (1µg) sont analysées par NanoLC-MS/MS sur un système NanoLC-2DPlus system couplé à un spectromètre de masse TripleTOF 5600 (ABSciex) (Chicher *et al.*, 2015).

6. Gel d'acide phénylboronique et Northern blot

Les gels de polyacrylamide contenant de l'acide phénylboronique ont été réalisées suivant les protocoles établis (Matuszek and Pan, 2019). Les ARN totaux (2µg) préalablement déacylés sont séparés sur gel de polyacrylamide, 12%, 8M urée, 0,5% APB pendant 3h30 à 13W constant. Les ARN sont ensuite transférés sur membrane de nitrocellulose Hybond N+ (GE Healthcare Life Sciences) par transfert semi-sec pendant 45 min à 10V (Trans-Blot semi-dry transfert cell, Biorad) et fixés par crosslink UV (Stratalinker 1800, Statagene). Les ARNt sont révélés par hybridation d'une sonde marquée au 32P (**Tableau 2**) et visualisés par autoradiographie.

7. Purification des ARNt

Les ARNt sont obtenus à partir d'extraits d'ARN totaux par filtration sur centricons 50 kDa (Amicon Ultra 0,5 mL, Millipore), 20 µg d'ARN total est déposé sur la membrane puis centrifugé 10 min, à 9000 rpm et température ambiante. Le filtrat est immédiatement précipité à -20°C durant la nuit avec 3 volumes d'éthanol contenant 0,1 M d'acétate d'ammonium. Après centrifugation 10 min à 13000 rpm et 4°C, le culot est rincé, séché puis repris dans 50 µL d'eau milliQ. 200 µL de résine streptavidine-sépharose sont préalablement incubée avec 400 µL de sonde spécifique biotinylée (7.5 µM) durant 30min à température ambiante puis rincée avec 400 µL de tampon (10mM Tris, HCl pH 7.5). Les ARNt sont incubés avec la résine streptavidine-sonde en présence de 900 mM de TEA-Cl et 0,1 mM d'EDTA pendant 5 min à 37°C. La résine est ensuite rincée 3 fois avec 400 µL de tampon. L'ARNt hybridé à la sonde est élué par chauffage à 60°C pendant 5 min suivi d'une centrifugation rapide (10 s, 13000 rpm, température ambiante). L'ARNt purifié est ensuite concentré par précipitation à l'éthanol (Yokogawa *et al.*, 2010).

8. Digestion à la RNAse U2 des ARNt purifiés.

La digestion des ARNt à la RNase U2 a été réalisée selon une adaptation de la méthode préalablement publiée (Wolff *et al.*, 2020). Brièvement, 20 ng d'ARNt purifié sont digérés avec 6 ng de RNase U2 produite au laboratoire dans 20 µL d'acétate d'ammonium 100mM à 37°C pendant 2h.

9. Modèlisation des structures de QueE et QueF de *S. aureus*

QueE et QueF *de S. aureus* ont été modélisées par homologie à l'aide du serveur tRosetta (Yang et al., 2020). L'alignement sur les modèles est amélioré par la réalisation d'alignement de séquence multiples (MSA : Multiple Sequence Alignment) utilisant les 1500 séquences disponibles pour chacune des deux protéines. Elles ont toutes deux été estimées comme étant de très haute confiance, avec des TM scores estimés de 0,91 pour QueE et 0,849 pour QueF. Le TM-score est une mesure permettant d'évaluer la similarité topologique des structures de protéines. Les valeurs de TM-score se situent entre 0 et 1, où 1 indique une parfaite correspondance entre deux structures. Les structures utilisées pour modéliser QueE sont les fichiers pdb 5TH5 (*B. subtilis*), 6NHL (*E. coli*), 4NJJ et 4NJH (*Burkholderia multivorans*). Celles utilisées pour modeliser QueF sont les fichiers pdb 4FGC, 4F8B et 5UDG (*B. subtilis*), 3S19 et 3UXJ (*Vibrio cholerae*).

10. Ribosome profiling à haute résolution

Les bactéries sont cultivées comme décrit précédemment. Les cultures (30 mL) sont congelées directement dans l'azote liquide avec le tampon de lyse (20mM Tris, HCl pH8 ; 150mM $MgCl_2$; 100 mM NH_4Cl ; 5 mM $CaCl_2$; 0,1% NP40 ; 0,4%triton X100 ; 100 U de DNaseI/mL de culture). Les billes de cellules congelées sont ensuite lysées au Fastprep 5 x 40s à vitesse maximale en présence de billes en acier. Les lysats sont ensuite décongelés 1 h à température ambiante et directement centrifugés 20 min à 3750 rpm, 4°C. Le surnageant est clarifié par une deuxième centrifugation, à 8000rpm, 4°C pendant 20 min avant d'être

déposé sur 4mL de coussin de sucrose (20 mM Tris HCl, pH8 ; 10 mM $MgCl_2$; 0.5 M NH_4Cl ; 0,5 mM EDTA ; 1,1M sucrose), puis ultracentrifugé 45000 rpm, 4°C, 3h30. Le culot est repris dans un tampon de resuspension (20 mM Tris HCl pH8 ; 10 mM $MgCl_2$; 5 mM $CaCl_2$; 0,1% NP40, 0,4% triton X100 ; 1 mM chloramphénicol) avant la digestion, ici à la MNase : 25 mM $CaCl_2$; 1000U MNase ; incubation à 25°C, 1 h, 1400 rpm. La digestion est arrêtée par l'ajout d'EGTA puis l'échantillon est déposé sur gradient de sucrose (5-50% ; 20 mM Tris, HCL pH7,5 ; 100mM NH_4Cl ; 10 mM $MgCl_2$; 1mM DTT) et ultracentrifugé à 39000 rpm 4°C pendant 2h46. Les ribosomes 70S sont récupérés, les ARN sont extraits par phénol chaud, précipités puis déposés sur gel de polyacrylamide afin de purifier sur gel les fragments correspondant à une taille d'environ 28 nt et les séquencer. En parallèle, une partie de la culture est gardée pour réaliser l'analyse transcriptomique. Le traitement informatique des données de séquençage est réalisé en collaboration avec Béatrice Chane-Woon-Ming suivant la pipeline développée par Mohammad en 2019 (Mohammad and Buskirk, 2019).

Références bibliographiques

Andersson, D.I. and Hughes, D. (2014) Microbiological effects of sublethal levels of antibiotics. *Nat Rev Microbiol* **12**: 465–478.

Antoine, L. and Wolff, P. (2020) Mapping of Posttranscriptional tRNA Modifications by Two-Dimensional Gel Electrophoresis Mass Spectrometry. *Methods Mol Biol Clifton NJ* **2113**: 101–110.

Antoine, L., Wolff, P., Westhof, E., Romby, P., and Marzi, S. (2019) Mapping post-transcriptional modifications in Staphylococcus aureus tRNAs by nanoLC/MSMS. *Biochimie* **164**: 60–69.

Arciola, C.R., Campoccia, D., Ravaioli, S., and Montanaro, L. (2015) Polysaccharide intercellular adhesin in biofilm: structural and regulatory aspects. *Front Cell Infect Microbiol* **5**:.

Ayadi, L., Motorin, Y., and Marchand, V. (2018) Quantification of 2'-O-Me Residues in RNA Using Next-Generation Sequencing (Illumina RiboMethSeq Protocol). *Methods Mol Biol Clifton NJ* **1649**: 29–48.

Barraud, P., Gato, A., Heiss, M., Catala, M., Kellner, S., and Tisné, C. (2019) Time-resolved NMR monitoring of tRNA maturation. *Nat Commun* **10**: 3373.

Beaber, J.W., Hochhut, B., and Waldor, M.K. (2004) SOS response promotes horizontal dissemination of antibiotic resistance genes. *Nature* **427**: 72–74.

Beasley, F.C., Vinés, E.D., Grigg, J.C., Zheng, Q., Liu, S., Lajoie, G.A., et al. (2009) Characterization of staphyloferrin A biosynthetic and transport mutants in Staphylococcus aureus. *Mol Microbiol* **72**: 947–963.

Berube, B.J. and Wardenburg, J.B. (2013) Staphylococcus aureus α-Toxin: Nearly a Century of Intrigue. *Toxins* **5**: 1140–1166.

Bisognano, C., Kelley, W.L., Estoppey, T., Francois, P., Schrenzel, J., Li, D., et al. (2004) A RecA-LexA-dependent Pathway Mediates Ciprofloxacin-induced Fibronectin Binding in Staphylococcus aureus*. *J Biol Chem* **279**: 9064–9071.

Bojer, M.S., Lindemose, S., Vestergaard, M., and Ingmer, H. (2018) Quorum Sensing-Regulated Phenol-Soluble Modulins Limit Persister Cell Populations in Staphylococcus aureus. *Front Microbiol* **9**: 255.

Bose, J.L., Fey, P.D., and Bayles, K.W. (2013) Genetic tools to enhance the study of gene function and regulation in Staphylococcus aureus. *Appl Environ Microbiol* **79**: 2218–2224.

Butala, M., Zgur-Bertok, D., and Busby, S.J.W. (2009) The bacterial LexA transcriptional repressor. *Cell Mol Life Sci CMLS* **66**: 82–93.

Cadet, J. and Wagner, J.R. (2013) DNA Base Damage by Reactive Oxygen Species, Oxidizing Agents, and UV Radiation. *Cold Spring Harb Perspect Biol* **5**: a012559.

Carnes, E.C., Lopez, D.M., Donegan, N.P., Cheung, A., Gresham, H., Timmins, G.S., and Brinker, C.J. (2010) Confinement-induced quorum sensing of individual Staphylococcus aureus bacteria. *Nat Chem Biol* **6**: 41–45.

Chang, W., Small, D.A., Toghrol, F., and Bentley, W.E. (2006) Global Transcriptome Analysis of Staphylococcus aureus Response to Hydrogen Peroxide. *J Bacteriol* **188**: 1648–1659.

Chen, X., Yin, H., Li, G., Wang, W., Wong, P.K., Zhao, H., and An, T. (2019) Antibiotic-resistance gene transfer in antibiotic-resistance bacteria under different light irradiation: Implications from oxidative stress and gene expression. *Water Res* **149**: 282–291.

Cheung, J., Beasley, F.C., Liu, S., Lajoie, G.A., and Heinrichs, D.E. (2009) Molecular characterization of staphyloferrin B biosynthesis in Staphylococcus aureus. *Mol Microbiol* **74**: 594–608.

Chicher, J., Simonetti, A., Kuhn, L., Schaeffer, L., Hammann, P., Eriani, G., and Martin, F. (2015) Purification of mRNA-programmed translation initiation complexes suitable for mass spectrometry analysis. *PROTEOMICS* **15**: 2417–2425.

Cho, K.H. and Caparon, M.G. (2008) tRNA Modification by GidA/MnmE Is Necessary for Streptococcus pyogenes Virulence: a New Strategy To Make Live Attenuated Strains. *Infect Immun* **76**: 3176–3186.

Cirz, R.T., Jones, M.B., Gingles, N.A., Minogue, T.D., Jarrahi, B., Peterson, S.N., and Romesberg, F.E. (2007) Complete and SOS-mediated response of Staphylococcus aureus to the antibiotic ciprofloxacin. *J Bacteriol* **189**: 531–539.

Clarke, S.R., Wiltshire, M.D., and Foster, S.J. (2004) IsdA of Staphylococcus aureus is a broad spectrum, iron-regulated adhesin. *Mol Microbiol* **51**: 1509–1519.

Clements, M.O., Watson, S.P., and Foster, S.J. (1999) Characterization of the major superoxide dismutase of Staphylococcus aureus and its role in starvation survival, stress resistance, and pathogenicity. *J Bacteriol* **181**: 3898–3903.

Cosgrove, K., Coutts, G., Jonsson, I.-M., Tarkowski, A., Kokai-Kun, J.F., Mond, J.J., and Foster, S.J. (2007) Catalase (KatA) and alkyl hydroperoxide reductase (AhpC) have compensatory roles in peroxide stress resistance and are required for survival, persistence, and nasal colonization in Staphylococcus aureus. *J Bacteriol* **189**: 1025–1035.

de Crécy-Lagard, V., Ross, R.L., Jaroch, M., Marchand, V., Eisenhart, C., Brégeon, D., et al. (2020) Survey and Validation of tRNA Modifications and Their Corresponding Genes in Bacillus subtilis sp Subtilis Strain 168. *Biomolecules* **10**:.

Davies, M.J. (2016) Protein oxidation and peroxidation. *Biochem J* **473**: 805–825.

Davies, M.J. (2005) The oxidative environment and protein damage. *Biochim Biophys Acta BBA - Proteins Proteomics* **1703**: 93–109.

Dean, R.T., Fu, S., Stocker, R., and Davies, M.J. (1997) Biochemistry and pathology of radical-mediated protein oxidation. *Biochem J* **324 (Pt 1)**: 1–18.

Dowling, D., Miles, Z., Kohrer, C., Maiocco, S., Elliott, S., Bandarian, V., and Drennan, C. (2016) Molecular basis of cobalamin-dependent RNA modification. *Nucleic Acids Res* **44**:.

Dryla, A., Gelbmann, D., von Gabain, A., and Nagy, E. (2003) Identification of a novel iron regulated staphylococcal surface protein with haptoglobin-haemoglobin binding activity. *Mol Microbiol* **49**: 37–53.

Eidhin, D.N., Perkins, S., Francois, P., Vaudaux, P., Höök, M., and Foster, T.J. (1998) Clumping factor B (ClfB), a new surface-located fibrinogen-binding adhesin of Staphylococcus aureus. *Mol Microbiol* **30**: 245–257.

Elmwall, J., Kwiecinski, J., Na, M., Ali, A.A., Osla, V., Shaw, L.N., et al. (2017) Galectin-3 Is a Target for Proteases Involved in the Virulence of Staphylococcus aureus. *Infect Immun* **85**:.

Eltzschig, H.K. and Carmeliet, P. (2011) Hypoxia and inflammation. *N Engl J Med* **364**: 656–665.

Falugi, F., Kim, H.K., Missiakas, D.M., and Schneewind, O. (2013) Role of Protein A in the Evasion of Host Adaptive Immune Responses by Staphylococcus aureus. *mBio* **4**:.

Fang, F.C. (2004) Antimicrobial reactive oxygen and nitrogen species: concepts and controversies. *Nat Rev Microbiol* **2**: 820–832.

Fedtke, I., Kamps, A., Krismer, B., and Götz, F. (2002) The nitrate reductase and nitrite reductase operons and the narT gene of Staphylococcus carnosus are positively controlled by the novel two-component system NreBC. *J Bacteriol* **184**: 6624–6634.

Fey, P.D., Endres, J.L., Yajjala, V.K., Widhelm, T.J., Boissy, R.J., Bose, J.L., and Bayles, K.W. (2013) A Genetic Resource for Rapid and Comprehensive Phenotype Screening of Nonessential Staphylococcus aureus Genes. *mBio* **4**: e00537-12.

Galvanin, A., Vogt, L.-M., Grober, A., Freund, I., Ayadi, L., Bourguignon-Igel, V., et al. (2020) Bacterial tRNA 2'-O-methylation is dynamically regulated under stress conditions and modulates innate immune response. *Nucleic Acids Res* **48**: 12833–12844.

Garcia, Y.M., Barwinska-Sendra, A., Tarrant, E., Skaar, E.P., Waldron, K.J., and Kehl-Fie, T.E. (2017) A Superoxide Dismutase Capable of Functioning with Iron or Manganese Promotes the Resistance of Staphylococcus aureus to Calprotectin and Nutritional Immunity. *PLoS Pathog* **13**:.

Giannouli, S., Kyritsis, A., Malissovas, N., Becker, H.D., and Stathopoulos, C. (2009) On the role of an unusual tRNAGly isoacceptor in Staphylococcus aureus. *Biochimie* **91**: 344–351.

Golubev, A., Fatkhullin, B., Khusainov, I., Jenner, L., Gabdulkhakov, A., Validov, S., et al. (2020) Cryo-EM structure of the ribosome functional complex of the human pathogen Staphylococcus aureus at 3.2 Å resolution. *FEBS Lett* **594**: 3551–3567.

Gordienko, I. and Rupp, W.D. (1997) UvrAB activity at a damaged DNA site: is unpaired DNA present? *EMBO J* **16**: 880–888.

Grimaud, R., Ezraty, B., Mitchell, J.K., Lafitte, D., Briand, C., Derrick, P.J., and Barras, F. (2001) Repair of oxidized proteins. Identification of a new methionine sulfoxide reductase. *J Biol Chem* **276**: 48915–48920.

Ha, K.P., Clarke, R.S., Kim, G.-L., Brittan, J.L., Rowley, J.E., Mavridou, D.A.I., et al. (2020a) Staphylococcal DNA Repair Is Required for Infection. *mBio* **11**:.

Hamill, R.J., Vann, J.M., and Proctor, R.A. (1986) Phagocytosis of Staphylococcus aureus by cultured bovine aortic endothelial cells: model for postadherence events in endovascular infections. *Infect Immun* **54**: 833–836.

Hassan, H.M. (1984) Exacerbation of superoxide radical formation by paraquat. *Methods Enzymol* **105**: 523–532.

Heilmann, C., Niemann, S., Sinha, B., Herrmann, M., Kehrel, B.E., and Peters, G. (2004) Staphylococcus aureus fibronectin-binding protein (FnBP)-mediated adherence to platelets, and aggregation of platelets induced by FnBPA but not by FnBPB. *J Infect Dis* **190**: 321–329.

Helm, M. and Motorin, Y. (2017) Detecting RNA modifications in the epitranscriptome: predict and validate. *Nat Rev Genet* **18**: 275–291.

Herbert, S., Ziebandt, A.-K., Ohlsen, K., Schäfer, T., Hecker, M., Albrecht, D., et al. (2010) Repair of global regulators in Staphylococcus aureus 8325 and comparative analysis with other clinical isolates. *Infect Immun* **78**: 2877–2889.

Igloi, G.L. and Kössel, H. (1985) Affinity electrophoresis for monitoring terminal phosphorylation and the presence of queuosine in RNA. Application of polyacrylamide containing a covalently bound boronic acid. *Nucleic Acids Res* **13**: 6881–6898.

Imlay, J.A. (2006) Iron-sulphur clusters and the problem with oxygen. *Mol Microbiol* **59**: 1073–1082.

Jarry, T.M., Memmi, G., and Cheung, A.L. (2008) The expression of alpha-haemolysin is required for Staphylococcus aureus phagosomal escape after internalization in CFT-1 cells. *Cell Microbiol* **10**: 1801–1814.

Jutkina, J., Rutgersson, C., Flach, C.-F., and Joakim Larsson, D.G. (2016) An assay for determining minimal concentrations of antibiotics that drive horizontal transfer of resistance. *Sci Total Environ* **548–549**: 131–138.

Karavolos, M.H., Horsburgh, M.J., Ingham, E., and Foster, S.J. (2003) Role and regulation of the superoxide dismutases of Staphylococcus aureus. *Microbiol Read Engl* **149**: 2749–2758.

Kellner, S., Neumann, J., Rosenkranz, D., Lebedeva, S., Ketting, R.F., Zischler, H., et al. (2014) Profiling of RNA modifications by multiplexed stable isotope labelling. *Chem Commun Camb Engl* **50**: 3516–3518.

Kellner, S., Ochel, A., Thüring, K., Spenkuch, F., Neumann, J., Sharma, S., et al. (2014) Absolute and relative quantification of RNA modifications via biosynthetic isotopomers. *Nucleic Acids Res* **42**: e142.

Keyer, K. and Imlay, J.A. (1996) Superoxide accelerates DNA damage by elevating free-iron levels. *Proc Natl Acad Sci U S A* **93**: 13635–13640.

Koh, C.S. and Sarin, L.P. (2018) Transfer RNA modification and infection – Implications for pathogenicity and host responses. *Biochim Biophys Acta BBA - Gene Regul Mech* **1861**: 419–432.

Lalaouna, D., Desgranges, E., Caldelari, I., and Marzi, S. (2018) Chapter Sixteen - MS2-Affinity Purification Coupled With RNA Sequencing Approach in the Human Pathogen Staphylococcus aureus. In *Methods in Enzymology*. High-Density

Sequencing Applications in Microbial Molecular Genetics. Carpousis, A.J. (ed). Academic Press, pp. 393–411.

Lechner, A., Wolff, P., Leize-Wagner, E., and François, Y.-N. (2020) Characterization of Post-Transcriptional RNA Modifications by Sheathless Capillary Electrophoresis-High Resolution Mass Spectrometry. *Anal Chem* **92**: 7363–7370.

Leiva, L.E., Pincheira, A., Elgamal, S., Kienast, S.D., Bravo, V., Leufken, J., et al. (2020) Modulation of Escherichia coli Translation by the Specific Inactivation of tRNAGly Under Oxidative Stress. *Front Genet* **11**:.

Liu, G.Y., Essex, A., Buchanan, J.T., Datta, V., Hoffman, H.M., Bastian, J.F., et al. (2005) Staphylococcus aureus golden pigment impairs neutrophil killing and promotes virulence through its antioxidant activity. *J Exp Med* **202**: 209–215.

Liu, M., Tanaka, W.N., Zhu, H., Xie, G., Dooley, D.M., and Lei, B. (2008) Direct hemin transfer from IsdA to IsdC in the iron-regulated surface determinant (Isd) heme acquisition system of Staphylococcus aureus. *J Biol Chem* **283**: 6668–6676.

Lowy, F.D. (1998) Staphylococcus aureus Infections. *N Engl J Med* **339**: 520–532.

Luong, T.T. and Lee, C.Y. (2002) Overproduction of Type 8 Capsular Polysaccharide Augments Staphylococcus aureus Virulence. *Infect Immun* **70**: 3389–3395.

Maiques, E., Ubeda, C., Campoy, S., Salvador, N., Lasa, I., Novick, R.P., et al. (2006) beta-lactam antibiotics induce the SOS response and horizontal transfer of virulence factors in Staphylococcus aureus. *J Bacteriol* **188**: 2726–2729.

Marchand, V., Ayadi, L., Ernst, F.G.M., Hertler, J., Bourguignon-Igel, V., Galvanin, A., et al. (2018) AlkAniline-Seq: Profiling of m7 G and m3 C RNA Modifications at Single Nucleotide Resolution. *Angew Chem Int Ed Engl* **57**: 16785–16790.

Marchand, V., Blanloeil-Oillo, F., Helm, M., and Motorin, Y. (2016) Illumina-based RiboMethSeq approach for mapping of 2'-O-Me residues in RNA. *Nucleic Acids Res* **44**: e135.

Marchand, V., Pichot, F., Neybecker, P., Ayadi, L., Bourguignon-Igel, V., Wacheul, L., et al. (2020) HydraPsiSeq: a method for systematic and quantitative mapping of pseudouridines in RNA. *Nucleic Acids Res* **48**: e110.

Maslowska, K.H., Makiela-Dzbenska, K., and Fijalkowska, I.J. (2019) The SOS system: A complex and tightly regulated response to DNA damage. *Environ Mol Mutagen* **60**: 368–384.

Matuszek, Z. and Pan, T. (2019) Quantification of Queuosine Modification Levels in tRNA from Human Cells Using APB Gel and Northern Blot. *Bio-Protoc* **9**: e3191–e3191.

McCarty, R.M., Krebs, C., and Bandarian, V. (2013) Spectroscopic, steady-state kinetic, and mechanistic characterization of the radical SAM enzyme QueE, which catalyzes a complex cyclization reaction in the biosynthesis of 7-deazapurines. *Biochemistry* **52**: 188–198.

Mengel-Jørgensen, J. and Kirpekar, F. (2002) Detection of pseudouridine and other modifications in tRNA by cyanoethylation and MALDI mass spectrometry. *Nucleic Acids Res* **30**: e135.

Mohammad, F. and Buskirk, A.R. (2019) Protocol for Ribosome Profiling in Bacteria. *Bio-Protoc* **9**: e3468.

Mohammad, F., Green, R., and Buskirk, A.R. (2019) A systematically-revised ribosome profiling method for bacteria reveals pauses at single-codon resolution. *eLife* **8**: e42591.

Motorin, Y. and Helm, M. (2019) Methods for RNA Modification Mapping Using Deep Sequencing: Established and New Emerging Technologies. *Genes* **10**: 35.

Motorin, Y., Muller, S., Behm-Ansmant, I., and Branlant, C. (2007) Identification of modified residues in RNAs by reverse transcription-based methods. *Methods Enzymol* **425**: 21–53.

Müller, M., Legrand, C., Tuorto, F., Kelly, V.P., Atlasi, Y., Lyko, F., and Ehrenhofer-Murray, A.E. (2019) Queuine links translational control in eukaryotes to a micronutrient from bacteria. *Nucleic Acids Res* **47**: 3711–3727.

Muryoi, N., Tiedemann, M.T., Pluym, M., Cheung, J., Heinrichs, D.E., and Stillman, M.J. (2008) Demonstration of the Iron-regulated Surface Determinant (Isd) Heme Transfer Pathway in Staphylococcus aureus. *J Biol Chem* **283**: 28125–28136.

Nakatsuji, T., Chiang, H.-I., Jiang, S.B., Nagarajan, H., Zengler, K., and Gallo, R.L. (2013) The microbiome extends to subepidermal compartments of normal skin. *Nat Commun* **4**: 1431.

Nilkens, S., Koch-Singenstreu, M., Niemann, V., Götz, F., Stehle, T., and Unden, G. (2014) Nitrate/oxygen co-sensing by an NreA/NreB sensor complex of Staphylococcus carnosus. *Mol Microbiol* **91**: 381–393.

Oh, J., Byrd, A.L., Park, M., Kong, H.H., and Segre, J.A. (2016) Temporal Stability of the Human Skin Microbiome. *Cell* **165**: 854–866.

Otto, M. (2018) Staphylococcal Biofilms. *Microbiol Spectr* **6**:.

Park, R.-Y., Sun, H.-Y., Choi, M.-H., Bai, Y.-H., and Shin, S.-H. (2005) Staphylococcus aureus siderophore-mediated iron-acquisition system plays a dominant and essential role in the utilization of transferrin-bound iron. *J Microbiol Seoul Korea* **43**: 183–190.

Periasamy, S., Chatterjee, S.S., Cheung, G.Y.C., and Otto, M. (2012) Phenol-soluble modulins in staphylococci. *Commun Integr Biol* **5**: 275–277.

Pidwill, G.R., Gibson, J.F., Cole, J., Renshaw, S.A., and Foster, S.J. (2021) The Role of Macrophages in Staphylococcus aureus Infection. *Front Immunol* **11**: 620339.

Podlesek, Z. and Žgur Bertok, D. (2020) The DNA Damage Inducible SOS Response Is a Key Player in the Generation of Bacterial Persister Cells and Population Wide Tolerance. *Front Microbiol* **11**:.

Postma, B., Poppelier, M.J., van Galen, J.C., Prossnitz, E.R., van Strijp, J.A.G., de Haas, C.J.C., and van Kessel, K.P.M. (2004) Chemotaxis inhibitory protein of Staphylococcus aureus binds specifically to the C5a and formylated peptide receptor. *J Immunol Baltim Md 1950* **172**: 6994–7001.

Puri, P., Wetzel, C., Saffert, P., Gaston, K.W., Russell, S.P., Cordero Varela, J.A., et al. (2014) Systematic identification of tRNAome and its dynamics in Lactococcus lactis. *Mol Microbiol* **93**: 944–956.

Puri, P., Wetzel, C., Saffert, P., W.Gaston, K., Russell, S.P., Varela, J.A.C., et al. (2014) Systematic identification of tRNAome and its dynamics in Lactococcus lactis. *Mol Microbiol* **93**: 944–956.

Reniere, M.L., Ukpabi, G.N., Harry, S.R., Stec, D.F., Krull, R., Wright, D.W., et al. (2010) The IsdG-family of haem oxygenases degrades haem to a novel chromophore. *Mol Microbiol* **75**: 1529–1538.

Rietmeyer, L., Fix-Boulier, N., Le Fournis, C., Iannazzo, L., Kitoun, C., Patin, D., et al. (2021) Partition of tRNAGly isoacceptors between protein and cell-wall peptidoglycan synthesis in Staphylococcus aureus. *Nucleic Acids Res* **49**: 684–699.

Rooijakkers, S.H.M., Ruyken, M., Roon, J.V., Kessel, K.P.M.V., Strijp, J.A.G.V., and Wamel, W.J.B.V. (2006) Early expression of SCIN and CHIPS drives instant immune evasion by Staphylococcus aureus. *Cell Microbiol* **8**: 1282–1293.

Rozov, A., Demeshkina, N., Khusainov, I., Westhof, E., Yusupov, M., and Yusupova, G. (2016) Novel base-pairing interactions at the tRNA wobble position crucial for accurate reading of the genetic code. *Nat Commun* **7**: 10457.

Seier-Petersen, M.A., Jasni, A., Aarestrup, F.M., Vigre, H., Mullany, P., Roberts, A.P., and Agersø, Y. (2014) Effect of subinhibitory concentrations of four commonly used

biocides on the conjugative transfer of Tn916 in Bacillus subtilis. *J Antimicrob Chemother* **69**: 343–348.

Sendi, P. and Proctor, R.A. (2009) Staphylococcus aureus as an intracellular pathogen: the role of small colony variants. *Trends Microbiol* **17**: 54–58.

Shaw, L., Golonka, E., Potempa, J., and Foster, S.J. (2004) The role and regulation of the extracellular proteases of Staphylococcus aureus. *Microbiol Read Engl* **150**: 217–228.

Skaar, E.P., Gaspar, A.H., and Schneewind, O. (2004) IsdG and IsdI, heme-degrading enzymes in the cytoplasm of Staphylococcus aureus. *J Biol Chem* **279**: 436–443.

Smagur, J., Guzik, K., Bzowska, M., Kuzak, M., Zarebski, M., Kantyka, T., et al. (2009) Staphylococcal cysteine protease staphopain B (SspB) induces rapid engulfment of human neutrophils and monocytes by macrophages. *Biol Chem* **390**: 361–371.

Soong, G., Paulino, F., Wachtel, S., Parker, D., Wickersham, M., Zhang, D., et al. (2015) Methicillin-resistant Staphylococcus aureus adaptation to human keratinocytes. *mBio* **6**: e00289-15.

Spaan, A.N., van Strijp, J.A.G., and Torres, V.J. (2017) Leukocidins: Staphylococcal bi-component pore-forming toxins find their receptors. *Nat Rev Microbiol* **15**: 435–447.

Stanczak-Mrozek, K.I., Manne, A., Knight, G.M., Gould, K., Witney, A.A., and Lindsay, J.A. (2015) Within-host diversity of MRSA antimicrobial resistances. *J Antimicrob Chemother* **70**: 2191–2198.

Stojković, V., Noda-Garcia, L., Tawfik, D.S., and Fujimori, D.G. (2016) Antibiotic resistance evolved via inactivation of a ribosomal RNA methylating enzyme. *Nucleic Acids Res* **44**: 8897–8907.

Surewaard, B.G.J., de Haas, C.J.C., Vervoort, F., Rigby, K.M., DeLeo, F.R., Otto, M., et al. (2013) Staphylococcal alpha-phenol soluble modulins contribute to neutrophil lysis after phagocytosis. *Cell Microbiol* **15**: 1427–1437.

Syed, A.K., Reed, T.J., Clark, K.L., Boles, B.R., and Kahlenberg, J.M. (2015) Staphlyococcus aureus Phenol-Soluble Modulins Stimulate the Release of Proinflammatory Cytokines from Keratinocytes and Are Required for Induction of Skin Inflammation. *Infect Immun* **83**: 3428–3437.

Tenover, F.C. and Goering, R.V. (2009) Methicillin-resistant Staphylococcus aureus strain USA300: origin and epidemiology. *J Antimicrob Chemother* **64**: 441–446.

Torres, V.J., Pishchany, G., Humayun, M., Schneewind, O., and Skaar, E.P. (2006) Staphylococcus aureus IsdB is a hemoglobin receptor required for heme iron utilization. *J Bacteriol* **188**: 8421–8429.

Treffon, J., Chaves-Moreno, D., Niemann, S., Pieper, D.H., Vogl, T., Roth, J., and Kahl, B.C. (2020) Importance of superoxide dismutases A and M for protection of Staphylococcus aureus in the oxidative stressful environment of cystic fibrosis airways. *Cell Microbiol* **22**: e13158.

Tuorto, F., Legrand, C., Cirzi, C., Federico, G., Liebers, R., Müller, M., et al. (2018) Queuosine-modified tRNAs confer nutritional control of protein translation. *EMBO J* **37**: e99777.

Vold, B. (1976) Modified nucleosides of Bacillus subtilis transfer ribonucleic acids. *J Bacteriol* **127**: 258–267.

Wang, B. and Muir, T.W. (2016) Regulation of virulence in Staphylococcus aureus: molecular mechanisms and remaining puzzles. *Cell Chem Biol* **23**: 214–224.

Wertheim, H.F.L., Melles, D.C., Vos, M.C., van Leeuwen, W., van Belkum, A., Verbrugh, H.A., and Nouwen, J.L. (2005) The role of nasal carriage in Staphylococcus aureus infections. *Lancet Infect Dis* **5**: 751–762.

Wolff, P., Villette, C., Zumsteg, J., Heintz, D., Antoine, L., Chane-Woon-Ming, B., et al. (2020) Comparative patterns of modified nucleotides in individual tRNA species from a mesophilic and two thermophilic archaea. *RNA* **26**: 1957–1975.

Xia, G. and Wolz, C. (2014) Phages of Staphylococcus aureus and their impact on host evolution. *Infect Genet Evol J Mol Epidemiol Evol Genet Infect Dis* **21**: 593–601.

Yang, J., Anishchenko, I., Park, H., Peng, Z., Ovchinnikov, S., and Baker, D. (2020) Improved protein structure prediction using predicted interresidue orientations. *Proc Natl Acad Sci U S A* **117**: 1496–1503.

Yokogawa, T., Kitamura, Y., Nakamura, D., Ohno, S., and Nishikawa, K. (2010) Optimization of the hybridization-based method for purification of thermostable tRNAs in the presence of tetraalkylammonium salts. *Nucleic Acids Res* **38**: e89–e89.

Young, B.C., Wu, C.-H., Gordon, N.C., Cole, K., Price, J.R., Liu, E., et al. (2017) Severe infections emerge from commensal bacteria by adaptive evolution. *eLife* **6**: e30637.

Zallot, R., Ross, R., Chen, W.-H., Bruner, S.D., Limbach, P.A., and de Crécy-Lagard, V. (2017) Identification of a Novel Epoxyqueuosine Reductase Family by Comparative Genomics. *ACS Chem Biol* **12**: 844–851.

Zhong, J., Xiao, C., Gu, W., Du, G., Sun, X., He, Q.-Y., and Zhang, G. (2015) Transfer RNAs Mediate the Rapid Adaptation of Escherichia coli to Oxidative Stress. *PLoS Genet* **11**:.

Zhu, H., Xie, G., Liu, M., Olson, J.S., Fabian, M., Dooley, D.M., and Lei, B. (2008) Pathway for heme uptake from human methemoglobin by the iron-regulated surface determinants system of Staphylococcus aureus. *J Biol Chem* **283**: 18450–18460.

Annexes

Annexe 1 : Tableau de la transcription différentielle durant le stress oxydant

Seuls les adjp<0,05 ont été conservés

UP regulated genes from the differencial transcriptomics analysis in oxidative stress						
id	gene	product	locus_tag_NCTC8325	gene_NCTC8325	log2FoldChange	padj
HG001_01893	-	single-strand DNA-binding protein, phage	SAOUHSC_02071	-	5,424	2,51E-104
HG001_01054	carB	Carbamoyl-phosphate synthase large chain	SAOUHSC_01170	carB	5,412	9,50E-104
HG001_01052	pyrC	Dihydroorotase	SAOUHSC_01168	pyrC	5,305	1,73E-65
HG001_01894	-	Phage protein	SAOUHSC_02072	-	5,302	3,29E-106
HG001_01055	pyrF	Orotidine 5'-phosphate decarboxylase	SAOUHSC_01171	-	5,29	3,09E-126
HG001_01053	carA	Carbamoyl-phosphate synthase small chain	SAOUHSC_01169	-	5,282	6,93E-63
HG001_01903	-	Putative phage protein	SAOUHSC_02081	-	5,257	6,13E-84
HG001_01051	pyrB	Aspartate carbamoyltransferase	SAOUHSC_01166	pyrB	5,174	1,60E-52
HG001_01904	-	Putative phage regulatory protein	SAOUHSC_02083	-	5,132	1,51E-76
HG001_01891	-	Putative phage replication protein	SAOUHSC_02069	-	5,128	7,84E-104
HG001_01895	-	Bacteriophage Mu Gam like protein	SAOUHSC_02073	-	5,122	1,86E-101
HG001_01898	-	Phage protein	SAOUHSC_02076	-	5,035	5,50E-64
HG001_01902	-	Phage antirepressor protein KilAC domain protein	SAOUHSC_02080	-	5,024	1,44E-91
HG001_01887	-	Phage protein	SAOUHSC_02065	-	5,004	2,05E-91
HG001_01885	-	Phage protein	SAOUHSC_02063	-	4,979	1,29E-122
HG001_01888	-	Putative phage protein	SAOUHSC_02066	-	4,979	1,64E-111
HG001_01056	pyrE	Orotate phosphoribosyltransferase	SAOUHSC_01172	pyrE	4,966	1,35E-105
HG001_01886	-	Phage protein	SAOUHSC_02064	-	4,939	3,02E-104
HG001_01889	dnaC_2	Replicative DNA helicase	SAOUHSC_02067	-	4,923	1,18E-111
HG001_01884	-	Putative phage regulatory protein; Helix-turn-helix domain protein	SAOUHSC_02062	-	4,889	3,62E-92
HG001_01883	-	Phage protein; PVL ORF-50-like family protein	SAOUHSC_02061	-	4,886	5,90E-94
HG001_01900	-	Phage protein	SAOUHSC_02078	-	4,885	1,40E-93
HG001_01890	-	Phage protein	SAOUHSC_02068	-	4,868	6,99E-99
HG001_02016	-	Phage protein	SAOUHSC_02213	-	4,856	5,76E-99
HG001_01896	-	Phage protein	SAOUHSC_02074	-	4,833	1,20E-88
HG001_01901	-	Putative phage protein	SAOUHSC_02079	-	4,811	2,42E-107
HG001_01050	pyrP	Uracil permease	SAOUHSC_01165	-	4,807	5,14E-46
HG001_01875	-	Transcriptional activator RinB (phage)	SAOUHSC_02053	-	4,754	1,21E-118
HG001_01868	-	Putative phage protein	SAOUHSC_02046	-	4,732	3,62E-66
HG001_01880	-	Putative phage protein	SAOUHSC_02058	-	4,7	1,30E-90
HG001_01881	-	Phage protein	SAOUHSC_02059	-	4,698	4,55E-98
HG001_01870	-	Phage portal protein%2C SPP1 Gp6-like	SAOUHSC_02048	-	4,694	1,57E-79
HG001_01876	-	Phage protein	SAOUHSC_02054	-	4,677	8,91E-80
HG001_01882	-	Phage protein	SAOUHSC_02060	-	4,659	8,31E-112
HG001_01869	-	Phage Mu protein F like protein	SAOUHSC_02047	-	4,631	3,92E-79
HG001_01899	-	Phage protein	SAOUHSC_02077	-	4,597	2,32E-83
HG001_01873	-	Transcriptional activator, phage-associated	SAOUHSC_02051	-	4,538	9,07E-91
HG001_01878	-	Putative phage protein	SAOUHSC_02056	-	4,536	2,16E-83
HG001_02037	-	Putative phage regulatory protein	SAOUHSC_02234	-	4,486	4,16E-70
HG001_02032	-	Phage protein	SAOUHSC_02228	-	4,457	4,05E-75
HG001_01874	-	Phage protein	SAOUHSC_02052	-	4,417	5,03E-104
HG001_01383	-	Phage protein	SAOUHSC_01550	-	4,412	8,41E-68
HG001_02034	-	AntA/AntB antirepressor	SAOUHSC_02229	-	4,402	3,05E-86
HG001_02036	-	Putative phage regulatory protein	SAOUHSC_02233	-	4,382	3,67E-72
HG001_01877	-	Phage protein	SAOUHSC_02055	-	4,379	1,19E-87
HG001_02727	glpE_3	Thiosulfate sulfurtransferase GlpE	SAOUHSC_03024	-	4,351	4,32E-96
HG001_02433	narH	Respiratory nitrate reductase 1 beta chain	SAOUHSC_02680	-	4,276	1,58E-52
HG001_02432	narW	putative nitrate reductase molybdenum cofactor assembly chaperone NarW	SAOUHSC_02679	-	4,264	4,39E-51
HG001_01897	-	Phage protein	SAOUHSC_02075	-	4,223	3,08E-83
HG001_01866	-	Phage capsid family protein	SAOUHSC_02043	-	4,199	1,95E-57
HG001_02033	-	Phage antirepressor protein KilAC domain protein	SAOUHSC_02229	-	4,185	1,60E-83
HG001_01867	-	Putative phage head protein	SAOUHSC_02044	-	4,145	1,63E-61
HG001_01871	-	Phage terminase large subunit	SAOUHSC_02049	-	4,14	4,87E-53
HG001_01865	-	Phage protein	SAOUHSC_02042	-	4,118	9,34E-51
HG001_01863	-	Putative phage protein	SAOUHSC_02040	-	4,069	1,18E-53
HG001_02023	-	Putative phage nuclease	SAOUHSC_02219	-	4,043	5,11E-85
HG001_01222	dinB_1	DNA polymerase IV	SAOUHSC_01363	MucB	4,037	1,46E-55
HG001_01858	-	Phage protein	SAOUHSC_02034	-	3,98	5,86E-61
HG001_02031	-	Putative phage protein	SAOUHSC_02227	-	3,978	1,83E-46
HG001_02029	-	Phage protein	SAOUHSC_02225	-	3,977	4,57E-80
HG001_02025	-	Phage protein	SAOUHSC_02221	-	3,951	6,11E-88
HG001_01861	-	Putative phage protein	SAOUHSC_02037	-	3,951	1,04E-58
HG001_02017	-	Putative phage protein	SAOUHSC_02214	-	3,883	2,85E-46
HG001_02028	-	Phage protein	SAOUHSC_02224	-	3,848	6,04E-45
HG001_01386	-	Phage protein; PVL orf 52-like protein; Phage phi 11 orf23 protein homolog	SAOUHSC_01553	-	3,847	2,70E-63
HG001_02024	-	Putative phage ssDNA binding protein	SAOUHSC_02220	-	3,831	7,83E-62
HG001_01860	-	Phage major tail protein 2	SAOUHSC_02036	-	3,821	7,08E-64
HG001_00085	deoD	Purine nucleoside phosphorylase DeoD-type	SAOUHSC_00097	-	3,814	5,29E-33
HG001_02026	-	Putative phage protein	SAOUHSC_02222	-	3,813	2,07E-65
HG001_02434	narG	Respiratory nitrate reductase 1 alpha chain	SAOUHSC_02681	-	3,796	2,96E-40
HG001_01859	-	Phage protein	SAOUHSC_02035	-	3,769	1,37E-55
HG001_01862	-	Phage protein	SAOUHSC_02038	-	3,765	3,25E-54
HG001_01872	-	Terminase small subunit	SAOUHSC_02050	-	3,652	1,14E-36
HG001_00308	-	HTH-type transcriptional regulator	SAOUHSC_00347	-	3,647	5,13E-32
HG001_02027	-	Phage protein	SAOUHSC_02223	-	3,634	5,40E-53
HG001_01057	-	hypothetical protein; same operon as pyrP-pyrB-pyrC-carA-carB-pyrF-pyrE	SAOUHSC_01173	-	3,505	8,10E-45

HG001_01200	-	hypothetical protein	SAOUHSC_01334	-	3,4	1,30E-23
HG001_02435	nasF	Uroporphyrinogen-III C-methyltransferase	SAOUHSC_02682	-	3,396	5,44E-37
HG001_02020	-	Phage protein	SAOUHSC_02217	-	3,323	8,20E-54
HG001_02436	nasE	Assimilatory nitrite reductase [NAD(P)H] small subunit	SAOUHSC_02683	-	3,321	1,65E-29
HG001_01343	-	Ferredoxin	SAOUHSC_01504	-	3,316	6,98E-40
HG001_01214	parC	DNA topoisomerase 4 subunit A	SAOUHSC_01352	-	3,261	8,08E-45
HG001_02246	aldC_1	Alpha-acetolactate decarboxylase	SAOUHSC_02467	-	3,236	1,69E-21
HG001_02437	nasD	Nitrite reductase [NAD(P)H]	SAOUHSC_02684	-	3,201	1,42E-25
HG001_02431	narX	Nitrate reductase-like protein NarX	SAOUHSC_02678	-	3,187	3,92E-36
HG001_01911	queE_2	7-carboxy-7-deazaguanine synthase	SAOUHSC_02090	-	3,185	6,19E-61
HG001_01856	-	Phage tail protein	SAOUHSC_02031	-	3,181	1,69E-41
HG001_01857	-	hypothetical protein	SAOUHSC_02033	-	3,18	1,86E-38
HG001_01855	-	Prophage endopeptidase tail	SAOUHSC_02030	-	3,152	4,30E-43
HG001_02018	-	hypothetical protein	SAOUHSC_02215	-	3,119	2,24E-22
HG001_02019	dnaC_3	DNA replication protein DnaC	SAOUHSC_02216	-	3,094	7,15E-45
HG001_00086	norB_2	Quinolone resistance protein NorB	SAOUHSC_00099	-	3,013	7,19E-23
HG001_01521	der_3	GTPase Der	SAOUHSC_01700	-	3,006	2,85E-48
HG001_02629	pyrD	Dihydroorotate dehydrogenase (quinone)	SAOUHSC_02909	-	2,959	6,09E-08
HG001_01213	parE	DNA topoisomerase 4 subunit B	SAOUHSC_01351	-	2,931	2,91E-45
HG001_00807	argH1	Argininosuccinate lyase 1	SAOUHSC_00898	-	2,89	2,12E-24
HG001_02429	nreB	Oxygen sensor histidine kinase NreB	SAOUHSC_02676	-	2,863	7,06112E-32
HG001_02609	isaA	putative transglycosylase IsaA precursor	SAOUHSC_02887	-	2,863	2,63E-30
HG001_01522	gph_2	Phosphoglycolate phosphatase	SAOUHSC_01701	-	2,849	2,29E-45
HG001_01854	-	hypothetical protein	SAOUHSC_02029	-	2,844	3,92E-38
HG001_02014	-	PVL ORF-50-like family protein	SAOUHSC_02211	-	2,814	1,25E-27
HG001_02166	dps	General stress protein 20U	SAOUHSC_02381	-	2,778	1,86E-35
HG001_01384	-	hypothetical protein	SAOUHSC_01551	-	2,772	2,91E-22
HG001_02483	-	UDP-glucose 4-epimerase	SAOUHSC_02737	-	2,762	8,31E-35
HG001_02015	-	hypothetical protein	SAOUHSC_02212	-	2,76	1,41E-24
HG001_01520	aroE	Shikimate dehydrogenase	SAOUHSC_01699	-	2,724	3,56E-42
HG001_02669	clfB	Clumping factor B precursor	SAOUHSC_02963	-	2,698	6,72E-44
HG001_01206	sbcC	Nuclease SbcCD subunit C	SAOUHSC_01343	-	2,692	2,90E-40
HG001_01518	nadD	putative nicotinate-nucleotide adenylyltransferase	SAOUHSC_01697	-	2,659	1,10E-38
HG001_02247	alsS	Acetolactate synthase	SAOUHSC_02468	-	2,641	1,58E-14
HG001_01250	yheS_1	putative ABC transporter ATP-binding protein YheS	SAOUHSC_01392	-	2,602	3,13E-29
HG001_01519	yhbY	RNA-binding protein YhbY	SAOUHSC_01698	-	2,596	2,07E-30
HG001_02438	shfC (nirR)	Sirohydrochlorin ferrochelatase	SAOUHSC_02685	-	2,585	3,49591E-19
HG001_00937	ythB	Putative cytochrome bd menaquinol oxidase subunit II	SAOUHSC_01032	-	2,584	6,91E-23
HG001_02430	-	hypothetical protein	SAOUHSC_02677	-	2,549	5,64788E-26
HG001_00670	nrdF	Ribonucleoside-diphosphate reductase subunit beta	SAOUHSC_00743	nrdF	2,532	5,81E-22
HG001_02428	nreC	Oxygen regulatory protein NreC	SAOUHSC_02675	-	2,512	1,59E-30
HG001_02340	hpxO	FAD-dependent urate hydroxylase	SAOUHSC_02579	-	2,511	2,42E-33
HG001_01853	-	hypothetical protein	SAOUHSC_02028	-	2,508	1,17E-27
HG001_02654	-	anaerobic ribonucleotide reductase-activating protein	SAOUHSC_02941	-	2,491	2,99E-23
HG001_02108	-	putative DEAD-box ATP-dependent RNA helicase	SAOUHSC_02316	-	2,477	6,34E-27
HG001_01682	bioB_1	Biotin synthase	SAOUHSC_01877	-	2,453	3,48E-34
HG001_02013	-	hypothetical protein	SAOUHSC_02210	-	2,441	8,25E-18
HG001_02657	p2d	Precorrin-2 dehydrogenase	SAOUHSC_02945	-	2,411	1,29E-19
HG001_00491	azo1	FMN-dependent NADPH-azoreductase	SAOUHSC_00543	-	2,408	5,19E-17
HG001_02655	nrdD	Anaerobic ribonucleoside-triphosphate reductase	SAOUHSC_02942	-	2,407	8,69E-18
HG001_02154	pyrG	CTP synthase	SAOUHSC_02368	pyrG	2,393	8,99E-22
HG001_01107	rpsB	30S ribosomal protein S2	-	-	2,389	2,03E-27
HG001_02006	-	hypothetical protein	SAOUHSC_02203	-	2,385	7,01E-22
HG001_00082	sodM	Superoxide dismutase [Mn/Fe] 2	SAOUHSC_00093	-	2,372	1,32E-34
HG001_01850	-	hypothetical protein	SAOUHSC_02025	-	2,354	1,71E-19
HG001_01523	mtnN	5'-methylthioadenosine/S-adenosylhomocysteine nucleosidase	SAOUHSC_01702	-	2,349	3,00E-29
HG001_01517	-	putative nicotinate-nucleotide adenylyltransferase	SAOUHSC_01696	-	2,346	1,82E-24
HG001_01925	cobQ	Cobyric acid synthase	SAOUHSC_02106	-	2,329	1,16E-29
HG001_01852	-	hypothetical protein	SAOUHSC_02027	-	2,308	6,85E-22
HG001_01092	rplS	50S ribosomal protein L19	SAOUHSC_01211	rplS	2,297	5,73E-24
HG001_02041	xerC_3	Tyrosine recombinase XerC	SAOUHSC_02239	-	2,297	9,53E-19
HG001_02042	hlb_2	Phospholipase C precursor	-	-	2,281	6,98E-20
HG001_01215	alsT_2	Amino-acid carrier protein AlsT	SAOUHSC_01354	-	2,273	1,10E-25
HG001_00139	ptsG_1	PTS system glucose-specific EIICBA component	SAOUHSC_00155	-	2,27	2,96E-05
HG001_00019	purA	Adenylosuccinate synthetase	SAOUHSC_00019	-	2,259	4,52562E-15
HG001_01765	hemY	Protoporphyrinogen oxidase	SAOUHSC_01960	-	2,248	1,57E-18
HG001_01766	hemH	Ferrochelatase	SAOUHSC_01961	hemH	2,233	2,42E-24
HG001_01941	-	Trp repressor protein	SAOUHSC_02125	-	2,207	2,38E-13
HG001_01851	-	hypothetical protein	SAOUHSC_02026	-	2,195	1,41E-12
HG001_01137	recA	Protein RecA	SAOUHSC_01262	recA	2,189	1,32E-20
HG001_01939	pcrA	ATP-dependent DNA helicase PcrA	SAOUHSC_02123	-	2,184	7,32E-27
HG001_02012	-	YopX protein	SAOUHSC_02209	-	2,168	1,58E-10
HG001_00951	ydcV	Inner membrane ABC transporter permease protein YdcV	SAOUHSC_01048	-	2,155	1,25E-14
HG001_02145	prfA	Peptide chain release factor 1	SAOUHSC_02359	prfA	2,153	1,46E-22
HG001_02424	narT	putative nitrate transporter NarT	SAOUHSC_02671	-	2,148	0,000554689
HG001_00808	argG	Argininosuccinate synthase	SAOUHSC_00899	-	2,134	7,77E-12
HG001_02005	-	Transcriptional activator RinB	SAOUHSC_02202	-	2,129	1,46E-09
HG001_01910	xerC_2	Tyrosine recombinase XerC	SAOUHSC_02089	-	2,121	6,78E-15
HG001_00512	-	hypothetical protein	SAOUHSC_00567	-	2,106	2,43E-16

HG001_00659	recQ_1	ATP-dependent DNA helicase RecQ	SAOUHSC_00730	-	2,104	4,16E-29
HG001_02008	-	dUTPase	SAOUHSC_02205	-	2,103	8,88E-15
HG001_02144	prmC	Release factor glutamine methyltransferase	SAOUHSC_02358	-	2,098	9,52E-18
HG001_02009	-	hypothetical protein	SAOUHSC_02206	-	2,09	9,66E-13
HG001_02004	-	hypothetical protein	-	-	2,09	1,02E-11
HG001_00002	dnaN	DNA polymerase III subunit beta	SAOUHSC_00002	-	2,088	1,57E-20
HG001_02256	truA	tRNA pseudouridine synthase A	SAOUHSC_02480	truA	2,083	4,31E-25
HG001_01957	-	YolD-like protein	SAOUHSC_02144	-	2,078	2,48E-10
HG001_02123	sceD	putative transglycosylase SceD precursor	SAOUHSC_02333	-	2,071	1,77E-15
HG001_02003	-	hypothetical protein	SAOUHSC_02200	-	2,062	4,14E-12
HG001_02007	-	hypothetical protein	SAOUHSC_02204	-	2,061	3,52E-10
HG001_02658	cysJ	Sulfite reductase [NADPH] flavoprotein alpha-component	SAOUHSC_02947	-	2,056	7,70E-15
HG001_02411	-	hypothetical protein	SAOUHSC_02656	-	2,046	8,86E-17
HG001_01184	nucH	Thermonuclease precursor	SAOUHSC_01316	-	2,044	5,01E-13
HG001_00878	-	hypothetical protein	SAOUHSC_00964	-	2,018	1,04E-14
HG001_00959	typA	GTP-binding protein TypA/BipA	SAOUHSC_01058	-	2,012	4,82E-20
HG001_00005	gyrB	DNA gyrase subunit B	SAOUHSC_00005	-	2,009	9,48E-24
HG001_01938	ligA	DNA ligase	SAOUHSC_02122	-	2,001	7,85E-21
HG001_00060	spa	Immunoglobulin G-binding protein A precursor	SAOUHSC_00069	-	1,993	1,52E-17
HG001_02155	rpoE	putative DNA-directed RNA polymerase subunit delta	SAOUHSC_02369	-	1,988	1,30E-24
HG001_02253	rpsI	30S ribosomal protein S9	SAOUHSC_02477	rpsI	1,964	2,69E-16
HG001_01574	mreC	Cell shape-determining protein MreC precursor	SAOUHSC_01759	-	1,96	2,51E-21
HG001_02750	rsmG	Ribosomal RNA small subunit methyltransferase G	SAOUHSC_03051	gidB	1,959	3,77E-16
HG001_01933	gatB_2	Aspartyl/glutamyl-tRNA(Asn/Gln) amidotransferase subunit B	SAOUHSC_02116	gatB	1,941	6,58E-17
HG001_01515	tylM1	dTDP-3-amino-3%2C6-dideoxy-alpha-D-glucopyranose N%2CN-dimethyltransferase	SAOUHSC_01694	-	1,94	4,98E-22
HG001_02090	-	Protein SprT-like protein	SAOUHSC_02296	-	1,936	1,20E-17
HG001_02388	emrB_1	Multidrug export protein EmrB	SAOUHSC_02629	-	1,932	6,19E-20
HG001_02751	mnmG	tRNA uridine 5-carboxymethylaminomethyl modification enzyme MnmG	SAOUHSC_03052	gidA	1,927	2,97E-16
HG001_00411	-	hypothetical protein	SAOUHSC_00465	-	1,925	1,56E-20
HG001_02010	-	hypothetical protein	SAOUHSC_02207	-	1,919	2,22E-11
HG001_01203	-	hypothetical protein	SAOUHSC_01338	-	1,913	9,09E-14
HG001_01048	rluD_2	Ribosomal large subunit pseudouridine synthase D	SAOUHSC_01163	lspA	1,91	9,54E-20
HG001_01790	tcyC_1	L-cystine import ATP-binding protein TcyC	SAOUHSC_01990	-	1,898	2,77E-15
HG001_01047	lspA	Lipoprotein signal peptidase	SAOUHSC_01162	lspA	1,894	3,62E-15
HG001_01995	-	Phage capsid family protein	SAOUHSC_02191	-	1,888	2,26E-10
HG001_01560	apt	Adenine phosphoribosyltransferase	SAOUHSC_01743	-	1,886	5,58131E-18
HG001_01791	artQ	Arginine transport system permease protein ArtQ	SAOUHSC_01991	-	1,882	1,63E-17
HG001_01479	znuB	High-affinity zinc uptake system membrane protein ZnuB	SAOUHSC_01656	-	1,875	5,45E-17
HG001_00324	ahpC	Alkyl hydroperoxide reductase subunit C	SAOUHSC_00365	-	1,874	1,93E-18
HG001_00067	sbnC	Staphyloferrin B synthase	SAOUHSC_00077	-	1,869	5,02E-14
HG001_00008	hutH	Histidine ammonia-lyase	SAOUHSC_00008	-	1,865	2,86E-15
HG001_01942	purB	Adenylosuccinate lyase	SAOUHSC_02126	-	1,864	6,42238E-15
HG001_00372	mccB	Cystathionine gamma-lyase	SAOUHSC_00422	-	1,855	6,45E-15
HG001_02257	ecfT	Energy-coupling factor transporter transmembrane protein EcfT	SAOUHSC_02481	-	1,847	2,29E-16
HG001_01992	-	Phage head-tail joining protein	SAOUHSC_02188	-	1,846	4,65E-09
HG001_02389	emrK	putative multidrug resistance protein EmrK	SAOUHSC_02630	-	1,843	3,22E-19
HG001_01339	-	Glucosaminate ammonia-lyase	SAOUHSC_01499	-	1,842	1,57E-12
HG001_02120	thiD	Hydroxymethylpyrimidine/phosphomethylpyrimidine kinase	SAOUHSC_02330	-	1,833	1,31E-13
HG001_02453	-	hypothetical protein	SAOUHSC_02702	-	1,832	2,04E-10
HG001_00468	rplA	50S ribosomal protein L1	SAOUHSC_00519	rplA	1,827	6,91E-18
HG001_01070	stp	Serine/threonine phosphatase stp	SAOUHSC_01186	-	1,827	1,16E-14
HG001_01573	-	rod shape-determining protein MreD	SAOUHSC_01758	-	1,827	1,44E-13
HG001_02754	rpmH	50S ribosomal protein L34	SAOUHSC_03055	rpmH	1,826	1,87E-12
HG001_01849	atl_3	Bifunctional autolysin precursor	SAOUHSC_02023	-	1,825	4,00E-18
HG001_01571	-	hypothetical protein	SAOUHSC_01756	-	1,817	9,94E-15
HG001_00351	hsdM	Type I restriction enzyme EcoKI M protein	SAOUHSC_00397	-	1,813	1,39E-14
HG001_01311	ponA	Penicillin-binding protein 1A/1B	SAOUHSC_01467	recU	1,795	7,85E-17
HG001_01461	gcvT	Aminomethyltransferase	SAOUHSC_01634	gcvT	1,793	1,02E-11
HG001_01481	nfo	putative endonuclease 4	SAOUHSC_01658	-	1,788	2,77E-17
HG001_00323	ahpF	Alkyl hydroperoxide reductase subunit F	SAOUHSC_00364	-	1,785	7,15E-17
HG001_00712	cggR	Central glycolytic genes regulator	SAOUHSC_00794	-	1,782	2,46E-12
HG001_00363	yciC_1	Putative metal chaperone YciC	SAOUHSC_00410	-	1,775	2,05E-11
HG001_01691	ribE	Riboflavin synthase	SAOUHSC_01888	-	1,773	3,31E-09
HG001_02156	bltD_2	Spermine/spermidine acetyltransferase	SAOUHSC_02370	-	1,769	1,48E-12
HG001_02243	mepM_2	Murein DD-endopeptidase MepM	SAOUHSC_02464	-	1,768	1,58E-17
HG001_02282	rplV	50S ribosomal protein L22	SAOUHSC_02507	rplV	1,745	2,26E-15
HG001_00408	ycfH	putative deoxyribonuclease YcfH	SAOUHSC_00462	-	1,743	4,29E-15
HG001_01764	ydeN	Putative hydrolase YdeN	SAOUHSC_01958	-	1,741	2,17E-11
HG001_02443	zinT	Metal-binding protein ZinT precursor	SAOUHSC_02690	-	1,737	8,57E-19
HG001_02022	-	hypothetical protein	-	-	1,734	1,56E-06
HG001_01634	-	hypothetical protein	SAOUHSC_01823	-	1,723	8,68E-16
HG001_01451	cfiB_2	2-oxoglutarate carboxylase small subunit	SAOUHSC_01623	-	1,72	2,22E-14
HG001_01934	gatA	Glutamyl-tRNA(Gln) amidotransferase subunit A	SAOUHSC_02117	gatA	1,717	4,02E-11
HG001_01142	korB	2-oxoglutarate oxidoreductase subunit KorB	SAOUHSC_01267	-	1,716	3,52E-09
HG001_02352	yifK	putative transport protein YifK	SAOUHSC_02590	-	1,709	7,42E-13
HG001_01572	rplU	50S ribosomal protein L21	SAOUHSC_01757	rplU	1,701	4,01E-16
HG001_01382	-	Transcriptional activator RinB	SAOUHSC_01549	-	1,701	2,86E-06
HG001_02586	pksG	Polyketide biosynthesis 3-hydroxy-3-methylglutaryl-ACP synthase PksG	SAOUHSC_02860	-	1,698	1,22E-14
HG001_02280	rplP	50S ribosomal protein L16	SAOUHSC_02505	rplP	1,696	3,18E-13

HG001_01848 -	hypothetical protein	SAOUHSC_02022	-	1,691	1,32E-13
HG001_02446 bdbD	Disulfide bond formation protein D precursor	SAOUHSC_02694	-	1,689	7,48E-17
HG001_02420 gltT	Proton/sodium-glutamate symport protein	SAOUHSC_02667	-	1,683	1,47E-12
HG001_02287 rplC	50S ribosomal protein L3	SAOUHSC_02512	rplC	1,68	6,59E-13
HG001_01689 ribH	6%2C7-dimethyl-8-ribityllumazine synthase	SAOUHSC_01886	ribH	1,678	1,28E-09
HG001_02258 ecfA2	Energy-coupling factor transporter ATP-binding protein EcfA2	SAOUHSC_02482	cbiO	1,674	5,77E-15
HG001_00475 rplGB	Ribosome-associated protein L7Ae-like protein	SAOUHSC_00526	-	1,666	1,59E-10
HG001_01846 -	Bacteriophage holin	SAOUHSC_02020	-	1,665	5,32E-14
HG001_01478 zur	Zinc-specific metallo-regulatory protein	SAOUHSC_01655	-	1,662	5,53E-11
HG001_01926 murE_2	UDP-N-acetylmuramoyl-L-alanyl-D-glutamate--2%2C6-diaminopimelate ligase	SAOUHSC_02107	-	1,66	3,56E-14
HG001_00352 -	Type I restriction modification DNA specificity domain protein	SAOUHSC_00398	-	1,66	7,19E-13
HG001_02284 rplB	50S ribosomal protein L2	SAOUHSC_02509	rplB	1,654	9,54E-14
HG001_02285 rplW	50S ribosomal protein L23	SAOUHSC_02510	rplW	1,649	7,01E-12
HG001_01831 -	Putative multidrug export ATP-binding/permease protein	SAOUHSC_02003	-	1,646	2,97E-16
HG001_00941 def	Peptide deformylase	SAOUHSC_01038	def	1,644	8,36E-15
HG001_01535 yhbU_1	putative protease YhbU precursor	SAOUHSC_01716	-	1,639	4,45E-16
HG001_00073 sbnI	L-serine kinase	SAOUHSC_00083	-	1,639	9,52E-15
HG001_02283 rpsS	30S ribosomal protein S19	SAOUHSC_02508	rpsS	1,639	1,08E-13
HG001_02286 rplD	50S ribosomal protein L4	SAOUHSC_02511	rplD	1,638	1,28E-16
HG001_01096 sucC	Succinyl-CoA ligase [ADP-forming] subunit beta	SAOUHSC_01216	sucC	1,633	1,64E-12
HG001_00949 potA	Spermidine/putrescine import ATP-binding protein PotA	SAOUHSC_01046	-	1,63	1,16E-07
HG001_02091 rpsA_2	30S ribosomal protein S1	SAOUHSC_02297	-	1,626	4,57E-11
HG001_02752 mnmE	tRNA modification GTPase MnmE	SAOUHSC_03053	trmE	1,624	2,36E-10
HG001_01690 ribBA	Riboflavin biosynthesis protein RibBA	SAOUHSC_01887	-	1,623	4,04E-09
HG001_02635 panD	Aspartate 1-decarboxylase precursor	SAOUHSC_02916	-	1,615	2,74E-13
HG001_01337 cmk	Cytidylate kinase	SAOUHSC_01496	cmk	1,612	3,25E-11
HG001_01338 ansA	putative L-asparaginase	SAOUHSC_01497	-	1,612	4,47E-10
HG001_01631 ackA	Acetate kinase	SAOUHSC_01820	-	1,611	8,50E-08
HG001_01564 tgt	Queuine tRNA-ribosyltransferase	SAOUHSC_01748	tgt	1,604	8,50E-13
HG001_02652 gloB_2	Hydroxyacylglutathione hydrolase	SAOUHSC_02936	-	1,602	1,24E-10
HG001_01516 rsfS	Ribosomal silencing factor RsfS	SAOUHSC_01695	-	1,601	1,58E-15
HG001_00936 ythA	Putative cytochrome bd menaquinol oxidase subunit I	SAOUHSC_01031	-	1,599	1,10E-10
HG001_00773 -	hypothetical protein	SAOUHSC_00862	-	1,59	1,85E-12
HG001_01683 rsmH_2	Ribosomal RNA small subunit methyltransferase H	SAOUHSC_01878	-	1,589	3,49E-07
HG001_00061 sarS	HTH-type transcriptional regulator SarS	SAOUHSC_00070	-	1,586	1,36E-13
HG001_01937 -	CamS sex pheromone cAM373 precursor	SAOUHSC_02121	-	1,573	4,16E-12
HG001_00496 folE2	GTP cyclohydrolase FolE2	SAOUHSC_00549	-	1,567	1,60E-14
HG001_00407 metG	Methionine--tRNA ligase	SAOUHSC_00461	-	1,553	1,43E-11
HG001_00467 rplK	50S ribosomal protein L11	SAOUHSC_00518	rplK	1,545	3,85E-12
HG001_02560 catE_2	Catechol-2%2C3-dioxygenase	SAOUHSC_02828	-	1,542	9,12E-13
HG001_00071 sbnG	Citrate synthase	SAOUHSC_00081	-	1,542	1,07E-11
HG001_02279 rpmC	50S ribosomal protein L29	SAOUHSC_02504	-	1,541	8,58E-15
HG001_00697 uvrA	UvrABC system protein A	SAOUHSC_00780	uvrA	1,54	4,12E-15
HG001_01735 -	EcoKI restriction-modification system protein HsdS	SAOUHSC_01932	-	1,538	1,51E-11
HG001_00879 -	CAAX amino terminal protease self- immunity	SAOUHSC_00965	-	1,531	1,49E-11
HG001_01158 -	methionine gamma-lyase	SAOUHSC_01284	-	1,53	1,45E-11
HG001_00469 -	L10_leader	-	-	1,525	3,10E-11
HG001_02244 -	putative hydrolase	SAOUHSC_02465	-	1,517	4,46E-11
HG001_00068 sbnD	Staphyloferrin B export protein	SAOUHSC_00078	-	1,513	6,73E-11
HG001_02109 murF	UDP-N-acetylmuramoyl-tripeptide--D-alanyl-D-alanine ligase	SAOUHSC_02317	-	1,513	4,28E-10
HG001_02278 rpsQ	30S ribosomal protein S17	SAOUHSC_02503	rpsQ	1,509	1,53E-11
HG001_02423 -	Acid shock protein	SAOUHSC_02670	-	1,507	4,26E-08
HG001_00497 mshB	1D-myo-inositol 2-acetamido-2-deoxy-alpha-D-glucopyranoside deacetylase	SAOUHSC_00550	-	1,502	1,24E-10
HG001_01499 rpsU	30S ribosomal protein S21	SAOUHSC_01678	rpsU	1,501	4,82E-13
HG001_02255 -	L13_leader	-	-	1,496	3,25E-09
HG001_02148 -	hypothetical protein	SAOUHSC_02362	rho	1,484	3,13E-11
HG001_00867 prfC	Peptide chain release factor 3	SAOUHSC_00956	prfC	1,483	3,26E-10
HG001_02439 ytml	putative N-acetyltransferase Ytml	SAOUHSC_02686	-	1,482	7,31E-09
HG001_01767 hemE	Uroporphyrinogen decarboxylase	SAOUHSC_01962	hemE	1,478	5,45E-13
HG001_00072 sbnH	2-[(L-alanin-3-ylcarbamoyl)methyl]-2-hydroxybutanedioate decarboxylase	SAOUHSC_00082	-	1,477	1,97E-12
HG001_00066 sbnB	N-[(2S)-2-amino-2-carboxyethyl]-L-glutamate dehydrogenase	SAOUHSC_00076	-	1,472	9,94E-09
HG001_00265 -	alpha/beta hydrolase fold protein	SAOUHSC_00301	-	1,471	1,57E-10
HG001_02119 thiM	Hydroxyethylthiazole kinase	SAOUHSC_02329	-	1,471	1,52E-07
HG001_01844 -	putative sapT prophage toxin	SAOUHSC_02018	-	1,468	1,33E-09
HG001_01792 -	Phosphotransferase system%2C EIIC	SAOUHSC_01992	-	1,457	1,70E-10
HG001_01994 -	hypothetical protein	SAOUHSC_02190	-	1,454	1,78E-05
HG001_02291 topB	DNA topoisomerase 3	SAOUHSC_02517	-	1,451	3,35E-11
HG001_01905 immR_1	HTH-type transcriptional regulator ImmR	SAOUHSC_02084	-	1,451	2,38E-10
HG001_00069 sbnE	L-2,3-diaminopropanoate--citrate ligase	SAOUHSC_00079	-	1,444	3,86E-09
HG001_02288 rpsJ	30S ribosomal protein S10	SAOUHSC_02512a	-	1,443	8,05E-09
HG001_02636 panC	Pantothenate synthetase	SAOUHSC_02918	panC	1,441	2,48E-12
HG001_01151 glpK	Glycerol kinase	SAOUHSC_01276	glpK	1,438	2,14E-09
HG001_02157 coaW	Type II pantothenate kinase	SAOUHSC_02371	-	1,438	9,09E-08
HG001_01071 prkC	Serine/threonine-protein kinase PrkC	SAOUHSC_01187	-	1,431	5,41E-10
HG001_01514 comEA	ComE operon protein 1	SAOUHSC_01693	-	1,43	2,04E-08
HG001_01310 recU	Holliday junction resolvase RecU	SAOUHSC_01466	recU	1,426	2,34E-09
HG001_00811 spsB_1	Signal peptidase IB	SAOUHSC_00902	-	1,425	2,71E-08
HG001_02277 rplN	50S ribosomal protein L14	SAOUHSC_02502	rplN	1,424	1,72E-12
HG001_02682 -	ABC-2 family transporter protein	SAOUHSC_02978	-	1,424	9,24E-12

HG001_00819 -	hypothetical protein	SAOUHSC_00910	-	1,422	2,89E-12
HG001_01653 fhs	Formate--tetrahydrofolate ligase	SAOUHSC_01845	-	1,419	1,14E-09
HG001_01591 clpX	ATP-dependent Clp protease ATP-binding subunit ClpX	SAOUHSC_01778	clpX	1,418	4,48E-12
HG001_00197 tagF	CDP-glycerol:poly(glycerophosphate) glycerophosphotransferase	SAOUHSC_00223	-	1,417	2,29E-11
HG001_01635 thiI	putative tRNA sulfurtransferase	SAOUHSC_01824	-	1,415	1,03E-11
HG001_01482 cshB	DEAD-box ATP-dependent RNA helicase CshB	SAOUHSC_01659	-	1,413	2,29E-11
HG001_01736 -	putative type I restriction enzymeP M protein	SAOUHSC_01933	-	1,412	3,19E-09
HG001_01091 trmD	tRNA (guanine-N(1)-)-methyltransferase	SAOUHSC_01210	trmD	1,409	2,36E-10
HG001_01645 ptsG_4	PTS system glucose-specific EIICBA component	SAOUHSC_01836	-	1,409	2,85E-07
HG001_00950 potB	Spermidine/putrescine transport system permease protein PotB	SAOUHSC_01047	-	1,408	1,02E-06
HG001_02275 rplE	50S ribosomal protein L5	SAOUHSC_02500	rplE	1,402	2,21E-11
HG001_00155 azoR	FMN-dependent NADH-azoreductase	SAOUHSC_00173	-	1,402	1,59E-10
HG001_01204 -	hypothetical protein	SAOUHSC_01340	-	1,402	1,01E-08
HG001_00517 -	putative heme peroxidase	SAOUHSC_00573	-	1,396	2,01E-11
HG001_01993 -	Phage gp6-like head-tail connector protein	SAOUHSC_02189	-	1,393	0,002756727
HG001_02276 rplX	50S ribosomal protein L24	SAOUHSC_02501	rplX	1,39	1,75E-10
HG001_01592 tig	Trigger factor	SAOUHSC_01779	tig	1,387	9,40E-11
HG001_01940 pcrB	Heptaprenylglyceryl phosphate synthase	SAOUHSC_02124	-	1,381	3,78E-08
HG001_01085 smc	Chromosome partition protein Smc	SAOUHSC_01204	-	1,379	4,98E-11
HG001_01141 korA	2-oxoglutarate oxidoreductase subunit KorA	SAOUHSC_01266	-	1,372	3,35E-06
HG001_01205 sbcD	Nuclease SbcCD subunit D	SAOUHSC_01341	-	1,371	2,58E-07
HG001_01561 recJ	Single-stranded-DNA-specific exonuclease RecJ	SAOUHSC_01744	-	1,366	2,90E-12
HG001_00669 nrdE2	Ribonucleoside-diphosphate reductase subunit alpha 2	SAOUHSC_00742	nrdI	1,363	7,99E-08
HG001_02011 -	hypothetical protein	SAOUHSC_02208	-	1,361	0,000139633
HG001_00871 ktrB_1	Ktr system potassium uptake protein B	SAOUHSC_00959	-	1,355	9,75E-10
HG001_01565 queA	S-adenosylmethionine:tRNA ribosyltransferase-isomerase	SAOUHSC_01749	queA	1,35	1,96E-08
HG001_02320 fhuD_2	Iron(3+)-hydroxamate-binding protein FhuD precursor	SAOUHSC_02554	-	1,349	9,45E-11
HG001_01562 secD	Protein translocase subunit SecD	SAOUHSC_01746	-	1,348	9,47E-09
HG001_00658 yjjK	putative ABC transporter ATP-binding protein YjjK	SAOUHSC_00729	-	1,344	8,80E-10
HG001_02121 tenA	Putative thiaminase-2	SAOUHSC_02331	-	1,343	3,22E-11
HG001_00993 mutS2	Endonuclease MutS2	SAOUHSC_01099	-	1,341	1,28E-10
HG001_02038 lexA_3	LexA repressor	SAOUHSC_02235	-	1,339	7,53E-11
HG001_02274 rpsN1	30S ribosomal protein S14	SAOUHSC_02499	rpsN	1,335	2,96E-09
HG001_02375 mro	Aldose 1-epimerase precursor	SAOUHSC_02614	-	1,334	1,27E-08
HG001_01509 lepA	Elongation factor 4	SAOUHSC_01688	-	1,332	2,76E-08
HG001_00473 rpoB	DNA-directed RNA polymerase subunit beta	SAOUHSC_00524	rpoB	1,33	3,07E-08
HG001_00377 -	hypothetical protein	SAOUHSC_00428	-	1,328	9,56E-10
HG001_02142 ptpB	Low molecular weight protein-tyrosine-phosphatase PtpB	SAOUHSC_02356	-	1,326	1,37E-06
HG001_00070 sbnF	2-[(L-alanin-3-ylcarbamoyl)methyl]-3-(2-aminoethylcarbamoyl)-2-hydroxypropanoate synt	SAOUHSC_00080	-	1,324	5,34E-07
HG001_01997 -	Phage portal protein	SAOUHSC_02194	-	1,323	8,17E-05
HG001_01907 -	hypothetical protein	SAOUHSC_02086	-	1,322	1,10E-08
HG001_01480 znuC_2	High-affinity zinc uptake system ATP-binding protein ZnuC	SAOUHSC_01657	-	1,32	3,39E-07
HG001_00490 ywpJ_1	Putative phosphatase YwpJ	SAOUHSC_00542	-	1,318	8,39E-08
HG001_01439 -	hypothetical protein	SAOUHSC_01610	-	1,317	8,45E-10
HG001_01829 hemL2	Glutamate-1-semialdehyde 2%2C1-aminomutase 2	SAOUHSC_02000	-	1,312	1,00E-08
HG001_00790 -	Na+/H+ antiporter family protein	SAOUHSC_00880	-	1,308	5,41E-06
HG001_01024 yfnB	Putative HAD-hydrolase YfnB	SAOUHSC_01137	-	1,307	7,96E-09
HG001_01788 trmL	tRNA (cytidine(34)-2'-O)-methyltransferase	SAOUHSC_01988	-	1,301	1,85E-08
HG001_01110 frr	Ribosome-recycling factor	SAOUHSC_01236	frr	1,301	8,66E-08
HG001_01534 udk	Uridine kinase	SAOUHSC_01715	-	1,298	2,62E-10
HG001_01847 -	hypothetical protein	SAOUHSC_02021	-	1,298	6,09E-08
HG001_00001 dnaA	Chromosomal replication initiator protein DnaA	SAOUHSC_00001	dnaA	1,297	1,34E-09
HG001_02290 pbuG	Guanine/hypoxanthine permease PbuG	SAOUHSC_02516	-	1,288	7,46E-07
HG001_01991 -	hypothetical protein	SAOUHSC_02187	-	1,284	0,001099013
HG001_00801 -	Putative peptidyl-prolyl cis-trans isomerase	SAOUHSC_00891	-	1,281	4,59E-10
HG001_00656 kipA_1	KipI antagonist	SAOUHSC_00727	-	1,279	9,23E-10
HG001_01781 liaR	Transcriptional regulatory protein LiaR	SAOUHSC_01980	-	1,277	2,06E-08
HG001_00654 -	hypothetical protein	SAOUHSC_00724	-	1,275	1,60E-08
HG001_02753 rnpA	Ribonuclease P protein component	SAOUHSC_03054	rnpA	1,275	5,73E-05
HG001_00499 nagB_1	Glucosamine-6-phosphate deaminase	SAOUHSC_00552	-	1,274	3,52E-10
HG001_01090 rimM	Ribosome maturation factor RimM	SAOUHSC_01209	rimM	1,272	2,35E-08
HG001_01996 -	Caudovirus prohead protease	SAOUHSC_02193	-	1,269	0,000998902
HG001_00943 pdhA	Pyruvate dehydrogenase E1 component subunit alpha	SAOUHSC_01040	-	1,268	8,46E-09
HG001_01089 rpsP	30S ribosomal protein S16	SAOUHSC_01208	rpsP	1,265	6,80E-07
HG001_02382 fni	Isopentenyl-diphosphate delta-isomerase	SAOUHSC_02623	-	1,263	7,86E-09
HG001_01208 opuD_1	Glycine betaine transporter OpuD	SAOUHSC_01346	-	1,26	2,14E-06
HG001_01288 -	hypothetical protein	SAOUHSC_01436	-	1,259	8,13E-09
HG001_01988 -	hypothetical protein	SAOUHSC_02184	-	1,259	0,000131299
HG001_02174 czcD_2	Cadmium%2C cobalt and zinc/H(+)-K(+) antiporter	SAOUHSC_02389	-	1,256	5,80E-08
HG001_02293 glcU_2	putative glucose uptake protein GlcU	SAOUHSC_02520	-	1,256	2,41E-07
HG001_00027 yfkN_1	Trifunctional nucleotide phosphoesterase protein YfkN precursor	SAOUHSC_00025	-	1,252	6,87E-07
HG001_00028 rlmH	Ribosomal RNA large subunit methyltransferase H	SAOUHSC_00027	-	1,247	2,75E-08
HG001_02143 ywlC_2	Threonylcarbamoyl-AMP synthase	SAOUHSC_02357	-	1,244	1,72E-07
HG001_02642 davT	5-aminovalerate aminotransferase DavT	SAOUHSC_02924	-	1,239	6,63E-06
HG001_01484 trmK	tRNA (adenine(22)-N(1))-methyltransferase	SAOUHSC_01661	-	1,236	3,25E-09
HG001_02210 -	hypothetical protein	SAOUHSC_02425	-	1,236	6,23E-06
HG001_02272 rplF	50S ribosomal protein L6	SAOUHSC_02496	rplF	1,235	2,98E-09
HG001_00137 yecD	Isochorismatase family protein YecD	SAOUHSC_00152	-	1,23	2,28E-06
HG001_00498 -	hypothetical protein	SAOUHSC_00551	-	1,229	1,89E-06

HG001_00138	ipdC	Indole-3-pyruvate decarboxylase	SAOUHSC_00153	-	1,229	3,85E-06
HG001_00417	prs_1	Ribose-phosphate pyrophosphokinase	SAOUHSC_00472	-	1,225	1,20E-07
HG001_02273	rpsH	30S ribosomal protein S8	SAOUHSC_02498	rpsH	1,221	4,91E-09
HG001_01146	-	Thiamine-precursor transporter protein (ThiW)	SAOUHSC_01271	-	1,22	1,83E-08
HG001_00812	spsB_2	Signal peptidase IB	SAOUHSC_00903	-	1,22	6,64E-08
HG001_00310	ssb_1	Single-stranded DNA-binding protein ssb	SAOUHSC_00349	-	1,214	7,79E-08
HG001_01449	-	hypothetical protein	SAOUHSC_01621	nusB	1,207	8,07E-08
HG001_02559	-	Acetyltransferase (GNAT) family protein	SAOUHSC_02827	-	1,207	3,61E-06
HG001_00299	metE	5-methyltetrahydropteroyltriglutamate--homocysteine methyltransferase	SAOUHSC_00338	-	1,201	1,59E-07
HG001_02585	mvaA	3-hydroxy-3-methylglutaryl-coenzyme A reductase	SAOUHSC_02859	-	1,198	2,10E-08
HG001_00944	pdhB	Pyruvate dehydrogenase E1 component subunit beta	SAOUHSC_01041	-	1,197	3,51E-07
HG001_01446	-	Farnesyl diphosphate synthase	SAOUHSC_01618	-	1,193	4,99E-07
HG001_02207	-	Haemolysin-III related	SAOUHSC_02422	-	1,192	6,17E-09
HG001_01452	accB_1	Biotin carboxyl carrier protein of acetyl-CoA carboxylase	SAOUHSC_01624	-	1,19	1,70E-08
HG001_02030	-	hypothetical protein	SAOUHSC_02226	-	1,19	5,52E-05
HG001_01906	-	hypothetical protein	SAOUHSC_02085	-	1,189	1,62E-06
HG001_01109	pyrH	Uridylate kinase	SAOUHSC_01235	pyrH	1,188	7,15E-06
HG001_01712	metK	S-adenosylmethionine synthase	SAOUHSC_01909	-	1,187	4,90E-08
HG001_01681	mdtH	Multidrug resistance protein MdtH	SAOUHSC_01876	-	1,185	1,09E-07
HG001_01132	phbB	Acetoacetyl-CoA reductase	SAOUHSC_01257	-	1,185	2,67E-06
HG001_02421	-	hypothetical protein	SAOUHSC_02668	-	1,185	2,63E-05
HG001_02208	-	putative uridylyltransferase	SAOUHSC_02423	-	1,184	1,20E-07
HG001_01990	-	hypothetical protein	SAOUHSC_02186	-	1,179	0,00182997
HG001_01235	femB	Aminoacyltransferase FemB	SAOUHSC_01374	-	1,174	2,25E-07
HG001_02372	lyrA	Lysostaphin resistance protein A	SAOUHSC_02611	-	1,173	9,52E-08
HG001_01989	-	Bacterial Ig-like domain (group 2)	SAOUHSC_02185	-	1,172	6,28E-07
HG001_01912	-	putative acyl-CoA thioester hydrolase	SAOUHSC_02091	-	1,17	5,82E-08
HG001_00065	sbnA	putative siderophore biosynthesis protein SbnA	SAOUHSC_00075	-	1,17	0,000501837
HG001_01460	gcvPA	putative glycine dehydrogenase (decarboxylating) subunit 1	SAOUHSC_01633	-	1,168	1,59E-05
HG001_00004	recF	DNA replication and repair protein RecF	SAOUHSC_00004	recF	1,166	6,04E-09
HG001_02383	corA	Magnesium transport protein CorA	SAOUHSC_02624	-	1,164	2,66E-07
HG001_02203	ylxH	Flagellum site-determining protein YlxH	SAOUHSC_02417	-	1,161	1,85E-07
HG001_00118	aldA	Putative aldehyde dehydrogenase AldA	SAOUHSC_00132	-	1,161	1,55E-06
HG001_01692	ribD	Riboflavin biosynthesis protein RibD	SAOUHSC_01889	-	1,16	1,76E-06
HG001_01334	gpsA	Glycerol-3-phosphate dehydrogenase [NAD(P)+]	SAOUHSC_01491	gpsA	1,156	3,00E-06
HG001_02118	thiE	Thiamine-phosphate synthase	SAOUHSC_02328	thiE	1,155	2,18E-05
HG001_01059	-	hypothetical protein	SAOUHSC_01175	-	1,151	1,08E-07
HG001_01620	accA	Acetyl-coenzyme A carboxylase carboxyl transferase subunit alpha	SAOUHSC_01808	-	1,151	1,21E-07
HG001_00476	rpsL	30S ribosomal protein S12	SAOUHSC_00527	rpsL	1,15	8,47E-06
HG001_01769	-	Bacterial ABC transporter protein EcsB	SAOUHSC_01966	-	1,148	1,95E-06
HG001_00821	clpB_1	Chaperone protein ClpB	SAOUHSC_00912	-	1,144	5,03E-07
HG001_01145	-	hypothetical protein	SAOUHSC_01270	-	1,143	2,04E-08
HG001_02607	oatA_2	O-acetyltransferase OatA	SAOUHSC_02885	-	1,14	3,32E-06
HG001_01447	xseB	Exodeoxyribonuclease 7 small subunit	SAOUHSC_01619	-	1,139	9,95E-05
HG001_00326	tcyP	L-cystine uptake protein TcyP	SAOUHSC_00367	-	1,134	8,75E-08
HG001_02270	rpsE	30S ribosomal protein S5	SAOUHSC_02494	rpsE	1,133	7,69E-09
HG001_01448	xseA	Exodeoxyribonuclease 7 large subunit	SAOUHSC_01620	xseA	1,128	5,09E-09
HG001_00641	corC	Magnesium and cobalt efflux protein CorC	SAOUHSC_00711	-	1,123	4,05E-06
HG001_01639	rpsD	30S ribosomal protein S4	SAOUHSC_01829	rpsD	1,121	1,96E-08
HG001_01095	rnhB	Ribonuclease HII	SAOUHSC_01215	rnhB	1,121	1,30E-06
HG001_02748	-	hypothetical protein	SAOUHSC_03048	-	1,121	6,74E-06
HG001_01636	iscS_2	Cysteine desulfurase	SAOUHSC_01825	-	1,121	1,38E-05
HG001_00870	-	Serine protease HtrA-like protein	SAOUHSC_00958	-	1,119	3,52E-05
HG001_01843	-	putative phage protein 2 of sapT operon	SAOUHSC_02017	-	1,117	2,82E-06
HG001_01391	-	hypothetical protein	SAOUHSC_01558	-	1,115	0,000846604
HG001_00992	polX	DNA polymerase/3'-5' exonuclease PolX	SAOUHSC_01098	-	1,111	2,71E-08
HG001_01069	rlmN	putative dual-specificity RNA methyltransferase RlmN	SAOUHSC_01185	-	1,111	4,03E-07
HG001_00655	kipI_1	Kinase A inhibitor	SAOUHSC_00726	-	1,108	1,75E-07
HG001_00428	ftsH	ATP-dependent zinc metalloprotease FtsH	SAOUHSC_00486	-	1,101	1,57E-07
HG001_02526	-	putative lipoprotein precursor	SAOUHSC_02789	-	1,098	6,92E-05
HG001_01983	-	hypothetical protein	SAOUHSC_02178	-	1,098	0,000787174
HG001_02068	-	putative inner membrane protein	SAOUHSC_02272	-	1,097	5,34E-05
HG001_02298	femX	Lipid II:glycine glycyltransferase	SAOUHSC_02527	-	1,096	8,84E-07
HG001_01140	-	Calcineurin-like phosphoesterase	SAOUHSC_01265	-	1,094	4,57E-06
HG001_00424	divIC	Cell division protein DivIC	SAOUHSC_00482	-	1,087	5,13E-06
HG001_02147	rpmE2	50S ribosomal protein L31 type B	SAOUHSC_02361	rpmE2	1,086	1,51E-07
HG001_01300	der_1	GTPase Der	SAOUHSC_01455	-	1,085	1,46E-05
HG001_00772	lipA_1	Lipoyl synthase	SAOUHSC_00861	-	1,081	4,80E-08
HG001_01044	ileS	Isoleucine--tRNA ligase	SAOUHSC_01159	ileS	1,079	0,000184868
HG001_02449	tcyC_2	L-cystine import ATP-binding protein TcyC	SAOUHSC_02697	-	1,078	4,12E-06
HG001_01315	asnS	Asparagine--tRNA ligase	SAOUHSC_01471	asnC	1,075	1,61E-05
HG001_01413	Int-Tn	Transposase from transposon Tn916	SAOUHSC_01582	-	1,071	2,88E-06
HG001_01475	rpmG2_2	50S ribosomal protein L33 2	SAOUHSC_01651	rpmG	1,064	0,000111302
HG001_00399	tmk	Thymidylate kinase	SAOUHSC_00451	tmk	1,061	4,06E-06
HG001_00305	ykuT	putative MscS family protein YkuT	SAOUHSC_00344	-	1,061	2,21E-05
HG001_00780	patA_1	Peptidoglycan O-acetyltransferase	SAOUHSC_00870	-	1,059	3,81E-06
HG001_02749	noc	Nucleoid occlusion protein	SAOUHSC_03049	-	1,058	9,40E-07
HG001_01607	coaE	Dephospho-CoA kinase	SAOUHSC_01795	coaE	1,057	1,39E-06
HG001_01953	rutB	Peroxyureidoacrylate/ureidoacrylate amidohydrolase RutB	SAOUHSC_02139	-	1,057	1,24E-05

HG001_00474	rpoC	DNA-directed RNA polymerase subunit beta'	SAOUHSC_00525	-	1,053	3,59E-06
HG001_00311	rpsR	30S ribosomal protein S18	SAOUHSC_00350	rpsR	1,046	1,58E-05
HG001_00146	-	hypothetical protein	SAOUHSC_00163	-	1,046	6,37E-05
HG001_01536	yhbU_2	putative protease YhbU precursor	SAOUHSC_01717	-	1,044	2,20E-07
HG001_01102	trmFO	Methylenetetrahydrofolate--tRNA-(uracil-5-)-methyltransferase TrmFO	SAOUHSC_01223	gid	1,043	3,65E-06
HG001_01715	-	Transposase IS200 like protein	SAOUHSC_01911	-	1,042	1,69E-06
HG001_02039	-	hypothetical protein	SAOUHSC_02237	-	1,042	4,26E-05
HG001_02630	-	hypothetical protein	SAOUHSC_02910	-	1,042	0,001620305
HG001_02310	-	tRNA-Gln(ttg)	-	-	1,04	0,002666821
HG001_01596	rpmI	50S ribosomal protein L35	SAOUHSC_01785	rpmI	1,037	2,31E-07
HG001_00393	dnaX_1	DNA polymerase III subunit tau	SAOUHSC_00442	-	1,034	4,83E-07
HG001_02117	yidC	Membrane protein insertase YidC precursor	SAOUHSC_02327	-	1,034	1,04E-05
HG001_02527	srmB	ATP-dependent RNA helicase SrmB	SAOUHSC_02790	-	1,034	3,15E-05
HG001_01342	-	hypothetical protein	SAOUHSC_01503	-	1,028	7,79E-05
HG001_02315	modA	Molybdate-binding periplasmic protein precursor	SAOUHSC_02549	-	1,024	6,61E-07
HG001_01124	rpsO	30S ribosomal protein S15	SAOUHSC_01250	rpsO	1,024	2,79E-06
HG001_00510	ung	Uracil-DNA glycosylase	SAOUHSC_00564	-	1,024	0,000840362
HG001_01299	ypcP	5'-3' exonuclease	SAOUHSC_01454	-	1,021	6,35E-05
HG001_01629	ald2	Alanine dehydrogenase 2	SAOUHSC_01818	-	1,02	1,41E-06
HG001_02450	tcyB	L-cystine transport system permease protein TcyB	SAOUHSC_02698	-	1,02	0,000167666
HG001_02481	-	hypothetical protein	SAOUHSC_02733	-	1,018	4,27E-06
HG001_02306	moaD	Molybdopterin synthase sulfur carrier subunit	SAOUHSC_02538	-	1,015	6,84E-05
HG001_01049	pyrR	Bifunctional protein PyrR	SAOUHSC_01164	-	1,013	0,000496863
HG001_01144	miaB	(Dimethylallyl)adenosine tRNA methylthiotransferase MiaB	SAOUHSC_01269	-	1,011	6,46E-06
HG001_00675	-	CHY zinc finger	SAOUHSC_00751	-	1,011	6,49E-06
HG001_01097	sucD	Succinyl-CoA ligase [ADP-forming] subunit alpha	SAOUHSC_01218	-	1,007	6,24E-06
HG001_01908	-	hypothetical protein	SAOUHSC_02087	-	1,006	1,32E-06
HG001_01450	-	hypothetical protein	SAOUHSC_01622	-	1,003	3,84E-06
HG001_01913	pepS	Aminopeptidase PepS	SAOUHSC_02092	-	1,003	1,30E-05
HG001_00771	yfkN_3	Trifunctional nucleotide phosphoesterase protein YfkN precursor	SAOUHSC_00860	-	1,002	1,76E-06
HG001_01566	ruvB	Holliday junction ATP-dependent DNA helicase RuvB	SAOUHSC_01750	ruvB	1,001	2,72E-05

DOWN regulated genes from the differencial transcriptomics analysis in oxidative stress						
id	gene	product	locus_tag_NCTC8325	gene_NCTC8325	log2FoldChange	padj
HG001_01009	hly	Alpha-hemolysin precursor	SAOUHSC_01121	-	-4,933	7,31E-95
HG001_00100	cap8A_1	Capsular polysaccharide type 8 biosynthesis protein cap8A	SAOUHSC_00114	-	-4,313	1,48E-50
HG001_00099	adhE	Aldehyde-alcohol dehydrogenase	SAOUHSC_00113	-	-3,985	1,68E-54
HG001_00101	ywqD_1	Tyrosine-protein kinase YwqD	SAOUHSC_00115	-	-3,82	4,93E-46
HG001_01030	ftsL	Cell division protein FtsL	SAOUHSC_01144	-	-3,572	1,09E-52
HG001_02245	-	65 kDa membrane protein precursor	-	-	-3,498	7,36E-32
HG001_00102	ywqE_1	Tyrosine-protein phosphatase YwqE	SAOUHSC_00116	-	-3,459	4,35E-38
HG001_00570	psaA	Manganese ABC transporter substrate-binding lipoprotein precursor	SAOUHSC_00634	-	-3,302	4,90E-40
HG001_00103	pglF	UDP-N-acetyl-alpha-D-glucosamine C6 dehydratase	SAOUHSC_00117	-	-3,2	1,99E-39
HG001_02045	dapE	putative succinyl-diaminopimelate desuccinylase	SAOUHSC_02244	-	-3,098	4,16E-35
HG001_00209	bglA	Aryl-phospho-beta-D-glucosidase BglA	SAOUHSC_00236	-	-3,079	3,93E-22
HG001_01028	mraZ	Protein MraZ	SAOUHSC_01142	-	-3,059	8,47E-48
HG001_00264	lip2	Lipase 2 precursor	SAOUHSC_00300	-	-2,999	3,65E-33
HG001_00206	lrgB	Antiholin-like protein LrgB	SAOUHSC_00233	-	-2,985	5,26E-07
HG001_00358	lpl2	putative lipoprotein precursor	SAOUHSC_00405	-	-2,962	3,88E-41
HG001_00331	xpt	Xanthine phosphoribosyltransferase	SAOUHSC_00372	-	-2,96	5,87E-31
HG001_00544	adh	Alcohol dehydrogenase	SAOUHSC_00608	adhA	-2,958	9,55E-47
HG001_01680	-	T-box	-	-	-2,95	4,37E-37
HG001_02709	lipA_2	Lipase 1 precursor	SAOUHSC_03006	-	-2,917	2,96E-27
HG001_00571	mntB	Manganese transport system membrane protein MntB	SAOUHSC_00636	-	-2,907	3,21E-40
HG001_02640	ldh2	L-lactate dehydrogenase 2	SAOUHSC_02922	-	-2,845	9,55E-43
HG001_00710	-	RsaH	-	-	-2,802	6,38E-21
HG001_00104	capD	UDP-glucose 4-epimerase	SAOUHSC_00118	-	-2,8	1,10E-29
HG001_01029	rsmH_1	Ribosomal RNA small subunit methyltransferase H	SAOUHSC_01143	mraW	-2,787	5,63E-50
HG001_00055	-	Oleate hydratase	SAOUHSC_00061	-	-2,771	9,85E-37
HG001_02756	-	RsaG	-	-	-2,762	2,92E-16
HG001_01172	-	hypothetical protein	SAOUHSC_01303	-	-2,749	2,42E-21
HG001_00318	-	Transglycosylase associated protein	SAOUHSC_00358	-	-2,721	5,70E-41
HG001_01548	-	hypothetical protein	SAOUHSC_01729	-	-2,699	4,62E-48
HG001_00359	-	hypothetical protein	SAOUHSC_00406	-	-2,659	1,15E-29
HG001_01297	tdcB	L-threonine dehydratase catabolic TdcB	SAOUHSC_01451	-	-2,654	1,59E-22
HG001_00106	wbpI	UDP-2%2C3-diacetamido-2%2C3-dideoxy-D-glucuronate 2-epimerase	SAOUHSC_00120	-	-2,572	4,15E-30
HG001_02103	kdpC	Potassium-transporting ATPase C chain	SAOUHSC_02310	-	-2,54	1,77E-27
HG001_00107	vatD	Streptogramin A acetyltransferase	SAOUHSC_00121	-	-2,527	2,76E-23
HG001_00105	fcl	GDP-L-fucose synthase	SAOUHSC_00119	-	-2,525	1,10E-29
HG001_00827	-	65 kDa membrane protein precursor	-	-	-2,514	9,85E-28
HG001_01684	rot	HTH-type transcriptional regulator rot	SAOUHSC_01879	-	-2,499	2,44E-25
HG001_02221	-	Transposase DDE domain protein	SAOUHSC_02437	-	-2,477	1,78E-19
HG001_00561	mrpA	Na(+)/H(+) antiporter subunit A	SAOUHSC_00625	-	-2,462	8,59E-28
HG001_01296	steT	Serine/threonine exchanger SteT	SAOUHSC_01450	-	-2,455	1,71E-29
HG001_02181	glmS	Glutamine--fructose-6-phosphate aminotransferase [isomerizing]	SAOUHSC_02399	-	-2,402	3,78E-28
HG001_02105	kdpA	Potassium-transporting ATPase A chain	SAOUHSC_02312	-	-2,4	1,65E-22
HG001_00241	-	hypothetical protein	SAOUHSC_00272	-	-2,382	5,63E-20
HG001_00274	-	PTS system ascorbate-specific transporter subunits IICB	SAOUHSC_00311	-	-2,378	7,71E-22
HG001_02104	kdpB	Potassium-transporting ATPase B chain	SAOUHSC_02311	-	-2,371	3,10E-18
HG001_01630	-	Putative universal stress protein	SAOUHSC_01819	-	-2,37	2,62E-31
HG001_01610	-	hypothetical protein	SAOUHSC_01798	-	-2,361	1,04E-22
HG001_02514	ahpD	Alkyl hydroperoxide reductase AhpD	SAOUHSC_02774	-	-2,352	2,77E-23
HG001_00273	ulaA	Ascorbate-specific permease IIC component UlaA	SAOUHSC_00310	ulaA	-2,348	3,96E-23
HG001_00562	mrpB	Na(+)/H(+) antiporter subunit B	SAOUHSC_00626	-	-2,342	4,97E-17
HG001_00360	-	hypothetical protein	SAOUHSC_00407	-	-2,333	8,89E-24
HG001_00556	sarA	Transcriptional regulator SarA	SAOUHSC_00620	-	-2,33	2,30E-20
HG001_02040	-	hypothetical protein	SAOUHSC_02238	-	-2,32	6,72E-25
HG001_02107	kdpE	KDP operon transcriptional regulatory protein KdpE	SAOUHSC_02315	-	-2,315	2,96E-19
HG001_02677	isaB	Immunodominant staphylococcal antigen B precursor	SAOUHSC_02972	-	-2,292	2,65E-22
HG001_00899	sspA	Glutamyl endopeptidase precursor	SAOUHSC_00988	-	-2,286	1,08E-22
HG001_00847	-	RsaE	-	-	-2,284	2,58E-06
HG001_01412	-	hypothetical protein	SAOUHSC_01580	-	-2,282	5,01E-24
HG001_00725	-	hypothetical protein	SAOUHSC_00808	-	-2,258	6,01E-20
HG001_02494	-	hypothetical protein	SAOUHSC_02753	-	-2,239	5,45E-25
HG001_02359	malP	PTS system maltose-specific EIICB component	SAOUHSC_02597	-	-2,234	2,88E-26
HG001_01744	-	hypothetical protein	SAOUHSC_01945	-	-2,233	2,77E-16
HG001_00120	-	hypothetical protein	SAOUHSC_00134	-	-2,232	4,58E-20
HG001_00108	-	hypothetical protein	SAOUHSC_00122	-	-2,231	3,19E-21
HG001_01075	rpmB	50S ribosomal protein L28	SAOUHSC_01191	rpmB	-2,228	1,21E-23
HG001_02398	-	FtsX-like permease family protein	SAOUHSC_02641	-	-2,222	1,28E-18
HG001_00564	mnhD1_1	Na(+)/H(+) antiporter subunit D1	SAOUHSC_00628	-	-2,22	1,74E-24
HG001_00275	cmtB	Mannitol-specific cryptic phosphotransferase enzyme IIA component	SAOUHSC_00312	-	-2,216	3,56E-20
HG001_00898	sspB	Staphopain B precursor	SAOUHSC_00987	-	-2,208	4,30E-17
HG001_02337	-	hypothetical protein	SAOUHSC_02575	-	-2,199	3,98E-20
HG001_00563	mrpC	Na(+)/H(+) antiporter subunit C	SAOUHSC_00627	-	-2,185	7,06E-20
HG001_02182	-	glmS	-	-	-2,182	1,02E-14
HG001_00724	-	hypothetical protein	SAOUHSC_00806	-	-2,175	5,66E-22

HG001_00545	-	hypothetical protein	SAOUHSC_00609	-	-2,173	0,000132078
HG001_01340	ebpS	Elastin-binding protein EbpS	SAOUHSC_01501	-	-2,155	3,66E-22
HG001_00573	ideR	Iron-dependent repressor IdeR	SAOUHSC_00638	mntR	-2,129	8,63E-19
HG001_00897	sspC	Staphostatin B	SAOUHSC_00986	-	-2,128	5,00E-17
HG001_02588	clpL	ATP-dependent Clp protease ATP-binding subunit ClpL	SAOUHSC_02862	-	-2,125	2,50E-18
HG001_02057	-	RNAIII	SAOUHSC_02260	-	-2,116	3,71E-27
HG001_01958	-	hypothetical protein	SAOUHSC_02145	-	-2,11	2,54E-23
HG001_02125	-	hypothetical protein	SAOUHSC_02335	-	-2,099	1,64E-14
HG001_02737	-	hypothetical protein	SAOUHSC_03035	-	-2,098	1,87E-19
HG001_00248	-	hypothetical protein	SAOUHSC_00280	-	-2,097	4,44E-17
HG001_00482	hchA	Molecular chaperone Hsp31 and glyoxalase 3	SAOUHSC_00533	-	-2,073	6,43E-21
HG001_01747	-	Thermophilic serine proteinase precursor	SAOUHSC_01949	-	-2,065	1,07E-15
HG001_01772	-	hypothetical protein	SAOUHSC_01969	-	-2,06	5,73E-24
HG001_00889	-	hypothetical protein	SAOUHSC_00977	-	-2,032	1,15E-14
HG001_01064	-	hypothetical protein	SAOUHSC_01180	-	-2,012	9,99E-13
HG001_01978	sak	Staphylokinase precursor	SAOUHSC_02171	-	-2,003	2,33E-19
HG001_02222	-	Alkaline shock protein 23	SAOUHSC_02441	-	-2,001	9,35E-17
HG001_01237	-	hypothetical protein	SAOUHSC_01376	-	-1,978	1,20E-22
HG001_00316	-	Peptidase propeptide and YPEB domain protein	SAOUHSC_00356	-	-1,978	1,39E-15
HG001_00046	plc	1-phosphatidylinositol phosphodiesterase precursor	SAOUHSC_00051	-	-1,97	2,79E-21
HG001_02062	agrA	Accessory gene regulator protein A	SAOUHSC_02265	-	-1,967	1,79E-14
HG001_02060	-	Staphylococcal AgrD protein	SAOUHSC_02262	-	-1,962	6,81E-14
HG001_00740	-	hypothetical protein	SAOUHSC_00825	-	-1,942	2,73E-16
HG001_02225	opuD_2	Glycine betaine transporter OpuD	SAOUHSC_02444	-	-1,94	1,98E-17
HG001_01065	-	TM2 domain protein	SAOUHSC_01181	-	-1,94	3,89E-16
HG001_00361	-	hypothetical protein	SAOUHSC_00408	-	-1,936	1,56E-15
HG001_01746	yxlF_2	putative ABC transporter ATP-binding protein YxlF	SAOUHSC_01948	-	-1,934	4,04E-14
HG001_01298	ald1	Alanine dehydrogenase 1	SAOUHSC_01452	-	-1,927	5,01E-13
HG001_02330	sarR	HTH-type transcriptional regulator SarR	SAOUHSC_02566	-	-1,925	2,59E-13
HG001_02601	crtN	Dehydrosqualene desaturase	SAOUHSC_02877	-	-1,921	8,97E-18
HG001_02347	-	RsaOG	-	-	-1,92	1,06E-12
HG001_01612	phoP	Alkaline phosphatase synthesis transcriptional regulatory protein PhoP	SAOUHSC_01800	-	-1,919	1,99E-20
HG001_02458	hlgC	Gamma-hemolysin component C precursor	SAOUHSC_02709	-	-1,911	6,49E-19
HG001_01445	argR_1	Arginine repressor	SAOUHSC_01617	-	-1,91	4,66E-16
HG001_00565	mrpE	Na(+)/H(+) antiporter subunit E	SAOUHSC_00629	-	-1,909	9,27E-16
HG001_00744	-	hypothetical protein	SAOUHSC_00830	-	-1,898	4,89E-10
HG001_01495	ybeZ	PhoH-like protein	SAOUHSC_01673	-	-1,893	1,72E-19
HG001_00567	mrpG	Na(+)/H(+) antiporter subunit G	SAOUHSC_00632	-	-1,891	7,48E-16
HG001_01955	alkH	Aldehyde dehydrogenase	SAOUHSC_02142	-	-1,887	2,51E-15
HG001_00058	-	hypothetical protein	SAOUHSC_00065	-	-1,881	4,25E-19
HG001_02397	hrtA_2	Putative hemin import ATP-binding protein HrtA	SAOUHSC_02640	-	-1,876	8,24E-11
HG001_01216	glcT	GlcA/glcB genes antiterminator	SAOUHSC_01356	-	-1,871	3,05E-15
HG001_01364	-	hypothetical protein	SAOUHSC_01527	-	-1,871	3,52E-09
HG001_00109	-	hypothetical protein	SAOUHSC_00123	-	-1,862	9,54E-17
HG001_00227	esxA	Virulence factor EsxA	SAOUHSC_00257	-	-1,858	1,52E-17
HG001_00566	mrpF	Na(+)/H(+) antiporter subunit F	SAOUHSC_00632	-	-1,851	2,38E-13
HG001_02365	yghA	putative oxidoreductase YghA	SAOUHSC_02604	-	-1,849	3,51E-16
HG001_00169	pflB	Formate acetyltransferase	SAOUHSC_00187	-	-1,839	9,01E-16
HG001_01751	gdmA	Lantibiotic gallidermin precursor	SAOUHSC_01953	-	-1,836	2,24E-13
HG001_02303	sarV	HTH-type transcriptional regulator SarV	SAOUHSC_02532	-	-1,834	1,02E-10
HG001_02106	kdpD	Sensor protein KdpD	SAOUHSC_02314	-	-1,818	2,02E-16
HG001_00330	-	Purine	-	-	-1,807	4,69E-05
HG001_01032	mraY	Phospho-N-acetylmuramoyl-pentapeptide-transferase	SAOUHSC_01146	mraY	-1,804	2,57E-19
HG001_00902	slyA_2	Transcriptional regulator SlyA	SAOUHSC_00992	-	-1,799	1,23E-11
HG001_00759	-	CsbD-like protein	SAOUHSC_00845	-	-1,797	8,91E-21
HG001_00560	xerD_2	Tyrosine recombinase XerD	SAOUHSC_00624	-	-1,786	3,23E-16
HG001_01704	tal	Transaldolase	SAOUHSC_01901	-	-1,785	5,82E-13
HG001_01173	-	hypothetical protein	SAOUHSC_01304	-	-1,783	4,77E-10
HG001_02061	dpiB	Sensor histidine kinase DpiB	SAOUHSC_02264	-	-1,782	1,04E-09
HG001_02223	-	hypothetical protein	SAOUHSC_02442	-	-1,781	3,39E-15
HG001_02059	agrB	Accessory gene regulator protein B	SAOUHSC_02261	-	-1,78	2,62E-12
HG001_01363	-	hypothetical protein	SAOUHSC_01526	-	-1,779	2,76E-06
HG001_02495	ybbL	putative ABC transporter ATP-binding protein YbbL	SAOUHSC_02754	-	-1,778	5,45E-17
HG001_00414	yabJ	Enamine/imine deaminase	SAOUHSC_00468	-	-1,767	5,40E-18
HG001_00110	-	hypothetical protein	SAOUHSC_00124	-	-1,764	5,05E-13
HG001_01174	-	hypothetical protein	SAOUHSC_01305	-	-1,758	6,40E-08
HG001_02627	-	hypothetical protein	SAOUHSC_02907	-	-1,755	7,58E-07
HG001_01031	pbpB	Penicillin-binding protein 2B	SAOUHSC_01145	-	-1,753	1,13E-15
HG001_01581	-	T-box	-	-	-1,751	1,14E-13
HG001_00728	clfA	Clumping factor A precursor	SAOUHSC_00812	-	-1,737	4,36E-13
HG001_00572	znuC_1	High-affinity zinc uptake system ATP-binding protein ZnuC	SAOUHSC_00637	-	-1,736	1,75E-12
HG001_02332	-	hypothetical protein	SAOUHSC_02569	-	-1,731	3,38E-13
HG001_01802	-	tRNA-Tyr(gta)	SAOUHSC_T00057	-	-1,726	8,71E-09
HG001_02112	-	hypothetical protein	SAOUHSC_02320	-	-1,718	4,31E-13
HG001_02195	-	tRNA-Tyr(gta)	SAOUHSC_T00058	-	-1,709	1,71E-08

HG001_02626	-	hypothetical protein	SAOUHSC_02906	-	-1,707	9,64E-08
HG001_00929	-	hypothetical protein	SAOUHSC_01024	-	-1,703	1,77E-15
HG001_01729	-	hypothetical protein	SAOUHSC_01925	-	-1,702	7,03E-05
HG001_02379	yhaI	Inner membrane protein YhaI	SAOUHSC_02620	-	-1,699	7,78E-15
HG001_01952	pfbA	Plasmin and fibronectin-binding protein A precursor	SAOUHSC_02138	-	-1,689	1,21E-14
HG001_01544	yrrB	TPR repeat-containing protein YrrB	SAOUHSC_01724	-	-1,689	6,62E-11
HG001_00111	cap5L	putative glycosyl transferase	SAOUHSC_00125	-	-1,68	1,13E-15
HG001_00174	fadA	3-ketoacyl-CoA thiolase	SAOUHSC_00195	-	-1,676	9,15E-07
HG001_01917	-	hypothetical protein	SAOUHSC_02097	-	-1,675	2,90E-13
HG001_01043	-	T-box	-	-	-1,666	1,53E-11
HG001_00267	limB_1	Limonene 1%2C2-monooxygenase	SAOUHSC_00304	-	-1,663	5,78E-14
HG001_01287	thyA	Thymidylate synthase	SAOUHSC_01435	thyA	-1,66	1,91E-14
HG001_01361	-	Phage tail protein	SAOUHSC_01524	-	-1,659	1,82E-09
HG001_02507	nikA	Nickel-binding periplasmic protein precursor	SAOUHSC_02767	-	-1,658	5,40E-12
HG001_02603	crtQ	4%2C4'-diaponeurosporenoate glycosyltransferase	SAOUHSC_02880	-	-1,657	9,84E-12
HG001_00329	-	hypothetical protein	SAOUHSC_00371	-	-1,652	2,45E-13
HG001_02697	-	hypothetical protein	SAOUHSC_02994	-	-1,651	3,15E-14
HG001_00709	-	Epimerase family protein	SAOUHSC_00792	-	-1,651	3,78E-13
HG001_02410	-	Ferredoxin--NADP reductase	SAOUHSC_02654	-	-1,649	1,26E-13
HG001_02459	hlgB	Gamma-hemolysin component B precursor	SAOUHSC_02710	-	-1,643	4,60E-15
HG001_00184	ldh1	L-lactate dehydrogenase 1	SAOUHSC_00206	-	-1,643	4,46E-09
HG001_00625	mgrA	HTH-type transcriptional regulator MgrA	SAOUHSC_00694	-	-1,638	1,53E-12
HG001_00617	-	hypothetical protein	SAOUHSC_00686	-	-1,635	4,47E-12
HG001_02399	hssR	Heme response regulator HssR	SAOUHSC_02643	-	-1,63	1,25E-12
HG001_00175	fadN	putative 3-hydroxyacyl-CoA dehydrogenase	SAOUHSC_00196	-	-1,63	2,14E-06
HG001_01444	recN	DNA repair protein RecN	SAOUHSC_01615	-	-1,619	5,84E-16
HG001_00214	degA	HTH-type transcriptional regulator DegA	SAOUHSC_00242	-	-1,616	4,49E-12
HG001_02093	rsbW	Serine-protein kinase RsbW	SAOUHSC_02299	-	-1,61	8,53E-13
HG001_00503	proP	Proline/betaine transporter	SAOUHSC_00556	-	-1,608	7,89E-14
HG001_01841	-	hypothetical protein	SAOUHSC_02014	-	-1,606	3,35E-09
HG001_01731	-	Transposase	SAOUHSC_01928	-	-1,605	1,71E-11
HG001_00130	psf-1	4'-phosphopantetheinyl transferase psf-1	SAOUHSC_00145	-	-1,599	1,64E-12
HG001_02545	-	hypothetical protein	SAOUHSC_02812	-	-1,599	3,25E-12
HG001_01745	-	ABC-2 family transporter protein	SAOUHSC_01947	-	-1,592	5,42E-10
HG001_02520	-	hypothetical protein	SAOUHSC_02781	-	-1,591	7,96E-13
HG001_01730	-	hypothetical protein	SAOUHSC_01926	-	-1,589	4,49E-12
HG001_00074	-	hypothetical protein	SAOUHSC_00084	-	-1,585	3,81E-10
HG001_00741	-	hypothetical protein	SAOUHSC_00826	-	-1,584	2,66E-11
HG001_01175	-	hypothetical protein	SAOUHSC_01306	-	-1,58	0,00276172
HG001_02415	sacX	Negative regulator of SacY activity	SAOUHSC_02661	-	-1,573	9,24E-14
HG001_01414	-	hypothetical protein	SAOUHSC_01583	-	-1,562	7,43E-12
HG001_02406	-	putative lipoprotein precursor	SAOUHSC_02650	-	-1,56	1,91E-11
HG001_01362	-	Glycyl-glycine endopeptidase ALE-1 precursor	SAOUHSC_01525	-	-1,558	8,74E-16
HG001_00415	spoVG	Putative septation protein SpoVG	SAOUHSC_00469	-	-1,553	3,09E-13
HG001_00678	-	hypothetical protein	SAOUHSC_00754	-	-1,546	6,31E-12
HG001_00738	-	hypothetical protein	SAOUHSC_00823	-	-1,536	1,36E-05
HG001_00303	-	T-box	-	-	-1,514	1,16E-06
HG001_02734	-	hypothetical protein	SAOUHSC_03032	-	-1,513	3,76E-09
HG001_00726	-	hypothetical protein	SAOUHSC_00810	-	-1,51	3,14E-09
HG001_01659	-	hypothetical protein	SAOUHSC_01854	-	-1,506	9,22E-12
HG001_00707	-	tRNA-Arg(ccg)	SAOUHSC_T0005	-	-1,503	0,031150464
HG001_00176	acdA	Acyl-CoA dehydrogenase	SAOUHSC_00197	-	-1,5	4,39E-06
HG001_02326	ureE	Urease accessory protein UreE	SAOUHSC_02562	ureE	-1,499	8,19E-10
HG001_00663	-	Putative 5'(3')-deoxyribonucleotidase	SAOUHSC_00734	-	-1,495	1,34E-09
HG001_00607	sarX	HTH-type transcriptional regulator SarX	SAOUHSC_00674	-	-1,492	6,69E-10
HG001_01654	acsA_1	Acetyl-coenzyme A synthetase	SAOUHSC_01846	-	-1,488	1,86E-09
HG001_02368	hutU	Urocanate hydratase	SAOUHSC_02607	-	-1,484	4,65E-09
HG001_00828	-	hypothetical protein	SAOUHSC_00919	-	-1,48	1,87E-11
HG001_02404	lctP_2	L-lactate permease	SAOUHSC_02648	-	-1,468	2,76E-08
HG001_00690	yvyD	Putative sigma-54 modulation protein	SAOUHSC_00767	-	-1,463	2,90E-11
HG001_02735	nixA	High-affinity nickel-transport protein NixA	SAOUHSC_03033	-	-1,46	2,10E-11
HG001_01927	ftnA	Ferritin	SAOUHSC_02108	-	-1,45	7,51E-13
HG001_00528	-	hypothetical protein	SAOUHSC_00586	-	-1,45	9,08E-09
HG001_02367	hutI	Imidazolonepropionase	SAOUHSC_02606	-	-1,45	1,31E-07
HG001_01428	proC	Pyrroline-5-carboxylate reductase	SAOUHSC_01597	-	-1,448	3,98E-10
HG001_01711	-	hypothetical protein	SAOUHSC_01908	-	-1,447	1,50E-11
HG001_01171	-	hypothetical protein	SAOUHSC_01301	-	-1,445	0,007144881
HG001_02162	-	hypothetical protein	SAOUHSC_02376	-	-1,444	1,50E-11
HG001_00736	-	hypothetical protein	SAOUHSC_00821	-	-1,442	2,29E-08
HG001_00047	-	putative lipoprotein precursor	SAOUHSC_00052	-	-1,441	7,53E-08
HG001_00618	-	Acetyltransferase (GNAT) family protein	SAOUHSC_00687	-	-1,439	3,28E-08
HG001_01336	rpsA_1	30S ribosomal protein S1	SAOUHSC_01493	rpsA	-1,438	9,56E-13
HG001_01004	-	hypothetical protein	SAOUHSC_01113	-	-1,431	2,16E-08
HG001_00332	pucK	Uric acid permease PucK	SAOUHSC_00373	-	-1,429	5,92E-06
HG001_02544	ywaC	GTP pyrophosphokinase YwaC	SAOUHSC_02811	-	-1,424	3,25E-11

HG001_01740 splC	Serine protease SplC precursor	SAOUHSC_01939	-	-1,419	2,47E-06
HG001_01974 scn_3	Staphylococcal complement inhibitor precursor	SAOUHSC_02167	-	-1,417	7,20E-08
HG001_00986 -	T-box	-	-	-1,414	1,11E-09
HG001_02543 zntR	HTH-type transcriptional regulator ZntR	SAOUHSC_02810	-	-1,41	2,68E-12
HG001_00131 yagU	Inner membrane protein YagU	SAOUHSC_00146	-	-1,409	9,97E-13
HG001_00362 -	hypothetical protein	SAOUHSC_00409	-	-1,403	4,73E-07
HG001_02172 yhfK	putative sugar epimerase YhfK	SAOUHSC_02387	-	-1,401	4,59E-10
HG001_01728 -	hypothetical protein	SAOUHSC_01923	-	-1,401	7,46E-08
HG001_02324 ureB	Urease subunit beta	SAOUHSC_02559	ureB	-1,398	7,41E-07
HG001_01524 -	hypothetical protein	SAOUHSC_01704	-	-1,397	0,004196363
HG001_02163 pdp	Pyrimidine-nucleoside phosphorylase	SAOUHSC_02377	-	-1,393	1,15E-10
HG001_02094 rsbV	Anti-sigma-B factor antagonist	SAOUHSC_02300	-	-1,39	1,11E-10
HG001_00553 -	hypothetical protein	SAOUHSC_00617	-	-1,389	1,30E-09
HG001_02418 ydaG	General stress protein 26	SAOUHSC_02665	-	-1,385	3,81E-10
HG001_00126 -	hypothetical protein	SAOUHSC_00141	-	-1,384	3,63E-10
HG001_00247 -	hypothetical protein	SAOUHSC_00279	-	-1,383	1,05E-08
HG001_01255 dapB	4-hydroxy-tetrahydrodipicolinate reductase	SAOUHSC_01397	-	-1,381	7,81E-10
HG001_01163 -	hypothetical protein	SAOUHSC_01290	-	-1,38	0,004802171
HG001_01787 nagB_2	Glucosamine-6-phosphate deaminase	SAOUHSC_01987	-	-1,379	4,97E-11
HG001_01611 phoR	Alkaline phosphatase synthesis sensor protein PhoR	SAOUHSC_01799	-	-1,376	4,07E-11
HG001_00743 argO	Arginine exporter protein ArgO	SAOUHSC_00828	-	-1,373	1,21E-06
HG001_00634 tetA_2	Tetracycline resistance protein%2C class B	SAOUHSC_00703	-	-1,371	5,57E-10
HG001_01256 dapH	2%2C3%2C4%2C5-tetrahydropyridine-2%2C6-dicarboxylate N-acetyltransferase	SAOUHSC_01398	-	-1,367	1,20E-09
HG001_00605 -	Inhibitor of apoptosis-promoting Bax1	SAOUHSC_00672	-	-1,365	1,33E-09
HG001_01186 -	hypothetical protein	SAOUHSC_01318	-	-1,365	1,56E-08
HG001_00990 zapA	Cell division protein ZapA	SAOUHSC_01096	-	-1,363	1,51E-07
HG001_00835 oppF_1	Oligopeptide transport ATP-binding protein OppF	SAOUHSC_00926	-	-1,359	2,68E-07
HG001_02164 deoC2	Deoxyribose-phosphate aldolase 2	SAOUHSC_02379	-	-1,357	8,55E-13
HG001_02666 -	hypothetical protein	-	-	-1,356	1,27E-09
HG001_01129 phnF	putative transcriptional regulator PhnF	SAOUHSC_01254	-	-1,353	4,60E-09
HG001_02676 aur	Zinc metalloproteinase aureolysin precursor	SAOUHSC_02971	-	-1,349	1,89E-07
HG001_00516 -	RsaA	-	-	-1,346	6,30E-09
HG001_02409 -	Acetyltransferase (GNAT) family protein	SAOUHSC_02653	-	-1,346	0,000139451
HG001_02407 paiA	Protease synthase and sporulation negative regulatory protein PAI 1	SAOUHSC_02651	-	-1,344	4,64E-08
HG001_02363 -	SAM	-	-	-1,344	8,59E-08
HG001_00850 yjbI	Group 2 truncated hemoglobin YjbI	SAOUHSC_00939	-	-1,34	1,68E-10
HG001_00891 -	Acetyltransferase (GNAT) family protein	SAOUHSC_00979	-	-1,339	2,03E-06
HG001_01660 -	hypothetical protein	SAOUHSC_01855	-	-1,336	1,87E-11
HG001_01192 -	hypothetical protein	SAOUHSC_01324	-	-1,335	6,09E-07
HG001_00170 pflA	Pyruvate formate-lyase-activating enzyme	SAOUHSC_00188	-	-1,334	8,75E-07
HG001_00249 focA	putative formate transporter 1	SAOUHSC_00281	-	-1,334	1,31E-05
HG001_00568 nhaK_1	Sodium%2C potassium%2C lithium and rubidium/H(+) antiporter	SAOUHSC_00633	-	-1,332	3,61E-11
HG001_01834 -	hypothetical protein	SAOUHSC_02006	-	-1,33	2,35E-11
HG001_00606 melR_1	Melibiose operon regulatory protein	SAOUHSC_00673	-	-1,329	1,23E-09
HG001_02325 ureC	Urease subunit alpha	SAOUHSC_02561	ureC	-1,329	9,64E-08
HG001_01360 -	Prophage endopeptidase tail	SAOUHSC_01523	-	-1,324	1,76E-07
HG001_00954 -	hypothetical protein	SAOUHSC_01051	-	-1,321	1,72E-07
HG001_00554 -	hypothetical protein	SAOUHSC_00618	-	-1,32	7,25E-09
HG001_00802 yugI_2	General stress protein 13	SAOUHSC_00892	-	-1,318	4,37E-09
HG001_01223 -	prephenate dehydrogenase	SAOUHSC_01364	-	-1,317	5,00E-09
HG001_02678 -	hypothetical protein	SAOUHSC_02973	-	-1,317	8,46E-09
HG001_02351 ybbH_3	putative HTH-type transcriptional regulator YbbH	SAOUHSC_02589	-	-1,314	1,04E-07
HG001_00183 hmp	Flavohemoprotein	SAOUHSC_00204	-	-1,312	1,40E-05
HG001_01909 -	hypothetical protein	SAOUHSC_02088	-	-1,309	6,86E-06
HG001_00836 dppE	Dipeptide-binding protein DppE precursor	SAOUHSC_00927	-	-1,309	1,00E-05
HG001_02732 yflS	Putative malate transporter YflS	SAOUHSC_03030	-	-1,306	6,81E-12
HG001_01033 murD	UDP-N-acetylmuramoylalanine--D-glutamate ligase	SAOUHSC_01147	murD	-1,306	1,01E-08
HG001_00704 aroK_1	Shikimate kinase	SAOUHSC_00787	-	-1,306	1,42E-08
HG001_00112 epsL	putative sugar transferase EpsL	SAOUHSC_00126	-	-1,304	4,34E-08
HG001_01756 -	tRNA-Ser(gga)	SAOUHSC_T00050	-	-1,294	0,00428682
HG001_00178 ydiF	Acetate CoA-transferase YdiF	SAOUHSC_00199	-	-1,291	3,53E-05
HG001_00129 grsB	Gramicidin S synthase 2	SAOUHSC_00144	-	-1,287	4,56E-08
HG001_01333 hup	DNA-binding protein HU	SAOUHSC_01490	-	-1,286	1,02E-09
HG001_01971 -	65 kDa membrane protein precursor	SAOUHSC_02160	-	-1,284	5,92E-06
HG001_02680 manP	PTS system mannose-specific EIIBCA component	SAOUHSC_02975	-	-1,283	8,48E-09
HG001_02719 -	Polysaccharide deacetylase	SAOUHSC_03016	-	-1,281	9,40E-07
HG001_02600 dapL	LL-diaminopimelate aminotransferase	SAOUHSC_02876	-	-1,276	3,98E-09
HG001_01164 -	hypothetical protein	SAOUHSC_01292	-	-1,275	0,01572951
HG001_02124 ssb_2	Single-stranded DNA-binding protein ssb	SAOUHSC_02334	-	-1,273	2,08E-06
HG001_01007 -	hypothetical protein	SAOUHSC_01119	-	-1,266	4,66E-05
HG001_00113 galE	UDP-glucose 4-epimerase	SAOUHSC_00127	-	-1,265	5,66E-09
HG001_01347 -	hypothetical protein	SAOUHSC_01510	-	-1,264	0,004493515
HG001_01415 -	hypothetical protein	SAOUHSC_01584	-	-1,259	1,47E-06
HG001_01542 -	T-box	-	-	-1,256	4,68E-05
HG001_00529 -	hypothetical protein	SAOUHSC_00587	-	-1,254	1,17E-06

HG001_01254	dapA	4-hydroxy-tetrahydrodipicolinate synthase	SAOUHSC_01396	-	-1,253	2,90E-08
HG001_02331	-	hypothetical protein	SAOUHSC_02568	-	-1,243	1,44E-08
HG001_02506	nikB_2	Nickel transport system permease protein NikB	SAOUHSC_02766	-	-1,234	1,11E-05
HG001_01759	-	tRNA-Gly(tcc)	SAOUHSC_T00022	-	-1,225	0,000540677
HG001_01786	-	hypothetical protein	SAOUHSC_01986	-	-1,212	3,05E-08
HG001_02354	-	hypothetical protein	SAOUHSC_02592	-	-1,212	2,81E-06
HG001_01295	norB_4	Quinolone resistance protein NorB	SAOUHSC_01448	-	-1,21	6,49E-06
HG001_00953	-	hypothetical protein	SAOUHSC_01050	-	-1,208	2,62E-08
HG001_01556	-	T-box	-	-	-1,208	1,06E-05
HG001_00834	oppD_1	Oligopeptide transport ATP-binding protein OppD	SAOUHSC_00925	-	-1,208	2,34E-05
HG001_01665	ytpP	Thioredoxin-like protein YtpP	SAOUHSC_01860	-	-1,207	2,01E-09
HG001_01742	splA	Serine protease SplA precursor	SAOUHSC_01942	-	-1,207	0,000610276
HG001_01365	-	Bacterial Ig-like domain (group 2)	SAOUHSC_01528	-	-1,195	2,05E-06
HG001_00048	-	putative lipoprotein precursor	SAOUHSC_00053	-	-1,192	1,21E-06
HG001_02292	-	hypothetical protein	SAOUHSC_02519	-	-1,19	6,11E-07
HG001_02489	opuCA	Carnitine transport ATP-binding protein OpuCA	SAOUHSC_02744	-	-1,189	5,16E-06
HG001_00864	ugtP	Processive diacylglycerol beta-glucosyltransferase	SAOUHSC_00953	-	-1,186	1,09E-08
HG001_02044	-	putative leukocidin-like protein 2 precursor	SAOUHSC_02243	-	-1,186	2,83E-06
HG001_01018	-	hypothetical protein	SAOUHSC_01131	-	-1,184	0,000125426
HG001_01260	-	hypothetical protein	SAOUHSC_01402	-	-1,184	0,013374835
HG001_01238	nikE	Nickel import ATP-binding protein NikE	SAOUHSC_01377	-	-1,182	4,27E-07
HG001_00268	gcvH_1	Glycine cleavage system H protein	SAOUHSC_00305	-	-1,179	2,04E-06
HG001_01332	-	Heptaprenyl diphosphate synthase (HEPPP synthase) subunit 1	SAOUHSC_01488	-	-1,179	3,22E-06
HG001_01494	ybeY	Endoribonuclease YbeY	SAOUHSC_01672	-	-1,175	9,41E-09
HG001_00952	potD	Spermidine/putrescine-binding periplasmic protein precursor	SAOUHSC_01049	-	-1,173	3,67E-08
HG001_01463	aroK_2	Shikimate kinase	SAOUHSC_01635	-	-1,168	5,44E-07
HG001_02371	hutG	Formimidoylglutamase	SAOUHSC_02610	-	-1,162	2,41E-08
HG001_00059	lctP_1	L-lactate permease	SAOUHSC_00067	-	-1,162	1,45E-06
HG001_02364	-	hypothetical protein	SAOUHSC_02603	-	-1,158	6,53E-06
HG001_00021	-	tRNA-Asp(gtc)	SAOUHSC_T00011	-	-1,158	0,000389585
HG001_01553	-	6S	-	-	-1,155	0,000116541
HG001_00826	-	putative kinase inhibitor	SAOUHSC_00917	-	-1,155	0,000367906
HG001_02327	ureF	Urease accessory protein UreF	SAOUHSC_02563	ureE	-1,14	1,55E-06
HG001_01211	-	Iron-sulphur cluster biosynthesis	SAOUHSC_01349	-	-1,14	8,82E-06
HG001_02625	-	hypothetical protein	SAOUHSC_02905	-	-1,139	0,001100864
HG001_00708	clpP	ATP-dependent Clp protease proteolytic subunit	SAOUHSC_00790	clpP	-1,137	5,17E-08
HG001_01455	-	hypothetical protein	SAOUHSC_01627	-	-1,136	0,000103352
HG001_01657	ccpA	Catabolite control protein A	SAOUHSC_01850	-	-1,134	4,30E-07
HG001_01757	-	tRNA-Glu(ttc)	SAOUHSC_T00019	-	-1,134	0,006684315
HG001_01826	perR	Peroxide-responsive repressor PerR	SAOUHSC_01997	-	-1,132	1,18E-06
HG001_01694	-	hypothetical protein	SAOUHSC_01890	-	-1,13	1,77E-07
HG001_01762	-	tRNA-Asp(gtc)	SAOUHSC_T00012	-	-1,129	0,000404503
HG001_00261	ybbH_2	putative HTH-type transcriptional regulator YbbH	SAOUHSC_00297	-	-1,128	3,10E-07
HG001_01602	-	T-box	SAOUHSC_01789	-	-1,127	6,79E-07
HG001_00647	-	Electron transfer DM13	SAOUHSC_00717	-	-1,124	1,27E-05
HG001_01808	-	tRNA-Asp(gtc)	SAOUHSC_T00014	-	-1,123	0,000512416
HG001_02197	-	tRNA-Glu(ttc)	SAOUHSC_T00020	-	-1,121	0,0067847
HG001_01737	splF	Serine protease SplF precursor	SAOUHSC_01935	-	-1,119	0,000404393
HG001_00706	whiA	Putative sporulation transcription regulator WhiA	SAOUHSC_00789	-	-1,115	4,52E-07
HG001_01202	tkt	Transketolase	SAOUHSC_01337	-	-1,114	1,46E-07
HG001_02572	-	hypothetical protein	SAOUHSC_02842	-	-1,113	0,012071358
HG001_01436	pepT_2	Peptidase T	SAOUHSC_01606	-	-1,112	1,22E-06
HG001_01650	mrcA	Penicillin-binding protein 1A	SAOUHSC_01840	-	-1,11	3,48E-05
HG001_02353	-	hypothetical protein	SAOUHSC_02591	-	-1,109	5,68E-07
HG001_00439	-	tRNA-Gly(gcc)	SAOUHSC_T00021	-	-1,103	0,000712167
HG001_01805	-	tRNA-Asp(gtc)	SAOUHSC_T00013	-	-1,102	0,000698607
HG001_00985	-	Putative TrmH family tRNA/rRNA methyltransferase	SAOUHSC_01091	-	-1,099	3,49E-07
HG001_02422	sarZ	HTH-type transcriptional regulator SarZ	SAOUHSC_02669	-	-1,099	1,11E-05
HG001_01221	-	putative tautomerase	SAOUHSC_01362	-	-1,095	1,27E-06
HG001_00868	-	yybP-ykoY	-	-	-1,095	0,004142821
HG001_01498	-	hypothetical protein	SAOUHSC_01677	-	-1,093	1,75E-08
HG001_00679	-	hypothetical protein	SAOUHSC_00755	-	-1,093	2,12E-07
HG001_01165	-	hypothetical protein	SAOUHSC_01293	-	-1,093	0,046553567
HG001_01627	gloB_1	Hydroxyacylglutathione hydrolase	SAOUHSC_01815	-	-1,089	9,83E-07
HG001_02688	secA_2	Protein translocase subunit SecA	SAOUHSC_02985	azi	-1,086	5,76E-07
HG001_01750	-	hypothetical protein	SAOUHSC_01952	-	-1,086	2,88E-06
HG001_01453	efp	Elongation factor P	SAOUHSC_01625	-	-1,084	3,07E-08
HG001_01253	asd	Aspartate-semialdehyde dehydrogenase	SAOUHSC_01395	-	-1,082	5,10E-07
HG001_00035	fccB	Sulfide dehydrogenase [flavocytochrome c] flavoprotein chain precursor	SAOUHSC_00037	-	-1,082	1,33E-05
HG001_00163	-	Xylose isomerase-like TIM barrel	SAOUHSC_00181	-	-1,082	3,25E-05
HG001_00502	gph_1	Phosphoglycolate phosphatase	SAOUHSC_00555	-	-1,082	0,000428418
HG001_00806	glpQ1_1	putative glycerophosphoryl diester phosphodiesterase 1	SAOUHSC_00897	-	-1,079	7,50E-06
HG001_00994	trxA_2	Thioredoxin	SAOUHSC_01100	-	-1,078	9,11E-07
HG001_01249	cvfB	Conserved virulence factor B	SAOUHSC_01391	-	-1,076	1,07E-06
HG001_01426	-	hypothetical protein	SAOUHSC_01595	-	-1,074	0,013872178

HG001_02574	lipR_2	Putative acetyl-hydrolase LipR precursor	SAOUHSC_02844	-	-1,07	9,83E-07
HG001_01258	alr2	Alanine racemase 2	SAOUHSC_01400	-	-1,069	1,81E-05
HG001_01824	-	tRNA-Ile(gat)	SAOUHSC_T00028	-	-1,066	0,002328113
HG001_01456	-	hypothetical protein	SAOUHSC_01628	-	-1,064	0,001185038
HG001_00758	metQ_2	Methionine-binding lipoprotein MetQ precursor	SAOUHSC_00844	-	-1,062	0,000103352
HG001_00495	tagE_2	putative poly(glycerol-phosphate) alpha-glucosyltransferase	SAOUHSC_00548	-	-1,06	2,16E-07
HG001_02647	hmoB	Heme-degrading monooxygenase HmoB	SAOUHSC_02930	-	-1,058	2,79E-07
HG001_02343	-	hypothetical protein	SAOUHSC_02581	-	-1,058	6,24E-05
HG001_02226	-	Zinc-type alcohol dehydrogenase-like protein	SAOUHSC_02445	-	-1,055	1,20E-07
HG001_00114	wbpA	UDP-N-acetyl-D-glucosamine 6-dehydrogenase	SAOUHSC_00128	-	-1,052	8,31E-07
HG001_00321	-	hypothetical protein	SAOUHSC_00362	-	-1,048	1,42E-06
HG001_00694	yfbR	5'-deoxynucleotidase YfbR	SAOUHSC_00774	-	-1,047	9,13E-06
HG001_01811	-	tRNA-Met(cat)	SAOUHSC_T00041	-	-1,044	0,002973751
HG001_02419	-	hypothetical protein	SAOUHSC_02666	-	-1,042	2,49E-05
HG001_00401	dnaX_2	DNA polymerase III subunit tau	SAOUHSC_00454	-	-1,041	8,09E-06
HG001_01977	-	Bacterial SH3 domain protein	SAOUHSC_02170	-	-1,04	0,000180039
HG001_00958	-	hypothetical protein	SAOUHSC_01055a	-	-1,038	1,44E-05
HG001_00182	-	hypothetical protein	SAOUHSC_00203	-	-1,038	4,52E-05
HG001_02686	gtf2	Glycosyltransferase-stabilizing protein Gtf2	SAOUHSC_02983	-	-1,036	5,89E-05
HG001_00340	qorB	Quinone oxidoreductase 2	SAOUHSC_00382	-	-1,035	9,37E-06
HG001_02097	mazE	Antitoxin MazE	SAOUHSC_02304	-	-1,031	4,06E-06
HG001_02604	crtP	Diapolycopene oxygenase	SAOUHSC_02881	-	-1,031	1,94E-05
HG001_00727	-	hypothetical protein	SAOUHSC_00811	-	-1,031	0,000125921
HG001_02530	-	hypothetical protein	SAOUHSC_02794	-	-1,028	0,00222342
HG001_01814	-	tRNA-Arg(acg)	SAOUHSC_T0007	-	-1,027	0,007388761
HG001_00626	yciC_2	Putative metal chaperone YciC	SAOUHSC_00695	-	-1,026	3,19E-05
HG001_00357	-	putative lipoprotein precursor	SAOUHSC_00404	-	-1,025	0,000831451
HG001_00436	-	tRNA-Val(tac)	SAOUHSC_T00059	-	-1,025	0,002443889
HG001_01578	comC	Type 4 prepilin-like proteins leader peptide-processing enzyme	SAOUHSC_01764	-	-1,025	0,03007429
HG001_02236	lacR	Lactose phosphotransferase system repressor	SAOUHSC_02456	-	-1,023	4,93E-06
HG001_01820	-	tRNA-Val(tac)	SAOUHSC_T00060	-	-1,023	0,002914399
HG001_00621	-	hypothetical protein	SAOUHSC_00690	-	-1,022	2,56E-06
HG001_01366	-	Phage major tail protein	SAOUHSC_01529	-	-1,022	5,07E-05
HG001_01749	nisC	Nisin biosynthesis protein NisC	SAOUHSC_01951	-	-1,018	0,000168582
HG001_00443	-	tRNA-Ala(tgc)	SAOUHSC_T0001	-	-1,018	0,001977909
HG001_01647	htrA	Serine protease Do-like HtrA	SAOUHSC_01838	-	-1,016	5,59E-06
HG001_00520	galK_1	Galactokinase	SAOUHSC_00577	-	-1,016	1,07E-05
HG001_01017	-	hypothetical protein	SAOUHSC_01130	-	-1,015	1,25E-06
HG001_00210	rebM	Demethylrebeccamycin-D-glucose O-methyltransferase	SAOUHSC_00237	-	-1,015	0,002756727
HG001_00437	-	tRNA-Thr(tgt)	SAOUHSC_T00053	-	-1,014	0,005170704
HG001_00507	-	hypothetical protein	SAOUHSC_00560	-	-1,014	0,008070658
HG001_00824	ywlC_1	Threonylcarbamoyl-AMP synthase	SAOUHSC_00915	-	-1,01	0,011835025
HG001_01294	ebh_1	Extracellular matrix-binding protein ebh precursor	SAOUHSC_01447	-	-1,009	1,21E-06
HG001_01359	-	hypothetical protein	SAOUHSC_01522	-	-1,008	0,007891537
HG001_01699	-	hypothetical protein	SAOUHSC_01896	-	-1,007	7,34E-05
HG001_02088	-	tRNA-Gly(tcc)	SAOUHSC_T00025	-	-1,005	0,002847856
HG001_00253	hrtA_1	Putative hemin import ATP-binding protein HrtA	SAOUHSC_00287	-	-1,004	1,03E-05
HG001_01738	splE	Serine protease SplE precursor	SAOUHSC_01936	-	-1,003	0,010082431
HG001_01251	-	Lysine	-	-	-1	2,32E-05

Annexe 2 : Tableau de l'expression différentielle des protéines durant le stress oxydant :

Liste de tous les gènes activés ou inhibés durant le stress oxydant.

UP regulated genes from the differencial proteomics analysis in oxidative stress			
accession	description	LogFC (MV/WT)	adjp
HG001_01897	HG001_01897|gene_NONE|hypothetical protein	9,14	1,96E-43
HG001_01902	HG001_01902|gene_NONE|Phage antirepressor protein KilAC domain protein	9,03	5,76E-54
HG001_00066	HG001_00066|gene_ala|Alanine dehydrogenase	8,63	5,62E-28
HG001_01894	HG001_01894|gene_NONE|hypothetical protein	7,72	8,10E-24
HG001_00070	HG001_00070|gene_iucC_2|Aerobactin synthase	7,41	3,27E-19
HG001_01895	HG001_01895|gene_NONE|Bacteriophage Mu Gam like protein	7,35	2,61E-18
HG001_01899	HG001_01899|gene_NONE|hypothetical protein	7,22	7,52E-17
HG001_00299	HG001_00299|gene_metE|5-methyltetrahydropteroyltriglutamate--homocysteine methyltransferase	7,16	7,63E-12
HG001_00071	HG001_00071|gene_garL|5-keto-4-deoxy-D-glucarate aldolase	6,79	1,54E-12
HG001_01880	HG001_01880|gene_NONE|hypothetical protein	6,23	1,47E-08
HG001_00072	HG001_00072|gene_btrK|L-glutamyl-[BtrI acyl-carrier protein] decarboxylase	6,11	7,21E-08
HG001_01879	HG001_01879|gene_dut_2|Deoxyuridine 5'-triphosphate nucleotidohydrolase	5,91	6,65E-07
HG001_01893	HG001_01893|gene_NONE|hypothetical protein	5,81	2,24E-29
HG001_01867	HG001_01867|gene_NONE|hypothetical protein	5,68	6,87E-06
HG001_00069	HG001_00069|gene_iucA_1|N(2)-citryl-N(6)-acetyl-N(6)-hydroxylysine synthase	5,59	1,37E-05
HG001_01873	HG001_01873|gene_NONE|hypothetical protein	5,50	2,76E-05
HG001_00073	HG001_00073|gene_NONE|ParB-like nuclease domain protein	5,50	2,76E-05
HG001_01900	HG001_01900|gene_NONE|hypothetical protein	5,30	1,17E-04
HG001_00067	HG001_00067|gene_iucC_1|Aerobactin synthase	5,19	2,32E-04
HG001_00218	HG001_00218|gene_NONE|Penicillin acylase precursor	5,07	4,70E-04
HG001_01891	HG001_01891|gene_NONE|hypothetical protein	4,93	9,83E-04
HG001_01232	HG001_01232|gene_trpB|Tryptophan synthase beta chain	4,79	2,09E-03
HG001_01883	HG001_01883|gene_NONE|PVL ORF-50-like family protein	4,44	8,53E-03
HG001_01866	HG001_01866|gene_NONE|Phage capsid family protein	4,23	1,64E-02
HG001_00064	HG001_00064|gene_yfiY|putative siderophore-binding lipoprotein YfiY precursor	3,99	8,34E-81
HG001_01859	HG001_01859|gene_NONE|Phage protein	3,98	3,18E-02
HG001_01886	HG001_01886|gene_NONE|hypothetical protein	3,98	3,18E-02
HG001_01884	HG001_01884|gene_NONE|Helix-turn-helix domain protein	3,68	6,59E-02
HG001_02384	HG001_02384|gene_lcdH|L-carnitine dehydrogenase	3,68	6,59E-02
HG001_00977	HG001_00977|gene_isdB|Iron-regulated surface determinant protein B precursor	3,68	6,59E-02
HG001_02135	HG001_02135|gene_atpE|ATP synthase subunit c	3,30	1,23E-01
HG001_02215	HG001_02215|gene_NONE|Alanine racemase	3,30	1,23E-01
HG001_00300	HG001_00300|gene_yitJ|Bifunctional homocysteine S-methyltransferase/5,10-methylenetetrahydrofolate reductase	3,30	1,23E-01
HG001_00269	HG001_00269|gene_ymdB|O-acetyl-ADP-ribose deacetylase	3,30	1,23E-01
HG001_01860	HG001_01860|gene_NONE|Phage major tail protein 2	3,30	1,23E-01
HG001_01877	HG001_01877|gene_NONE|hypothetical protein	3,30	1,23E-01
HG001_02727	HG001_02727|gene_glpE_3|Thiosulfate sulfurtransferase GlpE	3,20	2,44E-09
HG001_00979	HG001_00979|gene_isdC|Iron-regulated surface determinant protein C precursor	2,79	2,32E-01
HG001_02367	HG001_02367|gene_hutI|Imidazolonepropionase	2,79	2,32E-01
HG001_02216	HG001_02216|gene_iucA_2|N(2)-citryl-N(6)-acetyl-N(6)-hydroxylysine synthase	2,79	2,32E-01
HG001_01865	HG001_01865|gene_NONE|hypothetical protein	2,79	2,32E-01
HG001_00365	HG001_00365|gene_NONE|hypothetical protein	2,79	2,32E-01
HG001_00302	HG001_00302|gene_metI|Cystathionine gamma-synthase/O-acetylhomoserine (thiol)-lyase	2,79	2,32E-01
HG001_00065	HG001_00065|gene_sbnA|putative siderophore biosynthesis protein SbnA	2,79	2,32E-01
HG001_01769	HG001_01769|gene_NONE|Bacterial ABC transporter protein EcsB	2,79	2,32E-01
HG001_01887	HG001_01887|gene_NONE|hypothetical protein	2,79	2,32E-01
HG001_01890	HG001_01890|gene_NONE|hypothetical protein	2,79	2,32E-01
HG001_01049	HG001_01049|gene_pyrR|Bifunctional protein PyrR	2,76	4,52E-09
HG001_02166	HG001_02166|gene_dps|General stress protein 20U	2,71	1,02E-27
HG001_02214	HG001_02214|gene_yfmC_2|Fe(3+)-citrate-binding protein YfmC precursor	2,62	4,81E-52
HG001_01910	HG001_01910|gene_xerC_2|Tyrosine recombinase XerC	2,45	1,19E-01
HG001_02629	HG001_02629|gene_pyrD|Dihydroorotate dehydrogenase (quinone)	2,33	6,96E-12
HG001_00586	HG001_00586|gene_yusV_1|putative siderophore transport system ATP-binding protein YusV	2,24	6,82E-02
HG001_02658	HG001_02658|gene_cysJ|Sulfite reductase [NADPH] flavoprotein alpha-component	2,03	1,30E-11
HG001_00116	HG001_00116|gene_isdI|Heme oxygenase (staphylobilin-producing) 2	2,02	5,34E-05
HG001_01901	HG001_01901|gene_NONE|hypothetical protein	1,98	4,11E-01
HG001_01227	HG001_01227|gene_trpE|Anthranilate synthase component 1	1,98	4,11E-01
HG001_01579	HG001_01579|gene_fgs|Folylpolyglutamate synthase	1,98	4,11E-01
HG001_02668	HG001_02668|gene_NONE|S-formylglutathione hydrolase	1,98	4,11E-01
HG001_02600	HG001_02600|gene_dapL|LL-diaminopimelate aminotransferase	1,98	4,11E-01
HG001_01949	HG001_01949|gene_nos|Nitric oxide synthase oxygenase	1,98	4,11E-01
HG001_02029	HG001_02029|gene_NONE|hypothetical protein	1,98	4,11E-01
HG001_02034	HG001_02034|gene_NONE|AntA/AntB antirepressor	1,98	4,11E-01
HG001_02352	HG001_02352|gene_yifK|putative transport protein YifK	1,98	4,11E-01
HG001_02409	HG001_02409|gene_NONE|Acetyltransferase (GNAT) family protein	1,98	4,11E-01

HG001_01870	HG001_01870|gene_NONE|Phage portal protein, SPP1 Gp6-like	1,98	4,11E-01
HG001_00984	HG001_00984|gene_isdG|Heme oxygenase (staphylobilin-producing) 1	1,98	4,11E-01
HG001_01015	HG001_01015|gene_argF|Ornithine carbamoyltransferase	1,98	4,11E-01
HG001_01200	HG001_01200|gene_NONE|hypothetical protein	1,98	4,11E-01
HG001_02420	HG001_02420|gene_gltT|Proton/sodium-glutamate symport protein	1,98	4,11E-01
HG001_01903	HG001_01903|gene_NONE|hypothetical protein	1,98	4,11E-01
HG001_02024	HG001_02024|gene_NONE|hypothetical protein	1,98	4,11E-01
HG001_02731	HG001_02731|gene_NONE|DinB superfamily protein	1,98	4,11E-01
HG001_00277	HG001_00277|gene_slyA_1|Transcriptional regulator SlyA	1,98	4,11E-01
HG001_01177	HG001_01177|gene_NONE|hypothetical protein	1,98	4,11E-01
HG001_00525	HG001_00525|gene_NONE|Transcriptional regulator	1,98	4,11E-01
HG001_02639	HG001_02639|gene_aldC_2|Alpha-acetolactate decarboxylase	1,98	4,11E-01
HG001_02423	HG001_02423|gene_NONE|Acid shock protein	1,98	4,11E-01
HG001_00981	HG001_00981|gene_isdE|High-affinity heme uptake system protein IsdE precursor	1,98	4,11E-01
HG001_00324	HG001_00324|gene_ahpC|Alkyl hydroperoxide reductase subunit C	1,92	4,00E-77
HG001_00799	HG001_00799|gene_mnhA1|Na(+)/H(+) antiporter subunit A1	1,90	2,99E-01
HG001_02609	HG001_02609|gene_isaA|putative transglycosylase IsaA precursor	1,88	5,26E-02
HG001_00323	HG001_00323|gene_ahpF|Alkyl hydroperoxide reductase subunit F	1,86	3,84E-51
HG001_02123	HG001_02123|gene_sceD|putative transglycosylase SceD precursor	1,79	4,36E-02
HG001_01025	HG001_01025|gene_NONE|putative N-acetyltransferase	1,74	1,46E-01
HG001_02597	HG001_02597|gene_copA|Copper-exporting P-type ATPase A	1,74	1,46E-01
HG001_00752	HG001_00752|gene_NONE|hypothetical protein	1,69	1,53E-02
HG001_00978	HG001_00978|gene_isdA|Iron-regulated surface determinant protein A precursor	1,66	1,01E-04
HG001_00375	HG001_00375|gene_metQ_1|putative D-methionine-binding lipoprotein MetQ precursor	1,65	1,23E-01
HG001_00927	HG001_00927|gene_ykoE|Putative HMP/thiamine permease protein YkoE	1,57	2,12E-01
HG001_02507	HG001_02507|gene_nikA|Nickel-binding periplasmic protein precursor	1,57	1,48E-02
HG001_01912	HG001_01912|gene_NONE|putative acyl-CoA thioester hydrolase	1,53	4,35E-01
HG001_02673	HG001_02673|gene_arcB|Ornithine carbamoyltransferase, catabolic	1,53	4,35E-01
HG001_00674	HG001_00674|gene_yclQ|putative ABC transporter solute-binding protein YclQ precursor	1,45	5,00E-15
HG001_00696	HG001_00696|gene_uvrB|UvrABC system protein B	1,44	2,47E-02
HG001_00298	HG001_00298|gene_kynB|Kynurenine formamidase	1,43	3,54E-01
HG001_01024	HG001_01024|gene_yfnB|Putative HAD-hydrolase YfnB	1,43	3,54E-01
HG001_00186	HG001_00186|gene_rihA|Pyrimidine-specific ribonucleoside hydrolase RihA	1,39	2,99E-01
HG001_00712	HG001_00712|gene_cggR|Central glycolytic genes regulator	1,39	2,99E-01
HG001_00747	HG001_00747|gene_fbiB|Coenzyme F420:L-glutamate ligase	1,37	2,46E-01
HG001_01137	HG001_01137|gene_recA|Protein RecA	1,36	5,99E-05
HG001_02247	HG001_02247|gene_alsS|Acetolactate synthase	1,32	3,80E-06
HG001_00490	HG001_00490|gene_ywpJ_1|Putative phosphatase YwpJ	1,28	8,12E-05
HG001_02276	HG001_02276|gene_rplX|50S ribosomal protein L24	1,27	1,38E-04
HG001_02246	HG001_02246|gene_aldC_1|Alpha-acetolactate decarboxylase	1,26	6,63E-10
HG001_01052	HG001_01052|gene_pyrC|Dihydroorotase	1,22	8,22E-09
HG001_02320	HG001_02320|gene_fhuD_2|Iron(3+)-hydroxamate-binding protein FhuD precursor	1,18	2,08E-09
HG001_01119	HG001_01119|gene_rplGA|putative ribosomal protein YlxQ	1,18	4,09E-01
HG001_00328	HG001_00328|gene_NONE|hypothetical protein	1,13	4,56E-01
HG001_00476	HG001_00476|gene_rpsL|30S ribosomal protein S12	1,10	2,66E-03
HG001_00491	HG001_00491|gene_azo1|FMN-dependent NADPH-azoreductase	1,05	6,55E-04
HG001_00761	HG001_00761|gene_yurY|Vegetative protein 296	1,04	6,61E-06
HG001_01499	HG001_01499|gene_rpsU|30S ribosomal protein S21	1,03	1,27E-03
HG001_02752	HG001_02752|gene_mnmE|tRNA modification GTPase MnmE	1,02	2,12E-01
HG001_02228	HG001_02228|gene_NONE|hypothetical protein	1,01	6,28E-01
HG001_02190	HG001_02190|gene_disA|DNA integrity scanning protein DisA	1,01	6,28E-01
HG001_00411	HG001_00411|gene_NONE|hypothetical protein	1,01	6,28E-01
HG001_02649	HG001_02649|gene_betA|Oxygen-dependent choline dehydrogenase	1,01	6,28E-01
HG001_00379	HG001_00379|gene_bltD_1|Spermine/spermidine acetyltransferase	1,01	6,28E-01
HG001_02259	HG001_02259|gene_ecfA1|Energy-coupling factor transporter ATP-binding protein EcfA1	1,01	6,28E-01

DOWN regulated genes from the differencial proteomics analysis in oxidative stress			
accession	description	LogFC (MV/WT)	adjp
HG001_00725	HG001_00725|gene_NONE|hypothetical protein	-7,12	1,82E-14
HG001_02120	HG001_02120|gene_thiD|Hydroxymethylpyrimidine/phosphomethylpyrimidine kinase	-5,83	5,64E-06
HG001_00734	HG001_00734|gene_cspA_1|Cold shock protein CspA	-5,71	4,91E-04
HG001_00291	HG001_00291|gene_NONE|hypothetical protein	-5,56	4,83E-05
HG001_02681	HG001_02681|gene_yvyI|Putative mannose-6-phosphate isomerase YvyI	-5,40	1,34E-04
HG001_01211	HG001_01211|gene_NONE|Iron-sulphur cluster biosynthesis	-5,22	3,90E-04
HG001_00803	HG001_00803|gene_NONE|NADH oxidase	-5,13	6,61E-04
HG001_01144	HG001_01144|gene_miaB|(Dimethylallyl)adenosine tRNA methylthiotransferase MiaB	-5,02	1,32E-03
HG001_02534	HG001_02534|gene_sasG|Surface protein G precursor	-4,91	2,09E-03
HG001_02529	HG001_02529|gene_pgcA|Phosphoglucomutase	-4,79	3,37E-03
HG001_01115	HG001_01115|gene_polC_1|DNA polymerase III PolC-type	-4,79	3,37E-03
HG001_00422	HG001_00422|gene_mazG|Nucleoside triphosphate pyrophosphohydrolase/pyrophosphatase MazG	-4,79	3,37E-03
HG001_00774	HG001_00774|gene_NONE|hypothetical protein	-4,79	3,37E-03
HG001_01953	HG001_01953|gene_rutB|Peroxyureidoacrylate/ureidoacrylate amidohydrolase RutB	-4,66	5,75E-03
HG001_02343	HG001_02343|gene_NONE|hypothetical protein	-4,56	4,13E-08
HG001_00480	HG001_00480|gene_yxeP_2|putative hydrolase YxeP	-4,51	9,85E-03
HG001_00923	HG001_00923|gene_purH|Bifunctional purine biosynthesis protein PurH	-4,51	9,85E-03
HG001_00163	HG001_00163|gene_NONE|Xylose isomerase-like TIM barrel	-4,51	9,85E-03
HG001_00223	HG001_00223|gene_NONE|hypothetical protein	-4,51	9,85E-03
HG001_01432	HG001_01432|gene_malL|Oligo-1,6-glucosidase	-4,35	1,64E-02
HG001_00170	HG001_00170|gene_pflA|Pyruvate formate-lyase-activating enzyme	-4,35	1,64E-02
HG001_01129	HG001_01129|gene_phnF|putative transcriptional regulator PhnF	-4,35	1,64E-02
HG001_00317	HG001_00317|gene_NONE|hypothetical protein	-4,17	2,68E-02
HG001_02432	HG001_02432|gene_narW|putative nitrate reductase molybdenum cofactor assembly chaperone NarW	-4,17	2,68E-02
HG001_01917	HG001_01917|gene_NONE|hypothetical protein	-4,17	2,68E-02
HG001_02540	HG001_02540|gene_gntT|High-affinity gluconate transporter	-4,17	2,68E-02
HG001_00161	HG001_00161|gene_ycjS_1|putative oxidoreductase YcjS	-3,96	4,63E-02
HG001_02150	HG001_02150|gene_yodB|HTH-type transcriptional regulator YodB	-3,96	4,63E-02
HG001_00694	HG001_00694|gene_yfbR|5'-deoxynucleotidase YfbR	-3,96	4,63E-02
HG001_01034	HG001_01034|gene_divIB|Cell division protein DivIB	-3,96	4,63E-02
HG001_01645	HG001_01645|gene_ptsG_4|PTS system glucose-specific EIICBA component	-3,96	4,63E-02
HG001_02344	HG001_02344|gene_NONE|Putative formate dehydrogenase	-3,93	1,23E-21
HG001_01549	HG001_01549|gene_NONE|CsbD-like protein	-3,84	1,17E-04
HG001_00768	HG001_00768|gene_NONE|Nitronate monooxygenase	-3,72	7,39E-02
HG001_00999	HG001_00999|gene_murI|Glutamate racemase	-3,72	7,39E-02
HG001_00598	HG001_00598|gene_graR_1|Response regulator protein GraR	-3,72	7,39E-02
HG001_01028	HG001_01028|gene_mraZ|Protein MraZ	-3,72	7,39E-02
HG001_00180	HG001_00180|gene_gsiB|Glutathione-binding protein GsiB precursor	-3,72	7,39E-02
HG001_00142	HG001_00142|gene_NONE|PTS system EIIBC component	-3,72	7,39E-02
HG001_02625	HG001_02625|gene_NONE|hypothetical protein	-3,72	7,39E-02
HG001_01255	HG001_01255|gene_dapB|4-hydroxy-tetrahydrodipicolinate reductase	-3,72	7,39E-02
HG001_01150	HG001_01150|gene_glpF|Glycerol uptake facilitator protein	-3,72	7,39E-02
HG001_02424	HG001_02424|gene_narT|putative nitrate transporter NarT	-3,72	7,39E-02
HG001_01724	HG001_01724|gene_NONE|Telomeric repeat-binding factor 2	-3,71	7,39E-02
HG001_02099	HG001_02099|gene_acpS|Holo-[acyl-carrier-protein] synthase	-3,71	7,39E-02
HG001_01612	HG001_01612|gene_phoP|Alkaline phosphatase synthesis transcriptional regulatory protein PhoP	-3,42	1,23E-01
HG001_00916	HG001_00916|gene_purC|Phosphoribosylaminoimidazole-succinocarboxamide synthase	-3,42	1,23E-01
HG001_00826	HG001_00826|gene_NONE|putative kinase inhibitor	-3,42	1,23E-01
HG001_01319	HG001_01319|gene_pimB|GDP-mannose-dependent alpha-(1-6)-phosphatidylinositol monomannoside mannosy	-3,42	1,23E-01
HG001_00724	HG001_00724|gene_NONE|hypothetical protein	-3,42	1,23E-01
HG001_01351	HG001_01351|gene_NONE|hypothetical protein	-3,42	1,23E-01
HG001_00449	HG001_00449|gene_pdxT|Glutamine amidotransferase subunit PdxT	-3,42	1,23E-01
HG001_00793	HG001_00793|gene_mnhG1|Na(+)/H(+) antiporter subunit G1	-3,42	1,23E-01
HG001_00206	HG001_00206|gene_lrgB|Antiholin-like protein LrgB	-3,42	1,23E-01
HG001_00392	HG001_00392|gene_NONE|Acetyltransferase (GNAT) family protein	-3,42	1,23E-01
HG001_01537	HG001_01537|gene_NONE|Putative O-methyltransferase/MSMEI_4947	-3,42	1,23E-01
HG001_02483	HG001_02483|gene_NONE|UDP-glucose 4-epimerase	-3,42	1,23E-01
HG001_01079	HG001_01079|gene_fapR|Transcription factor FapR	-3,42	1,23E-01
HG001_01666	HG001_01666|gene_pepA_2|Glutamyl aminopeptidase	-3,42	2,68E-05
HG001_02592	HG001_02592|gene_ydfJ|Membrane protein YdfJ	-3,25	6,71E-08
HG001_00395	HG001_00395|gene_recR|Recombination protein RecR	-3,05	2,00E-01
HG001_01694	HG001_01694|gene_NONE|hypothetical protein	-3,05	2,00E-01
HG001_00274	HG001_00274|gene_NONE|PTS system ascorbate-specific transporter subunits IICB	-3,05	2,00E-01
HG001_01919	HG001_01919|gene_vraS|Sensor protein VraS	-3,05	2,00E-01

HG001_01216	HG001_01216|gene_glcT|GlcA/glcB genes antiterminator	-3,05	2,00E-01
HG001_00494	HG001_00494|gene_tagE_1|putative poly(glycerol-phosphate) alpha-glucosyltransferase	-3,05	2,00E-01
HG001_02500	HG001_02500|gene_gltB_2|Glutamate synthase [NADPH] large chain precursor	-3,05	2,00E-01
HG001_00262	HG001_00262|gene_nanE|Putative N-acetylmannosamine-6-phosphate 2-epimerase	-3,05	2,00E-01
HG001_01908	HG001_01908|gene_NONE|hypothetical protein	-3,05	2,00E-01
HG001_01164	HG001_01164|gene_NONE|hypothetical protein	-3,05	2,00E-01
HG001_02308	HG001_02308|gene_mobB|Molybdopterin-guanine dinucleotide biosynthesis adapter protein	-3,05	2,00E-01
HG001_01066	HG001_01066|gene_def1|Peptide deformylase 1	-3,05	2,00E-01
HG001_01299	HG001_01299|gene_ypcP|5'-3' exonuclease	-3,05	2,00E-01
HG001_01501	HG001_01501|gene_mtaB_2|Threonylcarbamoyladenosine tRNA methylthiotransferase MtaB	-3,05	2,00E-01
HG001_00784	HG001_00784|gene_NONE|hypothetical protein	-3,05	2,00E-01
HG001_00162	HG001_00162|gene_ycjS_2|putative oxidoreductase YcjS	-3,05	2,00E-01
HG001_00921	HG001_00921|gene_purM|Phosphoribosylformylglycinamidine cyclo-ligase	-3,05	2,00E-01
HG001_02576	HG001_02576|gene_NONE|hypothetical protein	-3,05	2,00E-01
HG001_02442	HG001_02442|gene_NONE|hypothetical protein	-3,05	2,00E-01
HG001_00885	HG001_00885|gene_NONE|hypothetical protein	-3,05	2,00E-01
HG001_02634	HG001_02634|gene_cocE|Cocaine esterase	-3,05	2,00E-01
HG001_00736	HG001_00736|gene_NONE|hypothetical protein	-3,05	2,00E-01
HG001_01470	HG001_01470|gene_NONE|putative metallo-hydrolase	-3,05	2,00E-01
HG001_01087	HG001_01087|gene_NONE|putative DNA-binding protein	-3,05	2,00E-01
HG001_00627	HG001_00627|gene_ydhF|Oxidoreductase YdhF	-3,05	2,00E-01
HG001_01674	HG001_01674|gene_rsuA|Ribosomal small subunit pseudouridine synthase A	-3,05	2,00E-01
HG001_02126	HG001_02126|gene_fabZ|3-hydroxyacyl-[acyl-carrier-protein] dehydratase FabZ	-3,05	2,00E-01
HG001_01697	HG001_01697|gene_arsC2|Arsenate-mycothiol transferase ArsC2	-3,05	2,00E-01
HG001_02680	HG001_02680|gene_manP|PTS system mannose-specific EIIBCA component	-3,04	6,72E-04
HG001_00940	HG001_00940|gene_NONE|hypothetical protein	-2,93	2,20E-02
HG001_00541	HG001_00541|gene_mshD_1|Mycothiol acetyltransferase	-2,93	2,20E-02
HG001_00331	HG001_00331|gene_xpt|Xanthine phosphoribosyltransferase	-2,84	8,52E-08
HG001_00410	HG001_00410|gene_rsmA|Ribosomal RNA small subunit methyltransferase A	-2,81	3,33E-02
HG001_00118	HG001_00118|gene_aldA|Putative aldehyde dehydrogenase AldA	-2,81	3,33E-02
HG001_01513	HG001_01513|gene_tadA_2|tRNA-specific adenosine deaminase	-2,77	4,33E-03
HG001_01905	HG001_01905|gene_immR_1|HTH-type transcriptional regulator ImmR	-2,69	6,50E-03
HG001_00420	HG001_00420|gene_mfd|Transcription-repair-coupling factor	-2,67	5,36E-02
HG001_01661	HG001_01661|gene_murC|UDP-N-acetylmuramate--L-alanine ligase	-2,61	1,00E-02
HG001_00145	HG001_00145|gene_hsdR|Type-1 restriction enzyme R protein	-2,57	2,96E-04
HG001_02434	HG001_02434|gene_narG|Respiratory nitrate reductase 1 alpha chain	-2,56	1,47E-13
HG001_02038	HG001_02038|gene_lexA_3|LexA repressor	-2,55	2,99E-01
HG001_00032	HG001_00032|gene_csoR_1|Copper-sensing transcriptional repressor CsoR	-2,55	2,99E-01
HG001_01551	HG001_01551|gene_rarA|Replication-associated recombination protein A	-2,55	2,99E-01
HG001_02090	HG001_02090|gene_NONE|Protein SprT-like protein	-2,55	2,99E-01
HG001_02542	HG001_02542|gene_ydfH|putative HTH-type transcriptional regulator YdfH	-2,55	2,99E-01
HG001_01298	HG001_01298|gene_ald1|Alanine dehydrogenase 1	-2,55	2,99E-01
HG001_02487	HG001_02487|gene_opuCC|Carnitine transport binding protein OpuCC precursor	-2,55	2,99E-01
HG001_01961	HG001_01961|gene_NONE|hypothetical protein	-2,55	2,99E-01
HG001_01132	HG001_01132|gene_phbB|Acetoacetyl-CoA reductase	-2,55	2,99E-01
HG001_00406	HG001_00406|gene_rsmI|Ribosomal RNA small subunit methyltransferase I	-2,55	2,99E-01
HG001_00228	HG001_00228|gene_NONE|hypothetical protein	-2,55	2,99E-01
HG001_00029	HG001_00029|gene_NONE|hypothetical protein	-2,55	2,99E-01
HG001_01136	HG001_01136|gene_cinA|Putative competence-damage inducible protein	-2,55	2,99E-01
HG001_01145	HG001_01145|gene_NONE|hypothetical protein	-2,55	2,99E-01
HG001_00914	HG001_00914|gene_purE|N5-carboxyaminoimidazole ribonucleotide mutase	-2,55	2,99E-01
HG001_02178	HG001_02178|gene_NONE|SAP domain protein	-2,55	2,99E-01
HG001_00609	HG001_00609|gene_NONE|hypothetical protein	-2,55	2,99E-01
HG001_02686	HG001_02686|gene_gtf2|Glycosyltransferase-stabilizing protein Gtf2	-2,55	2,99E-01
HG001_01931	HG001_01931|gene_NONE|putative RNA methyltransferase	-2,55	2,99E-01
HG001_00568	HG001_00568|gene_nhaK_1|Sodium, potassium, lithium and rubidium/H(+) antiporter	-2,55	2,99E-01
HG001_01163	HG001_01163|gene_NONE|hypothetical protein	-2,55	2,99E-01
HG001_01676	HG001_01676|gene_NONE|Ferredoxin--NADP reductase	-2,55	2,99E-01
HG001_00904	HG001_00904|gene_yjcF|putative N-acetyltransferase YjcF	-2,55	2,99E-01
HG001_02141	HG001_02141|gene_NONE|hypothetical protein	-2,55	2,99E-01
HG001_01833	HG001_01833|gene_yfhQ|putative A/G-specific adenine glycosylase YfhQ	-2,55	2,99E-01
HG001_00767	HG001_00767|gene_tlyC|Hemolysin C	-2,55	2,99E-01
HG001_00919	HG001_00919|gene_purL|Phosphoribosylformylglycinamidine synthase 2	-2,55	2,99E-01
HG001_02545	HG001_02545|gene_NONE|hypothetical protein	-2,55	2,99E-01
HG001_00175	HG001_00175|gene_fadN|putative 3-hydroxyacyl-CoA dehydrogenase	-2,55	2,99E-01
HG001_00616	HG001_00616|gene_NONE|hypothetical protein	-2,55	2,99E-01

HG001_00746	HG001_00746|gene_aroD|3-dehydroquinate dehydratase	-2,55	2,99E-01
HG001_01669	HG001_01669|gene_trmB|tRNA (guanine-N(7)-)-methyltransferase	-2,55	2,99E-01
HG001_01543	HG001_01543|gene_recD2|ATP-dependent RecD-like DNA helicase	-2,55	2,99E-01
HG001_00540	HG001_00540|gene_ywqN_2|Putative NAD(P)H-dependent FMN-containing oxidoreductase YwqN	-2,55	2,99E-01
HG001_00185	HG001_00185|gene_ptsG_2|PTS system glucose-specific EIICBA component	-2,55	2,99E-01
HG001_00926	HG001_00926|gene_ykoD_1|Putative HMP/thiamine import ATP-binding protein YkoD	-2,55	2,99E-01
HG001_00633		-2,55	2,99E-01
HG001_00378	HG001_00378|gene_nudC|NADH pyrophosphatase	-2,55	2,99E-01
HG001_01664	HG001_01664|gene_NONE|hypothetical protein	-2,55	2,99E-01
HG001_00305	HG001_00305|gene_ykuT|putative MscS family protein YkuT	-2,55	2,99E-01
HG001_02429	HG001_02429|gene_nreB|Oxygen sensor histidine kinase NreB	-2,55	2,99E-01
HG001_01682	HG001_01682|gene_bioB_1|Biotin synthase	-2,55	2,99E-01
HG001_00811	HG001_00811|gene_spsB_1|Signal peptidase IB	-2,55	2,99E-01
HG001_00377	HG001_00377|gene_NONE|hypothetical protein	-2,55	2,99E-01
HG001_01217	HG001_01217|gene_tqsA|AI-2 transport protein TqsA	-2,55	2,99E-01
HG001_01842	HG001_01842|gene_NONE|putative phage protein 3 of sapT operon	-2,55	2,99E-01
HG001_02480	HG001_02480|gene_nhaK_2|Sodium, potassium, lithium and rubidium/H(+) antiporter	-2,55	2,99E-01
HG001_01040	HG001_01040|gene_NONE|YGGT family protein	-2,55	2,99E-01
HG001_02035	HG001_02035|gene_NONE|hypothetical protein	-2,55	2,99E-01
HG001_00120	HG001_00120|gene_NONE|hypothetical protein	-2,55	2,99E-01
HG001_01667	HG001_01667|gene_NONE|Peptidase propeptide and YPEB domain protein	-2,55	2,99E-01
HG001_00125	HG001_00125|gene_NONE|hypothetical protein	-2,55	2,99E-01
HG001_00660	HG001_00660|gene_opuBA|Choline transport ATP-binding protein OpuBA	-2,43	2,30E-02
HG001_01478	HG001_01478|gene_zur|Zinc-specific metallo-regulatory protein	-2,19	1,80E-01
HG001_01069	HG001_01069|gene_rlmN|putative dual-specificity RNA methyltransferase RlmN	-2,19	1,80E-01
HG001_02183	HG001_02183|gene_mtlA|PTS system mannitol-specific EIICB component	-2,18	1,80E-01
HG001_00387	HG001_00387|gene_treA|Trehalose-6-phosphate hydrolase	-2,18	1,80E-01
HG001_01449	HG001_01449|gene_NONE|hypothetical protein	-2,18	2,04E-02
HG001_00358	HG001_00358|gene_lpl2|putative lipoprotein precursor	-2,13	1,19E-04
HG001_00579	HG001_00579|gene_tagX|Putative glycosyltransferase TagX	-2,12	7,39E-02
HG001_01788	HG001_01788|gene_trmL|tRNA (cytidine(34)-2'-O)-methyltransferase	-2,12	7,39E-02
HG001_01495	HG001_01495|gene_ybeZ|PhoH-like protein	-2,12	7,39E-02
HG001_02433	HG001_02433|gene_narH|Respiratory nitrate reductase 1 beta chain	-2,06	2,56E-04
HG001_00018	HG001_00018|gene_dnaC_1|Replicative DNA helicase	-2,00	1,08E-01
HG001_00819	HG001_00819|gene_NONE|hypothetical protein	-1,98	2,47E-01
HG001_01827	HG001_01827|gene_ghrB_2|Glyoxylate/hydroxypyruvate reductase B	-1,98	2,47E-01
HG001_00412	HG001_00412|gene_ispE|4-diphosphocytidyl-2-C-methyl-D-erythritol kinase	-1,98	2,47E-01
HG001_00857	HG001_00857|gene_kefC|Glutathione-regulated potassium-efflux system protein KefC	-1,98	2,47E-01
HG001_01091	HG001_01091|gene_trmD|tRNA (guanine-N(1)-)-methyltransferase	-1,98	2,47E-01
HG001_00594	HG001_00594|gene_aes|Acetyl esterase	-1,98	2,47E-01
HG001_00402	HG001_00402|gene_NONE|hypothetical protein	-1,98	2,47E-01
HG001_00865	HG001_00865|gene_murE_1|UDP-N-acetylmuramoyl-L-alanyl-D-glutamate--L-lysine ligase	-1,94	1,65E-04
HG001_01775	HG001_01775|gene_yhaM|3'-5' exoribonuclease YhaM	-1,88	3,47E-02
HG001_01118	HG001_01118|gene_NONE|hypothetical protein	-1,87	1,50E-01
HG001_00576	HG001_00576|gene_tagH_1|Teichoic acids export ATP-binding protein TagH	-1,87	1,50E-01
HG001_01783	HG001_01783|gene_rluD_3|Ribosomal large subunit pseudouridine synthase D	-1,85	1,95E-02
HG001_02693	HG001_02693|gene_sraP|Serine-rich adhesin for platelets precursor	-1,83	8,66E-02
HG001_02588	HG001_02588|gene_clpL|ATP-dependent Clp protease ATP-binding subunit ClpL	-1,81	8,88E-14
HG001_00849	HG001_00849|gene_NONE|hypothetical protein	-1,78	4,42E-01
HG001_01643	HG001_01643|gene_serA|D-3-phosphoglycerate dehydrogenase	-1,78	4,42E-01
HG001_00084	HG001_00084|gene_treR_1|Trehalose operon transcriptional repressor	-1,78	4,42E-01
HG001_02238	HG001_02238|gene_NONE|hypothetical protein	-1,78	4,42E-01
HG001_01967	HG001_01967|gene_ytrB_2|ABC transporter ATP-binding protein YtrB	-1,78	4,42E-01
HG001_01030	HG001_01030|gene_ftsL|Cell division protein FtsL	-1,78	4,42E-01
HG001_02185	HG001_02185|gene_mtlF|Mannitol-specific phosphotransferase enzyme IIA component	-1,78	4,42E-01
HG001_00709	HG001_00709|gene_NONE|Epimerase family protein	-1,78	4,42E-01
HG001_01308	HG001_01308|gene_NONE|hypothetical protein	-1,78	4,42E-01
HG001_01675	HG001_01675|gene_ytgP_2|putative cell division protein YtgP	-1,78	4,42E-01
HG001_02541	HG001_02541|gene_xylB|Xylulose kinase	-1,78	4,42E-01
HG001_00653	HG001_00653|gene_pabB|Aminodeoxychorismate synthase component 1	-1,78	4,42E-01
HG001_02304	HG001_02304|gene_moaA|Cyclic pyranopterin monophosphate synthase	-1,78	4,42E-01
HG001_01158	HG001_01158|gene_NONE|methionine gamma-lyase	-1,78	4,42E-01
HG001_01520	HG001_01520|gene_aroE|Shikimate dehydrogenase	-1,78	4,42E-01
HG001_01642	HG001_01642|gene_NONE|Soluble hydrogenase 42 kDa subunit	-1,78	4,42E-01
HG001_01159	HG001_01159|gene_glnR|HTH-type transcriptional regulator GlnR	-1,78	4,42E-01
HG001_02258	HG001_02258|gene_ecfA2|Energy-coupling factor transporter ATP-binding protein EcfA2	-1,78	4,42E-01

HG001_02521 HG001_02521|gene_NONE|putative lipoprotein precursor	-1,78	4,42E-01
HG001_01654 HG001_01654|gene_acsA_1|Acetyl-coenzyme A synthetase	-1,78	4,42E-01
HG001_00447 HG001_00447|gene_gabR|HTH-type transcriptional regulatory protein GabR	-1,78	4,42E-01
HG001_01944 HG001_01944|gene_NONE|Staphostatin A	-1,78	4,42E-01
HG001_01770 HG001_01770|gene_ecsA|ABC-type transporter ATP-binding protein EcsA	-1,78	4,42E-01
HG001_02377 HG001_02377|gene_NONE|ABC-2 family transporter protein	-1,78	4,42E-01
HG001_00744 HG001_00744|gene_NONE|hypothetical protein	-1,78	4,42E-01
HG001_02495 HG001_02495|gene_ybbL|putative ABC transporter ATP-binding protein YbbL	-1,78	4,42E-01
HG001_00844 HG001_00844|gene_mecA|Adapter protein MecA	-1,78	4,42E-01
HG001_01326 HG001_01326|gene_aroB|3-dehydroquinate synthase	-1,78	4,42E-01
HG001_00052 HG001_00052|gene_yxeP_1|putative hydrolase YxeP	-1,78	4,42E-01
HG001_02570 HG001_02570|gene_sdhB|L-serine dehydratase, beta chain	-1,78	4,42E-01
HG001_02359 HG001_02359|gene_malP|PTS system maltose-specific EIICB component	-1,78	4,42E-01
HG001_00092 HG001_00092|gene_phnD|Phosphate-import protein PhnD precursor	-1,78	4,42E-01
HG001_01410 HG001_01410|gene_NONE|hypothetical protein	-1,78	4,42E-01
HG001_00522 HG001_00522|gene_galK_2|Galactokinase	-1,78	4,42E-01
HG001_01176 HG001_01176|gene_ltaE|Low specificity L-threonine aldolase	-1,78	4,42E-01
HG001_01530 HG001_01530|gene_accB_2|Biotin carboxyl carrier protein of acetyl-CoA carboxylase	-1,78	4,42E-01
HG001_01945 HG001_01945|gene_NONE|hypothetical protein	-1,78	4,42E-01
HG001_02485 HG001_02485|gene_norB_5|Quinolone resistance protein NorB	-1,78	4,42E-01
HG001_01037 HG001_01037|gene_NONE|Laccase domain protein	-1,78	4,42E-01
HG001_00656 HG001_00656|gene_kipA_1|KipI antagonist	-1,78	4,42E-01
HG001_02422 HG001_02422|gene_sarZ|HTH-type transcriptional regulator SarZ	-1,78	4,42E-01
HG001_01011 HG001_01011|gene_NONE|hypothetical protein	-1,78	4,42E-01
HG001_00718 HG001_00718|gene_NONE|hypothetical protein	-1,78	4,42E-01
HG001_00554 HG001_00554|gene_NONE|hypothetical protein	-1,78	4,42E-01
HG001_01608 HG001_01608|gene_mutM|Formamidopyrimidine-DNA glycosylase	-1,78	4,42E-01
HG001_01095 HG001_01095|gene_rnhB|Ribonuclease HII	-1,78	4,42E-01
HG001_00972 HG001_00972|gene_rsmD|Ribosomal RNA small subunit methyltransferase D	-1,78	4,42E-01
HG001_02157 HG001_02157|gene_coaW|Type II pantothenate kinase	-1,78	4,42E-01
HG001_01084 HG001_01084|gene_rnc|Ribonuclease 3	-1,78	4,42E-01
HG001_00025 HG001_00025|gene_yycI|Two-component system YycFG regulatory protein	-1,78	4,42E-01
HG001_01365 HG001_01365|gene_NONE|Bacterial Ig-like domain (group 2)	-1,78	4,42E-01
HG001_01540 HG001_01540|gene_NONE|hypothetical protein	-1,78	4,42E-01
HG001_02628 HG001_02628|gene_NONE|Fructosamine kinase	-1,78	4,42E-01
HG001_01604 HG001_01604|gene_dnaB|Replication initiation and membrane attachment protein	-1,78	4,42E-01
HG001_00806 HG001_00806|gene_glpQ1_1|putative glycerophosphoryl diester phosphodiesterase 1	-1,78	4,42E-01
HG001_01792 HG001_01792|gene_NONE|Phosphotransferase system, EIIC	-1,78	4,42E-01
HG001_02063 HG001_02063|gene_iolC|5-dehydro-2-deoxygluconokinase	-1,78	4,42E-01
HG001_00461 HG001_00461|gene_mrnC|Mini-ribonuclease 3	-1,78	4,42E-01
HG001_00894 HG001_00894|gene_menD|2-succinyl-5-enolpyruvyl-6-hydroxy-3-cyclohexene-1-carboxylate synthase	-1,78	4,42E-01
HG001_00520 HG001_00520|gene_galK_1|Galactokinase	-1,78	4,42E-01
HG001_01218 HG001_01218|gene_mprF|Phosphatidylglycerol lysyltransferase	-1,78	4,42E-01
HG001_01536 HG001_01536|gene_yhbU_2|putative protease YhbU precursor	-1,78	4,42E-01
HG001_01518 HG001_01518|gene_nadD|putative nicotinate-nucleotide adenylyltransferase	-1,78	4,42E-01
HG001_00989 HG001_00989|gene_rnhC|Ribonuclease HIII	-1,78	4,42E-01
HG001_00027 HG001_00027|gene_yfkN_1|Trifunctional nucleotide phosphoesterase protein YfkN precursor	-1,78	4,42E-01
HG001_01297 HG001_01297|gene_tdcB|L-threonine dehydratase catabolic TdcB	-1,78	4,42E-01
HG001_02611 HG001_02611|gene_NONE|DNA-binding transcriptional regulator EnvR	-1,78	4,42E-01
HG001_01135 HG001_01135|gene_pgsA|CDP-diacylglycerol--glycerol-3-phosphate 3-phosphatidyltransferase	-1,78	4,42E-01
HG001_02101 HG001_02101|gene_NONE|Bacterial membrane flanked domain protein	-1,78	4,42E-01
HG001_00564 HG001_00564|gene_mnhD1_1|Na(+)/H(+) antiporter subunit D1	-1,78	4,42E-01
HG001_02616 HG001_02616|gene_NONE|hypothetical protein	-1,78	4,42E-01
HG001_00054 HG001_00054|gene_NONE|Na+/Pi-cotransporter	-1,78	4,42E-01
HG001_00610 HG001_00610|gene_NONE|hypothetical protein	-1,78	4,42E-01
HG001_01831 HG001_01831|gene_NONE|Putative multidrug export ATP-binding/permease protein	-1,78	4,42E-01
HG001_00780 HG001_00780|gene_patA_1|Peptidoglycan O-acetyltransferase	-1,78	4,42E-01
HG001_01262 HG001_01262|gene_NONE|hypothetical protein	-1,78	4,42E-01
HG001_02383 HG001_02383|gene_corA|Magnesium transport protein CorA	-1,78	4,42E-01
HG001_01207 HG001_01207|gene_mscL|Large-conductance mechanosensitive channel	-1,78	4,42E-01
HG001_02599 HG001_02599|gene_ldhD_2|D-lactate dehydrogenase	-1,78	4,42E-01
HG001_00247 HG001_00247|gene_NONE|hypothetical protein	-1,78	4,42E-01
HG001_01535 HG001_01535|gene_yhbU_1|putative protease YhbU precursor	-1,78	4,42E-01
HG001_02608 HG001_02608|gene_NONE|Acetyltransferase (GNAT) family protein	-1,78	4,42E-01
HG001_00099 HG001_00099|gene_adhE|Aldehyde-alcohol dehydrogenase	-1,78	4,42E-01
HG001_01032 HG001_01032|gene_mraY|Phospho-N-acetylmuramoyl-pentapeptide-transferase	-1,78	4,42E-01

HG001_02726	HG001_02726|gene_NONE|Lactonase drp35	-1,78	4,42E-01
HG001_02593	HG001_02593|gene_NONE|hypothetical protein	-1,78	4,42E-01
HG001_00974	HG001_00974|gene_NONE|hypothetical protein	-1,78	4,42E-01
HG001_01480	HG001_01480|gene_znuC_2|High-affinity zinc uptake system ATP-binding protein ZnuC	-1,78	4,42E-01
HG001_00664	HG001_00664|gene_NONE|Putative lipid kinase	-1,78	4,42E-01
HG001_00553	HG001_00553|gene_NONE|hypothetical protein	-1,77	1,54E-02
HG001_00967	HG001_00967|gene_NONE|Cysteine-rich secretory protein family protein	-1,73	3,26E-01
HG001_02489	HG001_02489|gene_opuCA|Carnitine transport ATP-binding protein OpuCA	-1,73	3,26E-01
HG001_02115	HG001_02115|gene_cls_2|Cardiolipin synthase	-1,73	3,26E-01
HG001_00668	HG001_00668|gene_nrdI|Protein NrdI	-1,73	3,26E-01
HG001_01063	HG001_01063|gene_priA|Primosomal protein N'	-1,73	3,26E-01
HG001_02326	HG001_02326|gene_ureE|Urease accessory protein UreE	-1,73	3,26E-01
HG001_02319	HG001_02319|gene_rihB|Pyrimidine-specific ribonucleoside hydrolase RihB	-1,73	3,26E-01
HG001_02373	HG001_02373|gene_rpiA|Ribose-5-phosphate isomerase A	-1,73	3,26E-01
HG001_00304	HG001_00304|gene_spo0C|Chromosome-partitioning protein Spo0J	-1,73	3,26E-01
HG001_02631	HG001_02631|gene_NONE|hypothetical protein	-1,73	3,26E-01
HG001_01424	HG001_01424|gene_nudF|ADP-ribose pyrophosphatase	-1,73	3,26E-01
HG001_00686	HG001_00686|gene_yigZ|IMPACT family member YigZ	-1,73	3,26E-01
HG001_00818	HG001_00818|gene_yidA|Sugar phosphatase YidA	-1,72	2,04E-01
HG001_00705	HG001_00705|gene_NONE|Gluconeogenesis factor	-1,72	2,04E-01
HG001_01237	HG001_01237|gene_NONE|hypothetical protein	-1,72	2,04E-01
HG001_00463	HG001_00463|gene_NONE|YacP-like NYN domain protein	-1,72	2,04E-01
HG001_02615	HG001_02615|gene_azoB|NAD(P)H azoreductase	-1,72	2,05E-01
HG001_01085	HG001_01085|gene_smc|Chromosome partition protein Smc	-1,72	1,23E-01
HG001_00022	HG001_00022|gene_walR|Transcriptional regulatory protein WalR	-1,72	6,91E-02
HG001_01279	HG001_01279|gene_NONE|Acetyltransferase (GNAT) family protein	-1,72	3,76E-02
HG001_00319	HG001_00319|gene_gpmA_1|2,3-bisphosphoglycerate-dependent phosphoglycerate mutase	-1,72	7,06E-02
HG001_02062	HG001_02062|gene_agrA|Accessory gene regulator protein A	-1,61	1,65E-01
HG001_01407	HG001_01407|gene_lexA_2|LexA repressor	-1,58	4,11E-03
HG001_01959	HG001_01959|gene_NONE|Acyl-coenzyme A:6-aminopenicillanic acid acyl-transferase	-1,56	2,80E-01
HG001_00493	HG001_00493|gene_sdrD|Serine-aspartate repeat-containing protein D precursor	-1,53	2,68E-05
HG001_01116	HG001_01116|gene_rimP|Ribosome maturation factor RimP	-1,47	7,39E-02
HG001_01939	HG001_01939|gene_pcrA|ATP-dependent DNA helicase PcrA	-1,45	5,72E-02
HG001_02527	HG001_02527|gene_srmB|ATP-dependent RNA helicase SrmB	-1,45	5,81E-02
HG001_00366	HG001_00366|gene_NONE|hypothetical protein	-1,44	4,42E-01
HG001_00181	HG001_00181|gene_NONE|hypothetical protein	-1,44	4,42E-01
HG001_02125	HG001_02125|gene_NONE|hypothetical protein	-1,44	4,42E-01
HG001_01419	HG001_01419|gene_scpB|Segregation and condensation protein B	-1,44	4,42E-01
HG001_01837	HG001_01837|gene_NONE|hypothetical protein	-1,44	4,42E-01
HG001_01606	HG001_01606|gene_gapA2|Glyceraldehyde-3-phosphate dehydrogenase 2	-1,44	4,42E-01
HG001_01257	HG001_01257|gene_yxeP_3|putative hydrolase YxeP	-1,44	4,42E-01
HG001_01268	HG001_01268|gene_cobT|Aerobic cobaltochelatase subunit CobT	-1,44	4,42E-01
HG001_01448	HG001_01448|gene_xseA|Exodeoxyribonuclease 7 large subunit	-1,44	4,42E-01
HG001_01074	HG001_01074|gene_thiN|Thiamine pyrophosphokinase	-1,38	3,46E-01
HG001_01219	HG001_01219|gene_msrA1|Peptide methionine sulfoxide reductase MsrA 1	-1,38	3,46E-01
HG001_00252	HG001_00252|gene_NONE|FtsX-like permease family protein	-1,36	2,83E-01
HG001_02446	HG001_02446|gene_bdbD|Disulfide bond formation protein D precursor	-1,35	2,84E-01
HG001_00359	HG001_00359|gene_NONE|hypothetical protein	-1,34	2,18E-01
HG001_01585	HG001_01585|gene_hemB|Delta-aminolevulinic acid dehydratase	-1,32	2,99E-02
HG001_00843	HG001_00843|gene_spxA|Regulatory protein Spx	-1,29	2,97E-03
HG001_01587	HG001_01587|gene_hemC|Porphobilinogen deaminase	-1,27	9,47E-02
HG001_00867	HG001_00867|gene_prfC|Peptide chain release factor 3	-1,26	1,23E-01
HG001_02121	HG001_02121|gene_tenA|Putative thiaminase-2	-1,25	1,00E-02
HG001_02408	HG001_02408|gene_yhfP|Putative quinone oxidoreductase YhfP	-1,23	2,81E-01
HG001_00640	HG001_00640|gene_nagA|N-acetylglucosamine-6-phosphate deacetylase	-1,23	2,81E-01
HG001_00641	HG001_00641|gene_corC|Magnesium and cobalt efflux protein CorC	-1,23	2,81E-01
HG001_00238	HG001_00238|gene_yezG_1|putative antitoxin YezG	-1,22	7,39E-02
HG001_00782	HG001_00782|gene_NONE|DltD central region	-1,22	2,14E-02
HG001_01451	HG001_01451|gene_cfiB_2|2-oxoglutarate carboxylase small subunit	-1,22	9,25E-02
HG001_02189	HG001_02189|gene_NONE|YbbR-like protein	-1,21	9,25E-02
HG001_01332	HG001_01332|gene_NONE|Heptaprenyl diphosphate synthase (HEPPP synthase) subunit 1	-1,21	3,44E-01
HG001_00836	HG001_00836|gene_dppE|Dipeptide-binding protein DppE precursor	-1,21	3,44E-01
HG001_02667	HG001_02667|gene_slyA_3|Transcriptional regulator SlyA	-1,21	3,44E-01
HG001_02382	HG001_02382|gene_fni|Isopentenyl-diphosphate delta-isomerase	-1,19	6,82E-02
HG001_02095	HG001_02095|gene_rsbU|Phosphoserine phosphatase RsbU	-1,17	2,06E-01
HG001_02537	HG001_02537|gene_gtaB|UTP--glucose-1-phosphate uridylyltransferase	-1,17	4,42E-01

HG001_01950	HG001_01950|gene_pheA|P-protein	-1,17	4,42E-01
HG001_00211	HG001_00211|gene_rbsK|Ribokinase	-1,17	4,42E-01
HG001_00699	HG001_00699|gene_lgt|Prolipoprotein diacylglyceryl transferase	-1,17	4,42E-01
HG001_00781	HG001_00781|gene_dltC|D-alanine--poly(phosphoribitol) ligase subunit 2	-1,17	4,42E-01
HG001_01254	HG001_01254|gene_dapA|4-hydroxy-tetrahydrodipicolinate synthase	-1,17	4,42E-01
HG001_00183	HG001_00183|gene_hmp|Flavohemoprotein	-1,17	2,97E-03
HG001_02428	HG001_02428|gene_nreC|Oxygen regulatory protein NreC	-1,17	4,42E-01
HG001_00931	HG001_00931|gene_rlmI|Ribosomal RNA large subunit methyltransferase I	-1,17	4,42E-01
HG001_02551	HG001_02551|gene_yxlF_5|putative ABC transporter ATP-binding protein YxlF	-1,17	4,42E-01
HG001_00432	HG001_00432|gene_folB|Dihydroneopterin aldolase	-1,17	4,42E-01
HG001_01128	HG001_01128|gene_ftsK|DNA translocase FtsK	-1,15	2,71E-01
HG001_01280	HG001_01280|gene_NONE|putative CtpA-like serine protease	-1,12	6,45E-02
HG001_00199	HG001_00199|gene_gutB_2|Sorbitol dehydrogenase	-1,12	1,21E-01
HG001_01776	HG001_01776|gene_NONE|Leucine-rich repeats of kinetochore protein Cenp-F/LEK1	-1,11	2,34E-04
HG001_01714	HG001_01714|gene_pckA|Phosphoenolpyruvate carboxykinase [ATP]	-1,11	9,00E-03
HG001_00679	HG001_00679|gene_NONE|hypothetical protein	-1,11	3,31E-01
HG001_01603	HG001_01603|gene_dnaI|Primosomal protein DnaI	-1,11	3,34E-01
HG001_01452	HG001_01452|gene_accB_1|Biotin carboxyl carrier protein of acetyl-CoA carboxylase	-1,10	1,48E-01
HG001_02646	HG001_02646|gene_acsA_2|Acetyl-coenzyme A synthetase	-1,10	8,88E-04
HG001_02118	HG001_02118|gene_thiE|Thiamine-phosphate synthase	-1,10	6,13E-02
HG001_00544	HG001_00544|gene_adh|Alcohol dehydrogenase	-1,10	2,42E-04
HG001_01624	HG001_01624|gene_nrnA_2|Bifunctional oligoribonuclease and PAP phosphatase NrnA	-1,09	2,59E-01
HG001_00998	HG001_00998|gene_frdB|Fumarate reductase iron-sulfur subunit	-1,08	2,00E-01
HG001_01261	HG001_01261|gene_cspA_2|Cold shock protein CspA	-1,07	2,30E-02
HG001_01031	HG001_01031|gene_pbpB|Penicillin-binding protein 2B	-1,07	2,77E-02
HG001_02436	HG001_02436|gene_nasE|Assimilatory nitrite reductase [NAD(P)H] small subunit	-1,07	1,46E-01
HG001_01148	HG001_01148|gene_mutL|DNA mismatch repair protein MutL	-1,07	5,82E-01
HG001_02614	HG001_02614|gene_NONE|Glyoxalase-like domain protein	-1,07	5,82E-01
HG001_01779	HG001_01779|gene_NONE|hypothetical protein	-1,07	5,82E-01
HG001_02045	HG001_02045|gene_dapE|putative succinyl-diaminopimelate desuccinylase	-1,07	5,82E-01
HG001_01692	HG001_01692|gene_ribD|Riboflavin biosynthesis protein RibD	-1,07	5,82E-01
HG001_01473	HG001_01473|gene_gluP|Rhomboid protease GluP	-1,07	5,82E-01
HG001_00515	HG001_00515|gene_NONE|hypothetical protein	-1,07	5,82E-01
HG001_01539	HG001_01539|gene_yrrK|Putative Holliday junction resolvase	-1,07	5,82E-01
HG001_01058	HG001_01058|gene_NONE|3-demethylubiquinone-9 3-methyltransferase	-1,07	5,82E-01
HG001_01197	HG001_01197|gene_guaC|GMP reductase	-1,07	5,82E-01
HG001_00352	HG001_00352|gene_NONE|Type I restriction modification DNA specificity domain protein	-1,07	5,82E-01
HG001_02346	HG001_02346|gene_suhB_2|Inositol-1-monophosphatase	-1,07	5,82E-01
HG001_02430	HG001_02430|gene_NONE|hypothetical protein	-1,07	5,82E-01
HG001_00851	HG001_00851|gene_NONE|CYTH domain protein	-1,07	5,82E-01
HG001_02421	HG001_02421|gene_NONE|hypothetical protein	-1,06	5,82E-01
HG001_01206	HG001_01206|gene_sbcC|Nuclease SbcCD subunit C	-1,06	5,82E-01
HG001_00575	HG001_00575|gene_tagA|Putative N-acetylmannosaminyltransferase	-1,06	5,82E-01
HG001_02745	HG001_02745|gene_cspLA|Cold shock-like protein CspLA	-1,06	5,82E-01
HG001_00542	HG001_00542|gene_NONE|HD domain protein	-1,06	5,82E-01
HG001_02094	HG001_02094|gene_rsbV|Anti-sigma-B factor antagonist	-1,06	1,05E-01
HG001_00872	HG001_00872|gene_yfkN_4|Trifunctional nucleotide phosphoesterase protein YfkN precursor	-1,05	4,35E-01
HG001_00243	HG001_00243|gene_yezG_3|putative antitoxin YezG	-1,05	4,35E-01
HG001_00386	HG001_00386|gene_treB|PTS system trehalose-specific EIIBC component	-1,05	4,35E-01
HG001_01487	HG001_01487|gene_yqfL|Putative pyruvate, phosphate dikinase regulatory protein	-1,05	4,35E-01
HG001_00376	HG001_00376|gene_sle1_1|N-acetylmuramoyl-L-alanine amidase sle1 precursor	-1,04	3,19E-01
HG001_00698	HG001_00698|gene_hprK|HPr kinase/phosphorylase	-1,04	1,34E-01
HG001_00728	HG001_00728|gene_clfA|Clumping factor A precursor	-1,02	1,27E-01
HG001_02181	HG001_02181|gene_glmS|Glutamine--fructose-6-phosphate aminotransferase [isomerizing]	-1,01	1,75E-04
HG001_02021	HG001_02021|gene_NONE|hypothetical protein	-1,01	6,59E-02
HG001_01918	HG001_01918|gene_vraR|Response regulator protein VraR	-1,01	2,35E-01

Annexe 3 : Tableau de l'expression différentielle selon les voies métaboliques impliquées.

Pyrimidine deoxyribonucleotides de novo biosyntheis					Diff. Transcriptomics MV/ctr		Diff. Proteomics MV/ctr	
id	gene	product	locus_tag_NCTC8325	gene_NCTC8325	log2FoldChange	padj	log2FoldChange	padj
HG001_01054	carB	Carbamoyl-phosphate synthase large chain	SAOUHSC_01170	carB	5,41	9,50E-104	0,12	7,76E-01
HG001_01052	pyrC	Dihydroorotase	SAOUHSC_01168	pyrC	5,31	1,73E-65	1,22	8,22E-09
HG001_01055	pyrF	Orotidine 5'-phosphate decarboxylase	SAOUHSC_01171	-	5,29	3,09E-126	0,59	2,47E-01
HG001_01053	carA	Carbamoyl-phosphate synthase small chain	SAOUHSC_01169	-	5,28	6,93E-63	0,67	1,04E-01
HG001_01051	pyrB	Aspartate carbamoyltransferase	SAOUHSC_01166	pyrB	5,17	1,60E-52	0,09	9,09E-01
HG001_01056	pyrE	Orotate phosphoribosyltransferase	SAOUHSC_01172	pyrE	4,97	1,35E-105	0,83	9,18E-02
HG001_01050	pyrP	Uracil permease	SAOUHSC_01165	-	4,81	5,14E-46	0,90	3,77E-01
HG001_01057	-	hypothetical protein; same operon as pyrP-pyrB-pyrC-carA-carB-pyrF-pyrI	SAOUHSC_01173	-	3,51	8,10E-45	ND	ND
HG001_00399	tmk	Thymidylate kinase	SAOUHSC_00451	tmk	1,06	4,06E-06	0,27	8,80E-01
HG001_00669	nrdE2	Ribonucleoside-diphosphate reductase subunit alpha 2	SAOUHSC_00742	nrdI	1,36	7,99E-08	0,40	8,71E-02
HG001_00670	nrdF	Ribonucleoside-diphosphate reductase subunit beta	SAOUHSC_00743	nrdF	2,53	5,81E-22	0,51	2,13E-02
HG001_01049	pyrR	Bifunctional protein PyrR	SAOUHSC_01164	-	1,01	0,000496863	2,76	4,52E-09
HG001_01109	pyrH	Uridylate kinase	SAOUHSC_01235	pyrH	1,19	7,15E-06	-0,67	2,35E-01
HG001_01337	cmk	Cytidylate kinase	SAOUHSC_01496	cmk	1,61	3,25E-11	-0,10	8,52E-01
HG001_01534	udk	Uridine kinase	SAOUHSC_01715	-	1,30	2,62E-10	-0,66	6,45E-01
HG001_02154	pyrG	CTP synthase	SAOUHSC_02368	pyrG	2,39	8,99E-22	-0,35	3,37E-01
HG001_02629	pyrD	Dihydroorotate dehydrogenase (quinone)	SAOUHSC_02909	-	2,96	6,09E-08	2,33	6,96E-12

Purine deoxyribonucleotides de novo biosyntheis					Diff. Transcriptomics MV/ctr		Diff. Proteomics MV/ctr	
id	gene	product	locus_tag_NCTC8325	gene_NCTC8325	log2FoldChange	padj	log2FoldChange	padj
HG001_00085	deoD	Purine nucleoside phosphorylase DeoD-type	SAOUHSC_00097	-	3,81	5,29E-33	ND	ND
HG001_00019	purA	Adenylosuccinate synthetase	SAOUHSC_00019	-	2,26	4,52562E-15	0,05	9,57E-01
HG001_01560	apt	Adenine phosphoribosyltransferase	SAOUHSC_01743	-	1,89	5,58131E-18	-0,37	7,86E-01
HG001_01942	purB	Adenylosuccinate lyase	SAOUHSC_02126	-	1,86	6,42238E-15	-0,34	2,32E-01
HG001_02655	nrdD	Anaerobic ribonucleoside-triphosphate reductase	SAOUHSC_02942	-	2,41	8,69131E-18	0,27	8,69E-01

Phage genes					Diff. Transcriptomics MV/ctr		Diff. Proteomics MV/ctr	
id	gene	product	locus_tag_NCTC8325	gene_NCTC8325	log2FoldChange	padj	log2FoldChange	padj
HG001_01894	-	Phage protein	SAOUHSC_02072	-	5,30	3,29E-106	7,72	8,10E-24
HG001_01903	-	Putative phage protein	SAOUHSC_02081	-	5,26	6,13E-84	1,98	4,11E-01
HG001_01904	-	Putative phage regulatory protein	SAOUHSC_02083	-	5,13	1,51E-76	ND	ND
HG001_01891	-	Putative phage replication protein	SAOUHSC_02069	-	5,13	7,84E-104	4,93	9,83E-04
HG001_01895	-	Bacteriophage Mu Gam like protein	SAOUHSC_02073	-	5,12	1,86E-101	7,35	2,61E-18
HG001_01898	-	Phage protein	SAOUHSC_02076	-	5,04	5,50E-64	ND	ND
HG001_01902	-	Phage antirepressor protein KilAC domain protein	SAOUHSC_02080	-	5,02	1,44E-91	9,03	5,76E-54
HG001_01887	-	Phage protein	SAOUHSC_02065	-	5,00	2,05E-91	2,79	2,32E-01
HG001_01888	-	Putative phage protein	SAOUHSC_02066	-	4,98	1,64E-111	ND	ND
HG001_01885	-	Phage protein	SAOUHSC_02063	-	4,98	1,29E-122	ND	ND
HG001_01886	-	Phage protein	SAOUHSC_02064	-	4,94	3,02E-104	3,98	3,18E-02
HG001_01884	-	Putative phage regulatory protein; Helix-turn-helix domain protein	SAOUHSC_02062	-	4,89	3,62E-92	3,68	6,59E-02
HG001_01883	-	Phage protein; PVL ORF-50-like family protein	SAOUHSC_02061	-	4,89	5,90E-94	4,44	8,53E-03
HG001_01900	-	Phage protein	SAOUHSC_02078	-	4,89	1,40E-93	5,30	1,17E-04
HG001_01890	-	Phage protein	SAOUHSC_02068	-	4,87	6,99E-99	2,79	2,32E-01
HG001_02016	-	Phage protein	SAOUHSC_02213	-	4,86	5,76E-99	ND	ND
HG001_01896	-	Phage protein	SAOUHSC_02074	-	4,83	1,20E-88	ND	ND
HG001_01901	-	Putative phage protein	SAOUHSC_02079	-	4,81	2,42E-107	1,98	4,11E-01
HG001_01875	-	Transcriptional activator RinB (phage)	SAOUHSC_02053	-	4,75	1,21E-118	ND	ND
HG001_01868	-	Putative phage protein	SAOUHSC_02046	-	4,73	3,62E-66	ND	ND
HG001_01880	-	Putative phage protein	SAOUHSC_02058	-	4,70	1,30E-90	6,23	1,47E-08
HG001_01881	-	Phage protein	SAOUHSC_02059	-	4,70	4,55E-98	ND	ND
HG001_01870	-	Phage portal protein%2C SPP1 Gp6-like	SAOUHSC_02048	-	4,69	1,57E-79	1,98	4,11E-01
HG001_01876	-	Phage protein	SAOUHSC_02054	-	4,68	8,91E-80	ND	ND
HG001_01882	-	Phage protein	SAOUHSC_02060	-	4,66	8,31E-112	ND	ND
HG001_01869	-	Phage Mu protein F like protein	SAOUHSC_02047	-	4,63	3,92E-79	ND	ND
HG001_01899	-	Phage protein	SAOUHSC_02077	-	4,60	2,32E-83	7,22	7,52E-17
HG001_01873	-	Transcriptional activator, phage-associated	SAOUHSC_02051	-	4,54	9,07E-91	5,50	2,76E-05
HG001_01878	-	Putative phage protein	SAOUHSC_02056	-	4,54	2,16E-83	ND	ND
HG001_02037	-	Putative phage regulatory protein	SAOUHSC_02234	-	4,49	4,16E-70	ND	ND
HG001_02032	-	Phage protein	SAOUHSC_02228	-	4,46	4,05E-75	ND	ND
HG001_01874	-	Phage protein	SAOUHSC_02052	-	4,42	5,03E-104	ND	ND
HG001_01383	-	Phage protein	SAOUHSC_01550	-	4,41	8,41E-68	ND	ND
HG001_02034	-	AntA/AntB antirepressor	SAOUHSC_02229	-	4,40	3,05E-86	1,98	4,11E-01
HG001_02036	-	Putative phage regulatory protein	SAOUHSC_02233	-	4,38	3,67E-72	ND	ND
HG001_01877	-	Phage protein	SAOUHSC_02055	-	4,38	1,19E-87	3,30	1,23E-01
HG001_01897	-	Phage protein	SAOUHSC_02075	-	4,22	3,08E-83	9,14	1,96E-43
HG001_01866	-	Phage capsid family protein	SAOUHSC_02043	-	4,20	1,95E-57	4,23	1,64E-02
HG001_02033	-	Phage antirepressor protein KilAC domain protein	SAOUHSC_02229	-	4,19	1,60E-83	ND	ND
HG001_01867	-	Putative phage head protein	SAOUHSC_02044	-	4,15	1,63E-61	5,68	6,87E-06
HG001_01871	-	Phage terminase large subunit	SAOUHSC_02049	-	4,14	4,87E-53	ND	ND
HG001_01865	-	Phage protein	SAOUHSC_02042	-	4,12	9,34E-51	2,79	2,32E-01
HG001_01863	-	Putative phage protein	SAOUHSC_02040	-	4,07	1,18E-53	ND	ND
HG001_02023	-	Putative phage nuclease	SAOUHSC_02219	-	4,04	5,11E-85	ND	ND
HG001_01858	-	Phage protein	SAOUHSC_02034	-	3,98	5,86E-61	ND	ND
HG001_02031	-	Putative phage protein	SAOUHSC_02227	-	3,98	1,83E-46	ND	ND
HG001_02029	-	Phage protein	SAOUHSC_02225	-	3,98	4,57E-80	1,98	4,11E-01
HG001_01861	-	Putative phage protein	SAOUHSC_02037	-	3,95	1,04E-58	ND	ND
HG001_02025	-	Phage protein	SAOUHSC_02221	-	3,95	6,11E-88	ND	ND
HG001_02017	-	Putative phage protein	SAOUHSC_02214	-	3,88	2,85E-46	ND	ND
HG001_02028	-	Phage protein	SAOUHSC_02224	-	3,85	6,04E-45	ND	ND
HG001_01386	-	Phage protein; PVL orf 52-like protein; Phage phi 11 orf23 protein homolc	SAOUHSC_01553	-	3,85	2,70E-63	ND	ND
HG001_02024	-	Putative phage ssDNA binding protein	SAOUHSC_02220	-	3,83	7,83E-62	1,98	4,11E-01
HG001_01860	-	Phage major tail protein 2	SAOUHSC_02036	-	3,82	7,08E-64	3,30	1,23E-01

HG001_02026	-	Putative phage protein	SAOUHSC_02222	-	3,81	2,07E-65	ND	ND
HG001_01859	-	Phage protein	SAOUHSC_02035	-	3,77	1,37E-55	3,98	3,18E-02
HG001_01862	-	Phage protein	SAOUHSC_02038	-	3,77	3,25E-54	ND	ND
HG001_01872	-	Terminase small subunit	SAOUHSC_02050	-	3,65	1,14E-36	ND	ND
HG001_02027	-	Phage protein	SAOUHSC_02223	-	3,63	5,40E-53	ND	ND
HG001_02020	-	Phage protein	SAOUHSC_02217	-	3,32	8,20E-54	ND	ND

DNA repair					Diff. Transcriptomics MV/ctr		Diff. Proteomics MV/ctr	
id	gene	product	locus_tag_NCTC8325	gene_NCTC8325	log2FoldChange	padj	log2FoldChange	padj
HG001_01889	dnaC_2	Replicative DNA helicase	SAOUHSC_02067	-	4,92	1,18E-111	ND	ND
HG001_01222	dinB_1	DNA polymerase IV	SAOUHSC_01363	MucB	4,04	1,46E-55	ND	ND
HG001_00018	dnaB	Replicative DNA helicase	SAOUHSC_00018	-	0,51	0,052192362	-2,00	1,08E-01
HG001_00004	recF	DNA replication and repair protein RecF	SAOUHSC_00004	recF	1,17	6,04E-09	ND	ND
HG001_00310	ssb_1	Single-stranded DNA-binding protein ssb	SAOUHSC_00349	-	1,21	7,79E-08	0,57	2,83E-01
HG001_00510	ung	Uracil-DNA glycosylase	SAOUHSC_00564	-	1,02	0,000840362	-0,66	6,45E-01
HG001_00659	recQ_1	ATP-dependent DNA helicase RecQ	SAOUHSC_00730	-	2,10	4,16E-29	ND	ND
HG001_00697	uvrA	UvrABC system protein A	SAOUHSC_00780	uvrA	1,54	4,12E-15	0,27	8,18E-01
HG001_00992	polX	DNA polymerase/3'-5' exonuclease PolX	SAOUHSC_01098	-	1,11	2,71E-08	-0,37	7,86E-01
HG001_00993	mutS2	Endonuclease MutS2	SAOUHSC_01099	-	1,34	1,28E-10	-0,86	3,26E-01
HG001_01095	rnhB	Ribonuclease HII	SAOUHSC_01215	rnhB	1,12	1,30E-06	-1,78	4,42E-01
HG001_01137	recA	Protein RecA	SAOUHSC_01262	recA	2,19	1,32E-20	1,36	5,99E-05
HG001_01205	sbcD	Nuclease SbcCD subunit D	SAOUHSC_01341	-	1,37	2,58E-07	ND	ND
HG001_01310	recU	Holliday junction resolvase RecU	SAOUHSC_01466	recU	1,43	2,34E-09	ND	ND
HG001_01481	nfo	putative endonuclease 4	SAOUHSC_01658	-	1,79	2,77E-17	-0,20	7,91E-01
HG001_01514	comEA	ComE operon protein 1	SAOUHSC_01693	-	1,43	2,04E-08	ND	ND
HG001_01561	recJ	Single-stranded-DNA-specific exonuclease RecJ	SAOUHSC_01744	-	1,37	2,90E-12	-0,03	9,83E-01
HG001_01566	ruvB	Holliday junction ATP-dependent DNA helicase RuvB	SAOUHSC_01750	ruvB	1,00	2,72E-05	ND	ND
HG001_01938	ligA	DNA ligase	SAOUHSC_02122	-	2,00	7,85E-21	-0,48	2,00E-01
HG001_01939	pcrA	ATP-dependent DNA helicase PcrA	SAOUHSC_02123	-	2,18	7,32E-27	-1,45	5,72E-02

Nitrate and Nitrite reduction. Porfirines biosisnthesis, anaerobic respiratory chain					Diff. Transcriptomics MV/ctr		Diff. Proteomics MV/ctr	
id	gene	product	locus_tag_NCTC8325	gene_NCTC8325	log2FoldChange	padj	log2FoldChange	padj
HG001_02438	shfC (nirR)	Sirohydrochlorin ferrochelatase	SAOUHSC_02685	nirR	2,59	3,49591E-19	ND	ND
HG001_02437	nasD	Nitrite reductase [NAD(P)H] large subunit - similar to tRNA U-34 5-methyl	SAOUHSC_02684	nasD	3,20	1,42E-25	-0,35	4,19E-01
HG001_02436	nasE	Nitrite reductase [NAD(P)H] small subunit	SAOUHSC_02683	nasE	3,32	1,65E-29	-1,07	1,46E-01
HG001_02435	nasF	Uroporphyrinogen-III C-methyltransferase - similar to queE	SAOUHSC_02682	nasF	3,40	5,44181E-37	0,66	5,51E-01
HG001_02434	narG	Respiratory nitrate reductase 1 alpha chain - molybdopterin [4Fe-4S] clus	SAOUHSC_02681	narG	3,80	2,96E-40	-2,56	1,47E-13
HG001_02433	narH	Respiratory nitrate reductase 1 beta chain - [4Fe-4S] cluster	SAOUHSC_02680	narH	4,28	1,58E-52	-2,06	2,56E-04
HG001_02432	narW	Nitrate reductase molybdenum cofactor assembly chaperone	SAOUHSC_02679	narJ	4,26	4,39E-51	-4,17	2,68E-02
HG001_02431	narX	Respiratory nitrate reductase subunit gamma	SAOUHSC_02678	narI	3,19	3,92E-36	ND	ND
HG001_02430	nreA	Nitrogen fixation regulatory protein	SAOUHSC_02677	nreA	2,55	5,64788E-26	-1,07	5,82E-01
HG001_02429	nreB	Oxygen sensor two-component histidine kinase [4Fe-4S] cluster	SAOUHSC_02676	nreB	2,86	7,06112E-32	-2,55	2,99E-01
HG001_02428	nreC	Oxygen regulatory protein regulator transcription factor of the two comp	SAOUHSC_02675	nreC	2,51	1,59378E-30	-1,17	4,42E-01
HG001_02344	-	Putative formate dehydrogenase	SAOUHSC_02582	fdhA	-0,69	0,002489064	-3,93	1,23E-21
HG001_02343	-	Putative formate dehydrogenase	SAOUHSC_02581	-	-1,06	6,23554E-05	-4,56	4,13E-08
HG001_02424	narT	putative nitrate transporter NarT	SAOUHSC_02671	-	2,15	0,000554689	-3,72	7,39E-02

Regulation of respiratory chain					Diff. Transcriptomics MV/ctr		Diff. Proteomics MV/ctr	
id	gene	product	locus_tag_NCTC8325	gene_NCTC8325	log2FoldChange	padj	log2FoldChange	padj
HG001_02428	nreC	Oxygen regulatory protein NreC	SAOUHSC_02675	-	2,51	1,59E-30	-1,17	4,42E-01
HG001_02069	rex	Redox-sensing transcriptional repressor Rex	SAOUHSC_02273	-	-0,25	0,272186609	0,05	9,53E-01

Protein Folding					Diff. Transcriptomics MV/ctr		Diff. Proteomics MV/ctr	
id	gene	product	locus_tag_NCTC8325	gene_NCTC8325	log2FoldChange	padj	log2FoldChange	padj
HG001_00429	hslO	33 kDa chaperonin	SAOUHSC_00487	hslO	0,95	8,36E-06	0,01	9,85E-01
HG001_00821	clpB_1	Chaperone protein ClpB	SAOUHSC_00912	-	1,14	5,03E-07	0,09	8,73E-01
HG001_01504	dnaJ	Chaperone protein DnaJ	SAOUHSC_01682	-	0,72	0,000696191	-0,31	5,20E-01
HG001_01506	grpE	Protein GrpE	SAOUHSC_01684	-	0,74	0,00066207	0,23	4,42E-01
HG001_01591	clpX	ATP-dependent Clp protease ATP-binding subunit ClpX	SAOUHSC_01778	clpX	1,42	4,48E-12	0,70	4,11E-03
HG001_01592	tig	Trigger factor	SAOUHSC_01779	tig	1,39	9,40E-11	0,90	5,36E-05

tRNA modification					Diff. Transcriptomics MV/ctr		Diff. Proteomics MV/ctr	
id	gene	product	locus_tag_NCTC8325	gene_NCTC8325	log2FoldChange	padj	log2FoldChange	padj
HG001_02727	glpE_3	Thiosulfate sulfurtransferase GlpE	SAOUHSC_03024	-	4,35	4,32E-96	3,20	2,44E-09
HG001_01911	queE_2	7-carboxy-7-deazaguanine synthase	SAOUHSC_02090	-	3,19	6,19E-61	0,93	5,04E-01
HG001_02256	truA	tRNA pseudouridine synthase A	SAOUHSC_02480	truA	2,08	4,31E-25	-0,63	7,17E-01
HG001_02751	mnmG	tRNA uridine 5-carboxymethylaminomethyl modification enzyme MnmG	SAOUHSC_03052	gidA	1,93	2,97E-16	0,65	5,36E-02
HG001_02752	mnmE	tRNA modification GTPase MnmE	SAOUHSC_03053	trmE	1,62	2,36E-10	1,02	2,12E-01
HG001_01564	tgt	Queuine tRNA-ribosyltransferase	SAOUHSC_01748	tgt	1,60	8,50E-13	-0,75	2,61E-01
HG001_01635	thiI	putative tRNA sulfurtransferase	SAOUHSC_01824	-	1,42	1,03E-11	-0,60	4,98E-01
HG001_01091	trmD	tRNA (guanine-N(1)-)-methyltransferase	SAOUHSC_01210	trmD	1,41	2,36E-10	-1,98	2,47E-01
HG001_01565	queA	S-adenosylmethionine:tRNA ribosyltransferase-isomerase	SAOUHSC_01749	queA	1,35	1,96E-08	0,15	9,06E-01
HG001_01788	trmL	tRNA (cytidine(34)-2'-O)-methyltransferase	SAOUHSC_01988	-	1,30	1,85E-08	-2,12	7,39E-02
HG001_01484	trmK	tRNA (adenine(22)-N(1))-methyltransferase	SAOUHSC_01661	-	1,24	3,25E-09	0,20	8,25E-01
HG001_01102	trmFO	Methylenetetrahydrofolate--tRNA-(uracil-5-)-methyltransferase TrmFO	SAOUHSC_01223	gid	1,04	3,65E-06	0,05	9,33E-01
HG001_01144	miaB	(Dimethylallyl)adenosine tRNA methylthiotransferase MiaB	SAOUHSC_01269	-	1,01	6,46E-06	-5,02	1,32E-03
HG001_01552	tcdA	tRNA threonylcarbamoyladenosine dehydratase	SAOUHSC_01735	-	0,88	0,000111308	-0,78	3,93E-01
HG001_02072	tsaD	tRNA N6-adenosine threonylcarbamoyltransferase	SAOUHSC_02277	gcp	0,75	0,000378128	-0,87	5,13E-01

HG001_01500	mtaB_1	Threonylcarbamoyladenosine tRNA methylthiotransferase MtaB	SAOUHSC_01679	-	0,69	0,001185038	ND	ND
HG001_00404	yfiC	tRNA1(Val) (adenine(37)-N6)-methyltransferase	SAOUHSC_00457	-	0,58	0,023934541	ND	ND
HG001_00462	-	Putative TrmH family tRNA/rRNA methyltransferase	SAOUHSC_00513	-	-0,43	0,074696654	-0,51	4,42E-01
HG001_02075	tsaE	tRNA threonylcarbamoyladenosine biosynthesis protein TsaE	SAOUHSC_02280	-	-0,83	0,016585893	ND	ND
HG001_01122	truB	tRNA pseudouridine synthase B	SAOUHSC_01248	-	-0,90	4,08E-05	0,44	6,84E-01
HG001_00036	dus_2	putative tRNA-dihydrouridine synthase	SAOUHSC_00039	-	-0,98	4,87E-06	0,66	5,51E-01
HG001_00985	-	Putative TrmH family tRNA/rRNA methyltransferase	SAOUHSC_01091	-	-1,10	3,49E-07	-0,04	9,76E-01
HG001_01537	trmR	Putative O-methyltransferase/MSMEI_4947 tRNA 5-hydroxyuridine meth	SAOUHSC_01718	-	0,94	0,004417914	-3,42	1,23E-01
HG001_00666	queF	NADPH-dependent 7-cyano-7-deazaguanine reductase	SAOUHSC_00739	-	0,60	0,00815737	0,49	4,42E-01
HG001_01789	queG	Epoxyqueuosine reductase	SAOUHSC_01989	-	0,54	0,030211245	ND	ND
HG001_00496	folE2	GTP cyclohydrolase FolE2	SAOUHSC_00549	-	1,57	1,60E-14	0,50	3,56E-01
HG001_01154	miaA	tRNA dimethylallyltransferase	SAOUHSC_01280	miaA	0,33	0,196377884	0,02	9,85E-01
HG001_00650	queD	6-carboxy-5%2C6%2C7%2C8-tetrahydropterin synthase	SAOUHSC_00720	-	-0,10	0,750041318	0,83	4,42E-01
HG001_00649	queE_1	7-carboxy-7-deazaguanine synthase	SAOUHSC_00719	-	0,39	0,083379277	ND	ND
HG001_00651	queC	7-cyano-7-deazaguanine synthase	SAOUHSC_00721	-	0,04	0,872388212	-0,28	8,73E-01

Fermentation					Diff. Transcriptomics MV/ctr		Diff. Proteomics MV/ctr	
id	gene	product	locus_tag_NCTC8325	gene_NCTC8325	log2FoldChange	padj	log2FoldChange	padj
HG001_02246	aldC_1	Alpha-acetolactate decarboxylase	SAOUHSC_02467	-	3,24	1,69E-21	1,26	6,63E-10

Detoxifying enzymes					Diff. Transcriptomics MV/ctr		Diff. Proteomics MV/ctr	
id	gene	product	locus_tag_NCTC8325	gene_NCTC8325	log2FoldChange	padj	log2FoldChange	padj
HG001_00082	sodM	Superoxide dismutase [Mn/Fe] 2	SAOUHSC_00093	-	2,37	1,32E-34	-0,18	7,14E-01
HG001_01477	sodA	Superoxide dismutase [Mn/Fe] 1	SAOUHSC_01653	-	0,47	0,05143839	0,34	3,51E-01
HG001_01194	katA	Catalase	SAOUHSC_01327	-	-0,499	0,052458991	0,91	3,55E-04
HG001_01633	tpx	putative thiol peroxidase	SAOUHSC_01822	tpx	0,445	0,051341102	0,20	6,15E-01
HG001_00324	ahpC	Alkyl hydroperoxide reductase subunit C	SAOUHSC_00365	-	1,87	1,93E-18	1,92	4,00E-77
HG001_00323	ahpF	Alkyl hydroperoxide reductase subunit F	SAOUHSC_00364	-	1,79	7,15E-17	1,86	3,84E-51
HG001_02514	ahpD	Alkyl hydroperoxide reductase AhpD	SAOUHSC_02774	-	-2,35	2,77E-23	-0,67	2,59E-01
HG001_00183	hmp	Flavohemoprotein	SAOUHSC_00204	-	-1,31	1,40E-05	-1,17	2,97E-03
HG001_02602	crtM	Dehydrosqualene synthase	SAOUHSC_02879	-	-1,57	NA	ND	ND
HG001_02601	crtN	Dehydrosqualene desaturase	SAOUHSC_02877	-	-1,92	8,97E-18	-0,66	6,45E-01

Regulation of detoxifying enzymes					Diff. Transcriptomics MV/ctr		Diff. Proteomics MV/ctr	
id	gene	product	locus_tag_NCTC8325	gene_NCTC8325	log2FoldChange	padj	log2FoldChange	padj
HG001_01826	perR	Peroxide-responsive repressor PerR	SAOUHSC_01997	-	-1,13	1,18E-06	ND	ND
HG001_02092	sigB	RNA polymerase sigma-B factor	SAOUHSC_02298	-	-0,94	5,31E-06	-0,91	2,71E-01
HG001_01423	fur	Ferric uptake regulation protein	SAOUHSC_01592	-	-0,447	0,080768103	0,53	3,07E-01
HG001_00556	sarA	Transcriptional regulator SarA	SAOUHSC_00620	-	-2,33	2,30E-20	0,31	2,99E-01

Metal homeostasis					Diff. Transcriptomics MV/ctr		Diff. Proteomics MV/ctr	
id	gene	product	locus_tag_NCTC8325	gene_NCTC8325	log2FoldChange	padj	log2FoldChange	padj
HG001_00116	isdI	Heme oxygenase (staphylobilin-producing) 2	SAOUHSC_00130	-	-0,663	0,020844767	2,02	5,34E-05
HG001_00981	isdE	High-affinity heme uptake system protein IsdE precursor	SAOUHSC_01085	-	-0,86	0,006277875	1,98	4,11E-01
HG001_02320	fhuD_2	Iron(3+)-hydroxamate-binding protein FhuD precursor	SAOUHSC_02554	-	1,35	9,45E-11	1,18	2,08E-09
HG001_02047	fhuD_1	Iron(3+)-hydroxamate-binding protein FhuD precursor	SAOUHSC_02246	-	-0,81	0,044043942	ND	ND
HG001_01927	ftnA	Ferritin	SAOUHSC_02108	-	-1,45	7,51E-13	0,16	6,45E-01
HG001_00625	mgrA	HTH-type transcriptional regulator MgrA	SAOUHSC_00694	-	-1,64	1,53E-12	-0,23	7,11E-01
HG001_01527	mntH_2	Divalent metal cation transporter MntH	SAOUHSC_01707	-	-0,88	0,001151062	ND	ND
HG001_00065	sbnA	putative siderophore biosynthesis protein SbnA	SAOUHSC_00075	-	1,17	0,000501837	2,79	2,32E-01
HG001_00066	sbnB	N-[(2S)-2-amino-2-carboxyethyl]-L-glutamate dehydrogenase	SAOUHSC_00076	-	1,47	9,94E-09	8,63	5,62E-28
HG001_00067	sbnC	Staphyloferrin B synthase	SAOUHSC_00077	-	1,87	5,02E-14	5,19	2,32E-04
HG001_00068	sbnD	Staphyloferrin B export protein	SAOUHSC_00078	-	1,51	6,73E-11	ND	ND
HG001_00069	sbnE	L-2,3-diaminopropanoate--citrate ligase	SAOUHSC_00079	-	1,44	3,86E-09	5,59	1,37E-05
HG001_00070	sbnF	2-[[(L-alanin-3-ylcarbamoyl)methyl]-3-(2-aminoethylcarbamoyl)-2-hydroxy	SAOUHSC_00080	-	1,32	5,34E-07	7,41	3,27E-19
HG001_00071	sbnG	Citrate synthase	SAOUHSC_00081	-	1,54	1,07E-11	6,79	1,54E-12
HG001_00072	sbnH	2-[[(L-alanin-3-ylcarbamoyl)methyl]-2-hydroxybutanedioate decarboxylase	SAOUHSC_00082	-	1,48	1,97E-12	6,11	7,21E-08
HG001_00073	sbnI	L-serine kinase	SAOUHSC_00083	-	1,64	9,52E-15	5,50	2,76E-05
HG001_00573	ideR	Iron-dependent repressor IdeR	SAOUHSC_00638	mntR	-2,13	8,63E-19	-0,58	5,48E-01
HG001_00572	**mntA**	High-affinity zinc uptake system ATP-binding protein ZnuC	SAOUHSC_00637	-	-1,74	1,75E-12	0,03	9,71E-01
HG001_00571	**mntB**	Manganese transport system membrane protein MntB	SAOUHSC_00636	-	-2,91	3,21E-40	ND	ND
HG001_00570	**mntC**	Manganese ABC transporter substrate-binding lipoprotein precursor	SAOUHSC_00634	-	-3,30	4,90E-40	0,34	9,47E-02

Electron transport chain					Diff. Transcriptomics MV/ctr		Diff. Proteomics MV/ctr	
id	gene	product	locus_tag_NCTC8325	gene_NCTC8325	log2FoldChange	padj	log2FoldChange	padj
HG001_01585	hemB	Delta-aminolevulinic acid dehydratase	SAOUHSC_01772	-	0,579	0,019809775	-1,32	2,99E-02

Transcription regulator					Diff. Transcriptomics MV/ctr		Diff. Proteomics MV/ctr	
id	gene	product	locus_tag_NCTC8325	gene_NCTC8325	log2FoldChange	padj	log2FoldChange	padj
HG001_00022	walR	Transcriptional regulatory protein WalR	SAOUHSC_00020	-	0,292	0,211077335	-1,72	6,91E-02
HG001_02667	slyA_3	Transcriptional regulator SlyA	SAOUHSC_02961	-	0,671	0,007078829	-1,21	3,44E-01
HG001_00061	sarS	HTH-type transcriptional regulator SarS	SAOUHSC_00070	-	1,59	1,36E-13	0,05	9,33E-01
HG001_02422	sarZ	HTH-type transcriptional regulator SarZ	SAOUHSC_02669	-	-1,10	1,11E-05	-1,78	4,42E-01
HG001_00607	sarX	HTH-type transcriptional regulator SarX	SAOUHSC_00674	-	-1,49	6,69E-10	-0,93	2,86E-01
HG001_02303	sarV	HTH-type transcriptional regulator SarV	SAOUHSC_02532	-	-1,83	1,02E-10	ND	ND
HG001_02330	sarR	HTH-type transcriptional regulator SarR	SAOUHSC_02566	-	-1,93	2,59E-13	-0,71	2,00E-01
HG001_00556	sarA	Transcriptional regulator SarA	SAOUHSC_00620	-	-2,33	2,30E-20	0,31	2,99E-01

Ethanol degradation	Diff. Transcriptomics MV/ctr	Diff. Proteomics MV/ctr

id	gene	product	locus_tag_NCTC8325	gene_NCTC8325	log2FoldChange	padj	log2FoldChange	padj
HG001_00118	aldA	Putative aldehyde dehydrogenase AldA	SAOUHSC_00132	-	1,16	1,55433E-06	-2,81	3,33E-02
HG001_00099	adhE	Aldehyde-alcohol dehydrogenase	SAOUHSC_00113	-	-3,99	1,68476E-54	-1,78	4,42E-01
HG001_00544	adh	Alcohol dehydrogenase	SAOUHSC_00608	adhA	-2,96	9,54629E-47	-1,10	2,42E-04
HG001_01654	acsA_1	Acetyl-coenzyme A synthetase	SAOUHSC_01846	-	-1,49	1,85733E-09	-1,78	4,42E-01
HG001_01955	alkH	Aldehyde dehydrogenase	SAOUHSC_02142	-	-1,89	2,51113E-15	-0,31	4,11E-01

tRNA charging					Diff. Transcriptomics MV/ctr		Diff. Proteomics MV/ctr	
id	gene	product	locus_tag_NCTC8325	gene_NCTC8325	log2FoldChange	padj	log2FoldChange	padj
HG001_00407	metG	Methionine--tRNA ligase	SAOUHSC_00461	-	1,55	1,42641E-11	-0,10	7,39E-01
HG001_01315	asnS	Asparagine--tRNA ligase	SAOUHSC_01471	asnC	1,08	1,60743E-05	-0,32	0,0861312
HG001_01044	ileS	Isoleucine--tRNA ligase	SAOUHSC_01159	ileS	1,08	0,000184868	0,07	0,6020900
HG001_01679	leuS	Leucine--tRNA ligase	SAOUHSC_01875	leuS	0,95	0,000494718	0,22	0,1775016
HG001_00434	lysS	Lysine--tRNA ligase	SAOUHSC_00493	lysS	0,683	0,004966781	0,30	0,0657212
HG001_00547	argS	Arginine--tRNA ligase	SAOUHSC_00611	argS	0,603	0,007896657	0,12	0,3623763
HG001_01114	proS	Proline--tRNA ligase	SAOUHSC_01240	-	0,80	0,000847588	-0,23	0,2029304
HG001_00457	gltX	Glutamate--tRNA ligase	SAOUHSC_00509	gltX	0,472	0,055358849	-0,02	0,9104106
HG001_01601	thrS	Threonine--tRNA ligase	SAOUHSC_01788	thrS	-0,45	0,061656411	-0,24	0,3307554
HG001_01555	hisS	Histidine--tRNA ligase	SAOUHSC_01738	hisS	-0,686	0,011301763	-0,51	0,1148211
HG001_00010	serS	Serine--tRNA ligase	SAOUHSC_00009	-	-0,80	0,000790321	-0,08	0,6029672
HG001_00842	trpS	Tryptophan--tRNA ligase	SAOUHSC_00933	-	-0,97	8,54628E-05	-0,54	0,0255249

Université de Strasbourg

Laura ANTOINE

École Doctorale des Sciences de la Vie et de la Santé STRASBOURG

Caractérisation des modifications post-transcriptionnelles des ARN non codants chez *Staphylococcus aureus* en réponse à divers stress environnementaux : analyse dynamique et fonctionnelle

Les modifications post-transcriptionnelles des ARN sont impliquées dans de nombreux processus biologiques. Elles sont constitutives ou modulées en réponse à des processus adaptatifs et remplissent de nombreuses fonctions. La cartographie des modifications dans les ARN du pathogène *S. aureus*, responsable d'un grand nombre d'infections de gravité variable et touchant un large éventail de tissus, reste encore peu connue ainsi que leurs implications dans l'adaptation de la bactérie à son environnement, notamment lors de l'infection.

Cette étude a pour but principal dans un premier temps d'établir une cartographie des modifications présentes dans les ARN non codants, plus spécifiquement dans les ARNt de *S. aureus* puis de révéler la dynamique des modifications en adaptation à différentes conditions environnementales rencontrées par la bactérie lors de l'infection.

Enfin, l'étude des causes ainsi que des conséquences traductionnelles des changements observés pourra être réalisée afin de déterminer le potentiel rôle des modifications post-transcriptionnelles dans l'adaptation aux stress

Mots clés : Modifications post-transcriptionnelles, *Staphylococcus aureus*, adaptation au stress

RNA post-transcriptionnal modifications are involved in numerous biological processes. They are constitutive or modulated in response to adaptive processes and play multiple functions. The mapping of RNA modifications on the pathogen *S. aureus*, responsible for several infections of variable severity and targeting several tissues, is still poorly known, as well as their involvement in the host adaptation processes.

This study aims to produce a first map of modifications that are present on *S. aureus* non coding RNAs, especially *S.aureus* tRNA and to reveal the dynamics of some of these modifications in a stress condition encountered during the infection.

Finally, the mechanisms promoting different modification levels and the impact that these variations might have on the translation processes could be studied.

Keywords : Post-transcriptionnal modifications, *Staphylococcus aureus*, stress adaptation.